



Published in final edited form as:

Chem Rev. 2022 June 08; 122(11): 10126–10169. doi:10.1021/acs.chemrev.1c00513.

Site-Selective Cross-Coupling of Polyhalogenated Arenes and Heteroarenes with Identical Halogen Groups

Vignesh Palani[†],

Department of Chemistry, University of California, California 94720, United States

Melecio A. Perea[†],

Department of Chemistry, University of California, California 94720, United States

Richmond Sarpong

Department of Chemistry, University of California, California 94720, United States

Abstract

Methods to functionalize arenes and heteroarenes in a site-selective manner are highly sought after for rapidly constructing value-added molecules of medicinal, agrochemical, and materials interest. One effective approach is the site-selective cross-coupling of polyhalogenated arenes bearing multiple, but identical, halogen groups. Such cross-coupling reactions have proven to be incredibly effective for site-selective functionalization. However, they also present formidable challenges due to the inherent similarities in the reactivities of the halogen substituents. In this Review, we discuss strategies for site-selective cross-couplings of polyhalogenated arenes and heteroarenes bearing identical halogens, beginning first with an overview of the reaction types that are more traditional in nature, such as electronically, sterically, and directing-group-controlled processes. Following these examples is a description of emerging strategies, which includes ligand- and additive/solvent-controlled reactions as well as photochemically initiated processes.

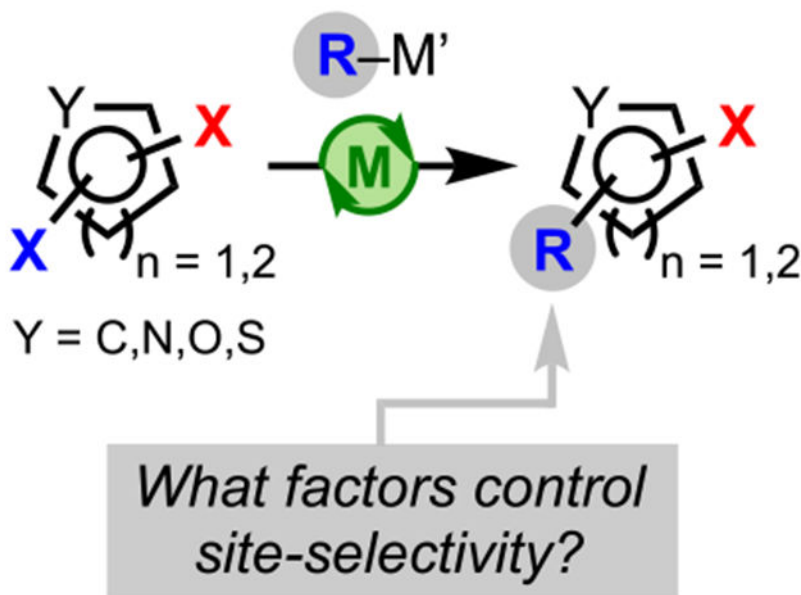
Graphical Abstract

Corresponding Author: Richmond Sarpong – *Department of Chemistry, University of California, California 94720, United States;* rsarpong@berkeley.edu.

[†]V.P. and M.A.P. contributed equally to this work.

Complete contact information is available at: <https://pubs.acs.org/10.1021/acs.chemrev.1c00513>

The authors declare no competing financial interest.



1. INTRODUCTION

Functionalized arenes and heteroarenes (collectively, (hetero)arenes) occur in a diverse array of secondary metabolites (i.e., natural products), drug candidates, ligands (e.g., those employed in transition-metal-catalyzed reactions), polymers, and electronic materials.^{1–3} Given the ubiquity of these structural motifs, synthetic chemists continue to seek efficient, generalizable syntheses to prepare these scaffolds.^{4–8} Two approaches have primarily been pursued. In the first approach, the core (hetero)arene is assembled from acyclic precursors already bearing key substituents that will reside on the periphery of the (hetero)arene.^{9–11} A second approach focuses on functionalizing the periphery of a preformed (hetero)arene core through sequential functionalizations.¹² Of the two approaches, the latter has become more commonly employed due to the widespread availability of the unfunctionalized (hetero)arene precursors and the broad range of functionalization strategies that currently exist, including aromatic substitution reactions,^{13–15} metal-mediated halogen-exchange reactions,^{16,17} C–H functionalization processes,¹⁸ cross-coupling reactions,¹⁹ and the more recently developed photoredox catalysis.⁶

In particular, cross-coupling reactions (selected examples shown in Figure 1),^{20,21} have been shown to be tremendously powerful tools for functionalizing halogenated/pseudohalogenated arenes by selectively replacing a halogen/pseudohalogen with a desired substituent. Since their inception over 40 years ago, cross-coupling reactions have continued to offer a highly convergent and streamlined approach for generating value-added complexity and are therefore invaluable in all areas of synthetic chemistry, in particular, the fine chemical industry.²² Indeed, it is no surprise that this powerful class of reactions was duly recognized with the 2010 Nobel Prize in Chemistry to Richard F. Heck, Ei-ichi Negishi, and Akira Suzuki.²⁰ The field of cross-coupling has continued to evolve since the pioneering work of Suzuki,^{23–25} Negishi,^{26,27} Stille,^{28,29} and Heck.³⁰ Recent decades

have seen the development of myriad new coupling strategies,²² many of which focus on addressing and improving several important aspects of cross-coupling chemistry, such as the site selectivity.³¹

The appeal of site-selective^{32,33} coupling reactions stems from the ability to functionalize one position of a multiply halogenated (hetero)arene over all other positions, thus providing a streamlined synthetic approach for structural diversification. Traditionally, site-selective couplings have been achieved by employing (hetero)arene electrophiles bearing multiple, nonidentical halogens or pseudohalogens, such as the triflyloxy ($-OTf$) group (Scheme 1A).^{12,34,35} In these cases, the site selectivity relates to the relative bond dissociation energies (BDEs) of carbon-halogen ($C-X$) bonds (lower $C-X$ BDE = preferred site of oxidative addition) and therefore follows the general reactivity trend: $C-I > C-Br > C-Cl > C-F$.³⁶⁻³⁸ This difference in reactivity ultimately facilitates the chemoselective installation of a substituent to a desired position.¹² This strategy, however, becomes challenging when the parent (hetero)arene bears identical halogen atoms, as there is little difference in the nature of the aryl-halide bonds (Scheme 1B). In these systems, site-selective coupling at the carbon bearing one halogen atom over another depends on other factors such as the electronic nature of the atom to which the halogen or pseudohalide is attached and the steric environment, which determines the preferred site of reactivity.³¹ Overall, achieving site-selective couplings is of great interest to the synthetic community not only because of the use of easily accessible polyhalogenated aryl precursors but also due to the effectiveness of these processes in generating complexity both rapidly and efficiently. Strategies for achieving site-selective couplings in polyhalogenated (hetero)arenes containing identical halogen atoms continue to emerge.³⁹⁻⁴⁴

In this Review, we present a comprehensive overview of the site-selective coupling of polyhalogenated (hetero)arenes bearing identical halogen groups by summarizing selected examples in this field, which highlight key factors that enable site selectivity. These examples are further categorized on the basis of factors that control the selectivity in each system, including electronic control, steric control, directing group (DG) control, ligand control, and additive/solvent control. The examples range from traditional approaches to controlling site selectivity, such as electronic and steric control, to more contemporary strategies, such as those that leverage additive/solvent control, to highlight the evolution of site-selective coupling. Additionally, the evolution in methods for achieving selective coupling is further supported with recent examples that deviate mechanistically from the norm, such as photochemical and $C-F$ activation processes. It is important to note that aspects of classical approaches to site-selective cross-couplings (e.g., those influenced by DGs and electronic/steric factors) discussed herein have also been discussed in previous, insightful reviews;^{31,39-42} however, more modern approaches, such as the aforementioned $C-F$ activation, additive/solvent-controlled, and photochemically initiated processes, have not been previously discussed. By focusing on a large array of examples, including those previously covered, we hope to place the methods in context, illustrate the growth of this field, and provide insight into the potential future directions of this highly valuable but rapidly evolving area of cross-coupling chemistry.

2. OVERVIEW OF MECHANISTIC CONSIDERATIONS AND EXISTING METHODS FOR PREDICTING SITE SELECTIVITY

To understand how selectivity arises in the cross-coupling of polyhalogenated (hetero)arenes, one must first consider the mechanism of cross-coupling. A simplistic depiction of the catalytic cycle for a transition-metal catalyzed cross-coupling, such as the Suzuki–Miyaura reaction, reveals three key elementary steps: oxidative addition, transmetalation, and reductive elimination (Scheme 2).^{34,35,45–48} The cycle begins with oxidative addition of the ligand-bound metal catalyst ($M^{\text{II}}L_n$) into one of the carbon–halogen bonds to generate a $M^{\text{IV}}L_n$ intermediate. This intermediate then transmetalates with a suitable organometallic reagent (RM') to generate a new $M^{\text{II}}L_n$ complex, where the halogen on the metal is displaced. This newly generated intermediate, when oriented in the cis geometry (with respect to the metal center), is primed to undergo reductive elimination to furnish the coupled product and regenerate the $M^{\text{II}}L_n$ complex.^{45–48} In most instances, the turnover-limiting (or selectivity-determining) step is oxidative addition, where selectivity arises due to differences in the relative electrophilicities of the carbons bound to halogen groups in the parent (hetero)arene.^{40–42} However, it should be noted that there are instances where transmetalation or reductive elimination are turnover-limiting, and such examples will be discussed on a case-by-case basis.^{48,49} Because oxidative addition formally involves the addition of electrons to a carbon–halogen bond, the most electrophilic carbon would be expected to be the preferred site of attack, and, in general, the selectivity of cross-coupling follows the same trend observed for nucleophilic aromatic substitution (S_NAr) reactions.^{13,50} Overall, the selectivity-determining step is influenced by several factors, including the electronics of the (hetero)arene, specifically, the relative electrophilicities of the carbon positions; the steric environment around the (hetero)arene, usually favoring positions that minimize steric interactions in the transition state; the reactivity of the ligand-bound catalyst from both an electronic and a steric standpoint; and the transmetalating reagent, in cases where transmetalation is turnover-limiting.⁵¹ Therefore, a site-selective coupling could be achieved by controlling any of these factors, depending on which step is turnover-limiting and irreversible.

In their highly informative review on site-selective Suzuki–Miyaura couplings of heteroaryl halides, Spivey and coworkers highlighted several key paradigms for predicting site selectivity.³¹ Because many of these factors will be invoked throughout our Review and to ensure comprehensive and consistent coverage, we will briefly summarize these key paradigms as well. Several methods have been employed in predicting the selectivity outcome in cross-couplings involving polyhalogenated (hetero)arenes. Often, empirically determined S_NAr data correlate with site-selective cross-coupling outcomes.^{42,52,53} In some cases, the reactivity trend observed with lithium–halogen exchange to generate a more stabilized aryllithium intermediate can also correlate with the preferred site for transition-metal-mediated coupling.^{54,55} Furthermore, ^{13}C NMR chemical shifts (δ_{C}) can provide insight into the most electrophilic carbon positions on a given system.^{41,56} Similarly, ^1H NMR chemical shifts (δ_{H}) of the C–H bonds in the corresponding nonhalogenated aromatic compounds can guide the prediction of site-selective transformations as well.⁵⁷ However, this method is not reliable for systems where δ_{H} is <0.3 ppm because the site selectivity for

such (hetero)arenes can be reversed depending on the reaction conditions.^{31,41,58} Another potential limitation in this NMR-guided approach to predicting reactivity order is that an initial substitution at one of the carbon–halogen bonds could affect the electronics of the remaining carbon positions, thus making subsequent substitutions more challenging to predict by NMR.

Recently, computational strategies have also been applied in predicting the selectivity outcome in cross-coupling for various heterocyclic systems.³⁸ Advantageously, computations evaluate several related factors, such as steric influences and neighboring group participation, in addition to the intrinsic electronic properties of the parent heterocycle, to predict selectivity outcomes. Overall, this represents a more comprehensive and practical approach to predicting site selectivity compared with previous methods like NMR, which rely solely on intrinsic electronic differences to rationalize preferred sites of coupling. For example, Houk, Merlic, and coworkers have recently determined that the site selectivity of Pd-catalyzed cross-couplings cannot be predicted/rationalized by analyzing only the BDEs of respective carbon–halogen bonds.³⁸ They have instead employed a density functional theory (DFT)-based “distortion–interaction” model to understand the factors that control oxidative addition (Figure 2A). This model considers both the energy required to distort the reactants (metal and heterocycle) to the oxidative addition transition-state geometry (known as the distortion energy, $E_{\text{dist}}^{\ddagger}$) and the energy from major orbital interactions between the distorted reactants (known as the interaction energy, $E_{\text{int}}^{\ddagger}$) to determine the activation energy for oxidative addition (E^{\ddagger}). In general, the distortion energy is related to the BDE of the C–X bond, and the interaction energy is related to the extent of stabilization that results from the overlap between the heterocycle π^* lowest unoccupied molecular orbitals (LUMOs) and the Pd d_{xy} highest occupied molecular orbitals (HOMOs) (Figure 2B).³⁸ For polyhalogenated arenes, both of these factors ($E_{\text{dist}}^{\ddagger}$ and $E_{\text{int}}^{\ddagger}$) determine the relative stabilities of oxidative addition transition states at different halogen positions (ultimately conveyed by relative E^{\ddagger} barriers). These data are, in turn, used to predict and rationalize the preferred site of oxidative addition.

Overall, these methods highlight the importance of considering multiple factors when predicting selectivity outcomes in cross-coupling. On this basis, we will highlight several strategies and tools for controlling site selectivity, beginning with a discussion of how innate electronic properties can guide selectivity outcomes in myriad cross-coupling processes (section 3). After establishing a fundamental understanding of electronic considerations and how they guide selectivity, we will continue our discussion of this expansive field by considering other strategies that can be employed to either reinforce or override innate electronics to control selectivity outcomes, such as leveraging steric, DG, ligand, and additive/solvent effects (sections 4–7). Finally, we will discuss modern photochemical approaches to execute site-selective cross-couplings (section 8).

3. ELECTRONIC CONTROL

The electronics of the (hetero)arene can provide insight into the site that is expected to undergo oxidative addition to predict selectivity outcomes for cross-couplings of polyhalogenated (hetero)arenes bearing the same type of halogen. In fact, unless there are

other factors that override electronics and perturb innate reactivity, such as strong steric influences or DGs, electronic effects will usually guide the reaction selectivity. Along these lines, there are two major factors to consider when assessing the electronics of a system: the (hetero)arene type and the substituent effects. For arenes (all-carbon framework), electronic effects from substituents (i.e., electron-withdrawing groups (EWGs) or electron-donating groups (EDGs)), beyond the two C–X bonds likely to undergo oxidative addition, often guide the selectivity outcomes (Scheme 3A). On the contrary, heteroarenes have intrinsic electronic properties by virtue of the embedded heteroatom, which can guide site selectivity even in the absence of substituents; in these cases, however, substituent effects can still play a role in guiding site selectivity (Scheme 3B).⁵⁹ In this section, we discuss representative examples that illustrate how the (hetero)arene type and the substituent effects influence the electronic properties and therefore control selectivity outcomes. We begin with a discussion of all-carbon systems followed by examples of various six- and five-membered heterocyclic systems. Whereas this section is categorized on the basis of (hetero)arene type, the discussion will focus on outlining the fundamental concepts surrounding the electronic effects and properties of each system. Overall, this section is meant to provide a general guide for understanding electronic properties of arenes and heteroarenes in the context of site-selective cross-coupling.

3.1. Selected Examples of Arenes (All-Carbon Framework)

Substituents play a major role in defining the electronic environment of arenes and therefore heavily influence the site of oxidative addition. One example of substituent effects on electronics and, by extension, guiding site selectivity was described by Hearn and coworkers in their syntheses of unsymmetrical *para*-terphenyl moieties, which have been shown to possess medicinally relevant biological properties (**4**, Scheme 4).⁶⁰ This transformation was achieved through a sequential ligand-free Suzuki–Miyaura coupling of 1,4-dibromonitrobenzene (**1**) and diverse arylboronic acids (**2** and **3**) with a Pd(OAc)₂ precatalyst (Scheme 4). By virtue of a nitro (–NO₂) substituent, cross-coupling to an electron-deficient polyhalogenated arene gave selectivities that mirrored that of an S_NAr reaction, where the first oxidative addition occurred preferentially at the more electrophilic C–Br bond ortho to the nitro group rather than the meta C–Br bond; this reaction resulted in the ortho-substituted (with respect to the NO₂ group) biaryl intermediate, which subsequently underwent a second coupling at the meta position upon the addition of the second arylboronic acid (**3**) to provide the desired terphenyl scaffold (**4**).

In addition to the work by Hearn and coworkers, site-selective cross-coupling has also been achieved in site-selective C–F bond cross-coupling reactions. Organofluorine compounds have proven valuable in pharmaceuticals because C–F bonds are bioisosteres of highly ubiquitous C–H bonds but are not susceptible to oxidation.⁶¹ For this reason, a considerable amount of research has been dedicated toward developing new C–F bond-forming processes.⁶² On the contrary, the functionalization of C–F bonds by transition-metal activation has been relatively less studied. Nonetheless, this alternative approach has proven to be an attractive strategy for diversifying organofluorine compounds. The main challenge associated with oxidative addition into C–F bonds arises from the strength of the C–F bond, which is not only the strongest bond in the aryl carbon–halide series (Figure 3) but also the

strongest carbon–heteroatom bond in nature.⁶¹ This bond strength is attributed to the strong electronegativity of fluorine, which polarizes the C–F bond and creates a strong electrostatic attraction between C^{δ+} and F^{δ-}.⁶³

Nonetheless, considerable progress has been made in the field of C–F bond activation,⁶⁴ in particular, for the site-selective cross-coupling of polyfluorinated arenes. In general, selectivity outcomes for cross-couplings of these systems can be understood by examining the analogous S_NAr reactivity (Scheme 5). In S_NAr reactions of these systems, nucleophilic addition is preferred at sites that result in a Meisenheimer⁶⁵ intermediate, with the anionic charge at a carbon bearing a nonfluorine substituent (usually R = H, EWG, or EDG) instead of one bearing a fluorine atom, which would otherwise result in destabilizing electron–electron repulsive interactions. To satisfy this preference, nucleophilic additions usually occur at a position that is not para to a fluorine atom.⁶⁶ Using pentafluorobenzene derivative **5** as a representative example, addition is favored para to the nonfluorine R group, which results in intermediate **6**, whereas, addition ortho to the R group (para to a fluorine substituent) is disfavored due to the formation of intermediate **7**, which is destabilized by electron–electron repulsion. Analogously, **8** would also favor oxidative addition para to R, providing intermediate **9**.

A prime example of this selectivity is the site-selective Pd-catalyzed C–F arylation of polyfluoroarenes that was demonstrated by Zhang and coworkers (Scheme 6).⁶⁷ This methodology involved the treatment of various polyfluoroarenes (**10**) with a diverse array of arylboronic acids and an *in situ* generated Pd(0) catalyst to synthesize monoarylated cross-coupled products. These reactions proceeded in accordance with their known S_NAr selectivity, where cross-coupling occurred para to a nonfluorine R substituent to provide monoarylated products **11a–d**. In addition to para-arylated products, the authors also reported ortho-arylated products, such as **11d**, where C–F activation selectivity was achieved between the two ortho sites by the strategic placement of the fluorine substituents. Similar to S_NAr, the site that was ortho to the ester but also para to a hydrogen atom (instead of a fluorine atom) was the preferred site of coupling.

Similarly, the base-free Ni(0)-catalyzed Hiyama coupling reported by Ogoshi and coworkers in 2014 (Scheme 7) proceeded with a similar selectivity outcome.⁶⁸ Using [Ni₂(^tPr₂Im)₄(cod)], the authors effectively coupled perfluorotoluene (**12**) with various arylsiloxanes (**13**) to furnish the corresponding para-arylated products (**14a–d**). One key feature of this work is that cross-coupling was achieved between arylsiloxanes and electron-rich (**14a** and **14b**) or electron-deficient (**14c** and **14d**) arenes. Of note, the site selectivity of this reaction could be rationalized similarly to the previous example, where selectivity analogous to an S_NAr reaction was observed.

3.2. Selected Examples of Six-Membered Heteroarenes

Heteroarenes, many of which are considered privileged scaffolds⁶⁹ in medicinal chemistry, have also gained significant traction in site-selective cross-coupling chemistry, which provides an effective and modular strategy for structural diversification. In fact, the majority of small-molecule drugs employed in human medicine are composed of heterocyclic

subunits, with >85% of all bioactive molecules containing some type of heterocycle.^{70,71} Unlike arenes, such as benzene and derivatives thereof, heteroarenes are inherently electronically biased due to inductive effects imparted by the embedded heteroatom(s).⁷² The selected examples of heteroarenes that will be discussed in this section (pyridine (**15**), diazines (pyridazine (**16**), pyrimidine (**17**), and pyrazine (**18**)), and 2-pyrone (**19**)) are shown in Figure 4.

3.2.1. Pyridine.—Pyridines (e.g., **20** and **20'**, Scheme 8) are inherently π -deficient by virtue of the embedded electronegative nitrogen atom, which inductively withdraws electron density from C2 (ortho) and C4 (para). The increased electrophilicity at these positions activates them toward nucleophilic attack in S_NAr (Scheme 8).⁷² In an analogous sense, for cross-couplings of polyhalogenated pyridines, oxidative addition is also favored at the C2 and C4 positions, but this selectivity also greatly depends on specific reaction conditions, other substituents, and substitution patterns.⁷³ In general, for 2,3-, 2,4-, and 2,5-dihalopyridines, oxidative addition is favored α to the nitrogen (i.e., at C2). Recently, Houk, Merlic, and coworkers calculated the BDEs of the C–Cl bonds in various dichloropyridines (Figure 5) and found that the C₂–Cl bond in each of these systems has the lowest calculated BDE, thus accounting for the observed selectivity in cross-coupling.⁷³ The lowest BDE associated with the C2 position can be rationalized by the α -nitrogen effect in which there is a stabilizing interaction between the nitrogen lone pair orbital and the C2 singly occupied molecular orbital (SOMO) resulting from homolysis.^{74,75} It is important to note, however, that whereas there is an overall preference for C2 oxidative addition in 2,4-dihalopyridines, site selectivity for the C4-position can be achieved under certain reaction conditions (see **29d**, Scheme 9B).⁷⁶

Preferential reactivity at the C2 position has been observed in many cross-coupling examples involving dihalogenated pyridines, such as the Pd-catalyzed allenylation of 2,5-dibromopyridine (**25**) described by Lee and coworkers (Scheme 9A).⁷⁷ In this work, the authors demonstrated C2-selective coupling with an *in situ* generated allenylindium reagent derived from the corresponding propargyl bromide. After installation of the C2 allene, the addition of a different allenylindium reagent resulted in C5 coupling, furnishing the C2/C5-allenylated product (**26**). Similarly, Kapdi and coworkers (Scheme 9B) demonstrated the C2- and C4-selective arylation of 2,5- and 2,4-dibromopyridines (**25** and **27**) with arylboronic acids using Pd(OAc)₂ and an *N*-heterocyclic carbene (NHC) ligand (**28**).⁷⁶ As expected, 2,5-dibromopyridines underwent monoarylation at the more electrophilic C2 position (**29a–c**). Interestingly, 2,4-dibromopyridine **27** underwent preferential arylation at C4 over C2 to furnish **29d**, thus demonstrating how under certain reaction conditions, selectivity can be achieved between two similarly electrophilic positions.

Along these lines, Gundersen and coworkers demonstrated how selectivity can be achieved between the electronically similar C2 and C4 positions of 2,4-dichloropyridines (**30**) by altering the substituent at the C3 position (Scheme 10).⁷⁸ The intrinsic reactivity (when R = H) of this system upon subjection to Stille coupling conditions with 2-furyl(tributyl) tin (**31**) favored cross-coupling at the C2 position to furnish **32**, albeit in low yields. Adding an EDG (R = NH₂) to the three-position also favored coupling at the C2 position, presumably due to

the deactivation of the C4 position. However, adding an EWG (R = NO₂) to C3 activated C4 toward oxidative addition, thus completely reversing the selectivity to favor C4 coupling and providing **33**. Overall, this example showcases how substituents can be used to alter intrinsic heteroarene electronics to control selectivity outcomes.

Complementary to Gundersen's work is the report by Langer and coworkers, who investigated site-selective cross-couplings of 2,6-dichloro-3-(trifluoromethyl)pyridines (**34**) to access myriad medicinally relevant trifluoromethyl-substituted pyridine derivatives (**35**, Scheme 11).⁷⁹ Focusing specifically on the monoarylation of these systems, the authors showcased how **34** in the presence of one equivalent of various arylboronic acids and a Pd(0) catalyst underwent selective arylation at C2 over C6. Whereas these two positions on unsubstituted pyridine systems are electronically equivalent, the presence of an adjacent trifluoromethyl (CF₃) group further activated the C2 position toward oxidative addition, thus rendering this reaction selective for C2 coupling. This preference for C2 selectivity has also been observed by Bourissou and coworkers in their studies of Suzuki–Miyaura couplings involving the similar substrate, 2,6-dichloro-3-nitropyridine.⁸⁰

In addition to investigating site-selective cross-coupling in dihalogenated pyridines, Langer and coworkers have also investigated these processes in more heavily substituted systems, such as perchloropyridine (**36**, Scheme 12).⁸¹ In this work, the authors investigated the selectivity of coupling pyridine **36** with various arylboronic acids through a Pd-catalyzed Suzuki–Miyaura coupling. This system underwent arylation only at the C2 and C6 positions, with no arylation observed at the electronically similar C4 position. It should also be noted that to achieve the second arylation, more forcing reaction conditions were required (i.e., higher temperatures around 90–100 °C). This is presumably because the aryl group is less electron-withdrawing than the chlorine atom that was substituted.

In contrast with the C2/C6 selectivity observed by Langer and coworkers, Zhang and coworkers observed completely different selectivity while investigating a Pd-catalyzed cross-coupling of perfluoropyridine (**38**, Scheme 13) with phenyl boronic acid. This cross-coupling was selective for the C4 position to provide 4-phenylpyridine **39**.⁶⁷ This selectivity can be explained through the same analysis that was applied to the polyfluorinated arenes discussed previously (Schemes 5 and 7), where coupling occurs preferentially at a position para to a nonfluorine substituent.

In addition to serving as a robust strategy for functionalizing the periphery of simple arenes, site-selective cross-coupling has also served as an effective approach for constructing even more complex polycyclic heteroarenes, such as the carbazole (**42**, Scheme 14A) and α -carboline (**45**, Scheme 14B) structural motifs.⁸² Ackermann and coworkers were one of the first to demonstrate this approach to construct these heterocycles using a Pd-catalyzed amination/C–H functionalization domino reaction between anilines (**40** and **43**) and dichlorinated arene electrophiles (**41** and **44**). These reactions generally first proceed through a Buchwald–Hartwig-type amination between the aniline and the more electrophilic C–Cl bond, which in **41** is the *para*-C–Cl bond (with respect to the ketone) and in **44** is the *ortho*-C–Cl bond (with respect to the nitrogen), both in accordance with predicted selectivity. This initial amination was then followed by a second oxidative

addition/intramolecular C–H functionalization event to provide either the carbazole (**42**) or the α -carboline (**45**) product. Following this work, a number of similar strategies for synthesizing α -carbolines were demonstrated by Maes and coworkers⁸³ and Cuny and coworkers.⁸⁴

3.2.2. Diazines: Pyrimidine, Pyridazine, and Pyrazine.—In addition to pyridines, polyhalogenated diazines (Figure 6), including pyrimidine (**46**), pyridazine (**47**), and pyrazine (**48**), have also been widely used as substrates in site-selective cross-couplings. Similar to pyridine, in general, oxidative addition in diazines occurs at the site with the lowest C–X BDE.⁷³

For polyhalogenated pyrimidines, the general order of reactivity is C4 > C2 > C5.⁷³ Analogous to the case for dichloropyridines, Houk, Merlic, and coworkers also calculated the relative BDEs for both 2,4- and 2,5-dichloropyrimidines and found that the C₄–Cl bond has the lowest BDE relative to the C2 and C5 positions (Figure 7). On the basis of the α -nitrogen effect observed in pyridine systems, one might have expected the C₂–X bond in pyrimidines, which is “doubly” α (situated next to two nitrogen atoms), to have a lower BDE compared with the C₄–X bond (due to added stabilization of the C2-pyrimidyl radical from an additional N(nonbonding orbital)–C2(SOMO) interaction). However, through computational studies, Hadad and coworkers found that the C4-pyrimidyl radical is actually more stable than the C2-pyrimidyl radical, thus accounting for the lower BDE at the C4 position.⁸⁵ Specifically, the authors reported that following C–H homolysis at C4, C2, and C5, the bond angles at these positions widen by 2.5, 3.8, and 5.0°, respectively. Overall, these data convey that less deviation from the ideal sp²-hybridized 120° bond angle provides greater radical stabilization and thus a lower BDE for the parent C–X bond.

The order of reactivity that was predicted computationally (C4 > C2 > C5) is supported by empirical observations by Undheim and Solberg, who reported identical trends from their studies of Stille couplings between various polychlorinated pyrimidines (**49**, **52**, and **54**, Scheme 15) and tributyl-styryl-stannane (**50**).⁸⁶ Ultimately, these reactions afforded the expected C4- and C2-vinylated adducts (C4: **51** and **55**; C2: **53**) in accordance with the selectivity trend predicted by relative BDE values.

Polyhalogenated pyridazines generally favor cross-coupling at C3, which has the lowest C–X BDE relative to the C5 position due to C3 being α to a nitrogen (Scheme 16).⁷³ Young and coworkers observed this selectivity trend in their Pd-catalyzed amidation reaction between 3,5-dichloropyridazine (**56**) and 2-pyrrolidinone (**57**) to give C3-amidated adduct **58**.⁸⁷

Unlike pyridine and pyrimidine derivatives, dihalogenated pyrazines are symmetrical for all substitution patterns, with both halogens residing α to a nitrogen in every case (Figure 6).³¹ These C–X bonds are electronically identical and, in the case of a C–Cl bond, have a calculated BDE of 92.9 kcal/mol (Figure 8).⁷³ Because these positions cannot be differentiated electronically, other strategies, such as employing a DG, are required to achieve site selectivity; such an example is described in section 5. (See Scheme 31.)

3.2.3. 2-Pyrone: The 2-pyrone motif (**19**, Figure 9) is found in a number of biologically active secondary metabolites and has also become a useful synthetic precursor to access numerous biologically important molecules.^{88–91} Specifically, various cross-coupling adducts originating from 2-pyrone derivatives exhibit promising anticancer activity. Given the promising bioactivity of 2-pyrone derivatives, 3,5-dibromo-2-pyrone (**59**) and 4,6-dichloro-2-pyrone (**60**) have been the subject of various studies on site-selective cross-coupling. The 3,5-dibromo-2-pyrone motif (**59**, Scheme 17A) has been shown to undergo C3-selective Sonogashira coupling with various terminal alkynes to afford the corresponding C3-alkynylated products (**61**).⁹² The selectivity observed under these conditions is in accordance with what would be predicted by ¹³C NMR shifts (Figure 9), where C3 is more deshielded (electron-deficient) than C5 ($\delta = 3.8$).^{93–95} With a decrease in electron density at C3, oxidative addition is more favorable at this position over the more shielded C5 position. Whereas reactivity at C3 of 3,5-dibromo-2-pyrone is favored by virtue of the innate electronics, the selectivity can be completely reversed to instead favor the C5 position under certain conditions.^{43,44} An example of employing additive/solvent control to reverse the intrinsic site selectivity of 3,5-dibromo-2-pyrone is discussed in section 7.

For 4,6-dichloro-2-pyrone (**60**), Sonogashira coupling with terminal alkynes preferentially gives C6-alkynylated products (**62**, Scheme 17B).⁹⁵ Similar to 3,5-dibromo-2-pyrone, the ¹³C NMR shifts for 4,6-dichloro-2-pyrone (C6: $\delta = 152.2$ vs C4: $\delta = 150.4$) also correlate with this observed selectivity (Figure 9). Upon analysis of the energy profile for both C4 and C6 oxidative addition (using PMe_3 model ligands), it can be seen that oxidative addition leading to intermediate **I** via **TS-I** is both kinetically and thermodynamically favored over the formation of intermediate **II** via **TS-II** (Figure 10). This favorability for C6 oxidative addition can be rationalized by the α -oxygen, which presumably stabilizes the developing positive charge in the transition state by serving as a π -donor.⁹⁵

3.3. Selected Examples of Five-Membered Heteroarenes

In addition to six-membered heteroarenes, five-membered heteroarenes (Figure 11) are also prevalent in many pharmaceuticals and therefore constitute an important class of medicinally relevant compounds.⁷⁰ In this section, we discuss selected examples of site-selective cross-couplings of five-membered polyhalogenated heteroarenes along with electronic considerations that help guide the prediction of site selectivity. As with the previous sections, these examples are further categorized based on the subclass of five-membered heterocycles they belong to, which in this section will include five-membered heterocycles with either one heteroatom or two heteroatoms (i.e., 1,3-azoles and 1,2-azoles).

3.3.1. Thiophene, Pyrrole, and Furan.—Polyhalogenated pyrroles, thiophenes, and furans are known, in general, to preferentially undergo oxidative addition α to the heteroatom (C2 or C5) in cross-coupling reactions. Unlike most of the six-membered aza-aromatics previously discussed (with the exception of pyrimidines), the site selectivity for oxidative addition involving polyhalogenated five-membered heteroarenes with one heteroatom (i.e., thiophene, pyrrole, and furan) does not necessarily correlate with relative BDEs.⁷³ In fact, for both 2,4- and 2,3-dichlorinated thiophene, pyrrole, and furan, the BDEs for both C–Cl bonds (Figure 12) are very similar, if not nearly identical, which means that

the experimentally observed C2/C5 selectivity is controlled by other factors that go beyond the relative bond strength.

A simple analysis of these systems using the Handy–Zhang⁵⁷ method of assessing electronics based on ¹H NMR chemical shifts shows that the C2/C5 positions for these systems are the most deshielded positions (i.e., most electron-deficient positions) relative to other positions, thus providing one rationalization as to why oxidative addition occurs preferentially at C2/C5 (Figure 13)^{41,96} Of course, this deshielding effect is more pronounced for thiophene and furan, as conveyed by the larger differences in ¹H NMR chemical shifts relative to pyrrole, due to sulfur and oxygen being more electronegative relative to nitrogen; this greater electronegativity ultimately causes the inductive effect imparted by the heteroatom to be the dominant effect, which results in an overall dipole moment directed toward the heteroatom. For pyrrole, the nitrogen is still somewhat inductively electron-withdrawing from the C2 position; however, in contrast with thiophene and furan, the mesomeric effect in pyrrole dominates over the inductive effect, thus accounting for the π -excessive character of pyrrole and producing an overall dipole directed away from the nitrogen.⁹⁶

In addition to considering inductive effects, a second, and more comprehensive, rationalization for C2 selectivity can be ascertained using Houk's distortion–interaction model. (See Figure 2.) In the case of 2,3-dibromofuran (**63**, Scheme 18A), the C2 and C3 positions have identical C–Br BDEs (88.9 kcal/mol). Because BDEs are related to the distortion energy, one can conclude, based on these identical BDEs, that the distortion energies for C2 and C3 oxidative addition do not play a prominent role in controlling the site selectivity. Instead, it is the interaction energy ($E_{\text{int}}^{\ddagger}$), the extent of stabilization from the interaction between the heterocycle π^* LUMOs and the Pd d_{xy} HOMOs, that controls the site selectivity for oxidative addition; for the C2 position of **63**, there is greater stabilization in the oxidative addition transition state and a lower activation barrier (lower E^{\ddagger}) for oxidative addition, thus leading to C2 selectivity.⁷³ Overall, the selectivity predicted by this model is in complete agreement with experimental results by Tang and coworkers, who showcased a Suzuki–Miyaura coupling between **63** and 4-methoxyphenylboronic acid, which provided the predicted C2-arylated product (**64**, Scheme 18B).⁹⁷

This preference for C2/C5 has also been observed for polyhalogenated pyrroles. One such example is 3,4,5-tribromopyrrole-2-carboxylate (**65**, Scheme 19A), which has been shown to undergo C5-selective arylation to give various cross-coupled adducts (**66a–g**).⁹⁸ Complementary to this study was additional work by Handy and Zhang, who demonstrated how electronic effects from substituents at the C2 and C5 positions can control cross-coupling selectivity at the C3 and C4 positions (Scheme 19B). Specifically, they showed how an electron-withdrawing ester moiety at the C2 position could facilitate C3 selectivity over C4 (due to the increased electrophilicity of C3 compared with C4).⁹⁹

Finally, similar C2/C5-favored selectivity outcomes have also been reported for thiophene derivatives, such as 2,3,5,6-tetrabromothiopheno[3,2-*b*]thiophene (**68**, Scheme 20). For **68**, Dang and coworkers reported a C2-selective Suzuki–Miyaura coupling with either one or

two equivalents of various arylboronic acids to afford the mono- or bisarylated products (**69** and **70**).¹⁰⁰

3.3.2. 1,3-Azoles: Thiazole, Imidazole, and Oxazole.—Unlike the five-membered heteroarenes that contain one heteroatom (i.e., thiophene, pyrrole, and furan), 1,3-azoles (i.e., thiazole, imidazole, and oxazole) have BDEs that differ significantly among the various positions, especially the C2 position, which has the lowest relative BDE in both mono- and dichloro-1,3-azole systems (Figure 14) by virtue of being α to two heteroatoms.⁷³

For 2,4- and 2,5-dibromothiazoles (**71** and **72**, Scheme 21A), cross-coupling selectivity has been observed to parallel these BDE trends, with coupling occurring preferentially at the C2 position with various arylboronic acids to give both the 2-aryl-4-bromothiazole (**74**) and the 2-aryl-5-bromothiazole (**75**) products.¹⁰¹ Similar to dibromothiazoles, 2,4-dibromoimidazoles (**76**, Scheme 21B) also exhibit a preference for the doubly α C2-position and undergo monoarylation with diverse arylboronic acids to give the corresponding C2-arylated products (**78**).¹⁰¹

Site-selective sequential Suzuki–Miyaura couplings of *N*-protected 2,4,5-tribromoimidazoles (**79**, Scheme 22A) have become a popular, effective strategy to access trisubstituted imidazoles (**80**), a common structural motif found in natural products with diverse biological activities ranging from anticancer to cell differentiation properties.^{102,103} In one study by Springer and coworkers, which focused on the synthesis of BRAF¹⁰⁴ inhibitors, the 2,4,5-tribromoimidazole scaffold underwent sequential Suzuki–Miyaura couplings in the order C2 > C5 > C4, demonstrating the modularity of this strategy in accessing diverse trisubstituted imidazoles (Scheme 22A).¹⁰² Along similar lines, in their total synthesis of topentin (Scheme 22B), Ohta and coworkers demonstrated a C5-selective Suzuki–Miyaura coupling between an *N*-SEM-protected-4,5-diiodoimidazole (**81**) and an indole boronic acid (**82**) to access the corresponding C5 coupled adduct (**83**).¹⁰⁵ The reactivity pattern C2 > C5 > C4 is the same as that observed in metal–halogen exchange reactions,^{106,107} and whereas the preference for oxidative addition at C2 over C5/C4 can be explained just as before (α to two heteroatoms), the preference for oxidative addition at C5 over C4 that is observed in both of these studies can potentially be understood by comparing the stereoelectronic environments of both positions. Analogous to the work of Sames and coworkers on the site-selective palladation/arylation of *N*-protected imidazoles,¹⁰⁸ the C₄–Pd(II)L₂X complex in this case may be less favored (relative to the alternative C₅–Pd(II)L₂X complex) due to destabilization by electron repulsion from the adjacent nitrogen lone pair at the three-position of the imidazole (highlighted in red; Scheme 22B).

It is important to note that the preference for C2 oxidative addition observed for many 1,3-azoles does not apply to all cases, as it has also been shown, namely, for *N*-methyl-2,5-dibromoimidazole (**84**, Figure 15) and 2,4-diiodooxazole (**85**), that selectivity can be reversed to favor C5 oxidative addition (for *N*-methyl-2,5-dibromoimidazole) or C4 oxidative addition (for 2,4-diiodooxazole) over C2 by simply altering the reaction conditions, specifically the metal/ligand complex (discussed in more detail in section 6; see Scheme 64).¹⁰¹ Finally, for ethyl 2,5-dibromooxazole-4-carboxylate (**86**), Hodgetts

and coworkers have reported that no selectivity could be achieved using standard Suzuki–Miyaura conditions, with a complex mixture of products resulting instead.¹⁰⁹

3.3.3. 1,2-Azoles: Pyrazole and Isothiazole.—The last series of heteroarenes to be discussed in this section are the 1,2-azoles, specifically pyrazole and isothiazole. To the best of our knowledge, there are currently no reports of site-selective cross-couplings of polyhalogenated isoxazoles substituted with the same type of halogen. For pyrazoles and isothiazoles, recent studies convey that there is no direct correlation between BDE trends and cross-coupling site selectivity.^{110,111} On the basis of relative BDE values (Figure 16), one would expect that oxidative addition would occur first at the C3 position because C3 has the lowest relative BDE.⁷³ However, for polyhalogenated pyrazoles and isothiazoles, cross-coupling has been shown to occur preferentially at the C5 position.^{110,111}

N-Protected 3,4,5-tribromopyrazoles (**87**, Scheme 23) have been observed to undergo oxidative addition (and subsequent cross-coupling) in the order C5 > C3 > C4.³¹ This preference for C5 coupling has been demonstrated before by Langer and coworkers, who synthesized a variety of C5-arylated pyrazoles (**88a–e**) from the corresponding arylboronic acids.¹¹⁰ Cross-coupling selectivity for *N*-protected 3,4,5-tribromopyrazoles follows the same selectivity pattern observed in the lithium–halogen exchange reaction for the *N*-vinyl system, where lithiation occurs first at the C5 position.¹¹² The preference for reactivity at C5/C3 over C4 arises from the inductive effect of the adjacent heteroatoms; as for the preference for C5 oxidative addition over C3, this may result from destabilizing electron repulsion at C3 by the adjacent nitrogen lone pair at C2, similar to the observed selectivity in imidazole systems.¹⁰⁸ (See Scheme 22B.)

In addition to pyrazole systems, the site-selective cross-coupling of isothiazoles such as 3,5-dichloroisothiazole-4-carbonitrile (**89**, Scheme 24) has been studied. These heterocycles are the basis for the observed antiviral properties of various derivatives.^{113,114} Therefore, the modular synthesis of these derivatives have garnered significant attention. Polyhalogenated isothiazole systems tend to undergo coupling at C5 followed by reaction at C3 and then C4, similar to pyrazoles.³¹ From their studies on site-selective Suzuki–Miyaura couplings between 3,5-dichloroisothiazole-4-carbonitrile (**89**) and one equivalent of various boronic acids, Koutentis and coworkers demonstrated that a series of diverse isothiazole products (**90a–l**) could be obtained following selective coupling at C5.¹¹¹

4. STERIC CONTROL

Whereas the relative carbon electrophilicities in a (hetero)aromatic ring play a prominent role in oxidative addition selectivity, as conveyed in the previous section, one must also consider the steric environment and its effect on site selectivity (Scheme 25). Overall, selectivity is often governed by the interplay between electronics and sterics,³¹ with the most electrophilic and most sterically accessible position being primed for oxidative addition.¹¹⁵ However, it is not always the case that these two factors will be additive (or multiplicative). Examples discussed herein illustrate instances where the steric environment of the aryl halide guides selectivity in a number of possible scenarios, including: steric effects overriding innate electronics, steric effects differentiating between two electronically

similar positions, and steric effects reinforcing the selectivity dictated by innate electronics. (Representative examples are shown in Scheme 26.) It should be noted that whereas the following examples focus on the intrinsic steric environment of the (hetero)arene, steric effects introduced by a metal complex can also play a primary role in governing selectivity;¹¹⁶ specific examples of this class of reactions are discussed in section 6 (Ligand Control).

One example of steric effects overriding electronic effects is shown in Scheme 26A, where coupling takes place at the more sterically accessible C5 position of 2,5-dibromo-3-furoate (**91**), despite the C2 position being electronically favored (i.e., most electron-deficient position) by virtue of being adjacent to both an oxygen atom and an electron-withdrawing ester moiety.¹¹⁷ In the case of 2,5-dibromothiophene **93** (Scheme 26B), there are no pronounced electronic effects from the pendant tetrahydroisoquinoline derivative.¹¹⁸ Therefore, the C2 and C5 positions are electronically similar, and in this case, the difference in the steric environments between these two positions facilitates reactivity at the more sterically accessible C5 position to give adduct **94**. For both **95** → **96** and **97** → **98** (Scheme 26C), the C2 positions of thiazoles **95** and **97** are both electronically preferred over the C5 and C3 positions and are more sterically accessible as well. Therefore, sterics reinforce the innate electronics of these systems, and coupling occurs at the C2 position in both cases.¹¹⁸

Sterically controlled cross-coupling has also proven to be an effective strategy in total synthesis, as exemplified by the synthesis of the thiazolyl peptide antibiotic GE2270 A (**102**)^{119,120} by Bach and coworkers in 2007 (Scheme 27).¹²¹ Here an 11-step sequence (longest linear sequence) was established to access peptide **99**, which features a key northern 2,6-dibromopyridine moiety poised to undergo sequential cross-couplings. The first coupling between peptide **99** and organozinc reagent **100** took place at the less sterically hindered C6 position (relative to the more sterically hindered C2 position) to install the northern C6 thiazole subunit. The target macrocycle was then forged downstream in the synthesis using an intramolecular Stille coupling at the remaining pyrido-C2 bromide.

Similar to Bach and coworkers' synthesis of GE2270 A, Miller and coworkers also leveraged steric control in their syntheses of atropisomerically defined biaryl scaffolds through a sequential cross-coupling strategy (Scheme 28).¹²² In 2010, Miller and coworkers described a peptide-catalyzed enantioselective bromination of atropisomeric compounds to access enantioenriched biaryls, such as the acid and free-hydroxy variant of **103**.¹²³ In 2011, they developed a sequential coupling approach to advance these tribrominated biaryls to diverse, medicinally relevant polyaryl systems without a loss of enantiopurity.¹²² One representative example of this is shown in Scheme 28, where tribromide **103a** first underwent selective coupling with a *N*-methyl-iminodiacetic acid (MIDA) boronate¹²⁴ at the more sterically accessible C1 position to give **105**. Coupling with a different boronate then occurred at the next sterically more accessible C5 position to give **106**, which was followed by a final coupling at the least sterically accessible C3 position to give the final polyaryl scaffold (**104a**) in an enantioenriched fashion.

Finally, it has also been shown that halogen atoms can also have a significant steric influence in guiding site-selective couplings (Scheme 29).^{115,125} In a 2005 study by Nakamura

and coworkers on Ni-catalyzed couplings of polyhalogenated arenes, it was shown that 1,2,3-trichlorobenzene (**107**) underwent coupling at the more sterically accessible C1 and C3 positions over the electronically favored but more sterically hindered C2 position.¹²⁵ Likewise, a similar trend was observed by Al-Zoubi and coworkers in 2015 when a variety of 1,2,3-triiodobenzene derivatives (**109**) underwent coupling with arylboronic acids at the more sterically accessible C1/C3 position over the C2 position to give myriad C1-arylated adducts (**110**).¹¹⁵

5. DIRECTING GROUP CONTROL

As discussed in the previous section, the steric influence of various groups can result in site selectivity, sometimes contrary to the outcome based solely on the difference in electron density at different carbons bearing an X group. However, for polyhalogenated arenes with electronically comparable C–X bonds and sterically less-pronounced substituents, a substrate-driven strategy becomes more challenging to execute. To obviate this challenge and achieve site-selective cross-couplings in such systems, synthetic chemists have often relied on a strategy that leverages the coordinating ability of a DG, a pendant functional group preinstalled on a molecule that can coordinate to a metal catalyst or ligand, to direct a metal catalyst to a proximal (or sometimes distal) C–X bond, thus enabling site-selective oxidative addition and subsequent functionalization.¹²⁶ Historically, there have been two major classes of DGs employed in such processes: (1) transition-metal-binding DGs, functional groups on the substrate that coordinate directly to a metal (Scheme 30A), and (2) ligand-binding DGs, functional groups on the substrate that coordinate to a ligand that is, in turn, bound to a transition-metal complex, thus linking the substrate and catalyst (Scheme 30B). Both classes of DGs have proven effective in facilitating site-selective oxidative addition, with transition-metal-binding DGs being optimal for proximal C–X bond cleavage, whereas ligand-binding DGs are applicable in both proximal and distal C–X bond cleavage.

Whereas DGs can be incredibly effective for enabling site selectivity, employing this strategy is often reserved for functional groups that either are ubiquitous in natural or commercially available compounds or do not negatively impact the step count and atom economy in a synthesis. Along these lines, one must be mindful of DGs that need to be removed in a later stage in a synthesis, which can ultimately inflate the step count and reduce the synthetic efficiency. Overall, these considerations have resulted in a collection of diverse functional groups, which have proven to be suitable DGs.¹²⁶ DG-controlled site-selective cross-coupling in polyhalogenated arenes first gained momentum in the early 2000s and has since experienced steady growth, as exemplified by several recent publications, many of which are discussed in this Review. In this section, we have categorized a wide array of examples based on the specific DG facilitating site-selective cross-coupling. Here the discussion focuses first on examples employing substrates with DGs that bind directly to a transition metal (section 5.1), which is then followed by examples employing DGs that interact with a ligand that links the substrate to a transition-metal complex (section 5.2).

5.1. Transition-Metal-Binding Directing Groups

The first category of DGs that we discuss here are those that reside on the substrate and have been shown to coordinate directly to the metal, thus enabling site-selective oxidative addition at a proximal C–X bond. This section is organized based on the specific DG employed. These are often ubiquitous functional groups with coordinating capabilities (e.g., amines, hydroxy groups, carboxylic acids, ketones, amides, etc.).

5.1.1. Amine.—An early example of using a DG to facilitate site-selective cross-coupling was reported by Nakamura and coworkers in 1995.¹²⁷ Their work entailed synthesizing 2-amino-3,5-disubstituted pyrazines en route to bioluminescent and chemiluminescent compounds such as coelenterazine¹²⁸ and analogues thereof. To develop a concise and convergent synthetic route, they chose to commence their synthesis from 2-amino-3,5-dibromo pyrazine (**111**). They initially adopted a sequential Pd-mediated Stille coupling strategy to access disubstituted pyrazines by using excess stannane. Interestingly, when an equimolar mixture of stannane and **111** was treated under the same reaction conditions, they mostly observed the formation of monocoupled pyrazines (**112**) substituted at the three-position, presumably directed by the nearby primary amino group (Scheme 31). This exceptional selectivity enabled them to introduce two different substituents on the 2-aminopyrazines. From these monosubstituted pyrazines (**112**), a second Stille coupling at C5 was effected with a different stannane to furnish disubstituted pyrazines (**113**). Finally, condensation with ketoaldehyde derivative **114** enabled access to a diverse range of coelenterazine analogues (**115a–c**, Scheme 31).¹²⁹

Following this initial report, several groups attempted to utilize the coordination ability of amines to selectively cleave a proximal C–X bond. Toward this end, Hikawa and Yokoyama presented an interesting example where they investigated the possibility of achieving the site-selective Suzuki–Miyaura coupling of *N*-(3,5-dibromo-2-pyridyl)piperazine **116** by coordinating the Pd complex to the tertiary piperazine nitrogen atom and directing it to the nearby C–Br bond (Scheme 32).¹³⁰ In their study, they analyzed the influence of several palladium catalyst precursors and solvents on the selectivity outcome. After extensive screening, they found that employing PdCl₂(dppf) as the precatalyst, KF as the base, and tetrahydrofuran (THF) as the solvent facilitated the site-selective Suzuki–Miyaura coupling between **116** and methylboronic acid to furnish the monomethylated derivative **117** in 71% yield. Eventually, they extended the scope of this reaction to other boronic acids to access a wide variety of monosubstituted products. In addition to primary (Scheme 31) and tertiary (Scheme 32) amines, secondary amines (not shown) were also identified as suitable DGs.¹³¹

More recently, amines have also been used as DGs to achieve site-selective C–F bond activation in difluorinated systems. As discussed in previous examples (section 3.1, Schemes 6 and 7), the selective functionalization of C–F bonds through direct C–F bond activation is of high significance. However, known methods for achieving this transformation are mainly limited to palladium and nickel catalysis. Whereas great effort has been devoted to the development and identification of highly effective phosphine and NHC ligands for Pd- and Ni-catalyzed C–F bond activation, there is a necessity to develop novel, alternative transition-metal-catalyzed approaches to enable the activation of these highly

stable bonds.^{132–134,64} Toward this end, Duan and coworkers reported a cobalt-catalyzed biaryl coupling reaction between aryl fluorides and aryl Grignard reagents in the presence of Ti(OEt)₄ (Scheme 33).¹³⁵ In the case of difluorinated systems, such as **118**, the authors identified the free amino group to be an effective ortho DG, exclusively furnishing the monoarylated product (**120**) in high yield (Scheme 33). Overall, these examples validate the versatility of using amino groups as a DG to facilitate site-selective cross-couplings under various transition-metal-catalyzed conditions.

5.1.2. Hydroxy Group.—Synthetic chemists have also explored the potential of other ubiquitous functional groups as DGs. Hydroxy groups have attracted particular attention. Much effort has been invested to effect the ortho functionalizations of polyhalogenated phenol and benzylic alcohol derivatives by tuning the coordinating ability of the hydroxy group. It is important to note that whereas hydroxy groups may serve as DGs (similar to amines in aniline derivatives), the electron-donating properties of hydroxy groups may result in the deactivation of the ortho position from both an electronic and a steric standpoint. To circumvent this inherent challenge, Manabe and coworkers developed a novel methodology to enable ortho-selective Kumada coupling in difluorinated phenol derivatives by using the nearby hydroxy group as a DG.¹³⁶ After screening several catalyst precursors, PdCl₂(PCy₃)₂ was identified as the most suitable precatalyst for this transformation. As an example, difluorinated phenol **121** and Grignard reagent **122** underwent ortho-selective Kumada coupling to provide the biaryl product (**123**) in good yield (Scheme 34). In addition to hydroxy groups, hydroxymethyl groups also worked well to give the ortho-substituted product, where difluorinated benzylic alcohol **124** and the corresponding Grignard reagent (**125**) gave the coupled adduct **126**. Importantly, Manabe and coworkers found that a protic DG was necessary to effect the desired Kumada coupling, as the use of a methyl ether led to unsatisfactory selectivities.¹³⁶

In most examples of DG-assisted site-selective cross-coupling, the identification of the most suitable catalyst precursors is of utmost importance. In this regard, Ackermann and coworkers observed that palladium complexes generated from air-stable heteroatom-substituted^{137,138} secondary phosphine oxide (HASPO) preligands^{139–141} could be used to achieve highly ortho-selective Kumada coupling involving dichloroarenes.¹⁴² Although originally developed for Kumada couplings with aryl and alkenyl tosylates,¹⁴³ the scope of this methodology was later extended to aryl chlorides^{144–146} as well. Specifically, they prepared a well-defined palladium complex (**128**) upon treating 4 equiv of an inexpensive HASPO preligand (**127**) with PdCl₂(PhCN)₂ (Scheme 35). The generated HASPO complex (**128**), which presumably interacts with the phenolic group by hydrogen bonding, was then used to accomplish the hydroxy-group-directed site-selective Kumada coupling of 2,4-dichlorophenol with a range of aryl Grignard reagents.¹⁴²

5.1.3. Carboxylic Acid.—Although carboxylic acids are ubiquitous functional groups, exploration into their potential as DGs only began in the late 2000s.^{147–149} In addition to their abundance, an added advantage of employing carboxylic acids as DGs is their versatility; they can be easily removed¹⁵⁰ or further diversified.^{151,152} However, carboxylates are known to coordinate weakly to catalysts and are therefore often disfavored

as DGs in the presence of other strongly coordinating DGs (e.g., pyridines, amides, etc.). In addition, under transition-metal catalysis, carboxylates can also undergo undesired side reactions (e.g., hydrodecarboxylation),¹⁵³ which are sometimes challenging to avoid. Despite these challenges, several groups have devised innovative strategies to leverage carboxylic acids as effective DGs in myriad cross-coupling processes.

Contemporaneous with Yu and coworkers' report on using sodium carboxylate as a DG in C–H activation methodology,¹⁴⁸ Houpis and coworkers devised a strategy to use lithium carboxylate as a DG in coupling reactions of brominated benzoic acid derivatives (Scheme 36).¹⁵⁴ During this study, initial attempts focused on coupling 2,5-dibromobenzoic acid (**131b**) to a dioxolane Grignard reagent. However, under almost all of the conditions that were investigated, they predominantly observed the formation of the undesired styrene derivative (**133**). Following extensive experimentation, the authors postulated that after an initial oxidative addition to furnish the magnesium salt of *trans*-Pd(II) species (**133a**), an undesired β -alkoxide elimination occurred to give enol ether complex **133b**. This was followed by an intramolecular migratory insertion to provide **133c**, which then underwent a second β -alkoxide elimination to form the styrene derivative (**133**). To outcompete this undesired pathway, they envisioned promoting the formation of the *cis*-Pd(II) intermediate after oxidative addition, which was then expected to undergo facile reductive elimination to furnish **132**. Toward this end, they anticipated beginning with a more nucleophilic carboxylate salt, which would favor the formation of a *cis*-Pd(II) intermediate through stronger coordination of the carboxylate group to the Pd center. This was ultimately realized by commencing with lithium salt **131a**, where the desired product (**132**) was isolated in 78% yield, and the undesired styrene derivative was limited to trace quantities.¹⁵⁴

Following this novel finding, the authors investigated the possibility of applying this concept to the widely used Suzuki–Miyaura coupling reaction.¹⁵⁵ They commenced their study with 2,4-dibromobenzoic acid (**134**) and *p*-tolylboronic acid (Scheme 37). After a thorough investigation, they concluded that the choice of the Pd precatalyst and the equivalents of an appropriate base were crucial for the carboxylate-assisted ortho-selective Suzuki–Miyaura coupling of **134**. Eventually, they found that using Pd₂(dba)₃ as the precatalyst in the presence of 2.2 equiv of LiOH furnished the desired product (**135**) with high selectivity, presumably via intermediate **135a**. Furthermore, carbonates were also identified as appropriate bases when the equivalents remained unchanged. In an attempt to reverse the selectivity, the authors chose to add an external phosphine ligand: bis[(2-diphenylphosphino)phenyl] ether (DPEPhos). They hypothesized that in the presence of this phosphine ligand, the coordination between the carboxylate and the Pd metal center would be disrupted, and consequently, the bulky Pd(0)L_n species would be oxidatively added into the less sterically hindered para C–Br bond to generate intermediate **136a**. Upon adding DPEPhos to the reaction mixture, the para-coupled product (**136**) was isolated in 68% yield.

Houpis and coworkers then attempted to extend the scope of the coordinating ability of the carboxylate group to other transformations such as Pd-catalyzed amination.¹⁵⁶ Their study included coupling reactions between 2,4-dibromobenzoic acid **134** and various electronically and sterically diverse amines (Scheme 38A). They observed that under the previously disclosed conditions to obtain para selectivity, they isolated the expected coupled product

(**137**) when benzylamine was treated with **134**. However, they were unable to reverse the selectivity under all of the conditions that they investigated, even when the phosphine ligand was excluded. They then examined other transition-metal complexes to achieve ortho selectivity. Taking inspiration from Ullmann and Goldberg's pioneering work¹⁵⁷ on Cu-catalyzed amination reactions with halobenzoic acids, Houpis and coworkers turned their attention toward investigating Cu-catalyzed conditions. They were also inspired by very similar work by Wolf and coworkers where an ortho-selective amination was achieved with both dichlorobenzoic acid **139** and dibromobenzoic acid **131b** when treated with phenethylamine in the presence of Cu/Cu₂O to furnish 2-aminobenzoic acid derivatives, **140** and **141**, respectively (Scheme 38B).¹⁵⁸ Eventually, Houpis and coworkers were also able to couple benzylamine to the ortho position of **134** in the presence of Cu₂O to give the desired 2-aminobenzoic derivative **138** in 91% yield (Scheme 38A).

The versatility of using a carboxylate as a DG was also extended to difluorobenzoic acid derivatives. In addition to exploring an amine as a DG in difluorinated systems (Scheme 33), Duan and coworkers also investigated the possibility of using a carboxylate as a DG in difluorobenzoic acids under Co-catalyzed conditions.¹³⁵ Gratifyingly, they observed that coupling between **142** and Grignard reagent **143** in the presence of CoCl₂ furnished the ortho-coupled product (**144**) in 81% yield (Scheme 39).

5.1.4. Ketone and Imine.—The ketone carbonyl group was one of the first DGs to be used in site-selective coupling chemistry.¹⁵⁹ New contributions continue to be made to expanding the scope of the coordination ability of the carbonyl group. In 2014, Wang and coworkers reported a coupling between aryl fluorides and organozinc reagents under Ni-catalyzed conditions.¹⁶⁰ When polyfluoroarenes were used as substrates, they introduced a suitable DG to avoid multiple substitutions as a result of ring-walking.¹⁶¹ As shown in Scheme 40, they showed that the installation of a benzoyl group [PhC(O)] enabled the selective functionalization of difluoroarene **145** in the cross-coupling with various organozinc reagents to favor the formation of the ortho-substituted product (**146**). In addition to this study, Kakiuchi and coworkers also showed that ketones can be employed as DGs to achieve the ortho-selective arylation of polyfluoroarenes with several arylboron reagents under Ru-catalyzed conditions (not shown).¹⁶²

Similar to ketones, imines have also been widely employed as DGs in recent years. One of the main approaches has been to leverage the “transient” directing ability of imines, that is, to install an imine for a directed site-selective functionalization with subsequent cleavage of the imine group, which ideally would all occur in a single pot. Along these lines, Love and coworkers devised several novel methodologies to achieve the ortho functionalization of polyfluoroarenes. Taking inspiration from work by Crespo and Martinez,¹⁶³ who achieved stoichiometric C–F activation in a series of polyfluoroaryl imines in the presence of [Me₂Pt(μ-SMe₂)]₂,¹⁶⁴ the Love group investigated the possibility of performing this transformation in a catalytic process. Toward this end, they found that by using [Me₂Pt(μ-SMe₂)]₂ as the catalyst with substoichiometric loading of Me₂Zn as the methylating agent, the ortho-methylation of a variety of polyfluoroaryl imines (**147**) could be achieved to furnish **148** (Scheme 41).^{165–168} Additionally, they extended the scope of this methodology

to achieve monomethoxylation in polyfluoroaryl imines by using tetramethoxysilane as the transmetalating reagent.¹⁶⁹

After their initial work exploiting the coordinating ability of imines to achieve the site-selective functionalization of the ortho C–F bond in various polyfluoroaryl imines, Love and coworkers extended this methodology to include other coupling processes as well. For example, they demonstrated a Ni-catalyzed cross-coupling reaction between several polyfluoroaryl imines (**150**) and 4-methoxyphenylboronic acid to access a wide variety of biaryl aldehydes (**151**) upon hydrolysis (Scheme 42).¹⁷⁰ This study showcases the “transient” nature of imines as DGs to achieve site-selective functionalization with the subsequent, *in situ* hydrolysis of the imine to unveil the corresponding aldehyde. Following these reports by the Love group, Li and coworkers extended the scope of employing imines as DGs to include the ortho-selective alkylative cross-coupling of polyfluoroarenes with various organozinc reagents under Ni-catalyzed conditions.¹⁷¹

5.1.5. Ester and Amide.—Esters are versatile functional groups because they can be either introduced or interconverted easily through a variety of methods; therefore, the development of strategies for ester-directed site-selective functionalization has become highly desirable. Although the directing potential of ester groups was first explored in the mid-1990s,^{172,173} very little progress has been made in this area. This is mainly attributed to the weak coordination of the carbonyl group of esters to metal catalysts. One of the first successful methodologies to enable the site-selective functionalization of polyhalogenated heterocycles directed by an ester group was reported by Yang and coworkers in 2003.¹⁷⁴ In their study, they observed that Suzuki–Miyaura coupling with the methyl ester of 2,6-dichloronicotinic acid (**152**) predominantly gave the six-substituted product (**154**) presumably due to the steric influence of the C3 ester (entry 1, Scheme 43A). To reverse the selectivity, they sought to coordinate the Pd(0) metal center to the ester group to promote oxidative addition into the C2 C–Cl bond. To enable this coordination, they envisioned reducing the ligand to palladium ratio to provide an open coordination site on the palladium. To test their hypothesis, they conducted the Suzuki–Miyaura coupling with a Pd/P^tBu₃ (1:1) catalyst system,¹⁷⁵ which had previously been employed by Hartwig and coworkers in their amination studies,^{176,177} where they proposed the generation of a monophosphine Pd(0) complex as the catalytically active species. As predicted, Yang and coworkers achieved the desired complementary selectivity, with the C2-coupled product (**153**) forming as the major product in a ratio of 1.7:1 (entry 2).

This promising initial result was followed by a thorough catalyst screening, where the best result was observed with an air-stable PXPd₂ system (a 1:1 Pd/chlorophosphine complex),^{178–181} which furnished **153/154** in a ratio of 2.5:1 (entry 3, Scheme 43A). With this newly identified catalyst, they anticipated being able to further improve the selectivity by employing a more strongly coordinating amide generated from 2,6-dichloronicotinic acid (**152d**). Indeed, Suzuki–Miyaura coupling with the nicotinamide substrate in the presence of PXPd₂ resulted in a 9:1 mixture of **153/154** (entry 4), thereby significantly enhancing selectivity. This chemistry was applied to the synthesis of novel negative allosteric modulator analogues,¹⁸² which included a C2-selective arylation of nicotinamide **152d** to access myriad biaryl compounds, such as **155** (Scheme 43B).^{183,184} The directing

ability of the amide group was also explored by Love and coworkers in their selective Ni-catalyzed trifluoromethylthiolation chemistry.¹⁸⁵ Over the course of their studies, they developed a novel protocol to access monotrifluoromethylthiolated adducts (**157**) starting from dichloronicotinamide **156** using AgSCF₃ as a nucleophilic trifluoromethylthiolating reagent in the absence of ligands and additives (Scheme 44).

5.1.6. N-Heterocycle.—*N*-Heterocycles are a very common class of DGs for the selective functionalization of polyhaloarenes. Several factors have contributed to their popularity as DGs, including: (1) *N*-heterocycles are found in various pharmaceutically relevant compounds, which helps facilitate late-stage modifications and prevents the need for additional DG installation/removal steps; (2) there are many strategies for introducing *N*-heterocycles; and (3) there is flexibility in introducing different substituents or heteroatoms to alter the coordinating ability for a specific transformation.¹⁸⁶ Consequently, several heterocycles have been exploited as DGs to facilitate the selective cleavage of a specific C–X bond in polyhaloarenes (Scheme 45).

Inspired by pioneering work in applying an oxazoline motif as a DG in C–H activation chemistry,^{187–189} Shen and Lu investigated the possibility of extending this strategy toward selective C–F bond activation in polyfluorinated arenes. They developed a Suzuki–Miyaura coupling between polyfluoroaryl oxazolines (**158**) and arylboronic acids to furnish ortho-arylated products (**159**) in the presence of Pd(CH₃CN)₂Cl₂ as the precatalyst and Cs₂CO₃ as the base (Scheme 46A).¹⁹⁰ It was concluded that 1,1'-ferrocenediyl-bis(diphenylphosphine) (DPPF) was the most effective ligand for this process because reactions using DPPF were much faster than reactions employing other phosphine ligands.

Following this report, the authors envisioned performing a C–F bond activation of a polyfluoroarene with a tandem C–H bond activation event^{191–197} occurring with a second coupling partner to achieve a more efficient synthesis of partially fluorinated arenes.^{198,199} This strategy came with its own synthetic challenge of suppressing the undesired, but kinetically favorable, activation of a C–H bond in the polyfluoroarene substrate. After a careful investigation, they ultimately accomplished this tandem C–F/C–H bond activation process between polyfluoroarenes **160** and benzothiazole by employing a pyridyl group as a DG to effect selective C–F bond cleavage. The authors found that when oxazoline was installed as the DG, the desired product could be obtained only in poor yields with the predominant formation of undesired side products. The highest yield was observed using lithium *tert*-butoxide as the base and a catalyst generated *in situ* from Pd(MeCN)₂Cl₂ and 1,2-bis(diphenylphosphino)benzene (DPPBz). Impressively, the scope of this methodology was extended to other heterocycles such as thiazole, benzothiazole, benzoimidazole, oxazole, and oxadiazole to access a wide variety of partially fluorinated arenes (**161**) (Scheme 46B).²⁰⁰

Having developed Pd-catalyzed conditions to leverage the directing ability of *N*-heterocycles, Shen and Lu began investigating other transition-metal-catalyzed conditions to effect other selective transformations. They developed the first Ni-catalyzed α -arylation using Reformatsky reagents (**163**) and polyfluorinated arenes (**162**) via an *N*-heterocycle-directed C–F bond activation process (Scheme 47).²⁰¹ Following optimization studies, they

identified DIOP to be the most suitable ligand for this process. Furthermore, they also showed that in addition to pyridine, quinoxaline and oxazoline groups were effective DGs to access a wide variety of α -arylated amides (**164**).

In a related study, Cao and coworkers demonstrated that organozinc reagents, such as Me_2Zn , Et_2Zn , and PhCH_2ZnBr , can also be selectively coupled to polyfluoroarenes using *N*-heterocycle DGs.²⁰² Additionally, in the methodology developed by Love and coworkers detailing amide-assisted ortho-selective trifluoromethylthiolation under Ni-catalyzed conditions (**156** \rightarrow **157**, Scheme 44), the authors demonstrated the same transformation by employing a pyridine DG to provide biaryl trifluoromethyl sulfide **166** (Scheme 48).¹⁸⁵

So far, we have mainly discussed strategies focused on the construction of C–C bonds through the transition-metal-catalyzed, site-selective C–F bond activation of polyfluoroarenes. Other types of couplings to install noncarbon substituents by the C–F bond activation of polyfluoroarenes enable the diversification of fluorinated molecules. Toward this end, Zhang and coworkers disclosed a novel strategy for achieving the *N*-heterocycle-directed ortho-borylation of polyfluoroarenes (**167**) to furnish boronate esters such as **168** (Scheme 49).²⁰³ Rh(I) catalysts were investigated, and after a comprehensive screen, $[\text{Rh}(\text{cod})_2]\text{BF}_4$ was identified as the most suitable catalyst for this process. Several *N*-heterocycles including pyridine, quinoline, and benzoxazole emerged as viable DGs in this methodology.

5.1.7. Other Miscellaneous Directing Groups.

5.1.7.1. Nitro.: In the early 2000s, strategies for the Pd-catalyzed C–F bond activation and functionalization of monofluorinated nitrobenzene derivatives were reported by the groups of Yu²⁰⁴ and Widdowson.²⁰⁵ In their studies, the authors proposed that in addition to its selectivity-enhancing electron-withdrawing properties, a nitro group also has the potential to direct a Pd catalyst to an adjacent C–F bond for its site-selective cleavage. Taking inspiration from these initial reports, Sandford and coworkers envisioned that a polyfluorinated nitroarene could also undergo a nitro-directed ortho functionalization via a Pd-catalyzed C–F bond activation event. When a Suzuki–Miyaura coupling reaction between perfluorinated nitroarene **169** and phenylboronate ester **170** was conducted in the presence of $\text{Pd}(\text{PPh}_3)_4$, the desired ortho-coupled product (**171**) was isolated in 80% yield (Scheme 50).²⁰⁶ Of note, the absence of the electronically favored para-coupled product (see Scheme 5) further supports transition state **172**, which depicts the directing ability of the nitro group. Additionally, the scope of the reaction was then expanded to include a variety of polyfluoro nitroarenes and arylboronic acids with equally satisfying results.

5.1.7.2. Aminide.: Pyridinium *N*-(3',5'-dibromopyrid-2'-yl)aminides (e.g., **173a**)^{207–210} have been employed as building blocks in the synthesis of various azine derivatives.^{211–214} When they possess two C–Br bonds, these compounds are primed to undergo late-stage modifications via cross-coupling reactions. Accordingly, Alvarez-Builla and coworkers observed that upon subjecting these compounds to Suzuki–Miyaura coupling conditions with one equivalent of a boronic acid, substitution occurred exclusively at C3 to afford the

monocoupled product (**174**) as the major product (Scheme 51). The authors attributed the observed site selectivity to the coordination ability of the aminide nitrogen to direct the Pd catalyst to the C3 position. On the basis of this result, a series of 3-(hetero)arylated derivatives were synthesized beginning from both **173a** and the analogous pyrazine derivative, **173b**.^{215,216}

5.1.7.3. Olefin.: The DGs that have been discussed thus far have mainly served to direct oxidative addition to a proximal C–X bond. Beaudry and coworkers reported the first example of using a coordinative functional group, such as an olefin, to achieve a site-selective coupling at a distal C–X bond. In their study, they observed that a Suzuki–Miyaura coupling between dibromostyrene **175** and boronate ester **176** predominantly furnished the monocoupled product (**177**) arylated at C4 (Scheme 52A).²¹⁷ From their subsequent mechanistic studies, they ruled out the possibility of the observed selectivity arising from either the sterics or the inherent electronics of **175**. They attributed the selectivity outcome to the relative rates of oxidative addition of the two bromides (Scheme 52B). Specifically, they proposed a reversible coordination of the Pd(0) species with the C–Br bond flanked by the alkene to generate the coordinately saturated complex **178**. This coordination decreases the rate of oxidative addition at the C1 position, which leads to the observed site selectivity. The effects of olefins²¹⁸ have been well studied, and it is reported that the rate of oxidative addition of Pd(0) into iodobenzene is significantly decreased in the presence of olefin additives;^{219–221} overall, this rationale is in agreement with the reactivity observed with olefin **175**.

Beaudry and coworkers then leveraged this observed selectivity in developing an elegant synthesis of target compound **184**, which was identified as a proteomimetic compound by Hamilton and coworkers.²²² A one-pot, three-component Suzuki–Miyaura reaction was developed to achieve the synthesis of terphenyl **183** in 54% overall yield as a single isomer, starting from **175** and boronate esters **181** and **182**. A subsequent hydrogenation furnished the target compound (**184**) in high yield (Scheme 52C). Overall, the authors accomplished an efficient synthesis of **184** compared with a previously established synthetic route involving seven steps.²¹⁷ Prior to this work, an analogous one-pot, three component Suzuki–Miyaura reaction was employed in the synthesis of the bisbibenzyl natural product (+)-cavicularin (**189**). Beaudry and coworkers found that dibromomethoxystyrene **185** and boronate esters **186** and **187** could react sequentially in a one-pot Suzuki–Miyaura coupling reaction to furnish triaryl compound **188** in 63% overall yield (Scheme 52D). The development of this reaction proved to be pivotal in achieving an efficient synthesis of **189**.^{223,224} In summary, these examples emphasize the significance of leveraging the coordinating ability of functional groups that are inherent in a target to achieve site-selective cross-couplings in various polyhalogenated (hetero)arenes. Furthermore, these tactics ultimately enabled the efficient syntheses of several target compounds.

5.2. Ligand-Binding Directing Groups

The examples that we have discussed thus far have employed DGs on substrates that coordinate directly to and guide the metal center to a proximal carbon position. However, some functional groups, depending on the reaction conditions, may retard the reaction

rate by altering the electronics of the substrate. Furthermore, for reactions where the functionalization of a distal C–X bond is desired, a transition-metal-binding DG may not be suitable if the metal center is too distant from the desired site of reactivity. To circumvent this challenge and achieve distal functionalization, certain ligands that are of adequate length and capable of binding to a DG on a substrate can serve as a linker between the substrate and the transition-metal complex, enabling the transition metal to get in reasonable proximity to the remote C–X bond for activation (Scheme 30B). In the following section, we discuss examples where this “ligand-binding directing group strategy” is employed to either enhance the rate of oxidative addition or achieve the selective cleavage of a distal C–X bond. It is important to note that whereas the following examples do illustrate a form of ligand control, we have chosen to include them in this Directing Group Control section, as opposed to the Ligand Control section (section 6), because their primary role is to interact with a directing functional group on the substrate. Ligands that do not interact with a DG but instead coordinate exclusively to a transition-metal complex will be discussed in section 6.

Kumada coupling reactions with hydroxylated aryl substrates generally suffer from reduced reaction rates because the Grignard reagent deprotonates the hydroxy group to generate a highly electron-donating oxido group, which electronically retards oxidative addition. A general strategy to overcome this challenge would involve binding the generated oxido group to a ligand (that is, in turn, bound to a transition metal), which would place the transition-metal center proximal to the C–X bond, thus accelerating the reaction. In this regard, Manabe and coworkers synthesized a series of hydroxylated oligoarene-type phosphine (HOP)^{225–228} ligands for transition-metal catalysis, which are based on the Buchwald-type biphenylphosphine ligands.^{229–232} Specifically, they synthesized mono-*hydroxy*terphenylphosphine (HTP) and di-*hydroxy*terphenylphosphine (DHTP) ligands (Scheme 53A), which were expected to perform as bifunctional ligands.^{233,234} Mechanistically, the authors anticipated that a linkage (via an electrostatic interaction) between the hydroxy group of the HOP ligand and the metal-oxido group of the substrate would increase the reaction rate by bringing the phosphino-coordinated transition-metal center closer to the desired C–X bond for site-selective oxidative addition (Scheme 53B).^{235,236}

To test this hypothesis, Manabe and coworkers conducted a Kumada coupling between 2,4-dibromophenol (**192**) and Grignard reagent **125** in the presence of Pd₂dba₃ and various ligands. Interestingly, employing Ph-HTP as the ligand promoted coupling ortho to the hydroxy group to furnish **193** with excellent selectivity. On the contrary, using DPPF as the ligand completely reversed the selectivity to provide the para-coupled product **194**, presumably due to steric effects (Scheme 54).²³⁷ Notably, the reaction was drastically accelerated with Ph-HTP and proceeded to completion in only 2 h; in contrast, the reaction with DPPF took 24 h to reach completion. Following mechanistic studies, the authors determined that HOP ligands favor ortho coupling, with poor selectivity occurring at both the meta and para positions.^{235,236} Altogether, these studies supported the mechanistic hypothesis of forming a bimetallic, bridged intermediate capable of facilitating site-selective ortho coupling.

In addition to the Ph-HTP ligand, the use of the HBF_4 salt of Cy-HTP was also found to be effective for Kumada coupling reactions; however, both of these ligands were limited in their substrate scope. Subsequently, Manabe and coworkers found that the DHTP ligands were more effective than the HTP ligands and significantly broadened the substrate scope with enhanced selectivity. The higher reactivity of the DHTP ligands is attributed to the higher probability of the palladium and magnesium phenoxide to be on the same face of the *para*-terphenyl system due to the presence of two hydroxy groups.²³⁸ Eventually, the scope of the Kumada coupling reaction in the presence of HTP/DHTP ligands was also extended to include dibromoaniline and dibromoindole derivatives (e.g., **195**) to give highly selective ortho-coupled products, such as **196** (Scheme 55).²³⁹

Manabe and coworkers then investigated the possibility of achieving HTP/DHTP-mediated ortho-selective Sonogashira coupling with dihalophenol and aniline derivatives. Toward this end, they devised a Sonogashira/cyclization sequence with dichlorophenols and terminal alkynes. Additionally, they also aimed to conduct a sequential Suzuki–Miyaura coupling at the unreacted C–X bond. Eventually, they achieved a one-pot synthesis for the preparation of myriad disubstituted benzo-*[b]*furans (**198**) from a series of dichlorophenols (**197**), terminal alkynes, and boronic acids (Scheme 56A).^{240–242} They identified the HBF_4 salt of Cy-DHTP as the most suitable ligand and $t\text{BuOLi}$ as the ideal base to effect ortho-selective Sonogashira coupling to arrive at alkynyl phenoxide **198b**, presumably through the formation of the heteroaggregate, **198a**. Mechanistically, a subsequent intramolecular cyclization and a sequential Suzuki–Miyaura coupling reaction afforded **198**. This development encouraged them to explore the Sonogashira/cyclization sequence with dihaloanilines as well. Analogous to the sequence with dichlorophenols, *N*-tosyldichloroanilines **199** were also transformed to disubstituted indoles (**200**) using various terminal alkynes and boronic acids (Scheme 56B).^{240,243}

In addition to tosylated aniline derivatives, acetylated aniline derivatives were also suitable substrates for this transformation. Specifically, *N*-acetyl-2,4,6-trichloroaniline **201** reacted with various terminal alkynes to furnish a series of 2-substituted 5,7-dichloroindoles (**202**). Mechanistically, similar to the previous examples, the Sonogashira coupling proceeds via the heteroaggregate intermediate **202a**, which installs the alkyne moiety ortho to the acetamido group. However, in contrast with the previously observed indole synthesis, **202b** cyclizes followed by a deacetylation of the resulting *N*-acetylated indole to furnish 1*H*-indole **202** (Scheme 57A). Importantly, this compound could be directly utilized in a subsequent C7-selective Kumada coupling with several aryl Grignard reagents under DHTP ligand conditions to furnish disubstituted indoles, such as **203** (Scheme 57B). This strategy allows for the stepwise substitution of each of the chloro groups to install different substituents in a well-controlled manner, thus proving to be effective for preparing a series of multisubstituted indoles.^{244,245}

Whereas the aforementioned reports by Manabe and coworkers exemplify the utility of bifunctional ligands (HTP and DHTP) in palladium catalysis to accelerate the rate of oxidative addition at a nearby ortho C–X bond, there currently exists a dearth in methodologies that address site-selective coupling at more distal positions with minimal steric or electronic bias. To address this challenge, Phipps and coworkers focused on

leveraging bifunctional phosphine ligands to direct oxidative addition at a distal position. They postulated a pseudointramolecular transition state stabilized by some noncovalent interactions between the substrate and the ligand,^{246–249} which would bring the phosphino-coordinated metal center in close proximity to a specific C–X bond. Toward this end, they considered sulfonylated phosphine ligands to serve this bifunctional purpose, where the sulfonate group was anticipated to engage the substrate via an electrostatic interaction. Accordingly, they chose to employ sSPhos and sXPhos, the sodium salts of sulfonylated SPhos and XPhos, which have been previously utilized by Anderson and Buchwald for the cross-coupling of aryl chlorides in water (Scheme 58A).^{250–255}

They probed the coordination ability of these ligands in the Suzuki–Miyaura coupling between *N*-acetyl-3,4-dichlorobenzylamine **204a** and boronic acid **205** (Scheme 58B).²⁵⁶ They hypothesized that the interaction between the ligand and the amine group of the substrate would result in site selectivity. Consistent with this notion, they observed no selectivity with either SPhos or XPhos (entries 1 and 2). In contrast, the addition of either sSPhos or sXPhos favored meta coupling to predominantly give **206** over **207** (entries 3 and 4). Subsequently, the *N*-group was varied to study the selectivity outcome. Interestingly, as the *N*-protecting groups became more electron-withdrawing, the selectivity was significantly enhanced. Whereas trifluoroacetyl gave poor selectivity (entry 5), tosyl increased the ratio to 7.5:1 (entry 6). Eventually, triflyl was identified to provide both excellent selectivity and conversion (entry 7). Overall, the authors rationalized the observed results by invoking an electrostatic interaction of the potassium salt of **204d** with the sulfonate group of the ligand to generate intermediate **208**. In this intermediate, the phosphine-bound Pd is proximal to the *meta*-C–Cl bond, thus enabling subsequent oxidative addition in a selective manner.

Next, the scope of the Suzuki–Miyaura coupling of **204d** was expanded to include various aromatic boronic acids, which led to the formation of biaryl products (**206d**) with excellent selectivity (Scheme 59A).²⁵⁶ Additionally, Sonogashira coupling to form Csp²–Csp bonds was investigated with several alkyne derivatives, and the corresponding aryl alkyne products (**209**) were isolated with superior selectivity. Furthermore, Buchwald–Hartwig amination was also explored with **204d** to access a variety of meta-substituted aryl amine products, such as **210** (Scheme 59B). Gratifyingly, aryl amines proved to be suitable substrates for this transformation, and after the optimization, *s*(*t*BuSPhos), the P(*t*Bu)₂ variant of sSPhos, was found to give the best selectivity. Applying these optimized conditions enabled a range of aryl amines to be successfully coupled.

Following this work, the authors then investigated the possibility of coupling **204d** to a suitable coupling partner via a C–H bond activation process (Scheme 60).²⁵⁷ This approach would be highly beneficial because it avoids the necessity of prefunctionalizing the second coupling partner; furthermore, this strategy would demonstrate the viability of concerted metalation–deprotonation (CMD) in this putative electrostatically bound transition state (**208**, Scheme 58B). Toward this end, fluoroarenes and fluoroheteroarenes (**211**) were chosen as the second coupling partner.^{258,259} Surprisingly, no product was observed under the previously disclosed conditions (Scheme 58B). However, on the basis of previous literature data, adding pivalic acid²⁶⁰ and switching the solvent to *i*PrOAc^{261,262} proved to be crucial for executing the desired C–H activation/C–C bond forming event. The yield

was substantially improved by using the more soluble tetrabutylammonium salt of sSPhos, sSPhos(NBu₄), instead of the typical sodium salt. In addition, following an evaluation of Pd precatalysts, [(cinnamyl)PdCl]₂ was identified to give the product in an enhanced yield. Next, several fluoroarenes were coupled to **204d** to produce myriad biaryl products (**212**) under this established set of optimized conditions (Scheme 60).

Phipps and coworkers next explored the dichloroarene component by varying the amino functional handle (Scheme 61). They established that extended triflamide derivatives were tolerated, albeit with reduced selectivity. Additionally, α -substitution with both methyl and phenyl groups did not interfere with the catalytic process. Interestingly, sulfamate, sulfonate, and phosphonate derivatives were all found to be suitable substrates for this site-selective cross-coupling process. Furthermore, carboxylic acid derivatives with an extended chain length resulted in excellent site selectivity, and the presence of an alkene in the chain also did not disrupt the observed selectivity.

Adding to their repertoire of site-selective cross-couplings, Phipps and coworkers next established a comprehensive “toolkit” where various ligand/base combinations were identified for site-selective Suzuki–Miyaura and Buchwald–Hartwig couplings via the electrostatic model proposed for intermediate **208**.²⁶³ (See Scheme 58.) Through a systematic screening process, the authors identified various ligand/base combinations for transforming dichlorinated arenes with diverse substitution patterns (**216–218**) into their corresponding monocoupled products (**219–221**) under both Suzuki–Miyaura and Buchwald–Hartwig conditions (Scheme 62A). In the same publication, the authors reported ligand/base combinations suitable for facilitating site-selective Suzuki–Miyaura and Buchwald–Hartwig couplings of various trichlorinated arenes (**222–224**) to monocoupled products (**225–227**) as well (Scheme 62B). Using the ligand/base combinations shown in Scheme 62, the authors successfully executed sequential Suzuki–Miyaura cross-couplings on both trichlorinated and tetrachlorinated arenes to obtain polyarylated products in a site-selective manner (not shown). In summary, Phipps and coworkers demonstrated that electrostatically directed palladium catalysis employing bifunctional sulfonylated biarylphosphine ligands is compatible with various cross-coupling and CMD-type C–H activation processes on several functionalized dichloroarene derivatives.

Overall, the contributions of Manabe and Phipps clearly mark the advent of employing bifunctional phosphine ligands to promote site-selective cross-coupling in polyhalogenated (hetero)arenes. This series of thought-provoking examples demonstrates how a ligand can be finely tuned to interact with halogenated precursors to facilitate site-selective oxidative addition. In this stage, one can anticipate the development of several new reactions that employ bifunctional ligands along with transition-metal catalysts to effect cross-couplings at positions that are otherwise challenging to activate under the previously disclosed strategies.

6. LIGAND CONTROL

The majority of examples for the site-selective cross-coupling of polyhalogenated arenes discussed so far have been based on a “substrate-controlled” strategy, which focuses on leveraging key differences in reactivity between various C–X bonds and DG abilities of

functional groups present on the substrate. Thus far, the preference for a reaction to occur at one C–X bond over another has been ascribed to three main factors: (1) the electronics of the carbon position, (2) the steric environment, and (3) the influence of nearby DGs. Examples relevant to these categories have been discussed in detail in sections 3–5. This section focuses on examples related to a “ligand-controlled” strategy (i.e., a non-substrate-controlled strategy), wherein ligands that bind exclusively to the transition metal (and not the substrate) can be used to alter/tune the electronic and steric properties of the transition-metal complex, thus controlling the selectivity outcome. In other words, depending on the choice of ligands, different products can be obtained selectively from the same polyhaloarene precursor. Employing this strategy would enable one to obtain a product selectively, regardless of the steric and electronic nature of the starting material. This provides an advantage over the previously described strategies in instances where the desired selectivity and electronically preferred outcomes are mismatched. Substrate control requires the preinstallation of either a sterically bulky substituent or a coordinating functional group to bias oxidative addition toward a specific C–X bond. However, this can decrease the atom and step economy if the added substituent must be removed later in the synthesis. Hence, strategies that enable site-selective reactivity without modification of the substrate are highly desirable. Recent reports of novel ligand platforms to guide site-selective couplings represent a significant advancement in this field.

In 2005, Chung and coworkers reported a Suzuki–Miyaura coupling between 5,7-dichloro-1-(2,6-dichlorophenyl)-1,6-naphthyridin-2-(1*H*)-one (**228**) and electron-deficient arylboronic acid **229** (Scheme 63).^{264–266} During their initial investigation, the authors observed selectivity between monocoupled products, with **230** being favored over **231**. However, in the case of both monocoupled products, the electron-deficient difluorophenyl group activated the second C–Cl bond toward a second coupling, which formed the bis-coupled product (**232**) in almost equal ratio to **230** (entry 1). Eventually, Chung and coworkers rationalized that the site selectivity observed with **228** was completely substrate-dependent, and they anticipated minimizing the second coupling by altering the ligand employed in the reaction. Consequently, they screened ~80 commercially available ligands with various bases and solvents,²⁶⁶ with selected results shown in Scheme 62 (see table). Furthermore, some improvements were also observed by either lowering the temperature or using a monodentate ligand, such as PPh₃ (entries 2 and 3). Interestingly, using SPhos, a highly activating ligand, enabled the reaction to occur at a lower temperature and gave a slightly improved selectivity for the monocoupled product **230** (entry 4). Further improvement in selectivity was observed using IMes•Cl, the NHC derived from 1,3-bis(2,4,6-trimethylphenyl)imidazolium chloride. A combination of this carbene along with Pd(OAc)₂ or Pd₂(dba)₃•CHCl₃ was identified as a suitable catalytic system for this transformation (entries 5 and 6). Additionally, for a large-scale manufacturing process, the precatalyst/ligand system of Pd₂(dba)₃•CHCl₃/P(2-MeOC₆H₄)₃ was revealed to be more robust and cost-effective, providing >99% conversion and **230** in 92% yield (entry 7).

These studies were followed by a report by Strotman, Chobanian, and coworkers, where various ligands (Scheme 64A) were identified to facilitate complementary selectivity outcomes in the cross-coupling of several dihaloazoles.²⁶⁷ Because oxazole, imidazole,

and thiazole frameworks are present in several bioactive and pharmaceutically relevant molecules,^{268,269} devising efficient strategies to access their derivatives is highly valuable. Toward this end, the authors investigated site-selective Suzuki–Miyaura couplings of dihaloimidazoles, dihalooxazoles, and dihalothiazoles as a strategy to rapidly diversify diarylazoles in a modular fashion (Scheme 64B). Taking inspiration from the work of Greaney and coworkers,²⁷⁰ the authors commenced their study with the Suzuki–Miyaura coupling of 2,4-diiodooxazole (**85**) and phenylboronic acid. The more reactive C2 position^{271,272} (as predicted by Handy's method²⁷³) was expected to be the preferred site of coupling; however, contrary to this expectation, the majority of ligands screened favored coupling at the C4 position. The highest yielding result was obtained by employing Xantphos (**X2**) as the ligand, which furnished the C4-phenylated product **233** in 64% yield. To explore C2-selective coupling, the authors next screened ~200 achiral phosphine ligands and identified 1,3,5-triaza-7-phosphaadamantane (**X4**) as a ligand that produced the desired C2-phenylated product (**234**) in 55% yield.

With these complementary conditions established, the authors next investigated a Suzuki–Miyaura coupling of other commercially available dihaloazoles. As with **85**, high C2 selectivity was observed with 2,5-dibromo-1-methylimidazole (**84**) when **X4** was employed as the ligand; these conditions provided **236** in 64% yield. Concurrently, C5 selectivity was also obtained with a wide variety of ligands, with bis(*p*-sulfonatophenyl)phenylphosphine dihydrate dipotassium salt (**X6**) furnishing **235** in 45% yield. While exploring C2 versus C4 site selectivity with 2,4-dibromo-1-methylimidazole (**76**), the previously described ligand choices were investigated. Surprisingly, the major site of reaction for all the explored ligands, including **X4** and **X2**, was at the C2 position. The best selectivity and highest yield of **238** (produced almost exclusively) were obtained using tri(4-fluorophenyl)phosphine ligand **X5**. Furthermore, no ligands in their collection provided any appreciable reaction at C4, which was the more reactive position observed for 2,4-diiodooxazole (**85**). A similar outcome was also observed with dibromothiazoles (**71** and **72**). Out of all of the investigated ligands, **X2** proved to be highly selective for C2 coupling in both 2,4- and 2,5-dibromothiazoles; notably, no ligand was identified that achieved selective coupling at either C4 or C5. These results stand in stark contrast with what was observed with both **84** and **85**, where coupling could take place at the C4 and C5 positions in a selective manner. The scope of the Suzuki–Miyaura coupling with these heterocycles was extended to include a wide variety of electron-rich, electron-poor, and sterically hindered arylboronic acids. Selectivity with heteroaryl and cyclopropylboronic acids followed similar trends to that observed with phenylboronic acid. The dependence of the relative rates of C2 versus C4 (or C5) coupling on the identity of the ligand is not fully understood but is believed to be a cumulative effect of both the steric and the electronic nature of the ligand.

The potential of ligand-controlled site-selective couplings has also been investigated by Dai and coworkers,²⁷⁴ who were interested in constructing a wide array of pyridazine derivatives from 3,5-dichloropyridazine (**56**) as part of a drug discovery program. The authors envisioned catalytic systems that could selectively favor coupling at either the C3 or the C5 positions of **56**, thus enabling a modular approach to accessing diverse diarylpyridazines. On the basis of the findings by Houk and Merlic,^{38,73} 3,5-dichloropyridazine is expected

to react more readily at C3 than C5 due to the lower BDE of the C–Cl bond α to the nitrogen atom. Dai and coworkers focused on a Suzuki–Miyaura coupling between **56** and phenylboronic acid under different ligand conditions (Scheme 65). They observed that electron-deficient bidentate ligands and PPh₃ favored the formation of the C3-coupled product (**241**), and DPPF was found to give the best yield and selectivity (entries 1–3). Notably, DTBPF, an electron-rich bidentate ligand, gave the opposite selectivity, albeit in a moderate ratio between mono- and bis-coupled products (entry 4). Alternatively, C5 selectivity was also achieved with electron-rich monodentate ligands (entries 5–7). Q-Phos gave the best selectivity and afforded the C5-coupled product (**242**) in 80% yield. Furthermore, Buchwald’s biaryl-based monophosphine ligands (e.g., RuPhos, DavePhos, and XPhos) predominantly favored the formation of the bis-coupled product (**243**), even when only 1 equiv of phenylboronic acid was used (entries 8–10).

Although the exact nature of how substrate–ligand interactions facilitate complementary selectivity remains unclear, one could envision selectivity arising from an effect of the steric and electronic influences of both the ligand and the substrate. For instance, electron-deficient ligands favor slower oxidative addition; therefore, the insertion of the metal center at the more reactive C3 position of **56** (Scheme 65) occurs, as predicted by the corresponding C–Cl BDE values reported by Houk and Merlic.^{38,73} On the contrary, electron-rich ligands bias the metal center to insert into the more sterically accessible C5 position of **56**. These principles guided Dai and coworkers in their investigation of a complementary C2 versus C4 coupling strategy for 2,4-dichloropyridine (**244**, Scheme 66). C2 coupling was achieved with DPPF, which furnished the desired product (**245**) in 90% yield. On the basis of the report by Houk and Merlic, coupling at C2 over C4 is favored by nearly 1000-fold;^{38,73} however, Dai and coworkers were able to overcome this preference by implementing their previously discovered conditions employing Q-Phos (see entry 7, Scheme 65) to give the C4-coupled product (**246**) in 36% yield. Despite the modest 36% yield of **246**, this is the first example of **244** undergoing a C4 coupling in the absence of a DG.

Recently, Yang and coworkers also investigated this challenging C4 coupling of 2,4-dichloropyridine (**244**).^{275–280} The authors began their exploration by using **244** and 4,4,5,5-tetramethyl-2-phenyl-1,3,2-dioxaborolane (PhBpin) (Scheme 67). They observed that using Pd(PPh₃)₄ as the catalyst afforded the C2-coupled product (**245**) in high yield (entry 1). Next, they conducted an extensive screening with Buchwald Pd-G3 precatalysts. Over the past decade, the Buchwald group has developed a series of Pd precatalysts from the corresponding family of biarylphosphine ligands.^{281–287} The Pd-G3 precatalysts are, in general, bulky, electron-rich ligands, which rapidly convert to the active L–Pd(0) species under mild reaction conditions; these catalysts have therefore been prominently used in various cross-coupling processes.^{284,288–293} Buchwald Pd-G3 precatalysts improved the ratio of C4:C2-coupled products, albeit with a moderate overall selectivity (entries 2–6). A plausible mechanistic rationale is that the precatalysts containing bulky electron-rich ligands favor oxidative addition at the more sterically accessible C4 position; this logic would be in agreement with what Dai and coworkers observed during their studies.²⁷⁴ (See Schemes 65 and 66.)

In an effort to further improve the yield of this C4 coupling, Yang and coworkers turned their attention toward “pyridine-enhanced precatalyst preparation stabilization and initiation” (PEPPSI) catalysts. These catalysts form highly stable organopalladium complexes containing bulky NHC ligands. PEPPSI catalysts were originally developed by Organ and coworkers and have since been found to accelerate various aminations and cross-coupling reactions.^{294–298} Gratifyingly, when the Suzuki–Miyaura coupling was conducted in the presence of a PEPPSI-IPr precatalyst, a large proportion of **246:245** (~4.5:1) was observed (entry 7, Scheme 67). This selectivity was attributed to the steric bulk of the PEPPSI-IPr precatalyst, which inserted into the more sterically accessible C4 position of **244**. However, a significant amount of the bis-coupled product (**247**) was also formed along with the desired C4-coupled product (**246**). Further optimization with PEPPSI-IPr was conducted to minimize the formation of **247**. Among the explored solvents, PEG400 was found to give the highest yield (entries 8–10). In varying the base, NaOAc emerged as beneficial for achieving a greater ratio of **246** to **245**; however, it drastically affected the conversion of **244** (entry 11). Eventually, using a combination of both Na₂CO₃ and NaOAc, along with employing KI as an additive, provided an optimal ratio of **246/245/247** (99:1:0), where **246** was isolated in 76% yield (entry 12). This optimized set of conditions was then utilized to couple **244** to both electron-donating and electron-withdrawing boronate esters to construct a variety of pyridine-based dyes.

In summary, the examples illustrated here demonstrate the role that ligands play in achieving unprecedented selectivity in cross-couplings. Notably, there are few reported cases where the careful tuning and choice of ligands were leveraged to achieve complementary selectivity outcomes. Whereas the origin of the site selectivity in many cases remains underexplored, further studies making use of Merlic and Houk’s DFT-based “distortion–interaction” model^{38,73} could prove useful in uncovering the underlying mechanisms governing observed selectivity patterns. As a deeper understanding of these mechanisms is obtained, “ligand-controlled” approaches will undoubtedly continue to move to the forefront of the field of site-selective cross-coupling due to the tunable nature of ligands in facilitating unique selectivity outcomes without the need for substrate modification or neighboring group effects.

7. SOLVENT/ADDITIVE CONTROL

The previous section discussed how ligands can be carefully tuned to favor coupling at a particular position with minimal substrate modification. In many of those examples, once the optimal ligand was identified, other factors such as the solvent, base, additives, and temperature were also tuned to further improve the selectivity and isolated yield of the desired coupling product. In one previous example (Scheme 67), Yang and coworkers showed that employing PEPPSI-IPr as a precatalyst, using a combination of two bases (Na₂CO₃ and NaOAc), along with KI as an additive and running the reaction in PEG400 proved to be essential for obtaining high selectivity for the C4 coupling of **244**.²⁷⁵ On the basis of these results, one could postulate that the selectivity, in both this and other examples, could be altered by manipulating variables other than the identity of the ligand (i.e., solvent, temperature, additives, etc.) in the reaction mixture. In principle, this practice

of modifying other variables besides metal salt/ligand mixtures, would present the added advantage of being more cost-effective as compared with screening catalysts and ligands, which can often be expensive. The following examples provide insight into the types of substrates that have proven competent in cross-couplings where selectivity is guided by modifying solvents and additives.

In 2008, while investigating the site selectivity of the Suzuki–Miyaura coupling of dihalopyrrole esters,^{99,299–301} the Handy group disclosed the first example of altering the site selectivity by modifying the reaction solvent (Scheme 68).³⁰² Specifically, they observed that Suzuki–Miyaura coupling between dibromopyrrole **248** and 4-methoxyphenylboronic acid using Pd(PPh₃)₄ as the catalyst with aqueous sodium carbonate as the base in a 3:1 mixture of toluene and ethanol afforded a mixture of **249** and **250** in a ratio of 22 to 1, where the C5-coupled product (**249**) was isolated in 70% yield. Alternatively, when the reaction solvent was changed to dimethylformamide (DMF), the C3-coupled product **250** was obtained in 53% yield. Intrigued by this reversal of selectivity upon changing the solvent, the authors investigated the reaction in other solvents as well. In doing so, they found that more polar solvents, such as DMF and dimethylsulfoxide (DMSO), favored C3 coupling, whereas relatively less polar solvents favored C5 coupling.

To explain this differential reactivity, the authors proposed two hypotheses. First, they envisioned that the nitrogen atom could direct C5 coupling^{303–305} in less polar solvents. This coordination could, however, be disrupted in solvents like DMF or DMSO, thus resulting in C3 coupling. Second, they proposed that the reversal of selectivity could also be attributed to changes in the electronics of C3 versus C5 caused by the differential solvation of **248** on the basis of solvent choice. To investigate this second hypothesis, they compared ¹H NMR chemical shifts of the nonhalogenated precursor of **248** in different solvents. In CDCl₃, the difference in ¹H NMR chemical shifts (δ_{H}) between the C3 and C5 protons was barely detectable ($\delta_{\text{H}} = 0.08$ ppm), and in DMSO-*d*₆, the difference was more pronounced ($\delta_{\text{H}} = 0.15$ ppm), with the C3 proton remaining more deshielded. However, in a 3:1 mixture of benzene-*d*₆ and methanol-*d*₄, the electronics were reversed, with the C5 proton being more deshielded ($\delta_{\text{H}} = -0.25$ ppm).

Given that oxidative addition is generally favored at the more electron-deficient positions,^{40–42} these NMR studies were in good agreement with this experimentally observed selectivity trend. Specifically, C3 coupling was favored in polar solvents (e.g., DMSO or DMF), whereas C5 coupling was preferred in nonpolar solvents (e.g., toluene).³⁰⁶ The authors ultimately proceeded to study the scope of this reaction, where both electron-rich and electron-deficient boronic acids were competent for obtaining complementary selectivity upon solvent changes. Finally, this novel protocol was applied in a second-generation synthesis of the lamellarins.³⁰⁷ In this context, Handy and coworkers performed a sequential, one-pot Suzuki–Miyaura coupling between **248** and boronic acids **251** and **252** to obtain the bis-coupled product (**253**) in 36% yield (Scheme 69). In summary, this report provides fascinating insight into the reversal in site selectivity that can result by merely changing the reaction solvent. Furthermore, this study clearly set the stage for future investigations into this exciting subfield of site-selective cross-coupling chemistry.

In 2019, Sarpong and coworkers studied the cross-coupling of 3,5-dibromo-2-pyrone (**59**), an α -pyrone-derived dihalogenated heterocycle bearing two chemically inequivalent C–Br bonds.⁴³ Building on the precedent for the site-selective cross-coupling of **59** established by Cho and coworkers,^{92,94,308} the authors sought to understand the underlying factors that guide selectivity, which was not easily explained using existing models.⁴¹ Consistent with the results of Cho and coworkers,⁹⁴ it was observed that Suzuki–Miyaura coupling between **59** and phenylboronic acid in nonpolar solvents,^{309,310} such as 1,2-DCE, THF, and toluene, and in both the presence and the absence of CuI predominantly delivered the C3-coupled product (**254**) (Scheme 70A). On the contrary, in more polar solvents, such as DMSO and DMF, and in the presence of CuI, the C5-coupled product **255** was generally formed as the major product. Notably, the C5-coupled product (**255**) was observed only in the presence of CuI, and conducting the reaction in the absence of CuI exclusively generated the C3-coupled product (**254**).

Additionally, experiments were conducted to study the oxidative addition of **59** in the presence of Pd(PPh₃)₄, which results in the formation of both the corresponding C3 and C5 oxidative adducts, **257** and **258** (Scheme 70B).³¹¹ Consistent with the Suzuki–Miyaura coupling results, C3 Pd complex **257** was formed in nonpolar solvents (toluene), irrespective of whether CuI was added. In polar solvents (DMF), the formation of **257** was favored in the absence of CuI, whereas C5 Pd complex **258** was formed as the major product in the presence of CuI. The C3 site selectivity was attributed to the lower BDE of the C₃–Br bond and the larger LUMO coefficient at the C3 position, which were both supported by computational findings on the basis of the conditions that favored C3 coupling. However, even more intriguing was the observed C5 site selectivity under a specified set of conditions. From both the Suzuki–Miyaura coupling and the oxidative addition results, it is clearly evident that C5 coupling was favored only in polar solvents and in the presence of CuI. To gain further insight into the effect of CuI and solvent on C5 selectivity, the authors chose to analyze the relative stabilities of the C3 and C5 Pd complexes (**257** and **258**) (Scheme 71).

When the oxidative addition was conducted in DMF and in the presence of CuI, it was determined that C5 Pd complex **258** is kinetically favored and gives rise to **255** following a relatively low barrier for transmetalation. The C3 Pd complex **257** was identified to be thermodynamically favored and possesses a relatively higher transmetalation barrier. In **257-cis**, the coordination of Cu to both the pyrone carbonyl oxygen and the bromide attached to the Pd center results in greater stabilization compared with **258**, and this coordination is favored in polar solvents. Subsequently, the corresponding kinetic and thermodynamic stabilities of **257** and **258** were both experimentally and computationally established to arise from an initial CuI-assisted PPh₃ dissociation^{312–314} to furnish the monophosphine ligated Pd complex **259**^{315–317} as the active catalyst for the oxidative addition. Additionally, under the conditions that favor C5 coupling, it was established that the isomeric Pd complexes are interconvertible. Overall, this describes a Curtin–Hammett scenario,³¹⁸ wherein rapid interconversion of the Pd complexes (**257** and **258**) occurs, and the ratio of the resulting cross-coupled products (i.e., **254/255**) is solely dependent on the energy difference between the two respective turnover-limiting transition states for transmetalation.

This enhanced mechanistic understanding of the site-selective cross-coupling of 3,5-dibromo-2-pyrone (**59**) facilitated a unified retrosynthetic disconnection of two structurally related natural products, delavatine A and incarvatonone A (Scheme 72).^{43,44} Consequently, a synthetic route was developed commencing with a sequential Stille–Stille coupling of **59** using stannanes **260a** and **260b** followed by the selective ring-opening of pyrone **261a**, which furnished methyl ester **261** in a single pot. The sequential Stille–Stille coupling involves a site-selective C5 coupling between **59** and stannane **260a** in *N*-methylpyrrolidone (NMP) (polar solvent) and in the presence of copper(I) thiophene-2-carboxylate (CuTC) (copper source), which is then followed by a second Stille coupling with stannane **260b** at the remaining C3–Br bond. Next, **261** was converted to intermediate **262** via an electrocyclization cascade sequence, which was then elaborated to delavatine A and incarvatonone A in two and eight steps, respectively.

Recently, Sarpong and coworkers also studied a method to access pyrido[1,2-*a*]indole scaffolds starting from indole–pyrone adducts (Scheme 73).³¹⁹ For one of the substrates, they conducted a site-selective C3 coupling between indole boronate ester **263** and 3,4-dibromo-2-pyrone (**59**) under the previously disclosed C3 coupling conditions^{92,94,308} to give the indole–pyrone adduct **264**. Upon the ring-opening of **264** with sodium methoxide to reveal intermediate **264a**, a spontaneous intramolecular cyclization proceeded to furnish pyrido[1,2-*a*]indole **264b** in 29% yield.

In summary, the studies by Sarpong and coworkers provide new insight into how solvents and additives can be tuned to achieve complementary selectivity. Many of the previous examples involving site-selective cross-coupling considered oxidative addition to be the rate-determining step (RDS) or the turnover-limiting step (TLS). However, this more recent study from Sarpong and coworkers provides an example of transmetalation as the TLS, thus underscoring the notion that other elementary steps in the catalytic cycle can be turnover-limiting as well.^{38,73} Furthermore, it is illustrated that for unbiased systems (i.e., those that contain C–X bonds with relatively little intrinsic electronic differences), solvents and additives can be leveraged to control site-selectivity outcomes. Currently, there are limited examples where this paradigm for selectivity has been applied; however, the two examples discussed in this section showcase the potential of this approach to serve as an effective strategy in chemical synthesis.

8. PHOTOCHEMICALLY INITIATED

The last set of site-selective cross-coupling reactions to be discussed are those we classify as photochemically initiated. Recently, there have been significant developments in photocatalytic strategies for chemical synthesis, including photoredox catalysis,^{320,321} which have drastically expanded the repertoire of radical-based couplings. In the context of the site-selective cross-coupling of polyhalogenated arenes bearing identical halogen groups, these processes are fairly new (only a handful of reported examples to date) but have nonetheless proven to be effective in accessing products that have remained elusive using the traditional cross-coupling or S_NAr chemistry. Photochemically initiated processes do not follow a traditional two-electron nucleophilic addition pathway but instead proceed through photomediated radical generation followed by the addition of this radical to a

suitable acceptor (Scheme 74), thus providing complementary reactivity to more traditional methods. Because either coupling partner can serve as the radical precursor or acceptor, there are diverse and tunable reaction manifolds that can be developed for diverse product generation. The examples shown here illustrate, through distinct radical-based mechanisms, general strategies for both C–C and C–heteroatom formation.

The first examples to be discussed are the photocatalytic C–F alkylation³²² and C–F arylation³²³ of perfluoroarenes developed by Weaver and coworkers. As discussed in section 3 (electronic control), polyfluorinated arenes are of particular interest from a medicinal chemistry perspective; however, accessing functionalized fluorinated aryls from readily available perfluoroarenes through direct C–F activation remains challenging due to the thermodynamic and kinetic robustness of the C–F bond. The studies by Weaver and coworkers circumvents this inherent challenge through a novel, divergent radical-based mechanism to access both alkylated and arylated perfluoroarenes (Scheme 75). The proposed mechanism^{322,323} for these processes begins with the formation of perfluoroaryl radical **265** following a single electron reduction facilitated by a photoexcited Ir catalyst and diisopropylethylamine (DIPEA) as an electron donor. At this point, depending on the acceptor, **265** can lead to either the alkylated product or the arylated product. For alkylation, radical **265** adds to an alkene to generate alkyl radical **266**, which then performs an H-atom abstraction from the DIPEA radical cation to give the final reduced alkylated perfluoroarene (**267**) and the iminium ion as a byproduct. Similarly, radical **265** can instead add to an arene to give aryl radical **268**. The rearomatization of this aryl radical intermediate via either **269a** or **269b** then leads to the final arylated product (**270**). Notably, the arylation pathway results in dual C–F and C–H functionalization.

For the reductive C–F alkylation (Scheme 76A), the treatment of various perfluoroarenes (**271**) with cyclic and acyclic alkenes, an Ir catalyst, and DIPEA under blue LED irradiation afforded a wide array of alkylated perfluoroarenes (**272a–g**). The C–F arylation (Scheme 76B) proceeded under similar Ir-catalyzed conditions to give fluorinated biaryls (**273a–f**) from the corresponding perfluoroarenes (**271**) and arene acceptors, which included both all-carbon and heteroarene acceptors.

In addition to the work by Weaver and coworkers, there have also been studies into leveraging photocatalysis for arene–heteroatom couplings, such as thiolation.³²⁴ Traditionally, the thiolation of halogenated arenes has been achieved via an S_NAr pathway using a thiol nucleophile and an electron-deficient arene. However, comparable thiolations to electron-rich arenes, which are not readily amenable to S_NAr, have proven to be challenging. In addition, such thiolations are not favored to proceed via traditional two-electron oxidative addition pathways. To obviate this clear challenge, in 2020, Glorius and coworkers developed a novel photo/Ir-catalyzed homolytic aromatic substitution reaction (Scheme 77A), which provided access to a variety of C5-thiolated heteroarenes (**275a–j**) from the corresponding polyhalogenated heteroarene precursors (**274**). This reaction is proposed to follow a radical chain mechanism (Scheme 77B) that initiates with the formation of a thiyl radical from thiol via a photocatalytic oxidation/deprotonation, which may either be stepwise or occur through an oxidative proton-coupled electron transfer (PCET).³²⁵ The thiyl radical then undergoes homolytic aromatic substitution at the more electron-rich C5

position of heteroarene **276** to give radical cation intermediate **277** with the concomitant extrusion of a chloride anion. Finally, electron transfer to **277** following a second oxidation/deprotonation of thiol provides product **275a** and subsequent chain propagation. Overall, this method, which facilitates the addition of a heteroatom to an electron-rich system, provides complementary reactivity to traditional S_NAr processes, which involve the addition of a nucleophile to electron-poor arenes.

9. CONCLUSIONS AND OUTLOOK

Site-selective cross-couplings of polyhalogenated (hetero)arenes have received widespread attention in recent years due to their importance in building complex molecules, in particular, in medicinal, agrochemical, and materials chemistry. Applications toward developing elegant syntheses of pharmaceutically relevant drugs have been particularly impactful and have been highlighted in this Review. Whereas the selective functionalization of a C–X bond in a molecule bearing multiple, distinct halogens might follow the trend of $I > Br > Cl > F$, predicting and rationalizing the selectivity outcome in an arene bearing multiple, but identical, halogen types has remained challenging. Therefore, several factors have been identified to enable the differentiation between carbon positions bearing identical halogen atoms. Initially, this distinction was achieved purely by leveraging the inherent electronics of the system, where the most electrophilic C–X bond would undergo faster oxidative addition. In addition to electronically driven site-selective cross-coupling processes, steric effects were also identified to guide oxidative addition to the least sterically encumbered carbon position. Following these advances, the coordinating ability of functional groups was leveraged to direct oxidative addition to a particular position. Subsequently, methods were developed to achieve site selectivity by tuning the electronic and steric influences of an external ligand. More recently, selectivity has been achieved by altering the choice of reaction solvents and additives.

Whereas leveraging the intrinsic electronic and sterics of a substrate remains the traditional approach to achieving site-selective cross-coupling, controlling site-selectivity outcomes by altering other factors, such as the metal precatalyst, external ligands, reaction solvent, or choice of additives, presents novel directions to further advance this highly valuable subfield of cross-coupling chemistry. Whereas current investigations have been mainly steered toward identifying conditions to obtain a desired selectivity, more effort is needed to gain a deeper understanding of the mechanistic rationale behind the selectivity observed in various (hetero)arenes. Better insight into these selectivity-guiding processes will provide a more methodical, and therefore more efficient, approach toward predicting conditions suitable for obtaining a particular selectivity outcome. Furthermore, on the basis of the large data sets that are emerging for site-selective cross-coupling, employing other modern strategies, such as linear regression models and machine-learning algorithms, to identify reaction conditions could also prove fruitful in further advancing this field.^{326,327} These systematic approaches could also prove to be particularly helpful for effecting site-selective cross-couplings in more complex systems, such as natural-product-like molecules.

Finally, an emerging area of interest includes achieving site-selective cross-couplings under photocatalytic conditions. Whereas many subfields of photocatalysis are still in their early

development, the examples discussed in this Review showcase how new, state-of-the-art reaction manifolds can be accessed, thus enabling nonintuitive, site-selective cross-couplings that do not abide by the traditional cross-coupling catalytic cycle (Scheme 2). Overall, the site-selective cross-coupling of (hetero)arenes with identical halogen substitution is a highly diverse and versatile field, which, as exemplified by this Review, presents countless future opportunities to not only advance this specific field but also help advance chemical synthesis as a whole.

Funding

V.P. acknowledges TRDRP for a predoctoral fellowship. M.A.P. acknowledges both the NSF (DGE 1752814) and the NIH (F31GM139368) for predoctoral fellowships. R.S. is grateful to the NSF (CHE-1856228) for funding of the work described here conducted in the Sarpong laboratory.

Biographies

Vignesh Palani received his B.S. in chemistry with honors (*summa cum laude*) from the University of Minnesota-Twin Cities in 2016. He earned his Ph.D. in chemistry from the University of California, Berkeley in 2020, where he carried out his research in the laboratory of Professor Richmond Sarpong. At UC Berkeley, he worked on the total synthesis of complex natural products and new reaction development.

Melecio Perea received his B.S. in chemistry (*graduating summa cum laude*) from New Mexico Highlands University in 2016. That same year he began his graduate studies at the University of California, Berkeley, working in the lab of Professor Richmond Sarpong. As an NSF and NIH predoctoral fellow, his research at Berkeley has focused on developing strategies for the synthesis of complex natural products.

Richmond Sarpong is a Professor of Chemistry at the University of California Berkeley, where his research group specializes in synthetic organic chemistry. He completed his undergraduate studies at Macalester College in St. Paul, Minnesota (with Prof. Rebecca C. Hoye) and his graduate work with Prof. Martin Semmelhack at Princeton. He conducted postdoctoral studies at Caltech with Prof. Brian Stoltz and joined the faculty at Berkeley in 2004.

REFERENCES

- (1). Carey JS; Laffan D; Thomson C; Williams MT Analysis of the Reactions Used for the Preparation of Drug Candidate Molecules. *Org. Biomol Chem* 2006, 4, 2337–2347. [PubMed: 16763676]
- (2). Pozharskii AF; Soldatenkov AT; Katrizky AR *Heterocycles in Life and Society*; Wiley: New York, 1997; pp 1–361.
- (3). Reis J; Gaspar A; Milhazes N; Borges F Chromone as a Privileged Scaffold in Drug Discovery: Recent Advances. *J. Med. Chem* 2017, 60, 7941–7957. [PubMed: 28537720]
- (4). Corbet J-P; Mignani G Selected Patented Cross-Coupling Reaction Technologies. *Chem. Rev* 2006, 106, 2651–2710. [PubMed: 16836296]
- (5). de Meijere A; Diederich F *Metal-Catalyzed Cross-Coupling Reactions*, 2nd ed.; Wiley-VCH: Weinheim, Germany, 2004; pp 1–882.
- (6). Boubertakh O; Goddard J-P Construction and Functionalization of Heteroarenes by Use of Photoredox Catalysis. *Eur. J. Org. Chem* 2017, 2017, 2072–2084.

- (7). Li JJ; Gribble GW *Palladium in Heterocyclic Chemistry*; Pergamon: Oxford, U.K., 2000; pp 1–650.
- (8). Bellina F; Rossi R Recent Advances in the Synthesis of (Hetero)Aryl-Substituted Heteroarenes via Transition Metal-Catalysed Direct (Hetero)Arylation of Heteroarene C–H Bonds with Aryl Halides or Pseudohalides, Diaryliodonium Salts, and Potassium Aryltrifluoroborates. *Tetrahedron* 2009, 65, 10269–10310.
- (9). Nair V; Rajesh C; Vinod AU; Bindu S; Sreekanth AR; Mathen JS; Balagopal L Strategies for Heterocyclic Construction via Novel Multicomponent Reactions Based on Isocyanides and Nucleophilic Carbenes. *Acc. Chem. Res* 2003, 36, 899–907. [PubMed: 14674781]
- (10). Andraos J A New Paradigm for Designing Ring Construction Strategies for Green Organic Synthesis: Implications for the Discovery of Multicomponent Reactions to Build Molecules Containing a Single Ring. *Beilstein J. Org. Chem* 2016, 12, 2420–2442. [PubMed: 28144310]
- (11). Keerthi Krishnan K; Ujwaldev SM; Saranya S; Anilkumar G; Beller M Recent Advances and Perspectives in the Synthesis of Heterocycles via Zinc Catalysis. *Adv. Synth. Catal* 2019, 361, 382–404.
- (12). Dobrounig P; Trobe M; Breinbauer R Sequential and Iterative Pd-Catalyzed Cross-Coupling Reactions in Organic Synthesis. *Monatsh. Chem* 2017, 148, 3–35. [PubMed: 28127089]
- (13). Rohrbach S; Smith AJ; Pang JH; Poole DL; Tuttle T; Chiba S; Murphy JA Concerted Nucleophilic Aromatic Substitution Reactions. *Angew. Chem., Int. Ed* 2019, 58, 16368–16388.
- (14). Galabov B; Nalbantova D; Schleyer P. v. R.; Schaefer HF III Electrophilic Aromatic Substitution: New Insights into an Old Class of Reactions. *Acc. Chem. Res* 2016, 49, 1191–1199. [PubMed: 27268321]
- (15). Bunnett JF; Zahler RE Aromatic Nucleophilic Substitution Reactions. *Chem. Rev* 1951, 49, 273–412.
- (16). Schnürch M; Spina M; Khan AF; Mihovilovic MD; Stanetty P Halogen Dance Reactions—A Review. *Chem. Soc. Rev* 2007, 36, 1046–1057. [PubMed: 17576473]
- (17). Evano G; Nitelet A; Thilmany P; Dewez DF Metal-Mediated Halogen Exchange in Aryl and Vinyl Halides: A Review. *Front. Chem* 2018, 6, 114. [PubMed: 29755967]
- (18). Davies HML; Morton D Recent Advances in C–H Functionalization. *J. Org. Chem* 2016, 81, 343–350. [PubMed: 26769355]
- (19). Jana R; Pathak TP; Sigman MS Advances in Transition Metal (Pd, Ni, Fe)-Catalyzed Cross-Coupling Reactions Using Alkyl-organometallics as Reaction Partners. *Chem. Rev* 2011, 111, 1417–1492. [PubMed: 21319862]
- (20). Wu X-F; Anbarasan P; Neumann H; Beller M From Noble Metal to Nobel Prize: Palladium-Catalyzed Coupling Reactions as Key Methods in Organic Synthesis. *Angew. Chem., Int. Ed* 2010, 49, 9047–9050.
- (21). Dorel R; Grugel CP; Haydl AM The Buchwald–Hartwig Amination After 25 Years. *Angew. Chem., Int. Ed* 2019, 58, 17118–17129.
- (22). Campeau L-C; Hazari N Cross-Coupling and Related Reactions: Connecting Past Success to the Development of New Reactions for the Future. *Organometallics* 2019, 38, 3–35. [PubMed: 31741548]
- (23). Suzuki A Cross-Coupling Reactions of Organoboranes: An Easy Way to Construct C–C Bonds (Nobel Lecture). *Angew. Chem., Int. Ed* 2011, 50, 6722.
- (24). Miyaura N; Yamada K; Suzuki A A New Stereospecific Cross-Coupling by the Palladium-Catalyzed Reaction of 1-Alkenylboranes with 1-Alkenyl or 1-Alkynyl Halides. *Tetrahedron Lett.* 1979, 20, 3437–3440.
- (25). Miyaura N; Suzuki A Stereoselective Synthesis of Arylated (*E*)-Alkenes by the Reaction of Alk-1-enylboranes with Aryl Halides in the Presence of Palladium Catalyst. *J. Chem. Soc., Chem. Commun* 1979, 866–867.
- (26). Negishi E Magical Power of Transition Metals: Past, Present, and Future (Nobel Lecture). *Angew. Chem., Int. Ed* 2011, 50, 6738–6764.
- (27). Negishi E; King AO; Okukado N Selective Carbon–Carbon Bond Formation via Transition Metal Catalysis. 3 A Highly Selective Synthesis of Unsymmetrical Biaryls and Diarylmethanes by the

Nickel- or Palladium-Catalyzed Reaction of Aryl- and Benzylzinc Derivatives with Aryl Halides. *J. Org. Chem* 1977, 42, 1821–1821.

- (28). Milstein D; Stille JK A General, Selective, and Facile Method for Ketone Synthesis from Acid Chlorides and Organotin Compounds Catalyzed by Palladium. *J. Am. Chem. Soc* 1978, 100, 3636–3638.
- (29). Milstein D; Stille JK Palladium-Catalyzed Coupling of Tetraorganotin Compounds with Aryl and Benzyl Halides. *Synthetic Utility and Mechanism. J. Am. Chem. Soc* 1979, 101, 4992–4998.
- (30). Heck RF; Nolley JP Jr. Palladium-Catalyzed Vinylic Hydrogen Substitution Reactions with Aryl, Benzyl, and Styryl Halides. *J. Org. Chem* 1972, 37, 2320–2322.
- (31). Almond-Thynne J; Blakemore DC; Pryde DC; Spivey AC Site-Selective Suzuki–Miyaura Coupling of Heteroaryl Halides – Understanding the Trends for Pharmaceutically Important Classes. *Chem. Sci* 2017, 8, 40–62. [PubMed: 28451148]
- (32). Whereas the term “regioselective” may be used, we prefer to use the term “site-selective” instead (see refs 32 and 33):Huang Z; Dong G Site-Selectivity Control in Organic Reactions: AQuest to Differentiate Reactivity Among the Same Kind of Functional Groups. *Acc. Chem. Res* 2017, 50, 465–471. [PubMed: 28945402]
- (33). Seebach D Methods of Reactivity Umpolung. *Angew. Chem., Int. Ed. Engl* 1979, 18, 239–258.
- (34). Shen C; Wei Z; Jiao H; Wu X-F Ligand- and Solvent-Tuned Chemoselective Carbonylation of Bromoaryl Triflates. *Chem. - Eur. J* 2017, 23, 13369–13378. [PubMed: 28650074]
- (35). Espino G; Kurbangaliev A; Brown JM Aryl Bromide/Triflate Selectivities Reveal Mechanistic Divergence in Palladium-Catalysed Couplings; The Suzuki–Miyaura Anomaly. *Chem. Commun* 2007, 1742–1744.
- (36). Miyaura N; Suzuki A Palladium-Catalyzed Cross-Coupling Reactions of Organoboron Compounds. *Chem. Rev* 1995, 95, 2457–2483.
- (37). Hassan Z; Patonay T; Langer P Regioselective Suzuki–Miyaura Reactions of Aromatic Bis-triflates: Electronic versus Steric Effects. *Synlett* 2013, 24, 412–423.
- (38). Legault CY; Garcia Y; Merlic CA; Houk KN Origin of Regioselectivity in Palladium-Catalyzed Cross-Coupling Reactions of Polyhalogenated Heterocycles. *J. Am. Chem. Soc* 2007, 129, 12664–12665. [PubMed: 17914827]
- (39). Wang J-R; Manabe K Transition-Metal-Catalyzed Site-Selective Cross-Coupling of Di- and Polyhalogenated Compounds. *Synthesis* 2009, 2009, 1405–1427.
- (40). Manabe K; Yamaguchi M Catalyst-Controlled Site-Selectivity Switching in Pd-Catalyzed Cross-Coupling of Dihaloarenes. *Catalysts* 2014, 4, 307–320.
- (41). Fairlamb IJS Regioselective (Site-Selective) Functionalisation of Unsaturated Halogenated Nitrogen, Oxygen and Sulfur Heterocycles by Pd-Catalysed Cross-Couplings and Direct Arylation Processes. *Chem. Soc. Rev* 2007, 36, 1036–1045. [PubMed: 17576472]
- (42). Schröter S; Stock C; Bach T Regioselective Cross-Coupling Reactions of Multiple Halogenated Nitrogen-, Oxygen-, and Sulfur-Containing Heterocycles. *Tetrahedron* 2005, 61, 2245–2267.
- (43). Palani V; Hugelshofer CL; Kevlishvili I; Liu P; Sarpong R A Short Synthesis of Delavatine A Unveils New Insights into Site-Selective Cross-Coupling of 3,5-Dibromo-2-pyrone. *J. Am. Chem. Soc* 2019, 141, 2652–2660. [PubMed: 30646686]
- (44). Palani V; Hugelshofer CL; Sarpong R A Unified Strategy for the Enantiospecific Total Synthesis of Delavatine A and Formal Synthesis of Incarviate A. *J. Am. Chem. Soc* 2019, 141, 14421–14432. [PubMed: 31433634]
- (45). For selected examples of the mechanism of cross-coupling reactions, see refs 45–48:Biffis A; Centomo P; Del Zotto A; Zecca M Pd Metal Catalysts for Cross-Couplings and Related Reactions in the 21st Century: A Critical Review. *Chem. Rev* 2018, 118, 2249–2295. [PubMed: 29460627]
- (46). Meconi GM; Vummaleti SVC; Luque-Urrutia JA; Belanzoni P; Nolan SP; Jacobsen H; Cavallo L; Solá M; Poater A Mechanism of the Suzuki–Miyaura Cross-Coupling Reaction Mediated by [Pd(NHC)(allyl)Cl] Precatalysts. *Organometallics* 2017, 36, 2088–2095.
- (47). Diccianni JB; Diao T Mechanisms of Nickel-Catalyzed Cross-Coupling Reactions. *Trends Chem.* 2019, 1, 830–844.

- (48). Espinet P; Echavarren AM The Mechanisms of the Stille Reaction. *Angew. Chem., Int. Ed* 2004, 43, 4704–4734.
- (49). Li J; Jin L; Liu C; Lei A Transmetalation of Ar^1ZnX with $[\text{Ar}^2\text{-Pd-X}]$ is the Rate-Limiting Step: Kinetic Insights from a Live Pd-Catalyzed Negishi Coupling. *Org. Chem. Front* 2014, 1, 50–53.
- (50). Stenlid JH; Brinck T Nucleophilic Aromatic Substitution Reactions Described by the Local Electron Attachment Energy. *J. Org. Chem* 2017, 82, 3072–3083. [PubMed: 28195731]
- (51). Busch M; Wodrich MD; Corminboeuf C A Generalized Picture of C–C Cross-Coupling. *ACS Catal.* 2017, 7, 5643–5653.
- (52). Fauvarque J-F; Pflüger F; Troupel M Kinetics of Oxidative Addition of Zerovalent Palladium to Aromatic Iodides. *J. Organomet. Chem* 1981, 208, 419–427.
- (53). Mortier J *Arene Chemistry: Reaction Mechanism and Methods for Aromatic Compounds*; John Wiley & Sons, Inc.: Hoboken, NJ, 2016; pp 131–295.
- (54). Gebauer J; Arseniyadis S; Cossy J A Concise Total Synthesis of Melithiazole C. *Org. Lett* 2007, 9, 3425–3427. [PubMed: 17637033]
- (55). Flegeau EF; Popkin ME; Greaney MF Direct Arylation of Oxazoles at C2. A Concise Approach to Consecutively Linked Oxazoles. *Org. Lett* 2008, 10, 2717–2720. [PubMed: 18540631]
- (56). Fairlamb IJS; O'Brien CT; Lin Z; Lam KC Regioselectivity in the Sonogashira Coupling of 4,6-Dichloro-2-pyrone. *Org. Biomol. Chem* 2006, 4, 1213–1216. [PubMed: 16557307]
- (57). Handy ST; Zhang Y A Simple Guide for Predicting Regioselectivity in the Coupling of Polyhaloheteroaromatics. *Chem. Commun* 2006, 299–301.
- (58). Ceide SC; Montalban AG Microwave-Assisted, Efficient and Regioselective Pd-Catalyzed C-Phenylation of Halopyrimidines. *Tetrahedron Lett.* 2006, 47, 4415–4418.
- (59). Maes BUW; Verbeeck S; Verhelst T; Ekomié A; von Wolff N; Lefèvre G; Mitchell EA; Jutand A Oxidative Addition of Haloheteroarenes to Palladium(0): Concerted versus $\text{S}_{\text{N}}\text{Ar}$ -Type Mechanism. *Chem. - Eur. J* 2015, 21, 7858–7865. [PubMed: 25858175]
- (60). Kazi SA; Campi EM; Hearn MTW A Convenient and Efficient One Pot Synthesis of Unsymmetrically Substituted *p*-Terphenyls via a Phosphine-Free Double Suzuki Cross-Coupling Protocol Using 1,4-Dibromo-2-nitrobenzene as the Substrate. *Tetrahedron* 2018, 74, 1731–1741.
- (61). Liu X-W; Echavarren J; Zarate C; Martin R Ni-Catalyzed Borylation of Aryl Fluorides via C–F Cleavage. *J. Am. Chem. Soc* 2015, 137, 12470–12473. [PubMed: 26397717]
- (62). Campbell MG; Ritter T Modern Carbon–Fluorine Bond Forming Reactions for Aryl Fluoride Synthesis. *Chem. Rev* 2015, 115, 612–633. [PubMed: 25474722]
- (63). O'Hagan D Understanding Organofluorine Chemistry. An Introduction to the C–F Bond. *Chem. Soc. Rev* 2008, 37, 308–319. [PubMed: 18197347]
- (64). Ahrens T; Kohlmann J; Ahrens M; Braun T Functionalization of Fluorinated Molecules by Transition-Metal-Mediated C–F Bond Activation to Access Fluorinated Building Blocks. *Chem. Rev* 2015, 115, 931–972. [PubMed: 25347593]
- (65). Lennox AJJ Meisenheimer Complexes in $\text{S}_{\text{N}}\text{Ar}$ Reactions: Intermediates of Transition States? *Angew. Chem. Int. Ed* 2018, 57, 14686–14688.
- (66). Chambers RD; Martin PA; Sandford G; Williams DLH Mechanisms of Reactions of Halogenated Compounds: Part 7. Effects of Fluorine and Other Groups as Substituents on Nucleophilic Aromatic Substitution. *J. Fluorine Chem* 2008, 129, 998–1002.
- (67). Luo Z-J; Zhao H-Y; Zhang X Highly Selective Pd-Catalyzed Direct C–F Bond Arylation of Polyfluoroarenes. *Org. Lett* 2018, 20, 2543–2546. [PubMed: 29667829]
- (68). Saijo H; Sakaguchi H; Ohashi M; Ogoshi S Base-Free Hiyama Coupling Reaction via a Group 10 Metal Fluoride Intermediate Generated by C–F Bond Activation. *Organometallics* 2014, 33, 3669–3672.
- (69). Welsch ME; Snyder SA; Stockwell BR Privileged Scaffolds for Library Design and Drug Discovery. *Curr. Opin. Chem. Biol* 2010, 14, 347–361. [PubMed: 20303320]
- (70). Jampilek J *Heterocycles in Medicinal Chemistry*. *Molecules* 2019, 24, 3839–3842.
- (71). Joule JA; Mills K *Heterocyclic Chemistry*, 5th ed.; Wiley-John Wiley & Sons Ltd.: West Sussex, U.K., 2014; pp 645–664.

- (72). Terrier F Modern Nucleophilic Aromatic Substitution; Wiley-VCH Verlag GmbH & Co. KGaA: Weinheim, Germany, 2013; pp 11–15.
- (73). Garcia Y; Schoenebeck F; Legault CY; Merlic CA; Houk KN Theoretical Bond Dissociation Energies of Halo-Heterocycles: Trends and Relationships to Regioselectivity in Palladium-Catalyzed Cross-Coupling Reactions. *J. Am. Chem. Soc* 2009, 131, 6632–6639. [PubMed: 19368385]
- (74). Kikuchi O; Hondo Y; Morihashi K; Nakayama M An Ab Initio Molecular Orbital Study of Pyridyl Radicals. *Bull. Chem. Soc. Jpn* 1988, 61, 291–292.
- (75). Jones J; Bacskay GB; Mackie JC; Doughty A Ab Initio Studies of the Thermal Decomposition of Azaaromatics: Free Radical versus Intramolecular Mechanism. *J. Chem. Soc., Faraday Trans* 1995, 91, 1587–1592.
- (76). Prajapati D; Schulzke C; Kindermann MK; Kapdi AR Selective Palladium-Catalyzed Arylation of 2,6-Dibromopyridine Using *N*-Heterocyclic Carbene Ligands. *RSC Adv.* 2015, 5, 53073–53085.
- (77). Lee K; Seomoon D; Lee PH Highly Efficient Catalytic Synthesis of Substituted Allenes Using Indium. *Angew. Chem., Int. Ed* 2002, 41, 3901–3903.
- (78). Khoje AD; Gundersen L-L Reactivity and Regioselectivity in Stille Couplings of 3-Substituted 2,4-Dichloropyridines. *Tetrahedron Lett.* 2011, 52, 523–525.
- (79). Ahmed A; Sharif M; Shoaib K; Reimann S; Iqbal J; Patonay T; Spannenberg A; Langer P Synthesis of 2,6-Diaryl-3-(trifluoromethyl)pyridines by Regioselective Suzuki–Miyaura Reactions of 2,6-Dichloro-3-(trifluoromethyl)pyridine. *Tetrahedron Lett.* 2013, 54, 1669–1672.
- (80). Malacea R; Chahdoura F; Devillard M; Saffon N; Gómez M; Bourissou D *Ortho*-(Dimesitylboryl)phenylphosphines: Positive Boryl Effect in the Palladium-Catalyzed Suzuki–Miyaura Coupling of 2-Chloropyridines. *Adv. Synth. Catal* 2013, 355, 2274–2284.
- (81). Ehlers P; Reimann S; Erfle S; Villinger A; Langer P Synthesis of 2-Aryl-3,4,5,6-tetrachloropyridines and 2,6-Diaryl-3,4,5-trichloropyridines by Site-Selective Suzuki–Miyaura Reactions of Pentachloropyridine. *Synlett* 2010, 2010, 1528–1532.
- (82). Ackermann L; Althammer A Domino N–H/C–H Bond Activation: Palladium-Catalyzed Synthesis of Annulated Heterocycles Using Dichloro(hetero)arenes. *Angew. Chem., Int. Ed* 2007, 46, 1627–1629.
- (83). Hostyn S; Van Baelen G; Lemièrè GLF; Maes BUW Synthesis of *r*-Carbolines Starting from 2,3-Dichloropyridines and Substituted Anilines. *Adv. Synth. Catal* 2008, 350, 2653–2660.
- (84). Laha JK; Petrou P; Cuny GD One-Pot Synthesis of *y*-Carbolines via Sequential Palladium-Catalyzed Aryl Amination and Intramolecular Arylation. *J. Org. Chem* 2009, 74, 3152–3155. [PubMed: 19323545]
- (85). Barckholtz C; Barckholtz TA; Hadad CM C–H and N–H Bond Dissociation Energies of Small Aromatic Hydrocarbons. *J. Am. Chem. Soc* 1999, 121, 491–500.
- (86). Solberg J; Undheim K; Pettersson L; Ohman L-O; Ruiz J; Colacio E; Mulichak AM; Alminger T; Erickson M; Grundevik I; Hagin I; Hoffman K-J; Johansson S; Larsson S; Lofberg I; Ohlson K; Persson B; Skanberg I; Tekenbergs-Hjelte L Regiochemistry in Pd-Catalyzed Organotin Reactions with Halopyrimidines. *Acta Chem. Scand* 1989, 43, 62–68.
- (87). Young IS; Glass A-L; Cravillion T; Han C; Zhang H; Gosselin F Palladium-Catalyzed Site-Selective Amidation of Dichloroazines. *Org. Lett* 2018, 20, 3902–3906. [PubMed: 29944383]
- (88). Dickinson JM Microbial Pyran-2-ones and Dihydropyran-2-ones. *Nat. Prod. Rep* 1993, 10, 71–98. [PubMed: 8451032]
- (89). McGlacken GP; Fairlamb IJS 2-Pyrone Natural Products and Mimetics: Isolation, Characterization, and Biological Activity. *Nat. Prod. Rep* 2005, 22, 369–385. [PubMed: 16010346]
- (90). Marrison LR; Dickinson JM; Fairlamb IJS Bioactive 4-Substituted-6-methyl-2-pyrones with Promising Cytotoxicity Against A2780 and K562 Cell Lines. *Bioorg. Med. Chem. Lett* 2002, 12, 3509–3513. [PubMed: 12443764]
- (91). Fairlamb IJS; Marrison LR; Dickinson JM; Lu F-J; Schmidt JP 2-Pyrones Possessing Antimicrobial and Cytotoxic Activities. *Bioorg. Med. Chem* 2004, 12, 4285–4299. [PubMed: 15246105]

- (92). Lee J-H; Park J-S; Cho C-G Regioselective Synthesis of 3-Alkynyl-5-bromo-2-pyrones via Pd-Catalyzed Couplings on 3,5-Dibromo-2-pyrone. *Org. Lett* 2002, 4, 1171–1173. [PubMed: 11922810]
- (93). Cho H-K; Cho C-G Preparation of 3,5-Dibromo-2-pyrone from Coumalic Acid. *Org. Synth* 2015, 92, 148–155.
- (94). Ryu K-M; Gupta AK; Han JW; Oh CH; Cho C-G Regiocontrolled Suzuki–Miyaura Couplings of 3,5-Dibromo-2-pyrone. *Synlett* 2004, 12, 2197–2199.
- (95). Fairlamb IJS; O'Brien CT; Lin Z; Lam KC Regioselectivity in the Sonogashira Coupling of 4,6-Dichloro-2-pyrone. *Org. Biomol. Chem* 2006, 4, 1213–1216. [PubMed: 16557307]
- (96). Joule JA; Mills K *Heterocyclic Chemistry*, 5th ed.; Wiley-John Wiley & Sons Ltd.: West Sussex, U.K., 2014; pp 9–10.
- (97). Liu J.-t.; Simmons CJ; Xie H; Yang F; Zhao X; Tang Y; Tang W Synthesis of Highly Substituted Benzofuran-Containing Natural Products via Rh-Catalyzed Carbonylative Benzannulation. *Adv. Synth. Catal* 2017, 359, 693–697.
- (98). Schröter S; Bach T Di- and Triarylsubstituted Pyrroles by Sequential Regioselective Cross-Coupling Reactions. *Heterocycles* 2007, 74, 569–594.
- (99). Handy ST; Zhang Y Regioselective Couplings of Dibromopyrrole Esters. *Synthesis* 2006, 2006, 3883–3887.
- (100). Nguyen H; Nguyen DX; Tran TQ; Vo BN; Nguyen TH; Vuong TMH; Dang TT Programmed Synthesis of Tetraarylthieno[3,2-*b*]Thiophene by Site-selective Suzuki Cross-Coupling Reactions of Tetrabromothieno[3,2-*b*]Thiophene. *Synlett* 2013, 25, 93–96.
- (101). Strotman NA; Chobanian HR; He J; Guo Y; Dormer PG; Jones CM; Steves JE Catalyst-Controlled Regioselective Suzuki Couplings at Both Positions of Dihaloimidazoles, Dihaloazoles, and Dihalothiazoles. *J. Org. Chem* 2010, 75, 1733–1739. [PubMed: 20141223]
- (102). Niculescu-Duvaz D; Niculescu-Duvaz I; Suijkerbuijk BMJM; Ménard D; Zambon A; Davies L; Pons J-F; Whittaker S; Marais R; Springer CJ Potent BRAF Kinase Inhibitors Based on 2,4,5-Trisubstituted Imidazole with Naphthyl and Benzothiophene 4-Substituents. *Bioorg. Med. Chem* 2013, 21, 1284–1304. [PubMed: 23376011]
- (103). Rečnik L-M; Abd El Hameid M; Haider M; Schnurch M; Mihovilovic M Selective Sequential Cross-Coupling Reactions on Imidazole towards Meurodazine and Analogues. *Synthesis* 2013, 45, 1387–1405.
- (104). Ascierto PA; Kirkwood JM; Grob J-J; Simeone E; Grimaldi AM; Maio M; Palmieri G; Testori A; Marincola FM; Mozzillo N The Role of BRAF V600 Mutation in Melanoma. *J. Transl. Med* 2012, 10, 1–9. [PubMed: 22214470]
- (105). Kawasaki I; Katsuma H; Nakayama Y; Yamashita M; Ohta S Total Synthesis of Topsisentin, Antiviral and Antitumor Bis(indolyl)imidazole. *Heterocycles* 1998, 48, 1887–1901.
- (106). Alford PE Lithiation-Based and Magnesium-Based Strategies for the Functionalization of Imidazole: 2001–2010. In *Metalation of Azoles and Related Five-Membered Ring Heterocycles. Topics in Heterocyclic Chemistry*; Gribble GW, Ed.; Springer: Berlin, 2012; Vol. 29, pp 77–102.
- (107). Yamauchi T; Shibahara F; Murai T Facile Synthetic Method for Diverse Polyfunctionalized Imidazoles by Means of Pd-Catalyzed C–H Bond Arylation of *N*-Methyl-4,5-dibromoimidazole. *J. Org. Chem* 2014, 79, 7185–7192. [PubMed: 25007133]
- (108). Joo JM; Touré BB; Sames D C–H Bonds as Ubiquitous Functionality: A General Approach to Complex Arylated Imidazoles via Regioselective Sequential Arylation of All Three C–H Bonds and Regioselective *N*-Alkylation Enabled by SEM-Group Transposition. *J. Org. Chem* 2010, 75, 4911–4920. [PubMed: 20608749]
- (109). Hodgetts KJ; Kershaw MT Ethyl 2-Chlorooxazole-4-carboxylate: A Versatile Intermediate for the Synthesis of Substituted Oxazoles. *Org. Lett* 2002, 4, 2905–2907. [PubMed: 12182585]
- (110). Khera RA; Ali A; Hussain M; Tatar J; Villinger A; Langer P Synthesis of Arylated Pyrazoles by Site-selective Suzuki–Miyaura Reactions of Tribromopyrazoles. *Synlett* 2010, 2010, 1923–1926.
- (111). Christoforou IC; Koutentis PA; Rees CW Regiospecific Suzuki Coupling of 3,5-Dichloroisothiazole-4-carbonitrile. *Org. Biomol. Chem* 2003, 1, 2900–2907. [PubMed: 12968340]

- (112). Iddon B; Tønder JE; Hosseini M; Begtrup M The *N*-vinyl Group as a Protection Group of the Preparation of 3(5)-Substituted Pyrazoles via Bromine–Lithium Exchange. *Tetrahedron* 2007, 63, 56–61.
- (113). Cutri CCC; Garozzo A; Siracusa MA; Sarvá MC; Tempera G; Geremia E; Pinizzotto MR; Guerrero F Synthesis and Antiviral Activity of a New Series of 4-Isothiazolecarbonitriles. *Bioorg. Med. Chem* 1998, 6, 2271–2280. [PubMed: 9925289]
- (114). Cutri CCC; Garozzo A; Siracusa MA; Sarvá MC; Castro A; Geremia E; Pinizzotto MR; Guerrero F Synthesis of New 3,4,5-Trisubstituted Isothiazoles as Effective Inhibitory Agents of Enteroviruses. *Bioorg. Med. Chem* 1999, 7, 225–230. [PubMed: 10218813]
- (115). Al-Zoubi RM; Al-Jammal WK; El-Khateeb MY; McDonald R Synthesis of Diiodinated Biphenyls and Iodinated *Meta*-Terphenyls by Regioselective Suzuki–Miyaura Cross-Coupling Reactions of 5-Substituted 1,2,3-Triiodobenzenes. *Eur. J. Org. Chem* 2015, 2015, 3374–3384.
- (116). For further discussions on the effects of catalyst/ligand sterics, see ref 19.
- (117). Cullis CA; Granger KE; Guo J; Hirose M; Li G; Mizutani M; Vos TJ Heteroaryls and Uses Thereof. Patent WO 2012021615 A1, 2012.
- (118). Freeze BS; Hirose M; Hu Y; Hu Z; Lee HM; Sells TB; Shi Z; Vyskocil S; Xu T Heteroaryls and Uses Thereof. Patent WO 2012021696 A1, 2012.
- (119). Selva E; Beretta G; Montanini N; Saddler GS; Gastaldo L; Ferrari P; Lorenzetti R; Landini P; Ripamonti F; Goldstein BP; et al. Antibiotic GE2270 A: A Novel Inhibitor of Bacterial Protein Synthesis. *J. Antibiot* 1991, 44, 693–701.
- (120). Tavecchia P; Gentili P; Kurz M; Sottani C; Bonfichi R; Selva E; Lociuoro S; Restelli E; Ciabatti R Degradation Studies of Antibiotic MDL 62,879 (GE2270A) and Revision of Structure. *Tetrahedron* 1995, 51, 4867–4890.
- (121). Müller HM; Delgado O; Bach T Total Synthesis of the Thiazolyl Peptide GE2270 A. *Angew. Chem., Int. Ed* 2007, 46, 4771–4774.
- (122). Gustafson JL; Lim D; Barrett KT; Miller SJ Synthesis of Atropisomerically Defined, Highly Substituted Biaryl Scaffolds through Catalytic Enantioselective Bromination and Regioselective Cross-Coupling. *Angew. Chem., Int. Ed* 2011, 50, 5125–5129.
- (123). Gustafson JL; Lim D; Miller SJ Dynamic Kinetic Resolution of Biaryl Atropisomers via Peptide-Catalyzed Asymmetric Bromination. *Science* 2010, 328, 1251–1255. [PubMed: 20522769]
- (124). Knapp DM; Gillis EP; Burke MD A General Solution for Unstable Boronic Acids: Slow-Release Cross-Coupling from Air-Stable MIDA Boronates. *J. Am. Chem. Soc* 2009, 131, 6961–6963. [PubMed: 19405470]
- (125). Yoshikai N; Mashima H; Nakamura E Nickel-Catalyzed Cross-Coupling Reaction of Aryl Fluorides and Chlorides with Grignard Reagents under Nickel/Magnesium Bimetallic Cooperation. *J. Am. Chem. Soc* 2005, 127, 17978–17979. [PubMed: 16366529]
- (126). Chen Z; Wang B; Zhang J; Yu W; Liu Z; Zhang Y Transition Metal-Catalyzed C–H Bond Functionalizations by the Use of Diverse Directing Groups. *Org. Chem. Front* 2015, 2, 1107–1295.
- (127). Nakamura H; Takeuchi D; Murai A Synthesis of 5- and 3,5-Substituted 2-Aminopyrazines by Pd Mediated Stille Coupling. *Synlett* 1995, 1995, 1227–1228.
- (128). Shimomura O; Musicki B; Kishi Y Semi-synthetic Aequorins with Improved Sensitivity to Ca²⁺Ions. *Biochem. J* 1989, 261, 913–920. [PubMed: 2803250]
- (129). Wu C; Nakamura H; Murai A; Shimomura O Chemi- and Bioluminescence of Coelenterazine Analogues with a Conjugated Group at the C-8 Position. *Tetrahedron Lett.* 2001, 42, 2997–3000.
- (130). Hikawa H; Yokoyama Y Cross-Coupling Reaction on *N*-(3,5-dibromo-2-pyridyl)piperazines: Regioselective Synthesis of 3,5-Disubstituted Pyridylpiperazines. *Tetrahedron* 2010, 66, 9552–9559.
- (131). Hilton S; Naud S; Caldwell JJ; Boxall K; Burns S; Anderson VE; Antoni L; Allen CE; Pearl LH; Oliver AW; et al. Identification and Characterisation of 2-Aminopyridine Inhibitors of Checkpoint Kinase 2. *Bioorg. Med. Chem* 2010, 18, 707–718. [PubMed: 20022510]

- (132). For selected reviews on C–F bond activation, see refs 132–134: Braun T; Perutz RN Routes to Fluorinated Organic Derivatives by Nickel Mediated C–F Activation of Heteroaromatics. *Chem. Commun* 2002, 2749–2757.
- (133). Amii H; Uneyama K C–F Bond Activation in Organic Synthesis. *Chem. Rev* 2009, 109, 2119–2183. [PubMed: 19331346]
- (134). Weaver J; Senaweera S C–F Activation and Functionalization of Perfluoro- and Polyfluoroarenes. *Tetrahedron* 2014, 70, 7413–7428.
- (135). Wei J; Liu K-M; Duan X-F Cobalt-Catalyzed Biaryl Couplings via C–F Bond Activation in the Absence of Phosphine or NHC Ligands. *J. Org. Chem* 2017, 82, 1291–1300. [PubMed: 27778507]
- (136). Manabe K; Ishikawa S *Ortho*-Selective Cross-Coupling of Fluorobenzenes with Grignard Reagents: Acceleration by Electron-Donating *Ortho*-Directing Groups. *Synthesis* 2008, 2008, 2645–2649.
- (137). For selected reviews on secondary phosphine oxide (SPO) preligands, see refs 137 and 138: Ackermann L Air- and Moisture-Stable Secondary Phosphine Oxides as Preligands in Catalysis. *Synthesis* 2006, 2006, 1557–1571.
- (138). Dubrovina NV; Börner A Enantioselective Catalysis with Chiral Phosphine Oxide Preligands. *Angew. Chem., Int. Ed* 2004, 43, 5883–5886.
- (139). For selected reviews on the application of HASPO preligands, see refs 139–141: Ackermann L Catalytic Arylations with Challenging Substrates: From Air-Stable HASPO Preligands to Indole Syntheses and C–H-Bond Functionalizations. *Synlett* 2007, 2007, 507–526.
- (140). Nemoto T; Hamada Y Pd-Catalyzed Asymmetric Allylic Substitution Reactions Using P-Chirogenic Diaminophosphine Oxides: DIAPHOXs. *Chem. Rec* 2007, 7, 150–158. [PubMed: 17551947]
- (141). Ackermann L Transition-Metal-Catalyzed Direct Arylations via C–H Bond Cleavages. *Pure Appl. Chem* 2010, 82, 1403–1413.
- (142). Ackermann L; Kapdi AR; Fenner S; Kornhaaß C; Schulzke C Well-Defined Air-Stable Palladium HASPO Complexes for Efficient Kumada–Corriu Cross-Couplings of (Hetero)Aryl or Alkenyl Tosylates. *Chem. - Eur. J* 2011, 17, 2965–2971. [PubMed: 21294197]
- (143). Ackermann L; Althammer A Air-Stable Pin P(O)H as Preligand for Palladium-Catalyzed Kumada Couplings of Unactivated Tosylates. *Org. Lett* 2006, 8, 3457–3460. [PubMed: 16869634]
- (144). For selected examples of coupling aryl bromides, chlorides, and fluorides using HASPO preligands, see refs 144–146: Ackermann L; Potukuchi HK; Althammer A; Born R; Mayer P Tetra-*Ortho*-Substituted Biaryls through Palladium-Catalyzed Suzuki–Miyaura Couplings with a Diaminochlorophosphine Ligand. *Org. Lett* 2010, 12, 1004–1007. [PubMed: 20131821]
- (145). Ackermann L; Spatz JH; Gschrei CJ; Born R; Althammer A A Diaminochlorophosphine for Palladium-Catalyzed Arylations of Amines and Ketones. *Angew. Chem., Int. Ed* 2006, 45, 7627–7630.
- (146). Ackermann L; Born R Modular Diamino- and Dioxophosphine Oxides and Chlorides as Ligands for Transition-Metal-Catalyzed C–C and C–N Couplings with Aryl Chlorides. *Angew. Chem., Int. Ed* 2005, 44, 2444–2447.
- (147). For selected initial reports of the carboxylate directing effect, see refs 147–149: Tanaka D; Romeril SP; Myers AG On the Mechanism of the Palladium(II)-Catalyzed Decarboxylative Olefination of Arene Carboxylic Acids. Crystallographic Characterization of Non-Phosphine Palladium(II) Intermediates and Observation of Their Stepwise Transformation in Heck-like Processes. *J. Am. Chem. Soc* 2005, 127, 10323–10333. [PubMed: 16028944]
- (148). Giri R; Mangel N; Li J-J; Wang D-H; Breazzano SP; Saunders LB; Yu J-Q Palladium-Catalyzed Methylation and Arylation of sp^2 and sp^3 C–H Bonds in Simple Carboxylic Acids. *J. Am. Chem. Soc* 2007, 129, 3510–3511. [PubMed: 17335217]
- (149). Mei T-S; Giri R; Mangel N; Yu J-Q Pd^{II}-Catalyzed Monoselective *Ortho*Halogenation of C–H Bonds Assisted by Counter Cations: A Complementary Method to Directed *Ortho*Li-thiation. *Angew. Chem., Int. Ed* 2008, 47, 5215–5219.

- (150). Font M; Quibell JM; Perry GJP; Larrosa I The Use of Carboxylic Acids as Traceless Directing Groups for Regioselective C–H Bond Functionalisation. *Chem. Commun* 2017, 53, 5584–5597.
- (151). Schwarz J; König B Decarboxylative Reactions with and without Light – A Comparison. *Green Chem.* 2018, 20, 323–361.
- (152). Wei Y; Hu P; Zhang M; Su W Metal-Catalyzed Decarboxylative C–H Functionalization. *Chem. Rev* 2017, 117, 8864–8907. [PubMed: 28266216]
- (153). Modak A; Maiti D Metal Catalyzed Defunctionalization Reactions. *Org. Biomol. Chem* 2016, 14, 21–35. [PubMed: 26565518]
- (154). Houpis IN; Van Hoeck J-P; Tilstam U Carboxylate-Directed Kumada Coupling of an Acetaldehyde Synthone with 2-Bromobenzoates Used towards the Synthesis of Isochromanes. *Synlett* 2007, 2007, 2179–2184.
- (155). Houpis IN; Huang C; Nettekoven U; Chen JG; Liu R; Canters M Carboxylate Directed Cross-Coupling Reactions in the Synthesis of Trisubstituted Benzoic Acids. *Org. Lett* 2008, 10, 5601–5604. [PubMed: 19053734]
- (156). Houpis IN; Weerts K; Nettekoven U; Canters M; Tan H; Liu R; Wang Y Palladium- and Copper-Catalyzed Site Selective Monoamination of Dibromobenzoic Acid. *Adv. Synth. Catal* 2011, 353, 538–544.
- (157). For a thorough review, see: Lindley J Copper Assisted Nucleophilic Substitution of Aryl Halogen. *Tetrahedron* 1984, 40, 1433–1456.
- (158). Liu S; Pestano JPC; Wolf C Regioselective Copper-Catalyzed C–N and C–S Bond Formation Using Amines, Thiols and Halobenzoic Acids. *Synthesis* 2007, 2007, 3519–3527.
- (159). Murai S; Kakiuchi F; Sekine S; Tanaka Y; Kamatani A; Sonoda M; Chatani N Efficient Catalytic Addition of Aromatic Carbon-Hydrogen Bonds to Olefins. *Nature* 1993, 366, 529–531.
- (160). Zhu F; Wang Z-X Nickel-Catalyzed Cross-Coupling of Aryl Fluorides and Organozinc Reagents. *J. Org. Chem* 2014, 79, 4285–4292. [PubMed: 24758137]
- (161). Nakamura Y; Yoshikai N; Ilies L; Nakamura E Nickel-Catalyzed Monosubstitution of Polyfluoroarenes with Organozinc Reagents Using Alkoxydiphosphine Ligand. *Org. Lett* 2012, 14, 3316–3319. [PubMed: 22691135]
- (162). Kawamoto K; Kochi T; Sato M; Mizushima E; Kakiuchi F Ruthenium-Catalyzed Arylation of Fluorinated Aromatic Ketones via *Ortho*-Selective Carbon–Fluorine Bond Cleavage. *Tetrahedron Lett.* 2011, 52, 5888–5890.
- (163). Crespo M; Martinez M; Sales J Effect of Fluorine Substituents in Intramolecular Activation of C–F and C–H Bonds by Platinum(II). *Organometallics* 1993, 12, 4297–4304.
- (164). Hill GS; Irwin MJ; Levy CJ; Rendina LM; Puddephatt RJ; Andersen RA; McLean L Platinum(II) Complexes of Dimethyl Sulfide. *Inorg. Synth* 2007, 32, 149–153.
- (165). Wang T; Alfonso BJ; Love JA Platinum(II)-Catalyzed Cross-Coupling of Polyfluoroaryl Imines. *Org. Lett* 2007, 9, 5629–5631. [PubMed: 18047367]
- (166). Wang T; Love JA Insight into the Mechanism of Platinum-Catalyzed Cross-Coupling of Polyfluoroaryl Imines. *Organometallics* 2008, 27, 3290–3296.
- (167). Buckley HL; Sun AD; Love JA User-Friendly Precatalyst for the Methylation of Polyfluoroaryl Imines. *Organometallics* 2009, 28, 6622–6624.
- (168). Sun AD; Love JA Pt(II)Cl₂(DMSO)₂-Catalyzed Cross-Coupling of Polyfluoroaryl Imines. *J. Fluorine Chem* 2010, 131, 1237–1240.
- (169). Buckley HL; Wang T; Tran O; Love JA Selective Platinum-Catalyzed C–F Bond Activation as a Route to Fluorinated Aryl Methyl Ethers. *Organometallics* 2009, 28, 2356–2359.
- (170). Sun AD; Love JA Nickel-Catalyzed Selective Defluorination to Generate Partially Fluorinated Biaryls. *Org. Lett* 2011, 13, 2750–2753. [PubMed: 21510620]
- (171). Yang X; Sun H; Zhang S; Li X Nickel-Catalyzed C–F Bond Activation and Alkylation of Polyfluoroaryl Imines. *J. Organomet. Chem* 2013, 723, 36–42.
- (172). Trost BM; Imi K; Davies IW Elaboration of Conjugated Alkenes Initiated by Insertion into a Vinylic C–H Bond. *J. Am. Chem. Soc* 1995, 117, 5371–5372.
- (173). Sonoda M; Kakiuchi F; Kamatani A; Chatani N; Murai S *Ruthenium-Catalyzed Addition of Aromatic Esters at the Ortho C–H Bonds to Olefins*. *Chem. Lett* 1996, 25, 109–110.

- (174). Yang W; Wang Y; Corte JR Efficient Synthesis of 2-Aryl-6-chloronicotinamides via PXPd₂-Catalyzed Regioselective Suzuki Coupling. *Org. Lett* 2003, 5, 3131–3134. [PubMed: 12916999]
- (175). Netherton MR; Fu GC Air-Stable Trialkylphosphonium Salts: Simple, Practical, and Versatile Replacements for Air-Sensitive Trialkylphosphines. Applications in Stoichiometric and Catalytic Processes. *Org. Lett* 2001, 3, 4295–4298. [PubMed: 11784201]
- (176). Hartwig JF; Kawatsura M; Hauck SI; Shaughnessy KH; Alcazar-Roman LM Room-Temperature Palladium-Catalyzed Amination of Aryl Bromides and Chlorides and Extended Scope of Aromatic C–N Bond Formation with a Commercial Ligand. *J. Org. Chem* 1999, 64, 5575–5580. [PubMed: 11674624]
- (177). Alcazar-Roman LM; Hartwig JF Mechanism of Aryl Chloride Amination: Base-Induced Oxidative Addition. *J. Am. Chem. Soc* 2001, 123, 12905–12906. [PubMed: 11749551]
- (178). Li GY; Zheng G; Noonan AF Highly Active, Air-Stable Versatile Palladium Catalysts for the C–C, C–N, and C–S Bond Formations via Cross-Coupling Reactions of Aryl Chlorides. *J. Org. Chem* 2001, 66, 8677–8681. [PubMed: 11735559]
- (179). Li GY The First Phosphine Oxide Ligand Precursors for Transition Metal Catalyzed Cross-Coupling Reactions: C–C, C–N, and C–S Bond Formation on Unactivated Aryl Chlorides. *Angew. Chem., Int. Ed* 2001, 40, 1513–1516.
- (180). Li GY Highly Active, Air-Stable Palladium Catalysts for the C–C and C–S Bond-Forming Reactions of Vinyl and Aryl Chlorides: Use of Commercially Available [(*t*-Bu)₂P(OH)]₂PdCl₂, [(*t*-Bu)₂P(OH)PdCl₂]₂, and [[(*t*-Bu)₂POPPPHHHOP(*t*-Bu)₂]PdCl]₂ as Catalysts. *J. Org. Chem* 2002, 67, 3643–3650. [PubMed: 12027675]
- (181). Li GY Catalysis Using Phosphine Oxide and Phosphine Sulfide Complexes with Pd and Ni for the Synthesis of Biaryls and Arylamines. Int. Patent WO2002000574A2, January 3, 2002.
- (182). Henderson BJ; Carper DJ; González-Cestari TF; Yi B; Mahasenan K; Pavlovicz RE; Dalefield ML; Coleman RS; Li C; McKay DB Structure–Activity Relationship Studies of Sulfonylpiperazine Analogues as Novel Negative Allosteric Modulators of Human Neuronal Nicotinic Receptors. *J. Med. Chem* 2011, 54, 8681–8692. [PubMed: 22060139]
- (183). Hu J; Jiang J; Costanzi S; Thomas C; Yang W; Feyen JHM; Jacobson KA; Spiegel AM A Missense Mutation in the Seven-Transmembrane Domain of the Human Ca²⁺ Receptor Converts a Negative Allosteric Modulator into a Positive Allosteric Modulator. *J. Biol. Chem* 2006, 281, 21558–21565. [PubMed: 16735501]
- (184). Yang W; Ruan Z; Wang Y; Van Kirk K; Ma Z; Arey BJ; Cooper CB; Seethala R; Feyen JHM; Dickson JK Discovery and Structure–Activity Relationships of Trisubstituted Pyrimidines/Pyridines as Novel Calcium-Sensing Receptor Antagonists. *J. Med. Chem* 2009, 52, 1204–1208. [PubMed: 19143533]
- (185). Nguyen T; Chiu W; Wang X; Sattler MO; Love JA Ligandless Nickel-Catalyzed *Ortho*-Selective Directed Trifluoromethylthiolation of Aryl Chlorides and Bromides Using AgSCF₃. *Org. Lett* 2016, 18, 5492–5495. [PubMed: 27736068]
- (186). Sambiasco C; Schönbauer D; Blicek R; Dao-Huy T; Pototschnig G; Schaaf P; Wiesinger T; Zia MF; Wencel-Delord J; Besset T; et al. A Comprehensive Overview of Directing Groups Applied in Metal-Catalyzed C–H Functionalization Chemistry. *Chem. Soc. Rev* 2018, 47, 6603–6743. [PubMed: 30033454]
- (187). Giri R; Chen X; Yu J-Q Palladium-Catalyzed Asymmetric Iodination of Unactivated C–H Bonds under Mild Conditions. *Angew. Chem., Int. Ed* 2005, 44, 2112–2115.
- (188). Giri R; Liang J; Lei J-G; Li J-J; Wang D-H; Chen X; Naggar IC; Guo C; Foxman BM; Yu J-Q Pd-Catalyzed Stereoselective Oxidation of Methyl Groups by Inexpensive Oxidants under Mild Conditions: A Dual Role for Carboxylic Anhydrides in Catalytic C–H Bond Oxidation. *Angew. Chem., Int. Ed* 2005, 44, 7420–7424.
- (189). Chen X; Li J-J; Hao X-S; Goodhue CE; Yu J-Q Palladium-Catalyzed Alkylation of Aryl C–H Bonds with sp³ Organotin Reagents Using Benzoquinone as a Crucial Promoter. *J. Am. Chem. Soc* 2006, 128, 78–79. [PubMed: 16390130]
- (190). Yu D; Shen Q; Lu L Selective Palladium-Catalyzed C–F Activation/Carbon–Carbon Bond Formation of Polyfluoroaryl Oxazolines. *J. Org. Chem* 2012, 77, 1798–1804. [PubMed: 22283549]

- (191). For selected reviews on C–X/C–H activation, see refs 191–194: Ackermann L; Vicente R; Kapdi AR Transition-Metal-Catalyzed Direct Arylation of (Hetero)Arenes by C–H Bond Cleavage. *Angew. Chem., Int. Ed* 2009, 48, 9792–9826.
- (192). Chen X; Engle KM; Wang D-H; Yu J-Q Palladium(II)-Catalyzed C–H Activation/C–C Cross-Coupling Reactions: Versatility and Practicality. *Angew. Chem., Int. Ed* 2009, 48, 5094–5115.
- (193). Alberico D; Scott ME; Lautens M Aryl–Aryl Bond Formation by Transition-Metal-Catalyzed Direct Arylation. *Chem. Rev* 2007, 107, 174–238. [PubMed: 17212475]
- (194). Campeau L-C; Fagnou K Applications of and Alternatives to I-Electron-Deficient Azine Organometallics in Metal Catalyzed Cross-Coupling Reactions. *Chem. Soc. Rev* 2007, 36, 1058–1068. [PubMed: 17576474]
- (195). For selected examples on C–X/C–H activation, see refs 195–197: Ye M; Gao G-L; Edmunds AJF; Worthington PA; Morris JA; Yu J-Q Ligand-Promoted C3-Selective Arylation of Pyridines with Pd Catalysts: Gram-Scale Synthesis of (γ)-Preclamol. *J. Am. Chem. Soc* 2011, 133, 19090–19093. [PubMed: 22059931]
- (196). Sun C-L; Li H; Yu D-G; Yu M; Zhou X; Lu X-Y; Huang K; Zheng S-F; Li B-J; Shi Z-J An Efficient Organo-catalytic Method for Constructing Biaryls through Aromatic C–H Activation. *Nat. Chem* 2010, 2, 1044–1049. [PubMed: 21107368]
- (197). Muto K; Yamaguchi J; Itami K Nickel-Catalyzed C–H/C–O Coupling of Azoles with Phenol Derivatives. *J. Am. Chem. Soc* 2012, 134, 169–172. [PubMed: 22148419]
- (198). Müller K; Faeh C; Diederich F Fluorine in Pharmaceuticals: Looking Beyond Intuition. *Science* 2007, 317, 1881–1886. [PubMed: 17901324]
- (199). Murphy AR; Fréchet MJJ Organic Semiconducting Oligomers for Use in Thin Film Transistors. *Chem. Rev* 2007, 107, 1066–1096. [PubMed: 17428023]
- (200). Yu D; Lu L; Shen Q Palladium-Catalyzed Coupling of Polyfluorinated Arenes with Heteroarenes via C–F/C–H Activation. *Org. Lett* 2013, 15, 940–943. [PubMed: 23391131]
- (201). Yu D; Wang C-S; Yao C; Shen Q; Lu L Nickel-Catalyzed α -Arylation of Zinc Enolates with Polyfluoroarenes via C–F Bond Activation under Neutral Conditions. *Org. Lett* 2014, 16, 5544–5547. [PubMed: 25321322]
- (202). Xiao S-H; Xiong Y; Zhang X-X; Cao S Nickel-Catalyzed *N*-Heterocycle-Directed Cross-Coupling of Fluorinated Arenes with Organozinc Reagents. *Tetrahedron* 2014, 70, 4405–4411.
- (203). Guo W-H; Min Q-Q; Gu J-W; Zhang X Rhodium-Catalyzed *Ortho*-Selective C–F Bond Borylation of Polyfluoroarenes with Bpin–Bpin. *Angew. Chem., Int. Ed* 2015, 54, 9075–9078.
- (204). Kim YM; Yu S Palladium(0)-Catalyzed Amination, Stille Coupling, and Suzuki Coupling of Electron-Deficient Aryl Fluorides. *J. Am. Chem. Soc* 2003, 125, 1696–1697. [PubMed: 12580584]
- (205). Widdowson DA; Wilhelm R Palladium Catalysed Suzuki Reactions of Fluoroarenes. *Chem. Commun* 2003, 34, 578–579.
- (206). Cargill MR; Sandford G; Tadeusiak AJ; Yufit DS; Howard JAK; Kilickiran P; Nelles G Palladium-Catalyzed C–F Activation of Polyfluoronitrobenzene Derivatives in Suzuki–Miyaura Coupling Reactions. *J. Org. Chem* 2010, 75, 5860–5866. [PubMed: 20704342]
- (207). Sucunza D; Cuadro AM; Alvarez-Builla J; Vaquero JJ Recent Advances in the Synthesis of Azonia Aromatic Heterocycles. *J. Org. Chem* 2016, 81, 10126–10135. [PubMed: 27385555]
- (208). José Reyes M; Luisa Izquierdo M; Alvarez-Builla J Suzuki Reaction on Pyridinium *N*-(5-Bromoheteroar-2-yl)aminides. *Tetrahedron Lett.* 2004, 45, 8713–8715.
- (209). Sliwa W; Bachowska B; Zelichowicz N Chemistry of Viologens. *Heterocycles* 1991, 32, 2241–2273.
- (210). Ollis WD; Stanforth SP; Ramsden CA Heterocyclic Mesomeric Betaines. *Tetrahedron* 1985, 41, 2239–2329.
- (211). Sánchez A; Núñez A; Alvarez-Builla J; Burgos C Pyridinium *N*-2'-Pyridylaminide: Synthesis of 3-Aryl-2-aminopyridines through an Intramolecular Radical Process. *Tetrahedron* 2004, 60, 11843–11850.
- (212). Nuñez A; de Viedma AG; Martínez-Barrasa V; Burgos C; Alvarez-Builla J *N*-Azinylpyridinium *N*-Aminides: An Approach to Pyrazolopyridines via an Intramolecular Radical Pathway. *Synlett* 2002, 2002, 1093–1096.

- (213). José Reyes M; Delgado F; Luisa Izquierdo M; Alvarez-Builla J Pyridinium *N*-(2'-Azinyl)Aminides: Regioselective Synthesis of *N*-(2-Pyridyl) Substituted Polyamines. *Tetrahedron* 2002, 58, 8573–8579.
- (214). Martínez-Barrasa V.in; Delgado F; Burgos C; Luis García-Navío J; Luisa Izquierdo M; Alvarez-Builla J Pyridinium *N*-(2'-Azinyl)Aminides: Regioselective Synthesis of 2-Alkylaminoazines. *Tetrahedron* 2000, 56, 2481–2490.
- (215). Castillo R; Reyes MJ; Izquierdo ML; Alvarez-Builla J Suzuki Reaction on Pyridinium *N*-Haloheteroarylaminides: Regioselective Synthesis of 3,5-Disubstituted 2-Aminopyrazines. *Tetrahedron* 2008, 64, 1351–1370.
- (216). Reyes MJ; Castillo R; Izquierdo ML; Alvarez-Builla J Regioselective Suzuki Coupling on Pyridinium *N*-(3,5-Dibromoheteroar-2-yl)Aminides. *Tetrahedron Lett.* 2006, 47, 6457–6460.
- (217). Zhao P; Young MD; Beaudry CM Regioselective Suzuki Couplings of Non-Symmetric Dibromobenzenes: Alkenes as Regiochemical Control Elements. *Org. Biomol. Chem* 2015, 13, 6162–6165. [PubMed: 25947551]
- (218). Johnson JB; Rovis T More Than Bystanders: The Effect of Olefins on Transition-Metal-Catalyzed Cross-Coupling Reactions. *Angew. Chem., Int. Ed* 2008, 47, 840–871.
- (219). Macé Y; Kapdi AR; Fairlamb IJS; Jutand A Influence of the *dba* Substitution on the Reactivity of Palladium(0) Complexes Generated from Pd⁰₂(*dba-n, n'-Z*)₂ and PPh₃ in Oxidative Addition with Iodobenzene. *Organometallics* 2006, 25, 1795–1800.
- (220). Amatore C; Broeker G; Jutand A; Khalil F Identification of the Effective Palladium(0) Catalytic Species Generated *in situ* from Mixtures of Pd(*dba*)₂ and Bidentate Phosphine Ligands. Determination of their Rates and Mechanism in Oxidative Addition. *J. Am. Chem. Soc* 1997, 119, 5176–5185.
- (221). Amatore C; Jutand A; Khalil F; M'Barki MA; Mottier L Rates and Mechanisms of Oxidative Addition to Zerovalent Palladium Complexes Generated *in situ* from Mixtures of Pd0(*dba*)₂ and Triphenylphosphine. *Organometallics* 1993, 12, 3168–3178.
- (222). Orner BP; Ernst JT; Hamilton AD Toward Proteomimetics: Terphenyl Derivatives as Structural and Functional Mimics of Extended Regions of an α -Helix. *J. Am. Chem. Soc* 2001, 123, 5382–5383. [PubMed: 11457415]
- (223). Zhao P; Beaudry CM Enantioselective and Regioselective Pyrone Diels–Alder Reactions of Vinyl Sulfones: Total Synthesis of (+)-Cavicularin. *Angew. Chem. Int. Ed* 2014, 53, 10500–10503.
- (224). Zhao P; Beaudry CM Total Synthesis of (γ)-Cavicularin: Control of Pyrone Diels–Alder Regiochemistry Using Isomeric Vinyl Sulfones. *Org. Lett* 2013, 15, 402–405. [PubMed: 23301524]
- (225). For selected examples of oligoarene-type phosphines, see refs 225–228; Matsui K; Takizawa S; Sasai H A Brønsted Acid and Lewis Base Organocatalyst for the Aza-Morita–Baylis–Hillman reaction. *Synlett* 2006, 5, 761–765.
- (226). Iwasawa T; Komano T; Tajima A; Tokunaga M; Obora Y; Fujihara T; Tsuji Y Phosphines Having a 2,3,4,5-Tetraphenylphenyl Moiety: Effective Ligands in Palladium-Catalyzed Transformations of Aryl Chlorides. *Organometallics* 2006, 25, 4665–4669.
- (227). Matsumoto T; Kasai T; Tatsumi K Chiral Crystallization of a Linear Two-coordinated Palladium(0) Complex Bearing Propeller-shaped Bulky Phosphine Ligands. *Chem. Lett* 2002, 31, 346–347.
- (228). Yu H-B; Hu Q-S; Pu L The First Optically Active BINOL–BINAP Copolymer Catalyst: Highly Stereoselective Tandem Asymmetric Reactions. *J. Am. Chem. Soc* 2000, 122, 6500–6501.
- (229). Martin R; Buchwald SL Pd-Catalyzed Kumada–Corriu Cross-Coupling Reactions at Low Temperatures Allow the Use of Knochel-type Grignard Reagents. *J. Am. Chem. Soc* 2007, 129, 3844–3845. [PubMed: 17352483]
- (230). Barder TE; Walker SD; Martinelli JR; Buchwald SL Catalysts for Suzuki–Miyaura Coupling Processes: Scope and Studies of the Effect of Ligand Structure. *J. Am. Chem. Soc* 2005, 127, 4685–4696. [PubMed: 15796535]
- (231). Huang X; Anderson KW; Zim D; Jiang L; Klapars A; Buchwald SL Expanding Pd-Catalyzed C–N Bond-Forming Processes: The First Amidation of Aryl Sulfonates, Aqueous Amination,

- and Complementarity with Cu-Catalyzed Reactions. *J. Am. Chem. Soc.* 2003, 125, 6653–6655. [PubMed: 12769573]
- (232). Parrish CA; Buchwald SL Use of Polymer-Supported Dialkylphosphinobiphenyl Ligands for Palladium-Catalyzed Amination and Suzuki Reactions. *J. Org. Chem.* 2001, 66, 3820–3827. [PubMed: 11375003]
- (233). For selected examples of phosphines with a hydroxy group, see refs 233 and 234: Yoshikai N; Matsuda H; Nakamura E Hydroxyphosphine Ligand for Nickel-Catalyzed Cross-Coupling through Nickel/Magnesium Bimetallic Cooperation. *J. Am. Chem. Soc.* 2009, 131, 9590–9599. [PubMed: 19522507]
- (234). Meng X; Huang Y; Chen R A Novel Selective Aza-Morita–Baylis–Hillman (Aza-MBH) Domino Reaction and Aza-MBH Reaction of N-Sulfonated Imines with Acrolein Catalyzed by a Bifunctional Phosphine Organocatalyst. *Chem. - Eur. J.* 2008, 14, 6852–6856. [PubMed: 18581386]
- (235). Ishikawa S; Manabe K Oligoarene Strategy for Catalyst Development. Hydroxylated Oligoarene-type Phosphines for Palladium-Catalyzed Cross-Coupling. *Chem. Lett.* 2007, 36, 1302–1303.
- (236). Ishikawa S; Manabe K Synthesis of Hydroxylated Oligoarene-type Phosphines by a Repetitive Two-Step Method. *Tetrahedron* 2010, 66, 297–303.
- (237). Ishikawa S; Manabe K *Ortho*-Selective Cross Coupling of Dibromophenols and Dibromoanilines with Grignard Reagents in the Presence of Palladium Catalysts Bearing Hydroxylated Oligoarene-type Phosphine. *Chem. Lett.* 2007, 36, 1304–1305.
- (238). Ishikawa S; Manabe K DHTP Ligands for the Highly *Ortho*-Selective, Palladium-Catalyzed Cross-Coupling of Dihaloarenes with Grignard Reagents: A Conformational Approach for Catalyst Improvement. *Angew. Chem. Int. Ed.* 2010, 49, 772–775.
- (239). Ishikawa S; Manabe K Hydroxylated Terphenylphosphine Ligands for Palladium-Catalyzed *Ortho*-Selective Cross-Coupling of Dibromophenols, Dibromoanilines, and their Congeners with Grignard Reagents. *Tetrahedron* 2011, 67, 10156–10163.
- (240). Yamaguchi M; Akiyama T; Sasou H; Katsumata H; Manabe K One-Pot Synthesis of Substituted Benzo[*b*]furans and Indoles from Dichlorophenols/Dichloroanilines Using a Palladium–Dihydroxyterphenylphosphine Catalyst. *J. Org. Chem.* 2016, 81, 5450–5463. [PubMed: 27267124]
- (241). Yamaguchi M; Katsumata H; Manabe K One-Pot Synthesis of Substituted Benzo[*b*]furans from Mono- and Dichlorophenols Using Palladium Catalysts Bearing Dihydroxyterphenylphosphine. *J. Org. Chem.* 2013, 78, 9270–9281. [PubMed: 23952238]
- (242). Wang J-R; Manabe K Hydroxyterphenylphosphine–Palladium Catalyst for Benzo[*b*]furan Synthesis from 2-Chlorophenols. Bifunctional Ligand strategy for Cross-Coupling of Chloroarenes. *J. Org. Chem.* 2010, 75, 5340–5342. [PubMed: 20578763]
- (243). Yamaguchi M; Manabe K One-Pot Synthesis of 2,4-Disubstituted Indoles from *N*-Tosyl-2,3-Dichloroaniline Using Palladium–Dihydroxyterphenylphosphine Catalyst. *Org. Lett.* 2014, 16, 2386–2389. [PubMed: 24742051]
- (244). Yamaguchi M; Manabe K Three-Step Synthesis of 2,5,7-Trisubstituted Indoles from *N*-Acetyl-2,4,6-trichloroaniline Using Pd-Catalyzed Site-Selective Cross-Coupling. *Org. Biomol. Chem.* 2017, 15, 6645–6655. [PubMed: 28752876]
- (245). Konishi H; Itoh T; Manabe K Site-Selective Cross-Coupling of Dichlorinated Benzo-Fused Nitrogen-Heterocycles with Grignard Reagents. *Chem. Pharm. Bull.* 2010, 58, 1255–1258.
- (246). Davis HJ; Phipps RJ Harnessing Non-Covalent Interactions to Exert Control Over Regioselectivity and Site-Selectivity in Catalytic Reactions. *Chem. Sci.* 2017, 8, 864–877. [PubMed: 28572898]
- (247). Zhang J; Sha S-C; Bellomo A; Trongsiwat N; Gao F; Tomson NC; Walsh PJ Positional Selectivity in C–H Functionalizations of 2-Benzylfurans with Bimetallic Catalysts. *J. Am. Chem. Soc.* 2016, 138, 4260–4266. [PubMed: 26937718]
- (248). Dydio P; Reek JNH Supramolecular Control of Selectivity in Transition-Metal Catalysis through Substrate Preorganization. *Chem. Sci.* 2014, 5, 2135–2145.

- (249). Raynal M; Ballester P; Vidal-Ferran A; van Leeuwen PWNM Supramolecular Catalysis. Part 1: Non-Covalent Interactions as a Tool for Building and Modifying Homogeneous Catalysts. *Chem. Soc. Rev* 2014, 43, 1660–1733. [PubMed: 24356298]
- (250). Anderson KW; Buchwald SL General Catalysts for the Suzuki–Miyaura and Sonogashira Coupling Reactions of Aryl Chlorides and for the Coupling of Challenging Substrate Combinations in Water. *Angew. Chem., Int. Ed* 2005, 44, 6173–6177.
- (251). Surry DS; Buchwald SL Biaryl Phosphane Ligands in Palladium-Catalyzed Amination. *Angew. Chem., Int. Ed* 2008, 47, 6338–6361.
- (252). For selected applications of sulfonylated phosphine ligands, see refs 252–255: Rojas AJ; Pentelute BL; Buchwald SL Water-Soluble Palladium Reagents for Cysteine S-Arylation under Ambient Aqueous Conditions. *Org. Lett* 2017, 19, 4263–4266. [PubMed: 28777001]
- (253). Janusson E; Zijlstra HS; Nguyen PPT; MacGillivray L; Martelino J; McIndoe JS Real-Time Analysis of Pd₂(dba)₃ Activation by Phosphine Ligands. *Chem. Commun* 2017, 53, 854–856.
- (254). Corr MJ; Sharma SV; Pubill-Ulldemolins C; Bown RT; Poirot P; Smith DRM; Cartmell C; Abou Fayad A; Goss RJM Sonogashira Diversification of Unprotected Halotryptophans, Halotryptophan Containing Tripeptides; and Generation of a New to Nature Bromo-Natural Product and its Diversification in Water. *Chem. Sci* 2017, 8, 2039–2046. [PubMed: 28451322]
- (255). Jiang H; Jia T; Zhang M; Walsh PJ Palladium-Catalyzed Arylation of Aryl Sulfenate Anions with Aryl Bromides under Mild Conditions: Synthesis of Diaryl Sulfoxides. *Org. Lett* 2016, 18, 972–975. [PubMed: 26878149]
- (256). Golding WA; Pearce-Higgins R; Phipps RJ Site-Selective Cross-Coupling of Remote Chlorides Enabled by Electrostatically Directed Palladium Catalysis. *J. Am. Chem. Soc* 2018, 140, 13570–13574. [PubMed: 30295472]
- (257). Golding WA; Phipps RJ Electrostatically-Directed Pd-Catalysis in Combination with C–H Activation: Site-Selective Coupling of Remote Chlorides with Fluoroarenes and Fluoroheteroarenes. *Chem. Sci* 2020, 11, 3022–3027. [PubMed: 34122805]
- (258). For selected reviews of C–H activation with fluoroarenes and fluoroheteroarenes, see refs 258 and 259: Eisenstein O; Milani J; Perutz RN Selectivity of C–H Activation and Competition between C–H and C–F Bond Activation at Fluorocarbons. *Chem. Rev* 2017, 117, 8710–8753. [PubMed: 28653537]
- (259). Clot E; Eisenstein O; Jasim N; Macgregor SA; McGrady JE; Perutz RN C–F and C–H Bond Activation of Fluorobenzenes and Fluoropyridines at Transition Metal Centers: How Fluorine Tips the Scales. *Acc. Chem. Res* 2011, 44, 333–348. [PubMed: 21410234]
- (260). Lafrance M; Fagnou K Palladium-Catalyzed Benzene Arylation: Incorporation of Catalytic Pivalic Acid as a Proton Shuttle and a Key Element in Catalyst Design. *J. Am. Chem. Soc* 2006, 128, 16496–16497. [PubMed: 17177387]
- (261). Lafrance M; Rowley CN; Woo TK; Fagnou K Catalytic Intermolecular Direct Arylation of Perfluorobenzenes. *J. Am. Chem. Soc* 2006, 128, 8754–8756. [PubMed: 16819868]
- (262). Lafrance M; Shore D; Fagnou K Mild and General Conditions for the Cross-Coupling of Aryl Halides with Penta-fluorobenzene and Other Perfluoroaromatics. *Org. Lett* 2006, 8, 5097–5100. [PubMed: 17048852]
- (263). Golding WA; Schmitt HL; Phipps RJ Systematic Variation of Ligand and Cation Parameters Enables Site-Selective C–C and C–N Cross-Coupling of Multiply Chlorinated Arenes through Substrate–Ligand Electrostatic Interactions. *J. Am. Chem. Soc* 2020, 142, 21891–21898. [PubMed: 33332114]
- (264). Chung JYL; Cai C; McWilliams JC; Reamer RA; Dormer PG; Cvetovich RJ Efficient Synthesis of a Trisubstituted 1,6-Naphthyridone from Acetonedicarboxylate and Regioselective Suzuki Arylation. *J. Org. Chem* 2005, 70, 10342–10347. [PubMed: 16323843]
- (265). Chung JYL Development of a Practical Synthesis of Naphthyridone p38 MAP Kinase Inhibitor MK-0913; Wiley-VCH Verlag GmbH & Co. KGaA: Weinheim, Germany, 2013; pp 39–56.
- (266). Cai C; Chung JYL; McWilliams JC; Sun Y; Shultz CS; Palucki M From High-Throughput Catalyst Screening to Reaction Optimization: Detailed Investigation of Regioselective Suzuki Coupling of 1,6-Naphthyridone Dichloride. *Org. Process Res. Dev* 2007, 11, 328–335.
- (267). For the cross-coupling of dihaloazoles by Strotman, Chobanian, and coworkers, see ref 101.

- (268). Wiglenda T; Gust R Structure–Activity Relationship Study to Understand the Estrogen Receptor-Dependent Gene Activation of Aryl- and Alkyl-Substituted 1*H*-Imidazoles. *J. Med. Chem* 2007, 50, 1475–1484. [PubMed: 17352461]
- (269). Stangeland EL; Sammakia T Use of Thiazoles in the Halogen Dance Reaction: Application to the Total Synthesis of WS75624 B. *J. Org. Chem* 2004, 69, 2381–2385. [PubMed: 15049634]
- (270). Flegeau EF; Popkin ME; Greaney MF Direct Arylation of Oxazoles at C2. A Concise Approach to Consecutively Linked Oxazoles. *Org. Lett* 2008, 10, 2717–2720. [PubMed: 18540631]
- (271). The preferred site of lithium halogen exchange on 2,4-dibromothiazole is C2: Martin T; Laguerre C; Hoarau C; Marsais F Highly Efficient Borylation Suzuki Coupling Process for 4-Bromo-2-ketothiazoles: Straightforward Access to Micrococinate and Saramycetate Esters. *Org. Lett* 2009, 11, 3690–3693. [PubMed: 19624105]
- (272). The preferred site of S_NAr on 2,4-dibromothiazoles with thiols is C2: Nicolaou KC; Sasmal PK; Rassias G; Reddy MV; Altmann K-H; Wartmann M; O’Brate A; Giannakakou P Design, Synthesis, and Biological Properties of Highly Potent Epothilone B Analogues. *Angew. Chem., Int. Ed* 2003, 42, 3515–3520.
- (273). Handy’s method for predicting the site of coupling in dihaloheteroaromatics using the 1H NMR shifts of the parent nonhalogenated compound incorrectly predicts reactivity at the C2 position of 2,4-diiodooxazole and 2,5-dibromo-1-methylimidazole; see ref 57.
- (274). Dai X; Chen Y; Garrell S; Liu H; Zhang L-K; Palani A; Hughes G; Nargund R Ligand-Dependent Site-Selective Suzuki Cross-Coupling of 3,5-Dichloropyridazines. *J. Org. Chem* 2013, 78, 7758–7763. [PubMed: 23848481]
- (275). Yang M; Chen J; He C; Hu X; Ding Y; Kuang Y; Liu J; Huang Q Palladium-Catalyzed C-4 Selective Coupling of 2,4-Dichloropyridines and Synthesis of Pyridine-Based Dyes for Live-Cell Imaging. *J. Org. Chem* 2020, 85, 6498–6508. [PubMed: 32329338]
- (276). Wang RX; Lai XJ; Qiu G; Liu JB Research Progress of Reactive Fluorescent Probe Based on ES IPT Principle. *Youji Huaxue* 2019, 39, 952–960.
- (277). Gong J; Li Y-H; Zhang C-J; Huang J; Sun Q A Thiazolo[4,5-*b*]Pyridine-Based Fluorescent Probe for Detection of Zinc Ions and Application for *in vitro* and *in vivo* Bioimaging. *Talanta* 2018, 185, 396–404. [PubMed: 29759218]
- (278). Zhang J; Wang H Photophysical Investigations and the Bioimaging of *i*-, -, -Pyridine-Based Terpyridine Derivatives. *J. Mol. Struct* 2018, 1157, 457–462.
- (279). Golden JH; Facendola JW; Sylvinson MR,D; Baez CQ; Djurovich PI; Thompson ME Boron Dipyritylmethene (DIPYR) Dyes: Shedding light on Pyridine-Based Chromophores. *J. Org. Chem* 2017, 82, 7215–7222. [PubMed: 28675038]
- (280). Chen J; Liu W; Ma J; Xu H; Wu J; Tang X; Fan Z; Wang P Synthesis and Properties of Fluorescence Dyes: Tetracyclic Pyrazolo[3,4-*b*]Pyridine-Based Coumarin Chromophores with Intramolecular Charge Transfer Character. *J. Org. Chem* 2012, 77, 3475–3482. [PubMed: 22428730]
- (281). Biscoe MR; Fors BP; Buchwald SL A New Class of Easily Activated Palladium Precatalysts for Facile C–N Cross-Coupling Reactions and the Low Temperature Oxidative Addition of Aryl Chlorides. *J. Am. Chem. Soc* 2008, 130, 6686–6687. [PubMed: 18447360]
- (282). Kinzel T; Zhang Y; Buchwald SL A New Palladium Precatalyst Allows for the Fast Suzuki–Miyaura Coupling Reactions of Unstable Polyfluorophenyl and 2-Heteroarylboronic Acids. *J. Am. Chem. Soc* 2010, 132, 14073–14075. [PubMed: 20858009]
- (283). Shu W; Buchwald SL Use of Precatalysts Greatly Facilitate Palladium-Catalyzed Alkynylations in Batch and Continuous-Flow Conditions. *Chem. Sci* 2011, 2, 2321–2325.
- (284). Yang Y; Oldenhuis NJ; Buchwald SL Mild and General Conditions for Negishi Cross-Coupling Enabled by the Use of Palladacycle Precatalysts. *Angew. Chem., Int. Ed* 2013, 52, 615–619.
- (285). Bruno NC; Niljianskul N; Buchwald SL *N*-Substituted 2-Aminobiphenylpalladium Methanesulfonate Precatalysts and Their Use in C–C and C–N Cross-Couplings. *J. Org. Chem* 2014, 79, 4161–4166. [PubMed: 24724692]
- (286). Friis SD; Skrydstrup T; Buchwald SL Mild Pd-Catalyzed Aminocarbonylation of (Hetero)Aryl Bromides with a Palladacycle Precatalyst. *Org. Lett* 2014, 16, 4296–4299. [PubMed: 25090373]

- (287). Ingoglia BT; Buchwald SL Oxidative Addition Complexes as Precatalysts for Cross-Coupling Reactions Requiring Extremely Bulky Biarylphosphine Ligands. *Org. Lett* 2017, 19, 2853–2856. [PubMed: 28498667]
- (288). Ruiz-Castillo P; Buchwald SL Applications of Palladium-Catalyzed C–N Cross-Coupling Reactions. *Chem. Rev* 2016, 116, 12564–12649. [PubMed: 27689804]
- (289). Bruno NC; Tudge MT; Buchwald SL Design and Preparation of New Palladium Precatalysts for C–C and C–N Cross-Coupling Reactions. *Chem. Sci* 2013, 4, 916–920. [PubMed: 23667737]
- (290). Bruno NC; Buchwald SL Synthesis and Application of Palladium Precatalysts that Accommodate Extremely Bulky Di-*tert*-butylphosphino Biaryl Ligands. *Org. Lett* 2013, 15, 2876–2879. [PubMed: 23675976]
- (291). Cheung CW; Surry DS; Buchwald SL Mild and Highly Selective Palladium-Catalyzed Monoarylation of Ammonia Enabled by the Use of Bulky Biarylphosphine Ligands and Palladacycle Precatalysts. *Org. Lett* 2013, 15, 3734–3737. [PubMed: 23815096]
- (292). Cheung CW; Buchwald SL Mild and General Palladium-Catalyzed Synthesis of Methyl Aryl Ethers Enabled by the Use of a Palladacycle Precatalyst. *Org. Lett* 2013, 15, 3998–4001. [PubMed: 23883393]
- (293). Cheung CW; Buchwald SL Palladium-Catalyzed Hydroxylation of Aryl and Heteroaryl Halides Enabled by the Use of a Palladacycle Precatalyst. *J. Org. Chem* 2014, 79, 5351–5358. [PubMed: 24762125]
- (294). Hadei N; Kantchev EAB; O'Brien CJ; Organ MG The First Negishi Cross-Coupling Reaction of Two Alkyl Centers Utilizing a Pd–N-Heterocycle Carbene (NHC) Catalyst. *Org. Lett* 2005, 7, 3805–3807. [PubMed: 16092880]
- (295). Nasielski J; Hadei N; Achonduh G; Kantchev EAB; O'Brien CJ; Lough A; Organ MG Structure–Activity Relationship Analysis of Pd–PEPPSI Complexes in Cross-Couplings: A Close Inspection of the Catalytic Cycle and the Precatalyst Activation Model. *Chem. - Eur. J* 2010, 16, 10844–10853. [PubMed: 20665575]
- (296). Valente C; Belowich ME; Hadei N; Organ MG Pd-PEPPSI Complexes and the Negishi Reaction. *Eur. J. Org. Chem* 2010, 2010, 4343–4354.
- (297). O'Brien CJ; Kantchev EAB; Valente C; Hadei N; Chass GA; Lough A; Hopkinson AC; Organ MG Easily Prepared Air- and Moisture-Stable Pd-NHC (NHC = N-Heterocyclic Carbene) Complexes: A Reliable, User-Friendly, Highly Active Palladium Precatalyst for the Suzuki–Miyaura Reaction. *Chem. - Eur. J* 2006, 12, 4743–4748. [PubMed: 16568494]
- (298). Organ MG; Avola S; Dubovyk I; Hadei N; Kantchev EAB; O'Brien CJ; Valente C A User-Friendly, All-Purpose Pd-NHC (NHC = N-Heterocyclic Carbene) Precatalyst for the Negishi Reaction: A Step Towards a Universal Cross-Coupling Catalyst. *Chem. - Eur. J* 2006, 12, 4749–4755. [PubMed: 16568493]
- (299). For selected examples of the Handy group's work on the development of one-pot polycoupling approaches to substituted heteroaromatics, see refs 99 and 299–301: Handy ST; Sabatini JJ Regioselective Dicouplings: Application to Differentially Substituted Pyrroles. *Org. Lett* 2006, 8, 1537–1539. [PubMed: 16597104]
- (300). Handy ST; Wilson T; Muth A Disubstituted Pyridines: The Double-Coupling Approach. *J. Org. Chem* 2007, 72, 8496–8500. [PubMed: 17918901]
- (301). Handy ST; Mayi D Regioselective Double Suzuki Couplings of 4,5-Dibromothiophene-2-carboxylate. *Tetrahedron Lett.* 2007, 48, 8108–8110. [PubMed: 19008934]
- (302). Zhang Y; Handy ST A Solvent-Induced Reversal of Regioselectivity in the Suzuki Coupling of Pyrrole Esters. *Open Org. Chem. J* 2008, 2, 58–64.
- (303). For selected examples of the chelation of the nitrogen atom in pyrrole to transition-metal catalysts, see refs 303–305: Wiest JM; Pöthig A; Bach T Pyrrole as a Directing group: Regioselective Pd(II)-Catalyzed Alkylation and Benzylolation at the Benzene Core of 2-Phenylpyrroles. *Org. Lett* 2016, 18, 852–855. [PubMed: 26845081]
- (304). Jiao L; Bach T Palladium-Catalyzed Direct C–H Alkylation of Electron-Deficient Pyrrole Derivatives. *Angew. Chem., int. Ed* 2013, 52, 6080–6083.

- (305). Zhang M; Zhang Y; Jie X; Zhao H; Li G; Su W Recent Advances in Directed C–H Functionalizations Using Monodentate Nitrogen-based Directing Groups. *Org. Chem. Front* 2014, 1, 843–895.
- (306). The Suzuki coupling of **248** in a 3:1 mixture of benzene and methanol proceeded to give an outcome indistinguishable from that of the toluene/ethanol mixture.
- (307). Handy ST; Zhang Y; Bregman H A Modular Synthesis of the Lamellarins: Total Synthesis of Lamellarin G Trimethyl Ether. *J. Org. Chem* 2004, 69, 2362–2366. [PubMed: 15049631]
- (308). For the site-selective Stille coupling of 3,5-dibromo-2-pyrone, see: Kim W-S; Kim H-J; Cho C-G Regioselectivity in the Stille Coupling Reactions of 3,5-Dibromo-2-pyrone. *J. Am. Chem. Soc* 2003, 125, 14288–14289. [PubMed: 14624572]
- (309). The polarity of the solvents is described based on the reported dielectric constants. For context, see refs 309 and 310: Vogel AI; Furniss BS; Hannaford AJ; Smith PWG; Tatchell AR Vogel's Textbook of Practical Organic Chemistry, 5th ed.; Pearson Education Limited: Essex, U.K., 1989; pp 395–468.
- (310). Common Solvents Used in Organic Chemistry: Table of Properties. https://www.organicdivision.org/wp-content/uploads/2016/12/organic_solvents.html (accessed 2020-07-10).
- (311). Interestingly and in contrast with ref 94, when the oxidative addition was carried out with a stoichiometric amount of Pd(PPh₃)₄, the formation of C5–Pd complex **258** was not observed, and only C3–Pd complex **257** could be isolated.
- (312). Farina V; Kapadia S; Krishnan B; Wang C; Liebeskind LS On the Nature of the “Copper Effect” in the Stille Cross-Coupling. *J. Org. Chem* 1994, 59, 5905–5911.
- (313). Beaupérin M; Job A; Cattey H; Royer S; Meunier P; Hierso J-C Copper(I) Iodide Polyphosphine Adducts at Low Loading for Sonogashira Alkynylation of Demanding Halide Substrates: Ligand Exchange Study between Copper and Palladium. *Organometallics* 2010, 29, 2815–2822.
- (314). Aufero M; Proutiere F; Schoenebeck F Redox Reactions in Palladium Catalysis: On the Accelerating and/or Inhibiting Effects of Copper and Silver Salt Additives in Cross-Coupling Chemistry Involving Electron-Rich Phosphine Ligands. *Angew. Chem., Int. Ed* 2012, 51, 7226–7230.
- (315). Li Z; Fu Y; Guo Q-X; Liu L Theoretical Study on Monoligated Pd-Catalyzed Cross-Coupling Reactions of Aryl Chlorides and Bromides. *Organometallics* 2008, 27, 4043–4049.
- (316). Lam KC; Marder TB; Lin Z DFT Studies on the Effect of the Nature of the Aryl Halide Y–C₆H₄–X on the Mechanism of its Oxidative Addition to Pd⁰L versus Pd⁰L₂. *Organometallics* 2007, 26, 758–760.
- (317). Ahlquist M; Norrby P-O Oxidative Addition of Aryl Chlorides to Monoligated Palladium(0): A DFT-SCRF study. *Organometallics* 2007, 26, 550–553.
- (318). Seeman JI Effect of Conformational Change on Reactivity in Organic Chemistry. Evaluations, Applications, and Extensions of Curtin-Hammett Winstein-Holness Kinetics. *Chem. Rev* 1983, 83, 83–134.
- (319). Palani V; Perea MA; Gardner KE; Sarpong R A Pyrone Remodeling Strategy to Access Diverse Heterocycles: Application to the Synthesis of Fascaplysin Natural Products. *Chem. Sci* 2021, 12, 1528–1534.
- (320). Shaw MH; Twilton J; MacMillan DWC Photoredox Catalysis in Organic Chemistry. *J. Org. Chem* 2016, 81, 6898–6926. [PubMed: 27477076]
- (321). Matsui JK; Lang SB; Heitz DR; Molander GA Photoredox-Mediated Routes to Radicals: The Value of Catalytic Radical Generation in Synthetic Methods Development. *ACS Catal.* 2017, 7, 2563–2575. [PubMed: 28413692]
- (322). Singh A; Kubik JJ; Weaver JD Photocatalytic C–F Alkylation; Facile Access to Multifluorinated Arenes. *Chem. Sci* 2015, 6, 7206–7212. [PubMed: 29861956]
- (323). Senaweera S; Weaver JD Dual C–F, C–H Functionalization via Photocatalysis: Access to Multifluorinated Biaryls. *J. Am. Chem. Soc* 2016, 138, 2520–2523. [PubMed: 26890498]

- (324). Sandfort F; Knecht T; Pinkert T; Daniliuc CG; Glorius F Site-Selective Thiolation of (Multi)Halogenated Heteroarenes. *J. Am. Chem. Soc* 2020, 142, 6913–6919. [PubMed: 32237706]
- (325). Weinberg DR; Gagliardi CJ; Hull JF; Murphy CF; Kent CA; Westlake BC; Paul A; Ess DH; McCafferty DG; Meyer TJ Proton-Coupled Electron Transfer. *Chem. Rev* 2012, 112, 4016–4093. [PubMed: 22702235]
- (326). Ahneman DT; Estrada JG; Lin S; Dreher SD; Doyle AG Predicting Reaction Performance in C–N Cross-Coupling Using Machine Learning. *Science* 2018, 360, 186–190. [PubMed: 29449509]
- (327). Shen Y; Borowski JE; Hardy MA; Sarpong R; Doyle AG; Cernak T Automation and Computer-Assisted Planning for Chemical Synthesis. *Nat. Rev. Methods Primers* 2021, 1, 23 DOI: 10.1038/s43586-021-00022-5.

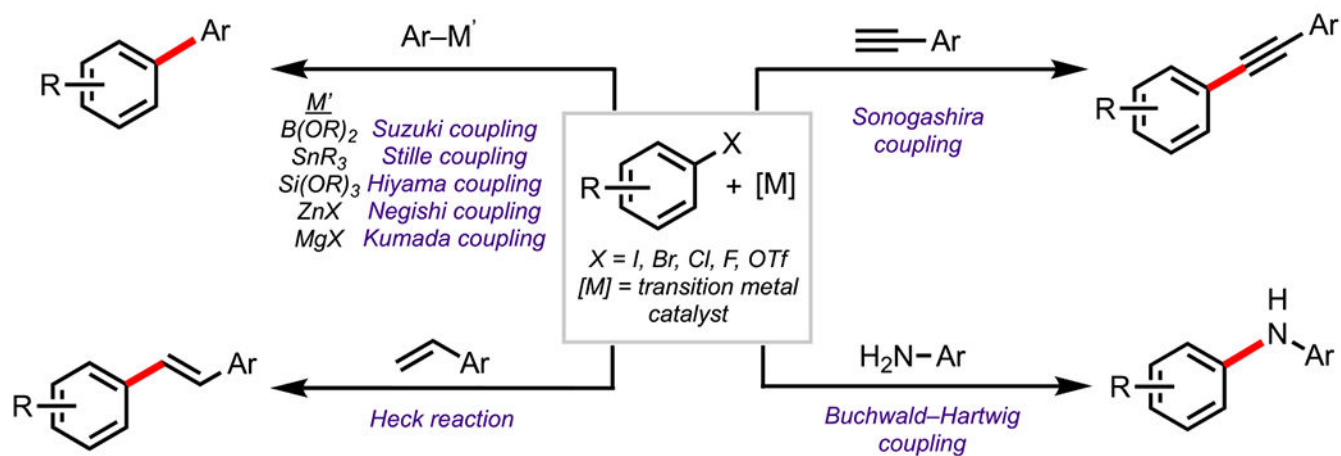
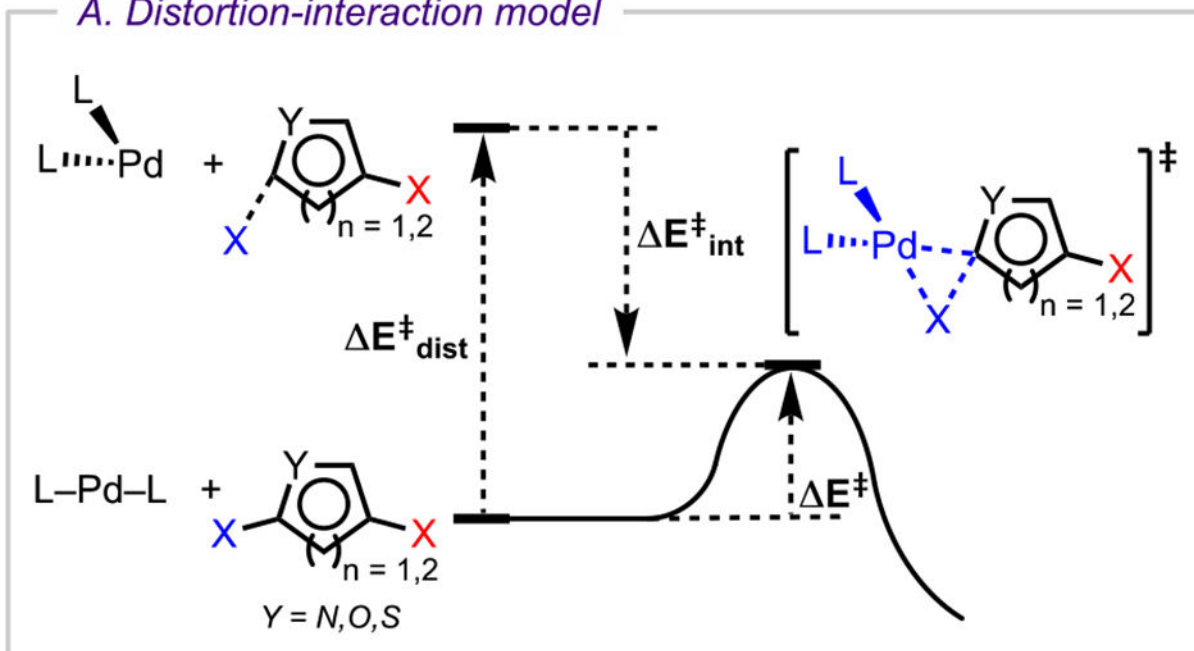


Figure 1.
Selected cross-coupling examples.

A. Distortion-interaction model



B. Orbital interactions in oxidative addition

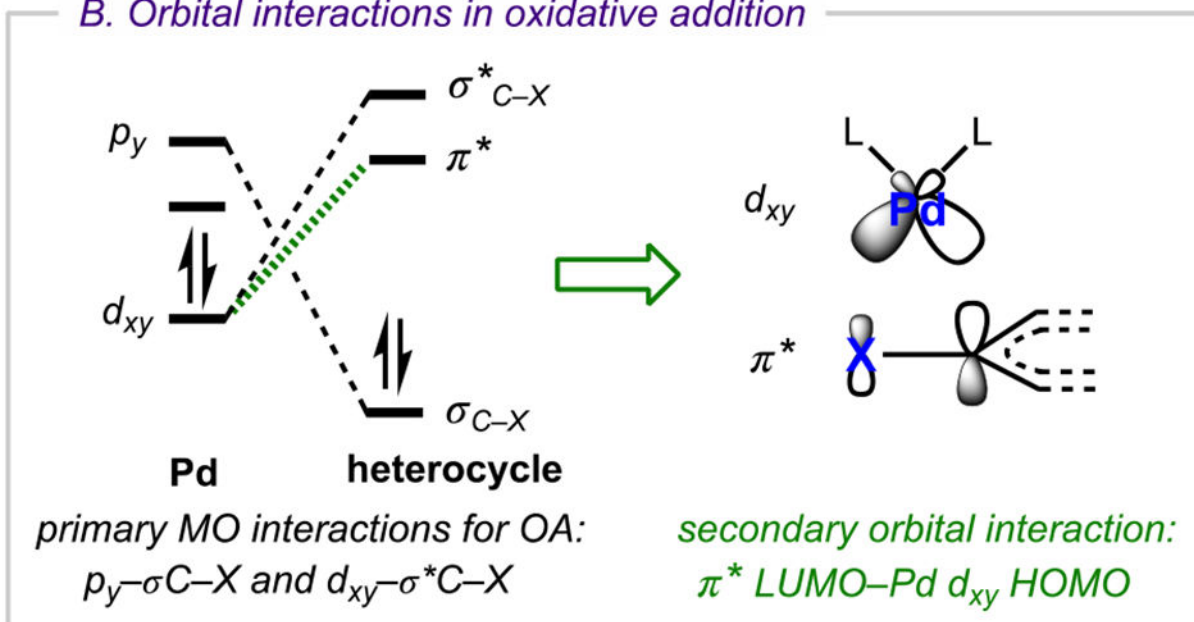


Figure 2.

(A) Distortion–interaction model and (B) major orbital interactions between PdL_2 and ArX in oxidative addition.

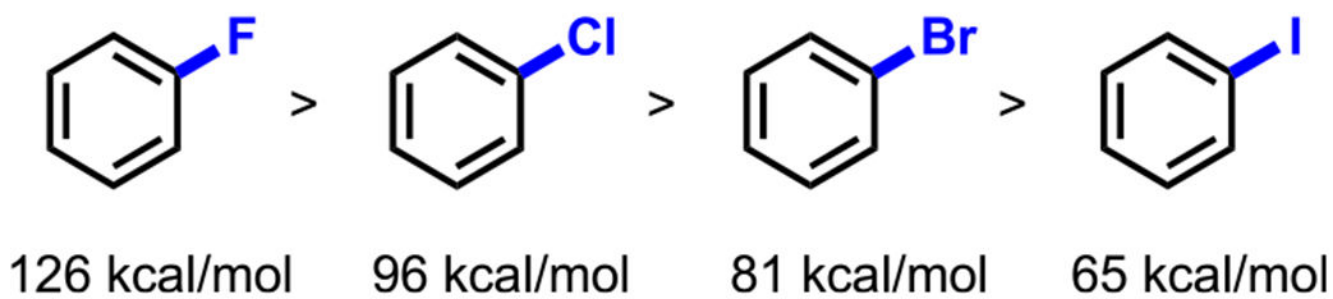


Figure 3.
Relative BDEs of aryl C–X bonds.

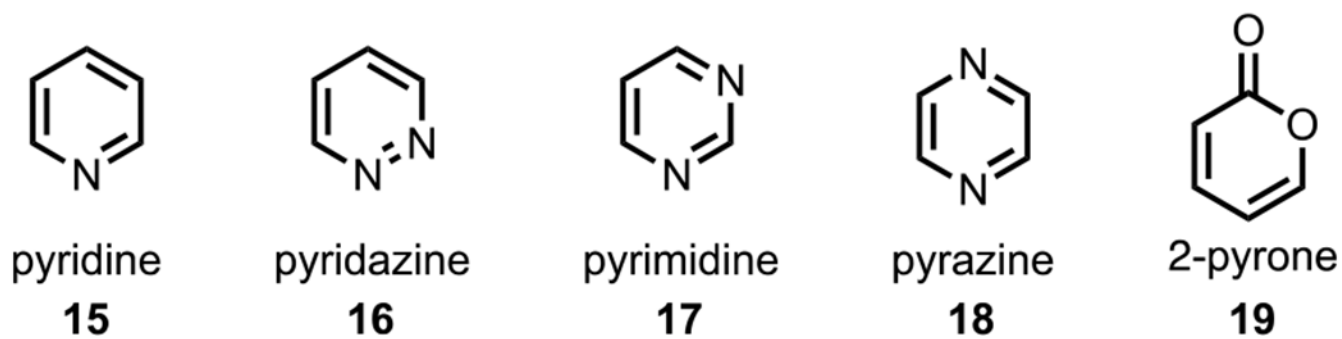


Figure 4.
Selected six-membered heterocycles employed in site-selective cross-coupling.

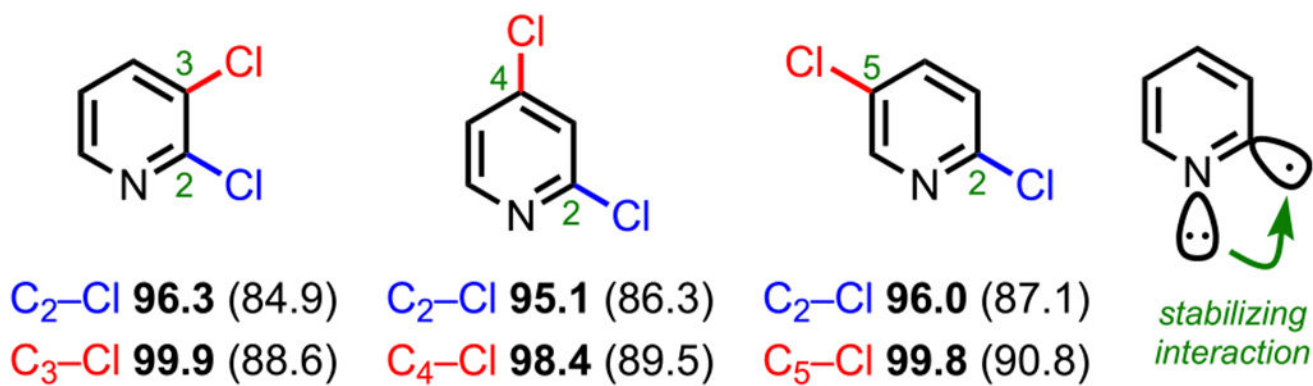
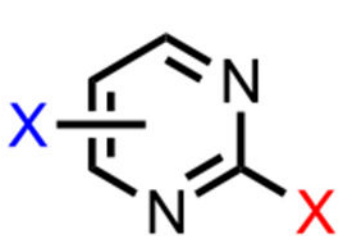
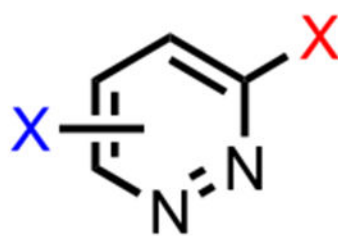


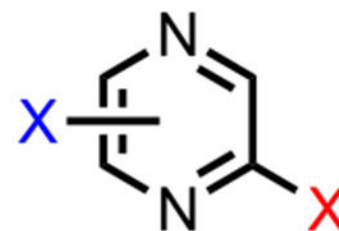
Figure 5.
C-Cl BDEs (kcal/mol) of dichloropyridines using G3B3 (bold) and B3LYP (in parentheses).



pyrimidine

46

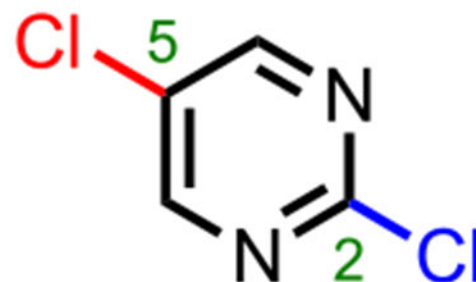
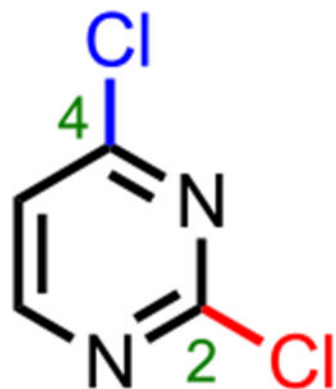
pyridazine

47

pyrazine

48

Figure 6.
Selected diazines: pyrimidine, pyridazine, and pyrazine.



C₂-Cl 94.9 (87.2)

C₄-Cl 93.8 (85.9)

C₂-Cl 96.5 (87.7)

C₅-Cl 99.6 (91.0)

Figure 7.
C-Cl BDEs (kcal/mol) of dichloropyrimidines using G3B3 (bold) and B3LYP (in parentheses).

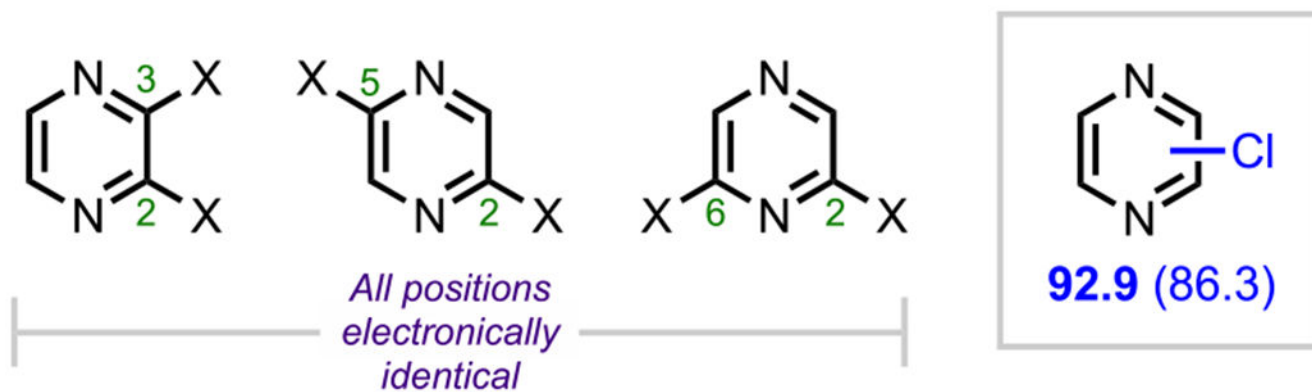


Figure 8. Electronically identical dihalogenated pyrazines and the pyrazine C–Cl BDE in kcal/mol (in box) using G3B3 (bold) and B3LYP (in parentheses).

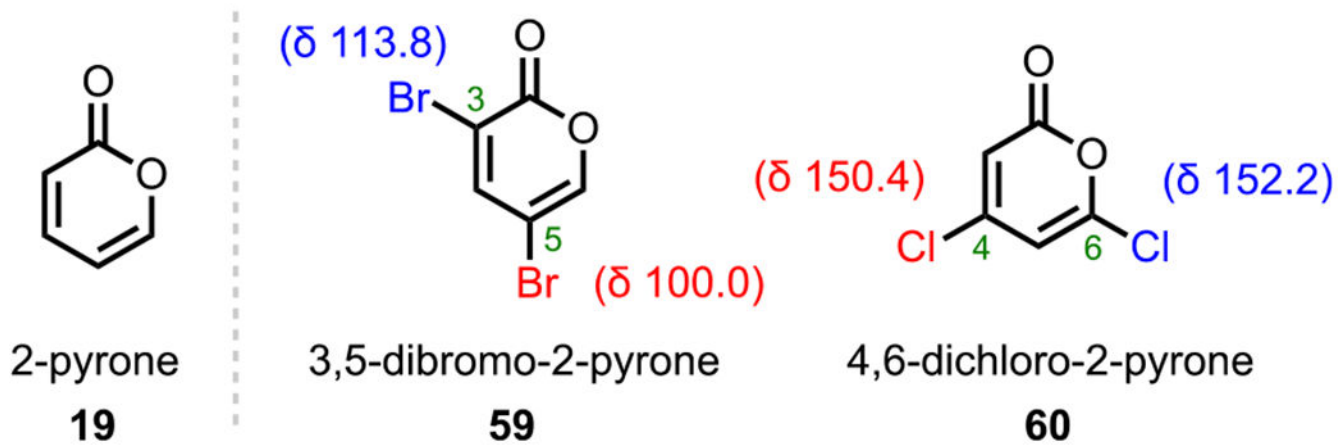


Figure 9. 2-Pyrone and ^{13}C NMR shifts for 3,5-dibromo-2-pyrone and 4,6-dichloro-2-pyrone.

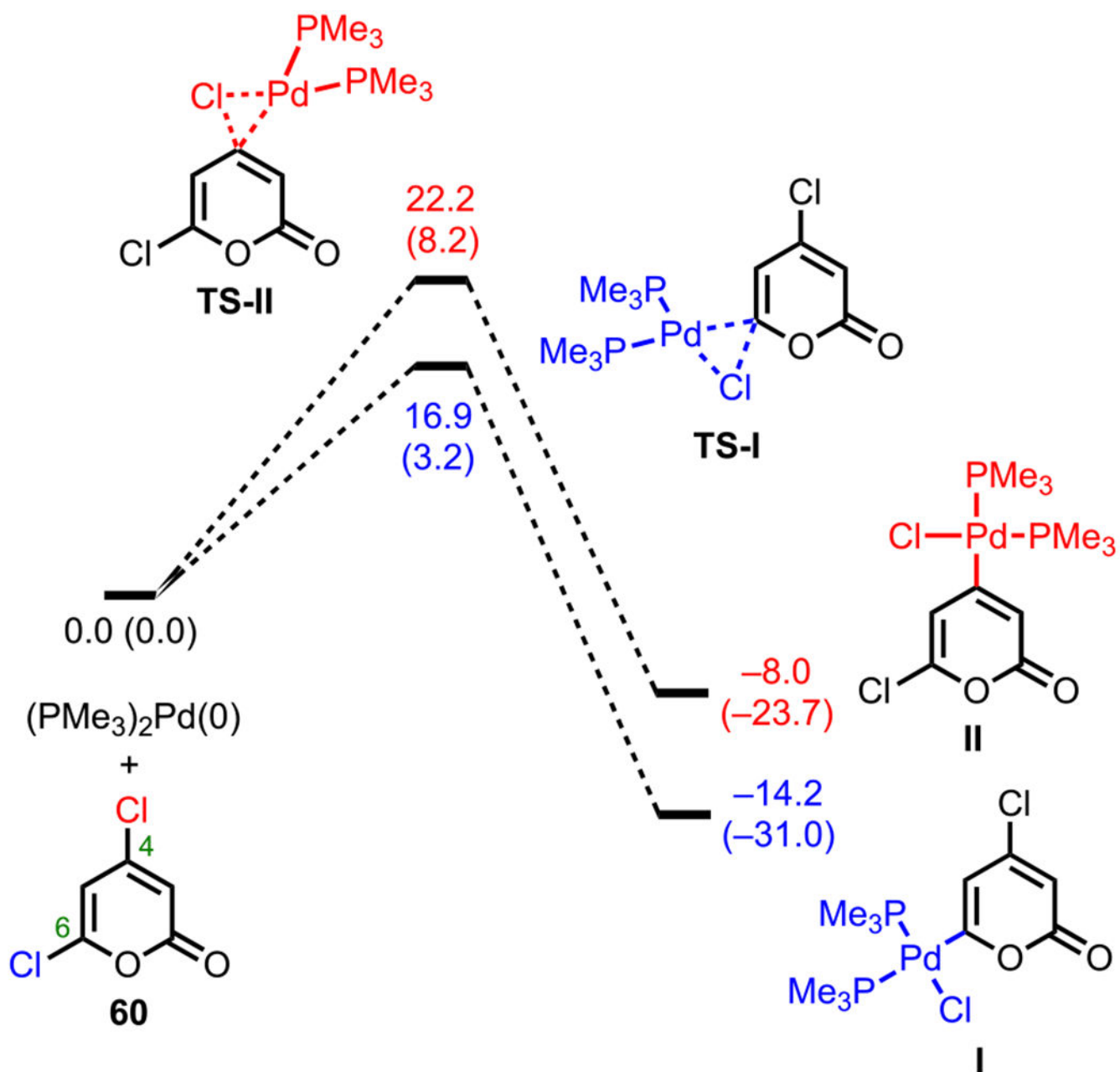


Figure 10. Energy profiles for C4 versus C6 oxidative addition of 4,6-dichloro-2-pyrone. Relative free energies and reaction energies (in parentheses) listed in kcal/mol (ref 95).

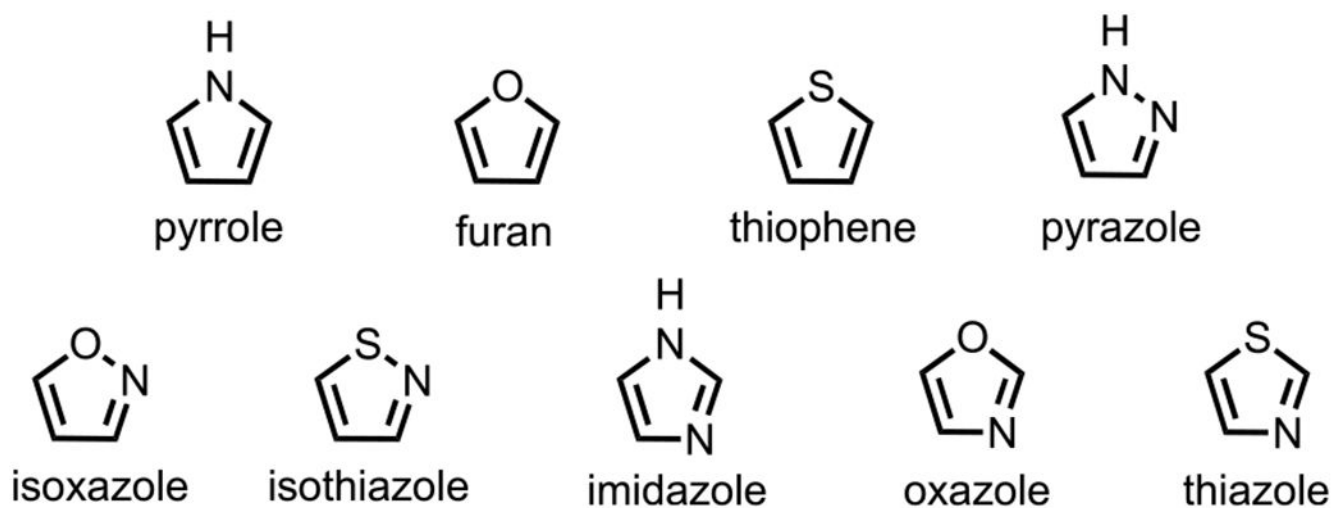


Figure 11.
Selected five-membered heterocycles.

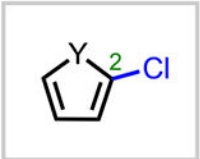
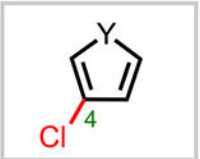
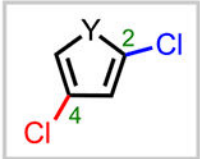
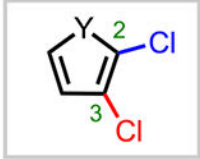
| |  |  |  | |  | |
|------|---|---|--|---------------------|---|---------------------|
| | C ₂ -Cl | C ₄ -Cl | C ₂ -Cl | C ₄ -Cl | C ₂ -Cl | C ₃ -Cl |
| Y=S | 98.8 (92.5) | 98.6 (92.2) | 98.9 (91.9) | 98.7 (91.4) | 100.7 (92.8) | 100.3 (92.1) |
| Y=NH | 101.9 (96.3) | 101.5 (96.3) | 101.9 (95.5) | 101.4 (95.4) | 103.0 (95.8) | 102.6 (95.9) |
| Y=O | 102.0 (96.5) | 101.4 (96.5) | 102.1 (94.9) | 101.4 – | 103.9 (96.0) | 102.8 (95.4) |

Figure 12.

2,4- and 2,3-Thiophene, pyrrole, and furan C–Cl BDEs in kcal/mol using G3B3 (bold) and B3LYP (in parentheses).

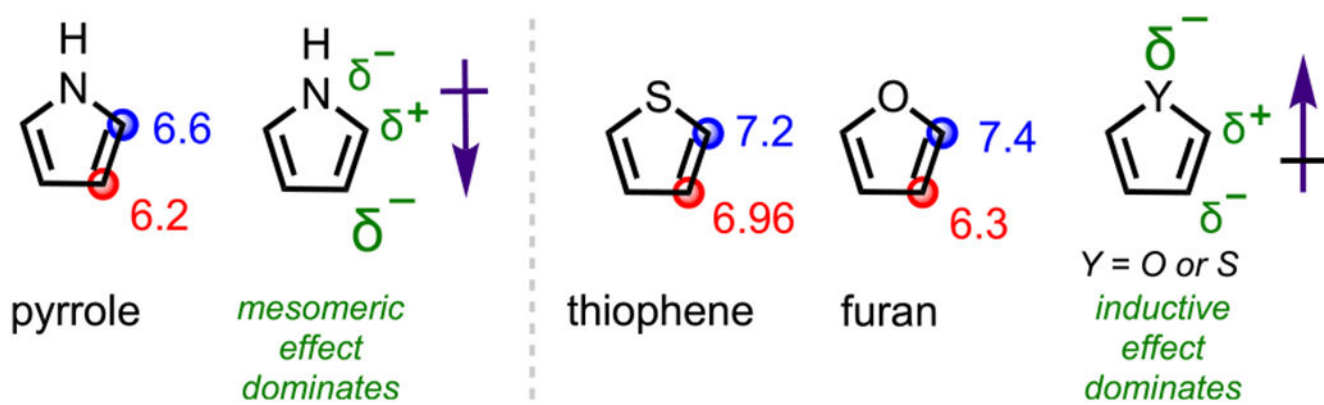


Figure 13. ^1H NMR chemical shifts (highlighted in blue and red) and major electronic effects for pyrrole, thiophene, and furan.

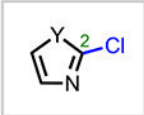
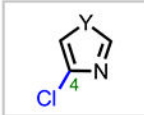
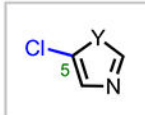
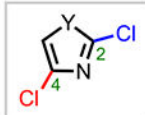
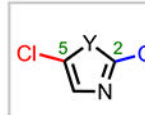

| |  |  |  |  | |  | |  | |
|------|---|---|---|---|---------------------|---|---------------------|---|---------------------|
| | C ₂ -Cl | C ₄ -Cl | C ₅ -Cl | C ₂ -Cl | C ₄ -Cl | C ₂ -Cl | C ₅ -Cl | C ₄ -Cl | C ₅ -Cl |
| Y=S | 93.7 (87.4) | 97.8 (90.8) | 98.8 (92.4) | 94.5 (87.4) | 97.9 (90.3) | 93.6 (86.4) | 98.7 (91.8) | 99.7 (90.7) | 100.4 (92.5) |
| Y=NH | 99.4 (93.3) | 100.4 (94.3) | 101.3 (95.4) | 99.9 (93.0) | 100.5 (93.9) | 99.1 (92.4) | 101.2 (94.9) | 101.6 (94.0) | 103.0 (95.7) |
| Y=O | 100.3 (94.0) | 101.1 (94.3) | 102.3 (95.7) | - | - | - | - | - | - |

Figure 14.

C–Cl BDEs in kcal/mol of mono- and dichloro-1,3-azoles using G3B3 (bold) and B3LYP (in parentheses).

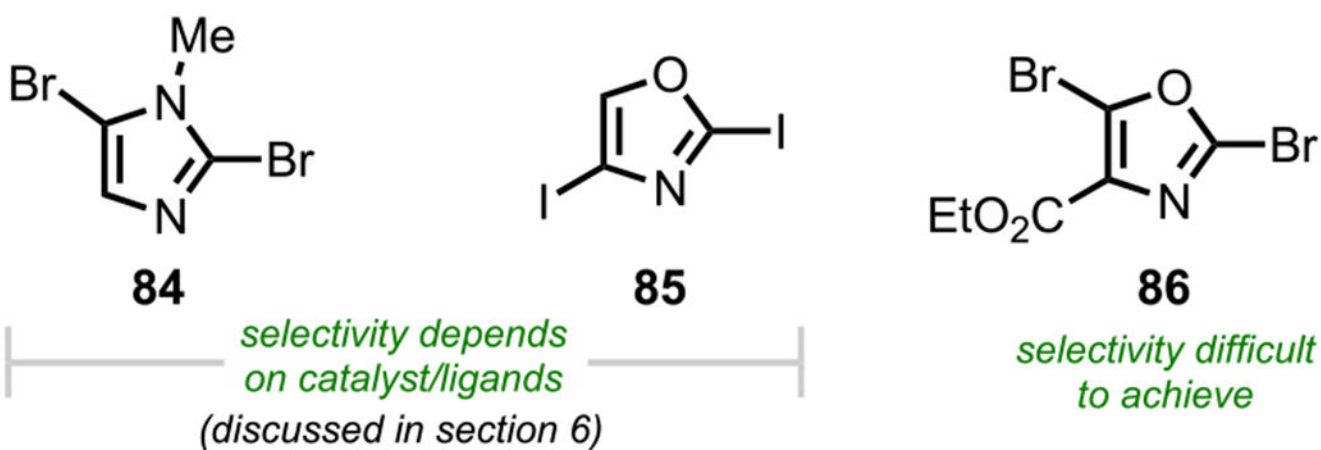


Figure 15. Selectivity outcomes for *N*-methyl-2,5-dibromimidazole, 2,4-diiodooxazole, and ethyl 2,5-dibromooxazole-4-carboxylate.

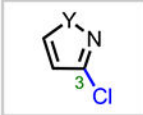
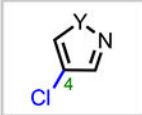
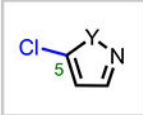
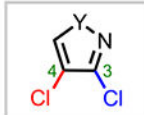
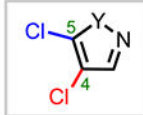
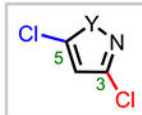
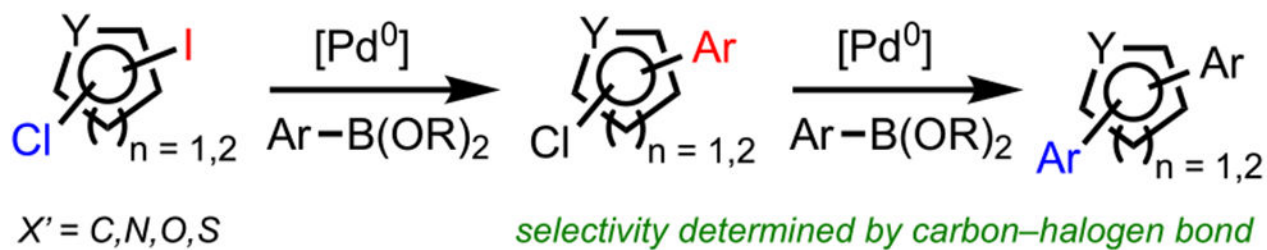
| |  |  |  |  | |  | |  | |
|------|---|---|---|---|-------------------------|---|-------------------------|---|-------------------------|
| | C₃-Cl | C₄-Cl | C₅-Cl | C₃-Cl | C₄-Cl | C₄-Cl | C₅-Cl | C₃-Cl | C₅-Cl |
| Y=S | 94.7 (87.9) | 98.6 (92.1) | 97.9 (91.5) | 96.3 (87.6) | 99.3 (91.5) | - | - | 100.2 (92.0) | 99.7 (91.7) |
| Y=NH | 100.3 (94.3) | 101.5 (95.9) | 101.1 (95.0) | - | - | - | - | - | - |
| Y=O | 99.0 (92.2) | 103.6 (95.2) | 100.5 (93.4) | - | - | - | - | - | - |

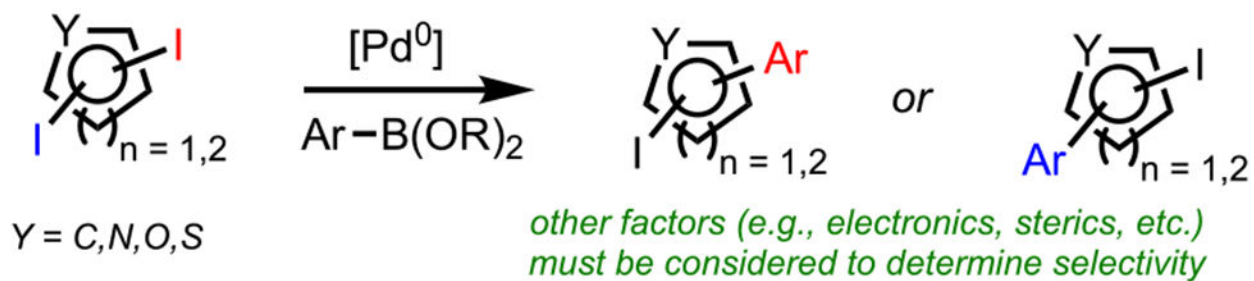
Figure 16.

C–Cl BDEs in kcal/mol of mono- and dichloro-1,2-azoles using G3B3 (bold) and B3LYP (in parentheses).

A. Non-Identical Halogens

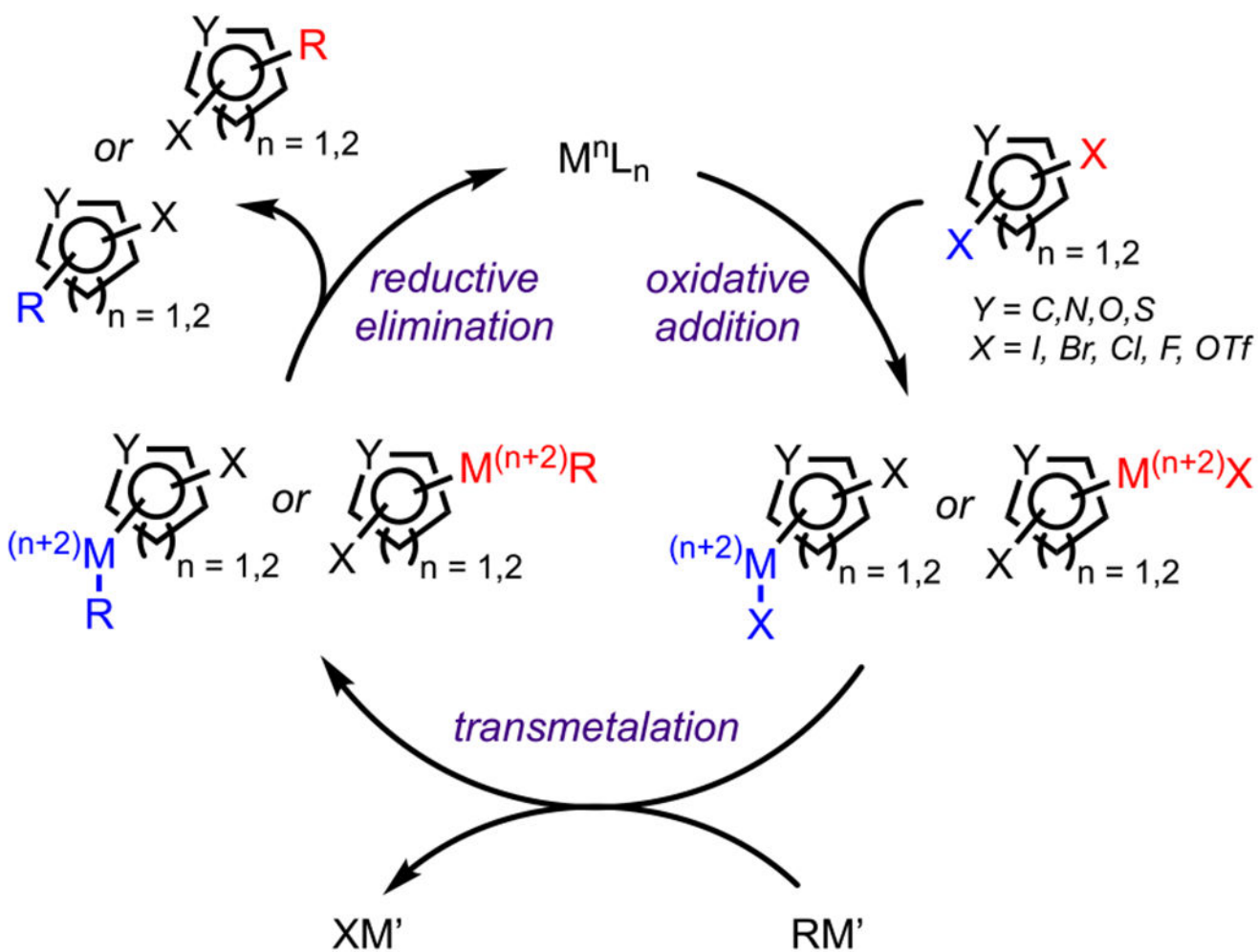


B. Identical Halogens

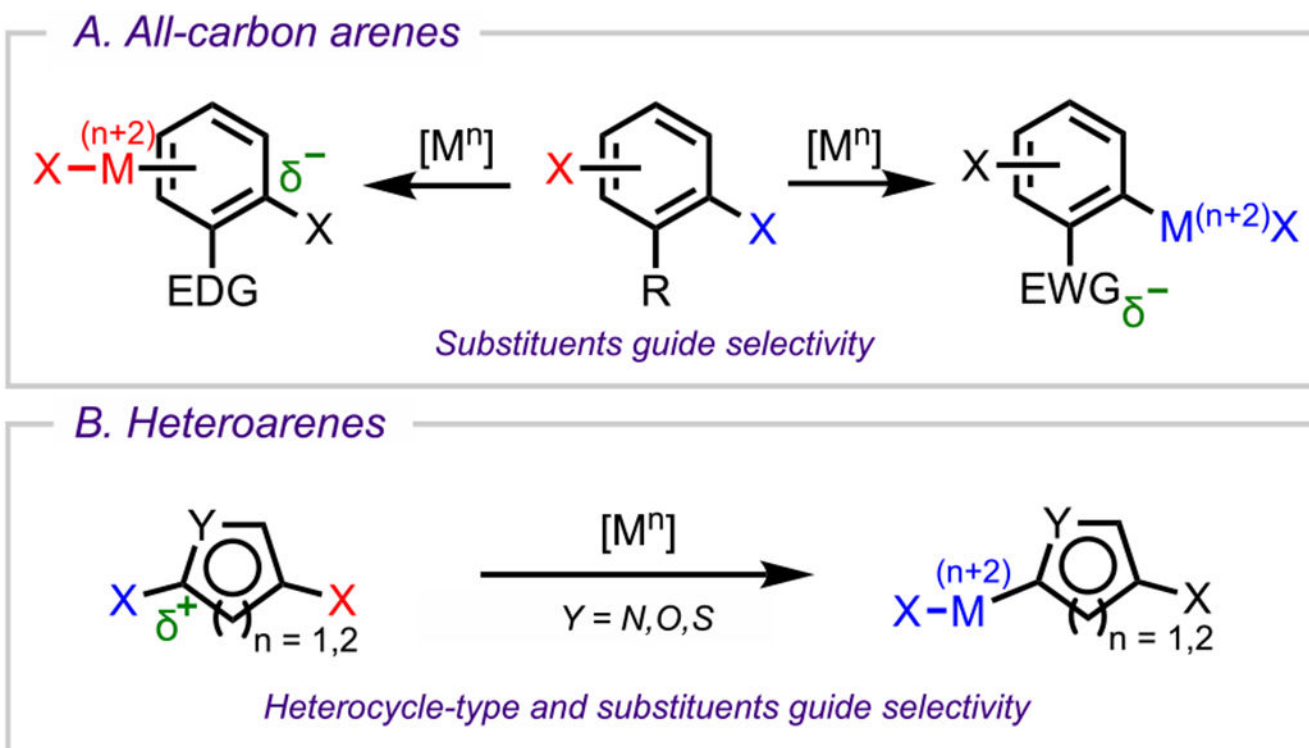


Scheme 1.

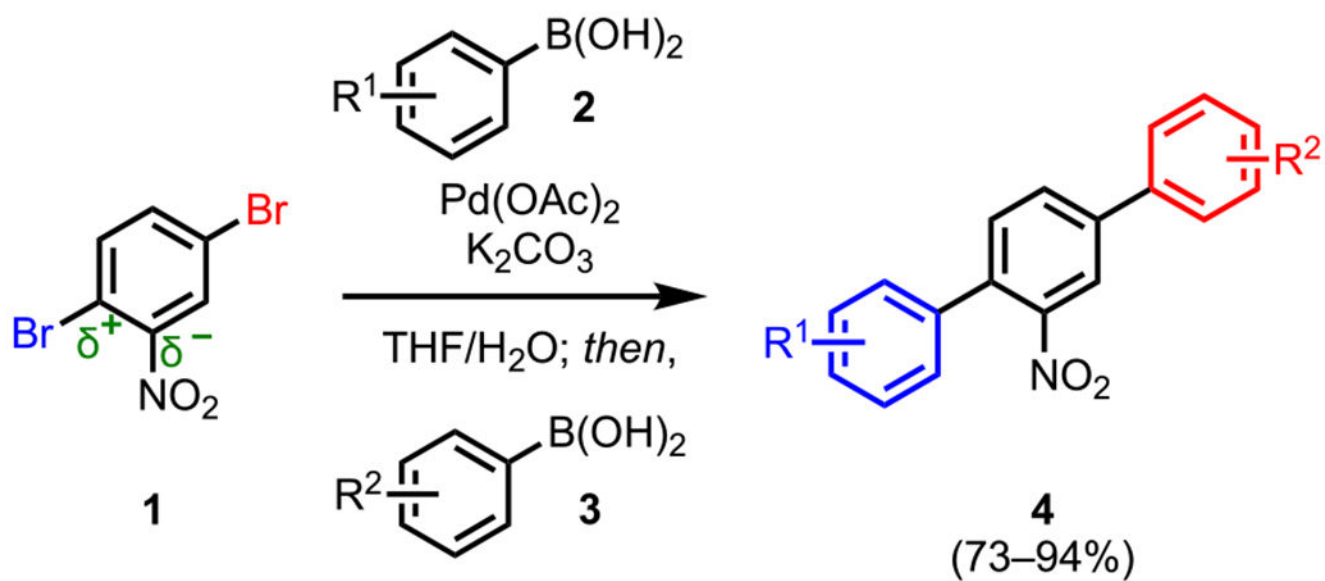
Cross-Couplings of Polyhalogenated Arenes Substituted with (A) Nonidentical Halogens or (B) Identical Halogens



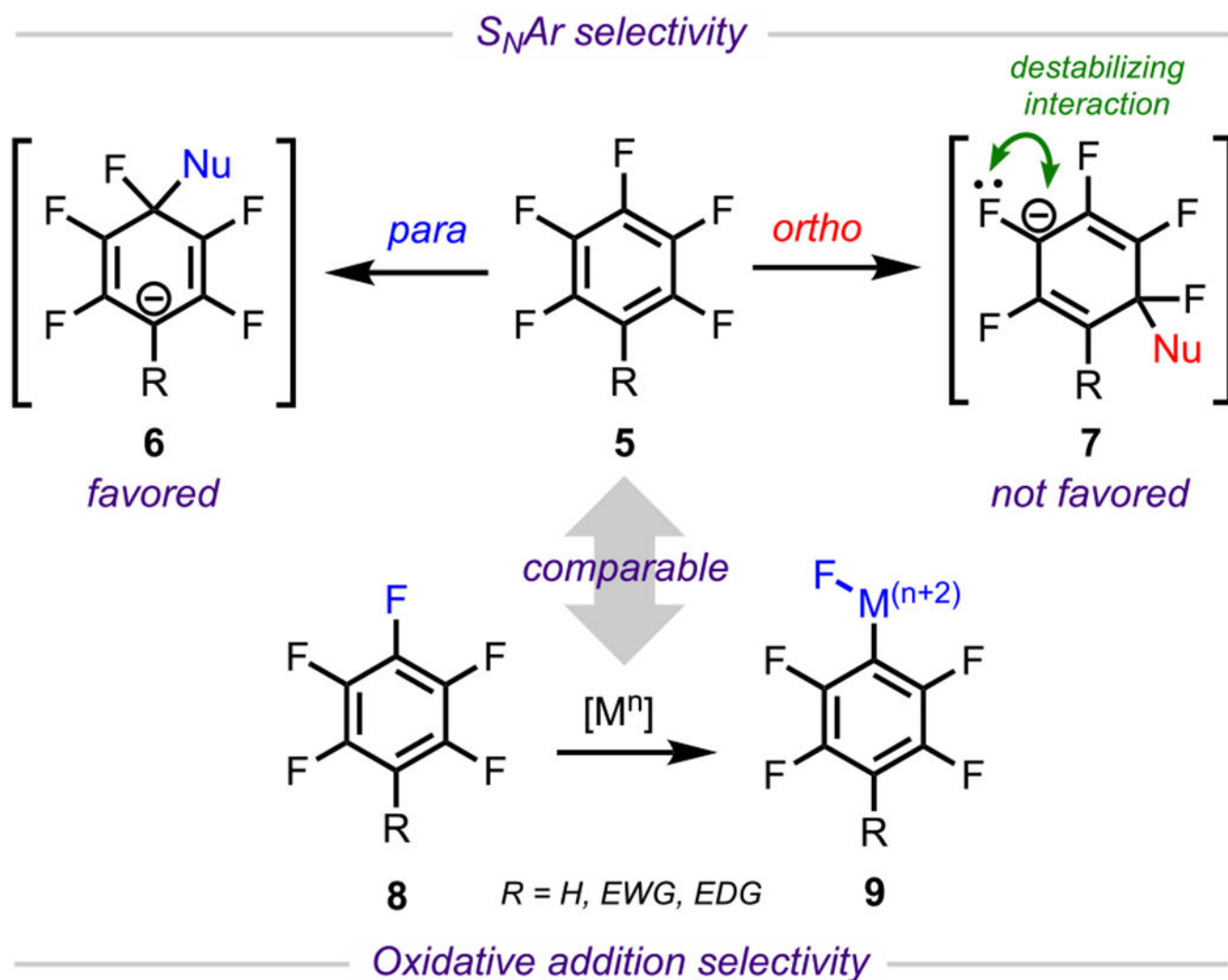
Scheme 2.
General Reaction Mechanism for Transition Metal-Catalyzed Cross-Coupling

**Scheme 3.**

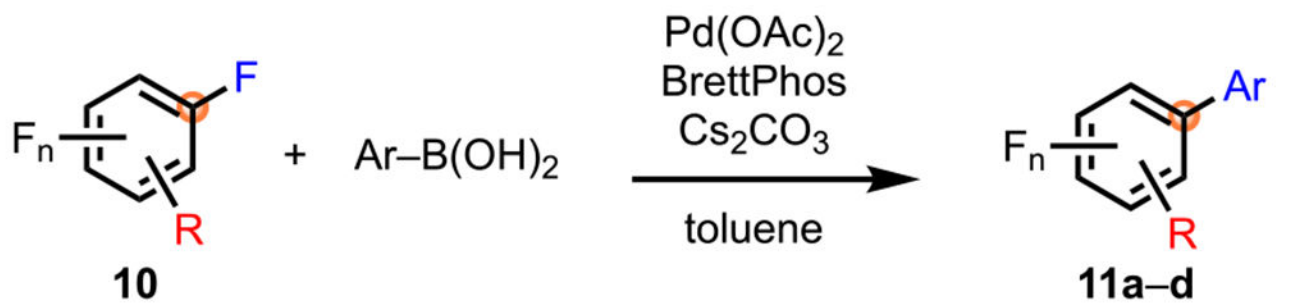
General Electronic Considerations for Both (A) Arenes (All-Carbon) and (B) Heteroarenes



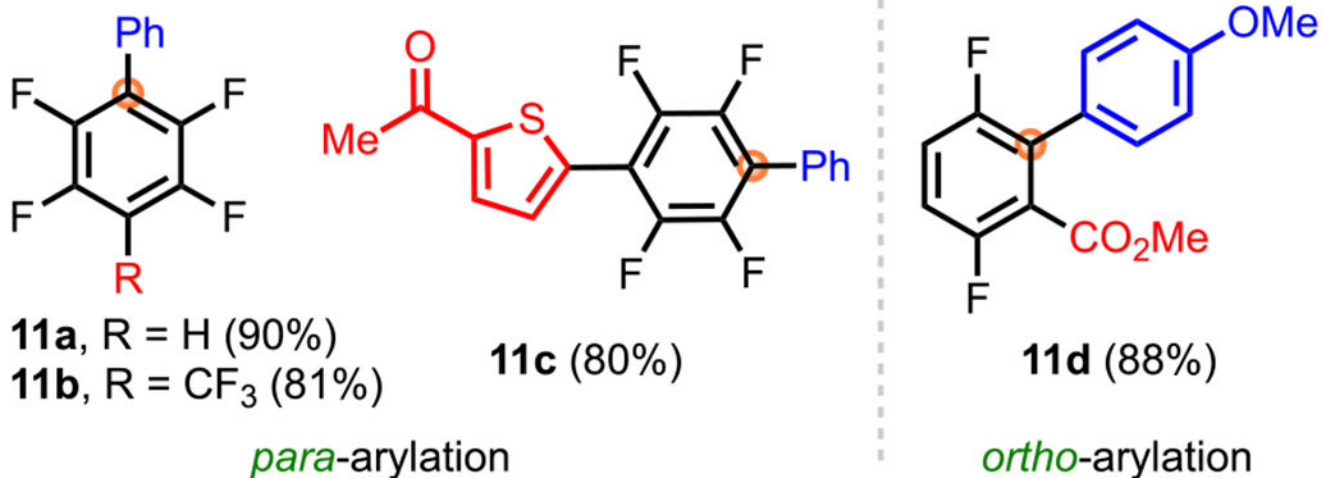
Scheme 4.
Site-Selective, One-Pot Suzuki–Miyaura Coupling to Form Unsymmetrical Terphenyl Cores



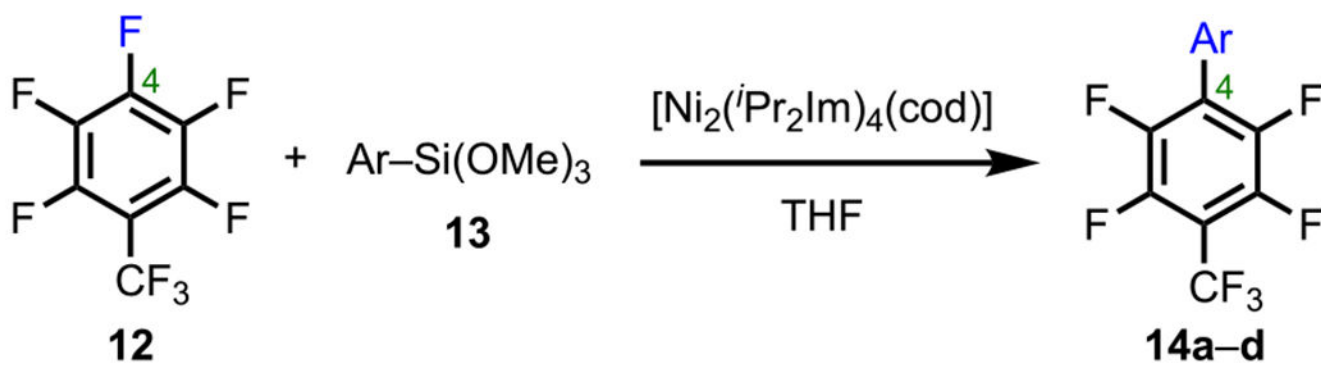
Scheme 5.
Electronic Considerations of Polyfluorinated Arenes and General Reactivity toward S_NAr and Cross-Coupling



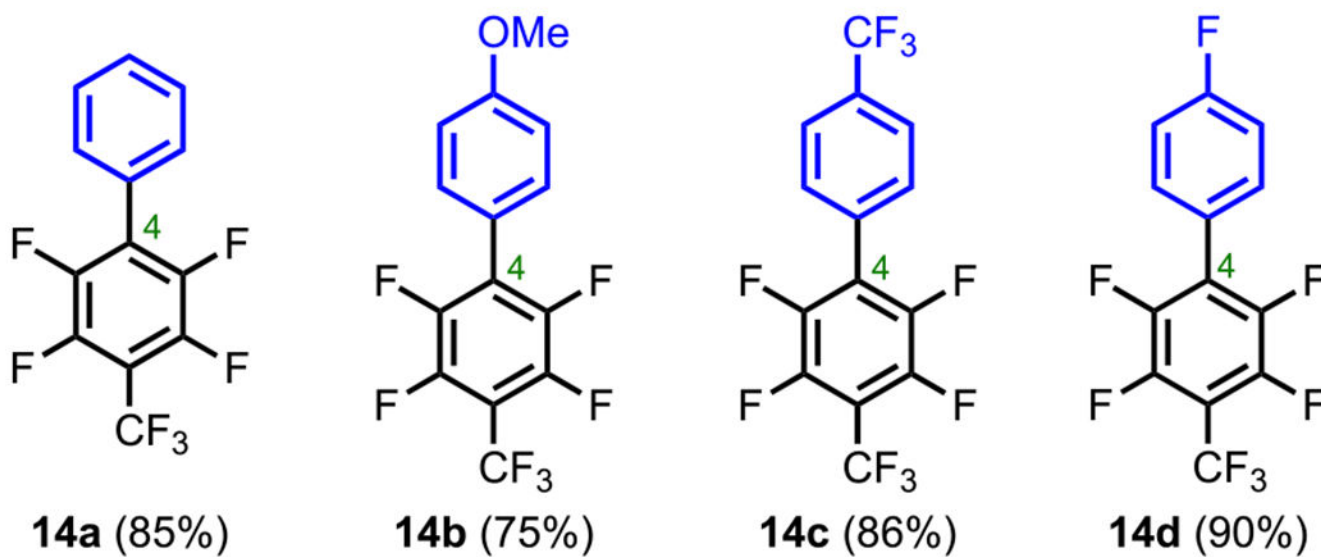
Mono-arylation



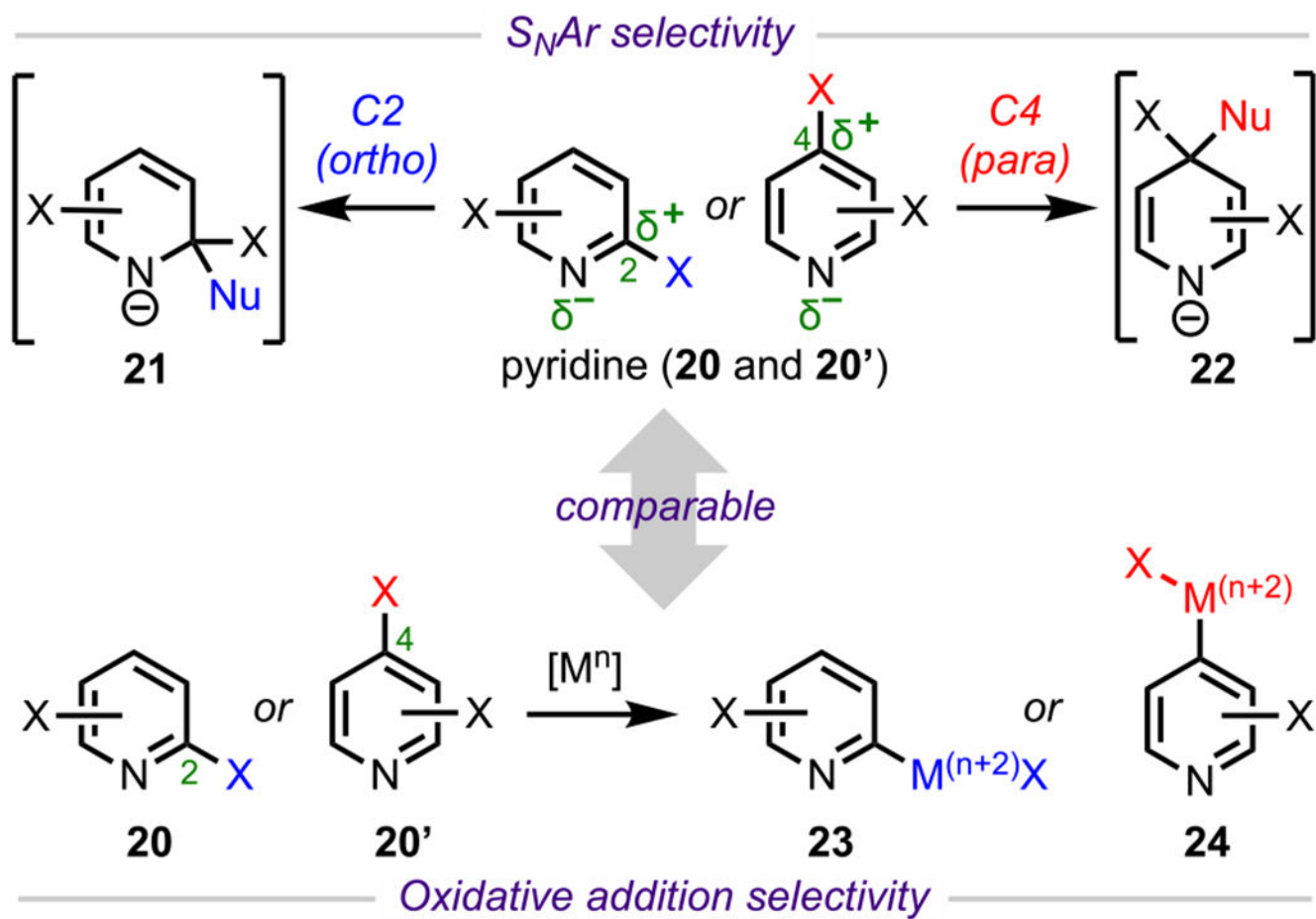
Scheme 6.
Site-Selective Cross-Coupling of Polyfluorinated Arenes



Mono-arylation

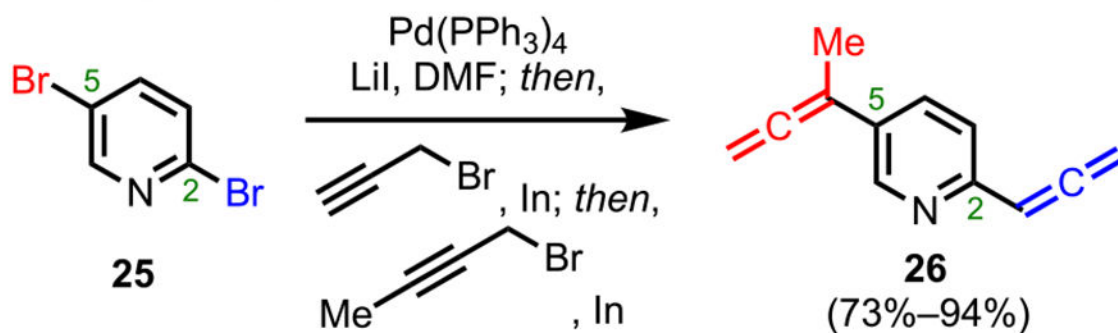


Scheme 7.
Site-Selective Monoarylation of Perfluorotoluene

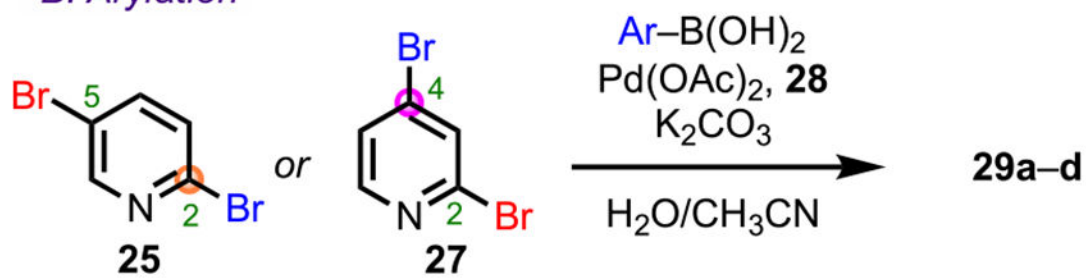


Scheme 8.
Electronic Considerations of Pyridine and General Reactivity toward S_NAr and Cross-Coupling

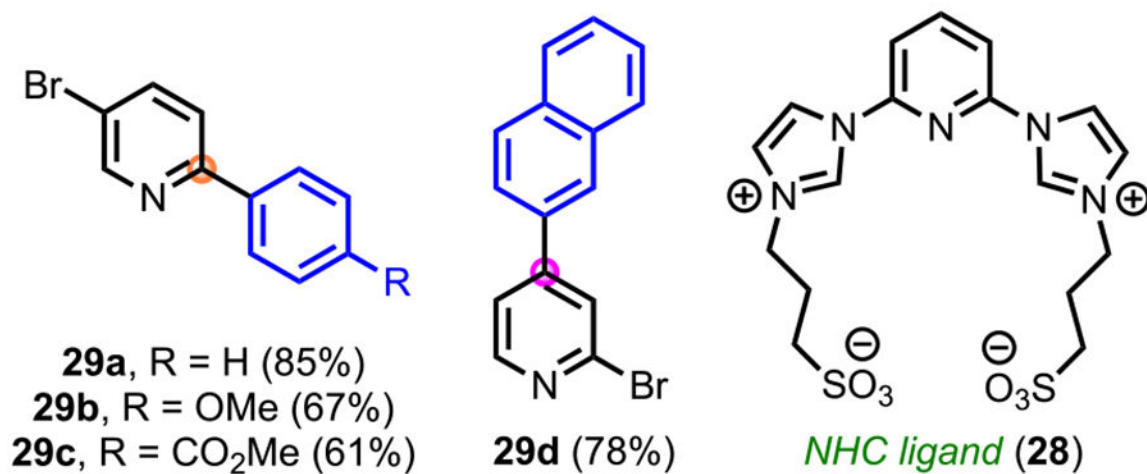
A. Allenylation



B. Arylation

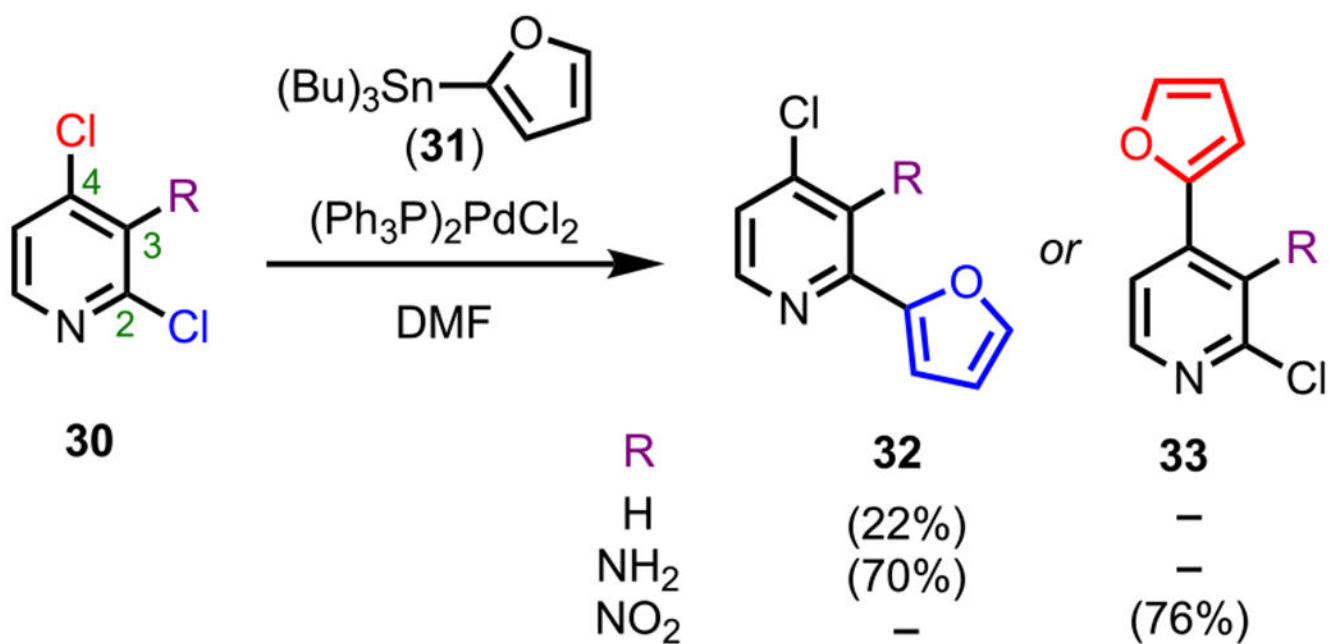


Mono-arylation

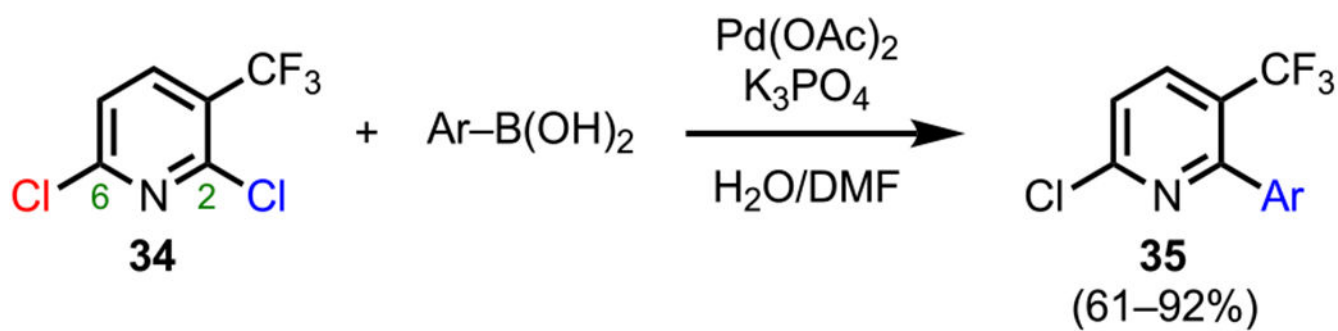


Scheme 9.

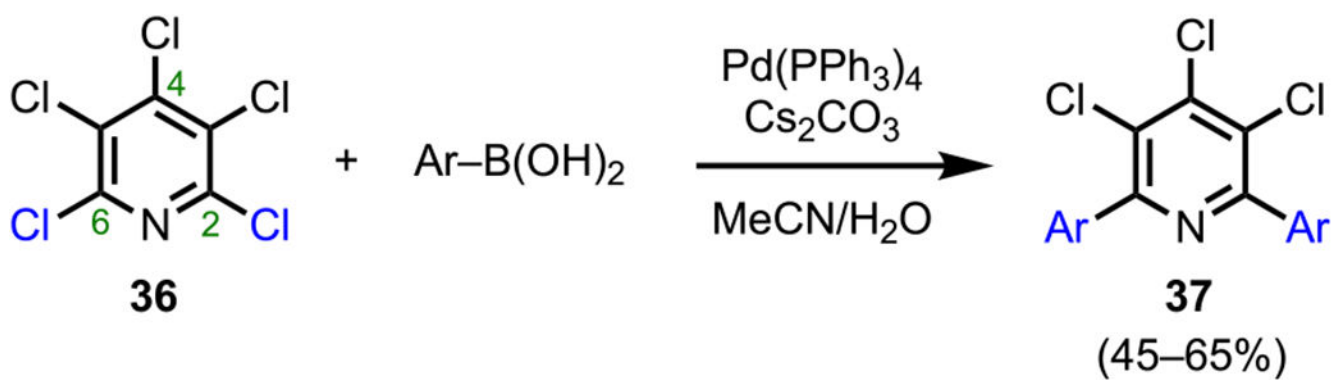
Site-Selective (A) Allenylation and (B) Arylation of Dibrominated Pyridines



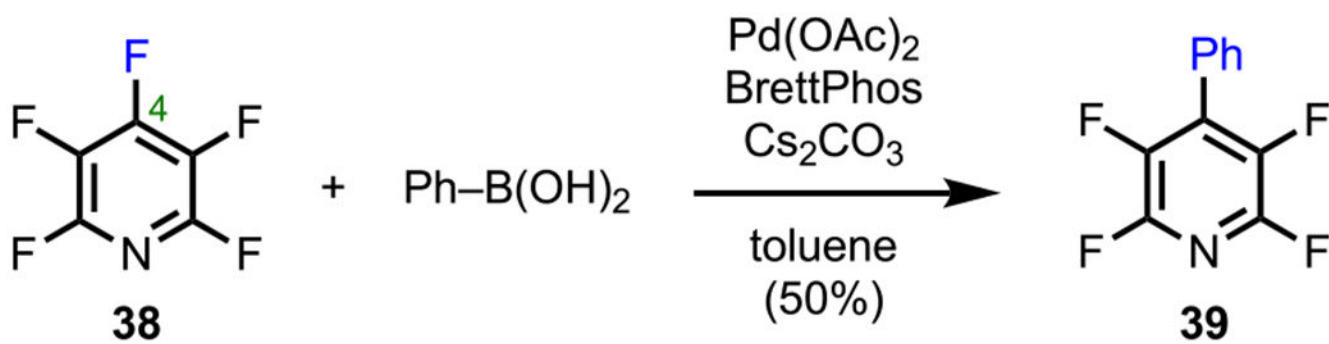
Scheme 10.
Substituent Effects in C2 versus C4 Stille Coupling



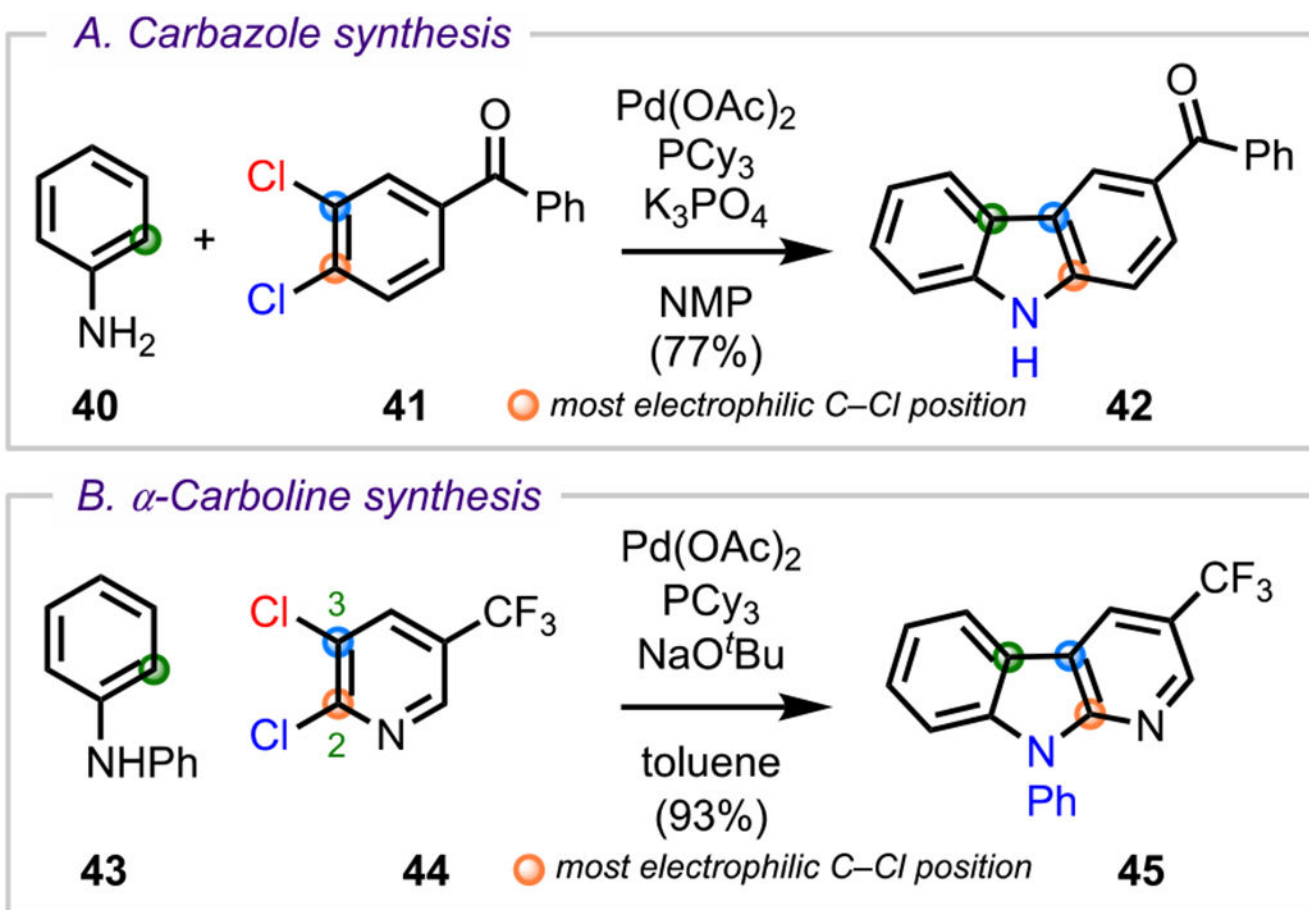
Scheme 11.
Site-Selective Monoarylation of 2,6-Dichloro-4-(trifluoromethyl)pyridines



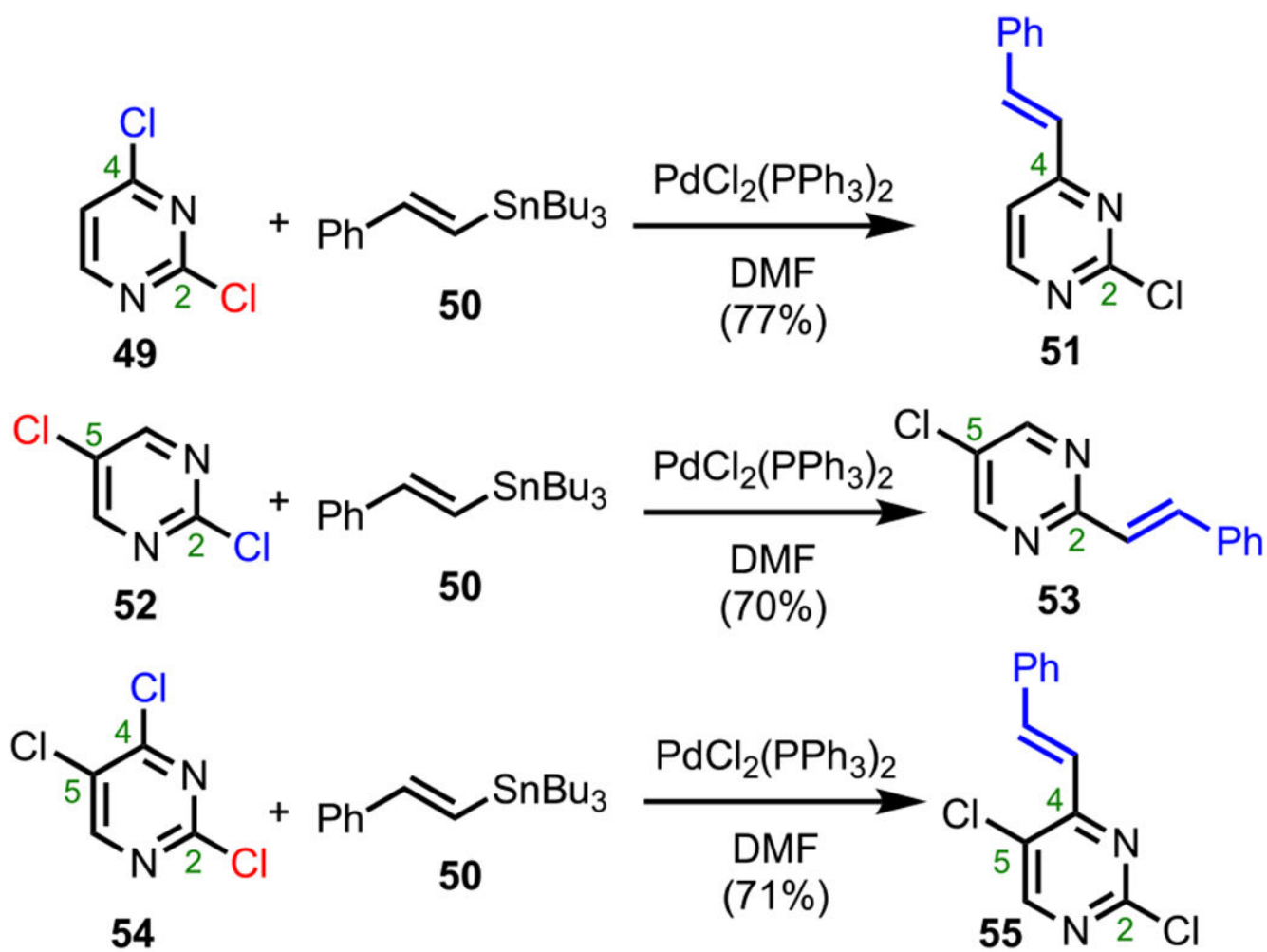
Scheme 12.
Site-Selective Bisarylation of Perchloropyridine



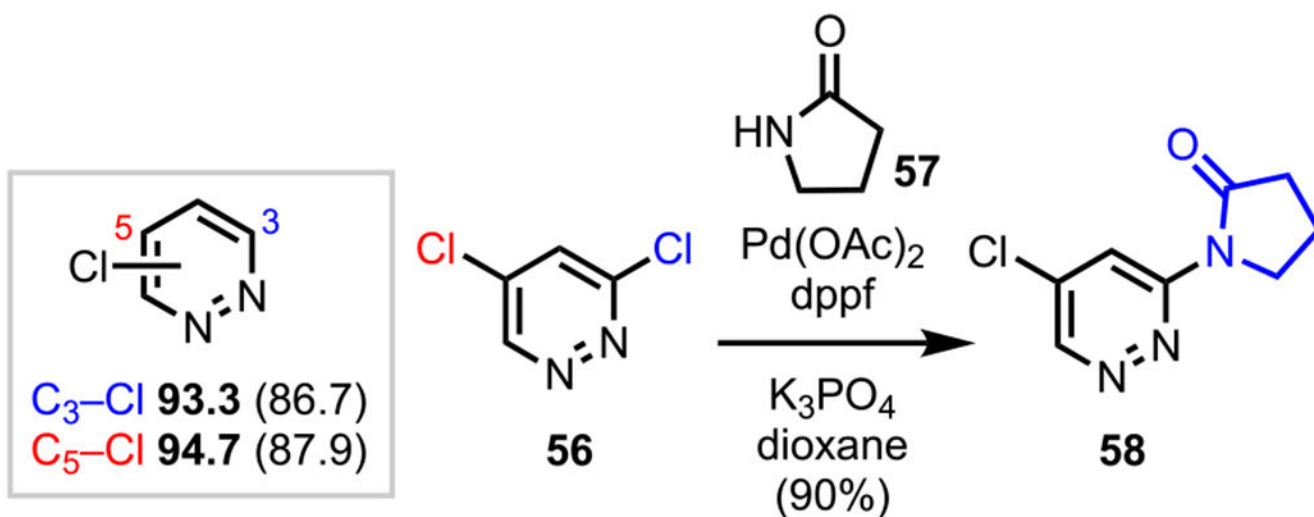
Scheme 13.
Site-Selective Monoarylation of Perfluoropyridine

**Scheme 14.**

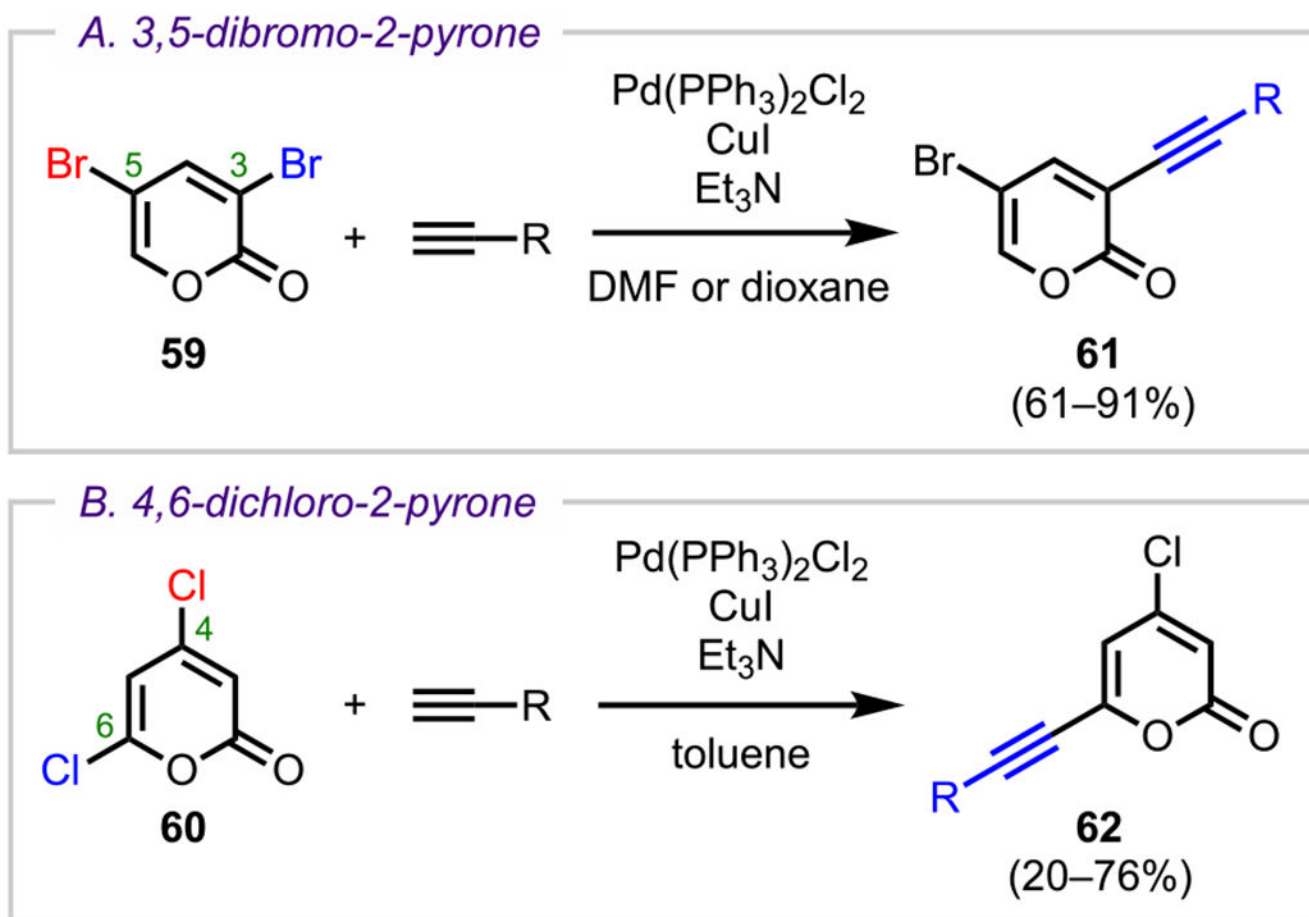
(A) Carbazole and (B) α -Carboline Synthesis Using a Site-Selective Domino Cross-Coupling Reaction



Scheme 15.
Site-Selective Stille Coupling of Polyhalogenated Pyrimidines

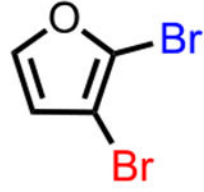
**Scheme 16.**

Pyridazine C-Cl BDEs in kcal/mol (in Box) Using G3B3 (Bold) and B3LYP (in Parentheses) and Site-Selective Amidation of 3,5-Dichloropyridazine

**Scheme 17.**

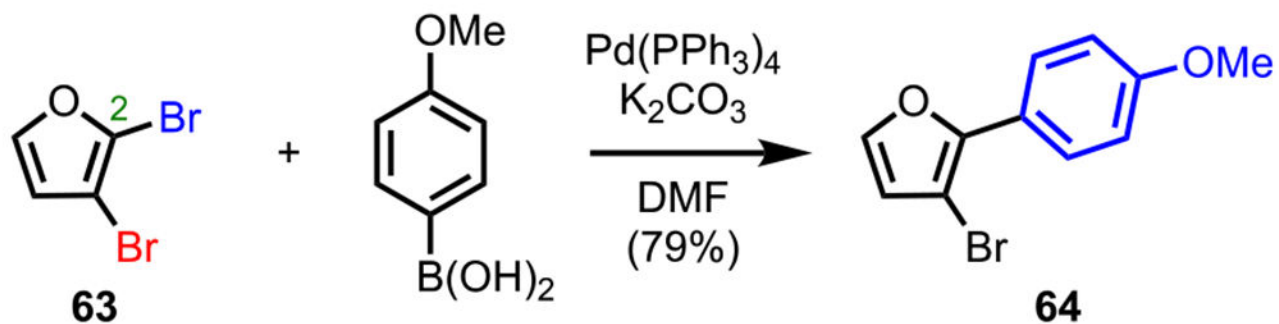
Site-Selective Sonogashira Coupling of (A) 3,5-Dibromo-2-pyrone and (B) 4,6-Dichloro-2-pyrone

A. Distortion–interaction model

| | | BDE (kcal/mol) | $\Delta E^\ddagger_{\text{dist}}$ (Het) | $\Delta E^\ddagger_{\text{dist}}$ (Pd) | $\Delta E^\ddagger_{\text{int}}$ | ΔE^\ddagger |
|--|------------|-------------------|--|---|----------------------------------|---------------------|
|  63 | 2 → | 88.9 | 18.7 | 12.7 | −21.6 | 9.8 |
| | 3 → | 88.9 | 19.8 | 12.9 | −18.7 | 14.0 |

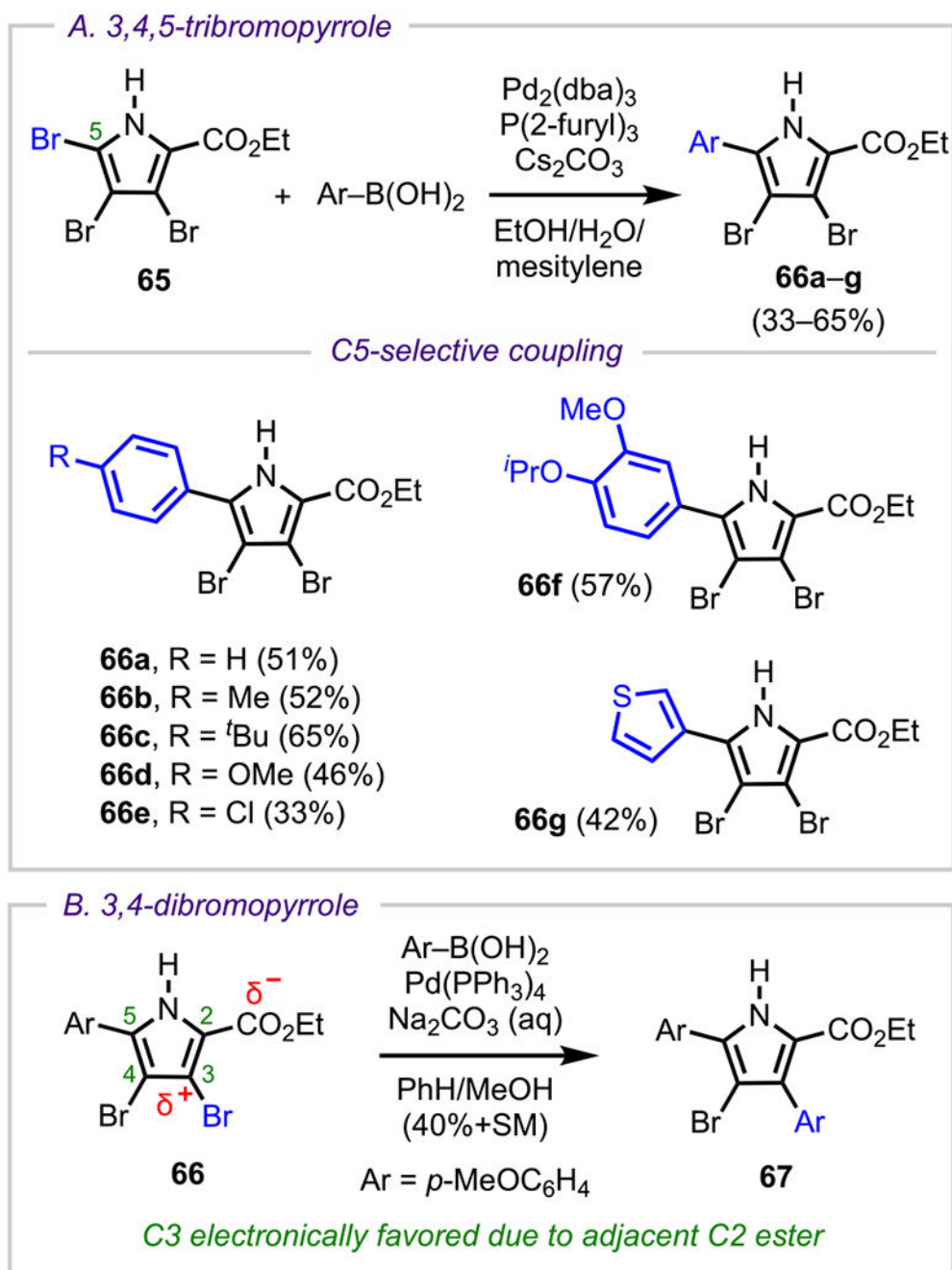
Selectivity controlled by interaction energy (ΔE^\ddagger)

B. Experimental confirmation

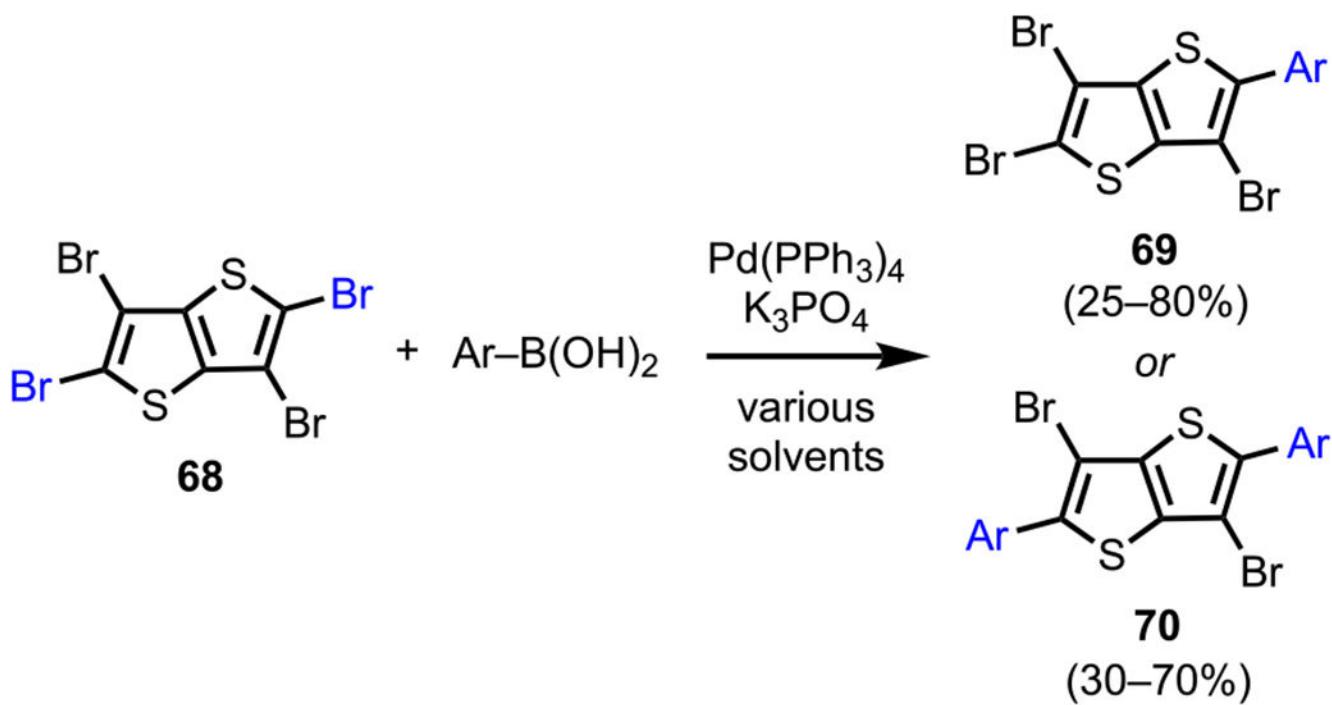


Scheme 18.

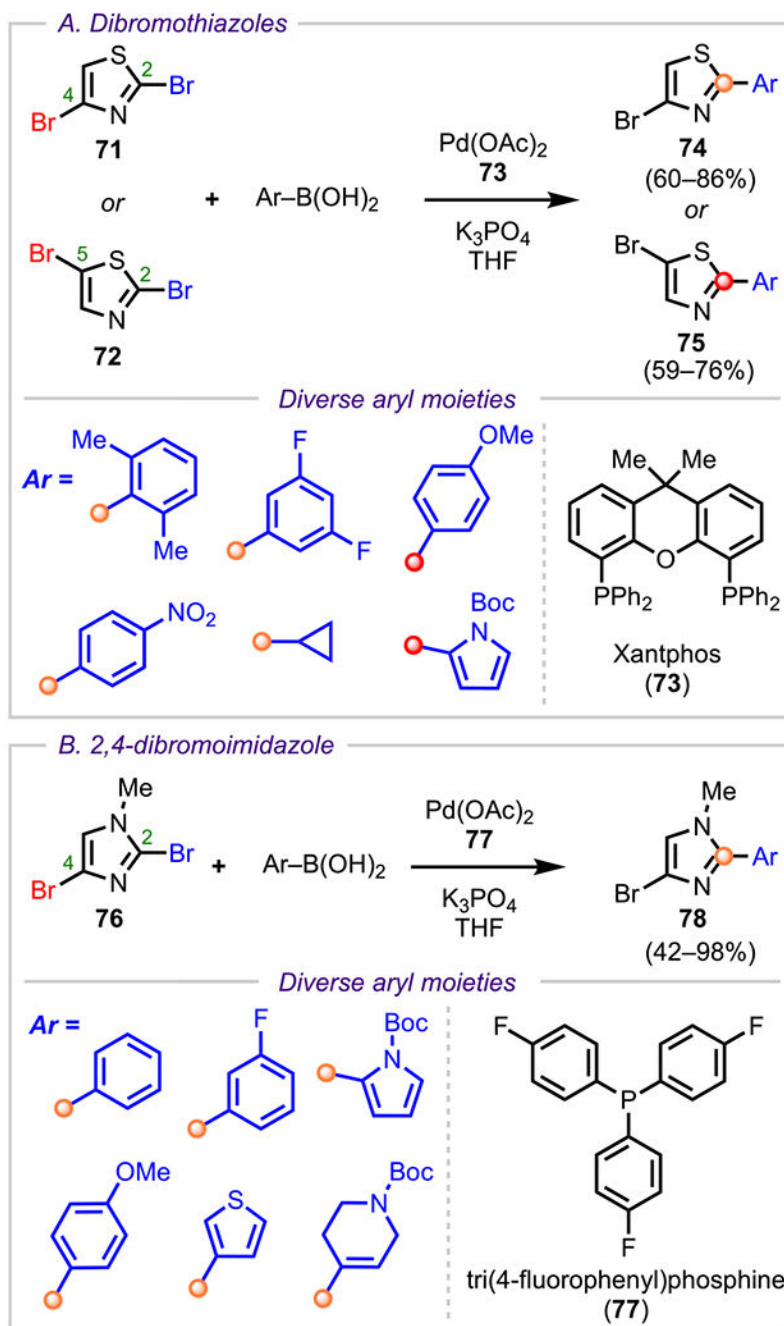
(A) Distortion–Interaction Analysis for the Oxidative Addition of a Model Pd(PH₃)₂ Catalyst into the C2 and C3 C–Br Bonds of 2,3-Dibromofuran and (B) Experimental Confirmation of Predicted Selectivity

**Scheme 19.**

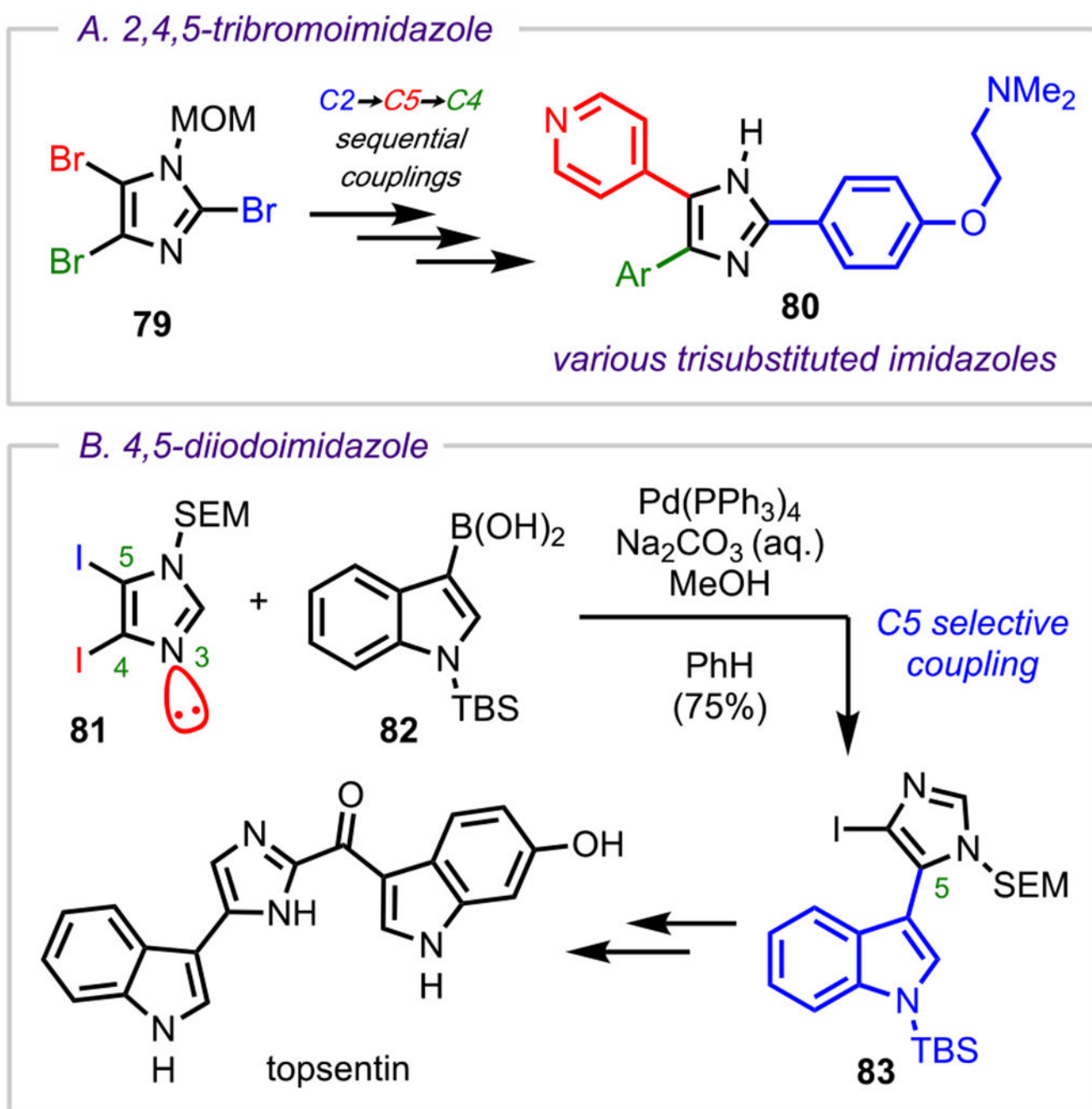
(A) C5- and (B) C3-Selective Arylation of Polybrominated Pyrroles



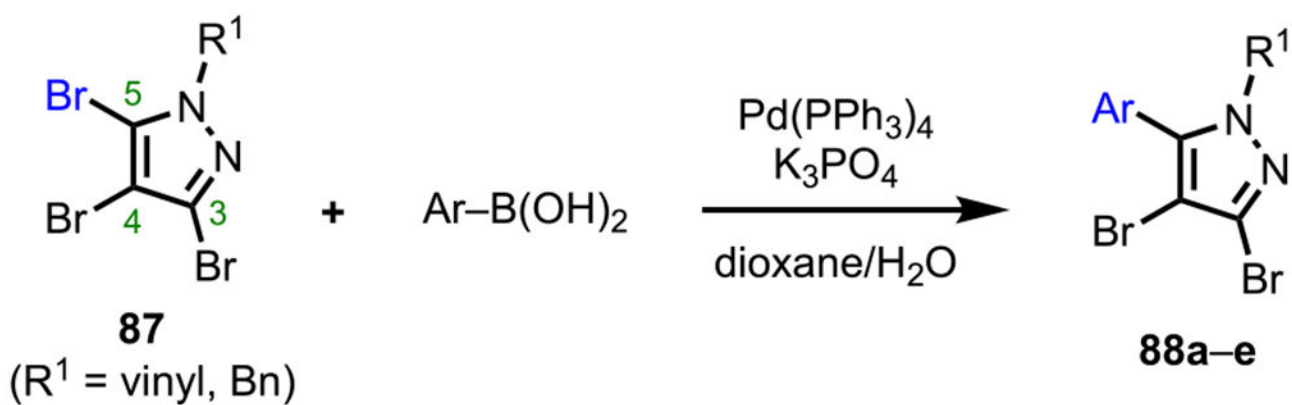
Scheme 20.
Site-Selective Mono/Bis-Arylation of 2,3,5,6-Tetrabromothieno[3,2-*b*]thiophene



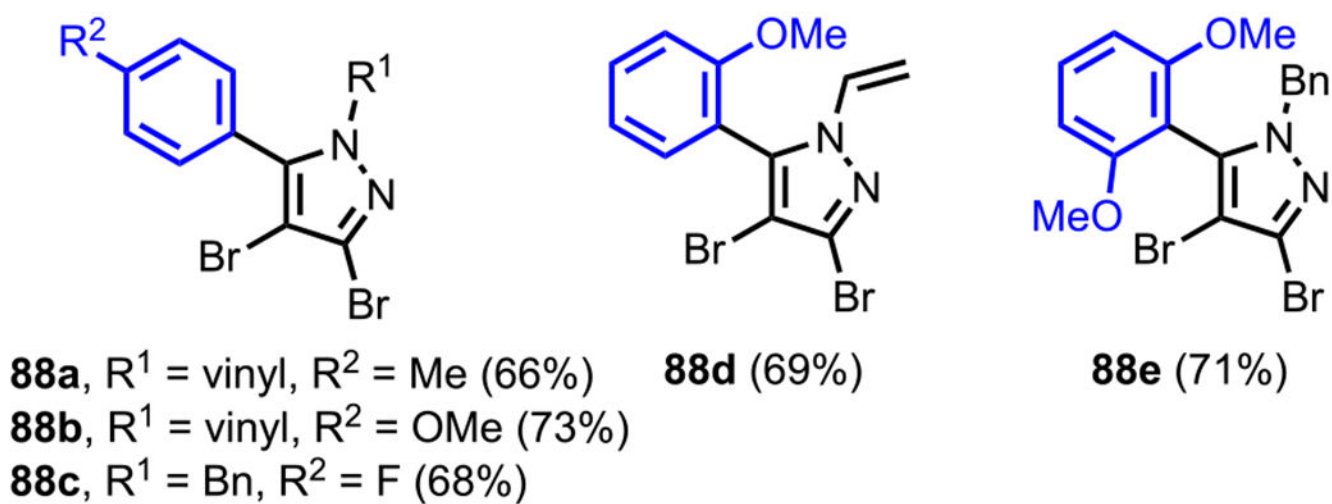
Scheme 21. Selectivity Outcomes for (A) 2,4- and 2,5-Dibromothiazole and (B) *N*-Methyl-2,4-dibromoimidazole

**Scheme 22.**

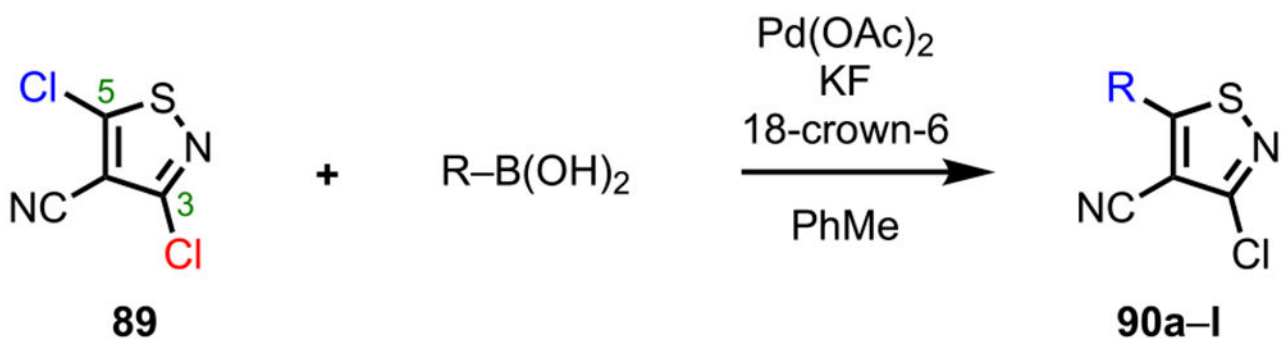
Selectivity Outcomes for (A) *N*-MOM-2,4,5-Tribromoimidazole and (B) *N*-SEM-4,5-Diiodoimidazole



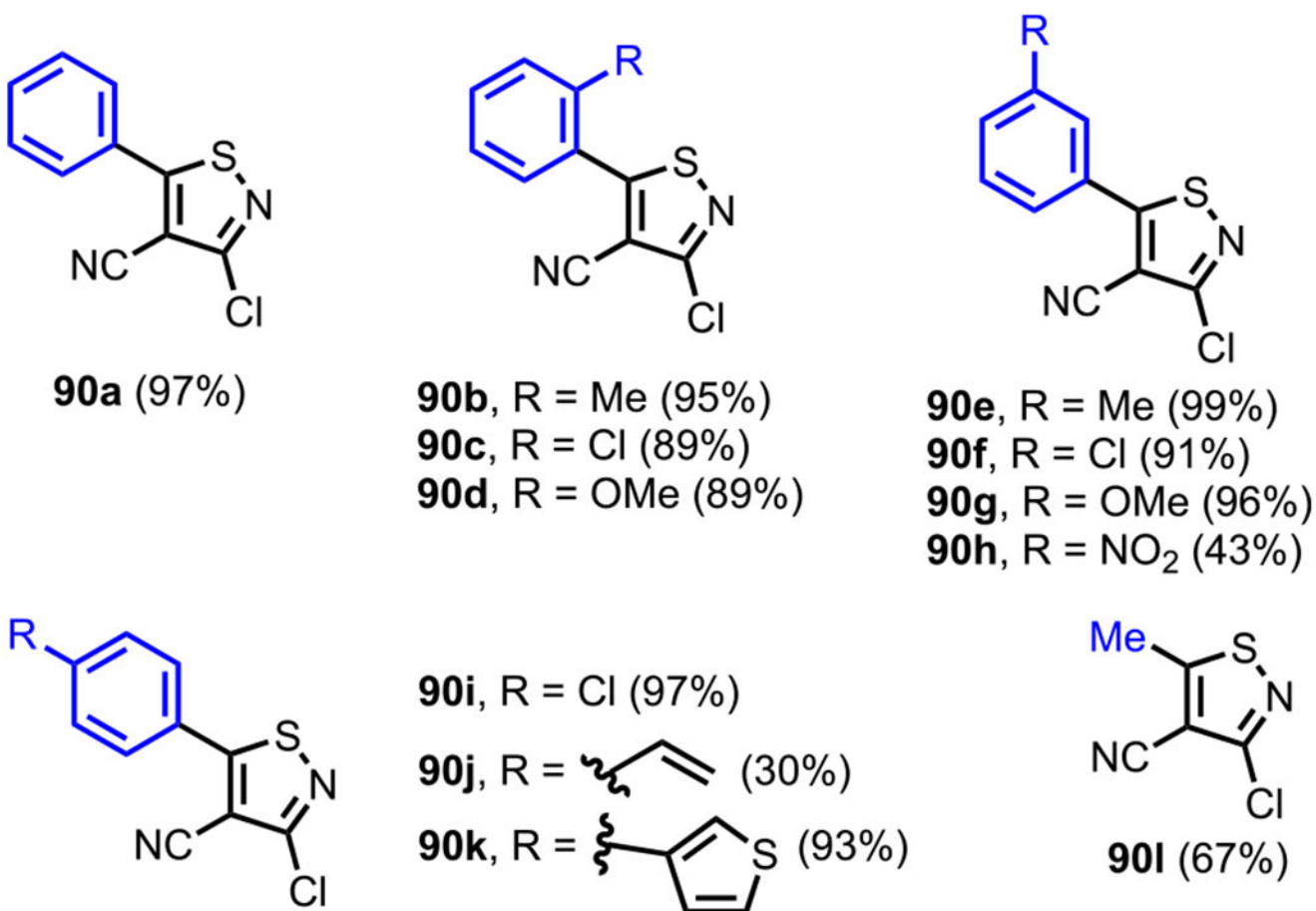
C5-selective coupling



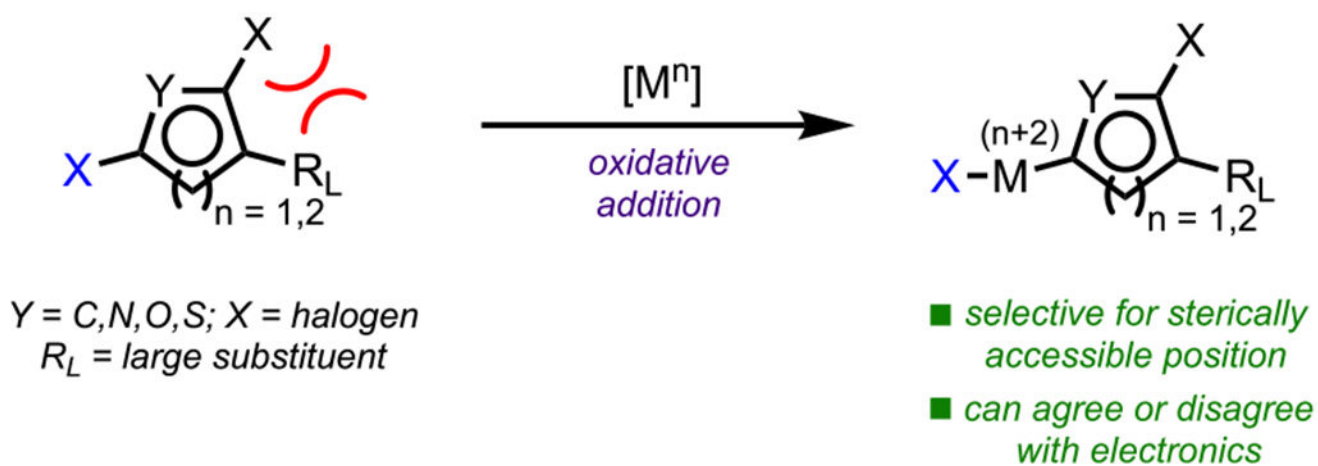
Scheme 23.
Site-Selective Coupling of *N*-Protected 3,4,5-Tribromoimidazole



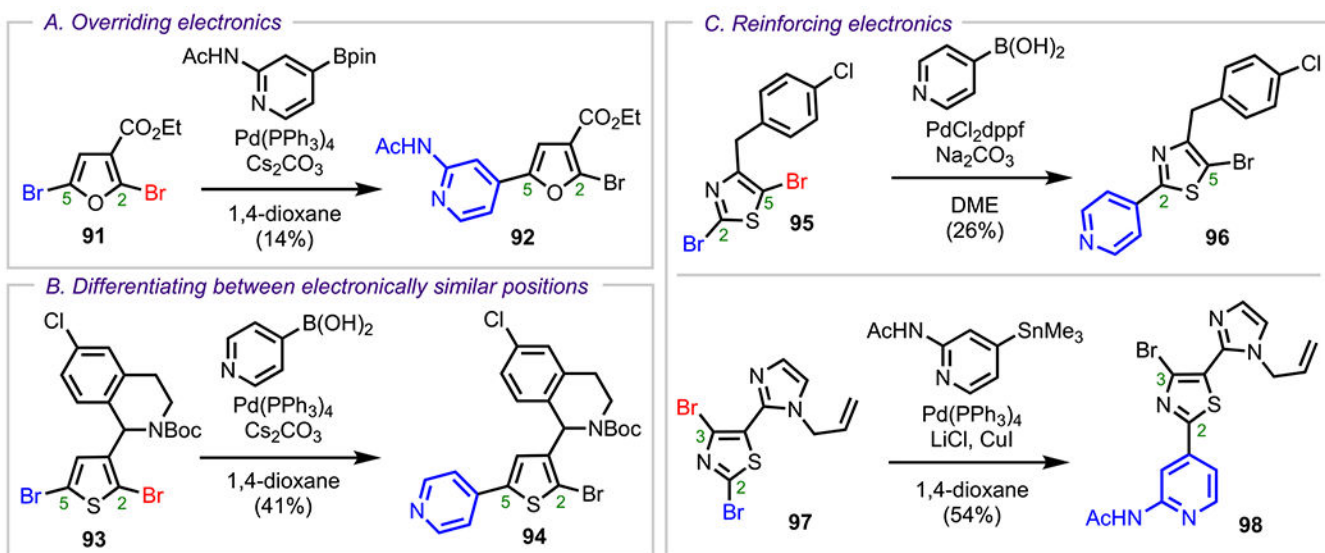
C5-selective coupling



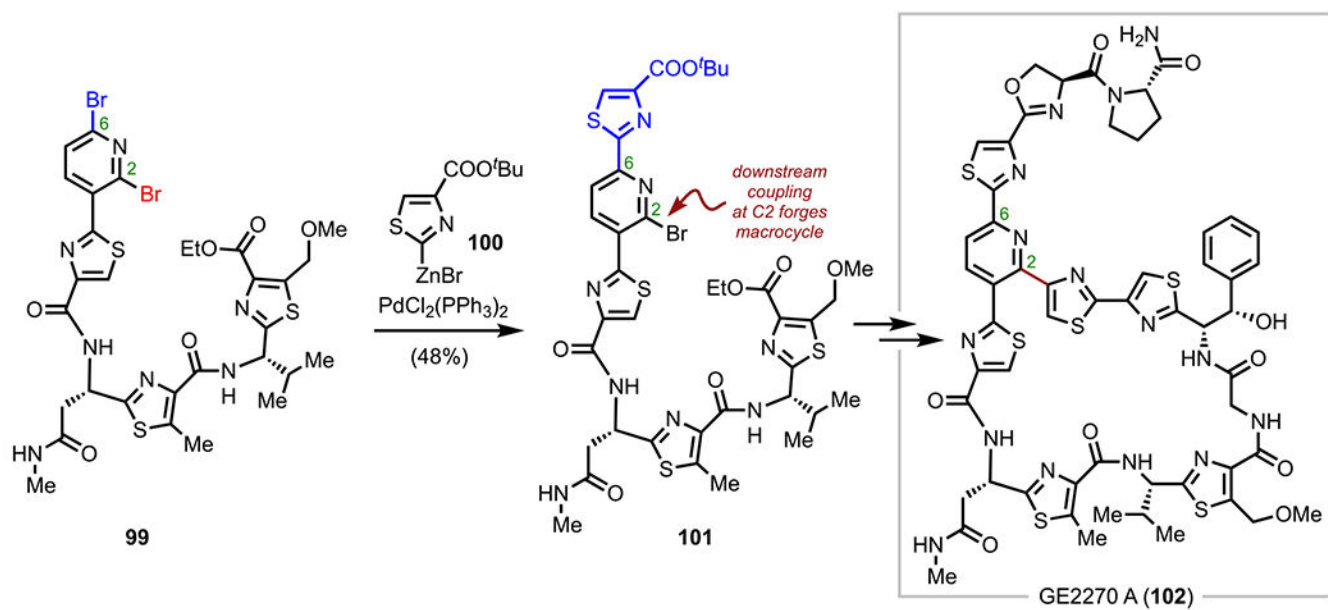
Scheme 24.
Site-Selective Coupling of 3,5-Dichlorothiazole-4-carbonitrile



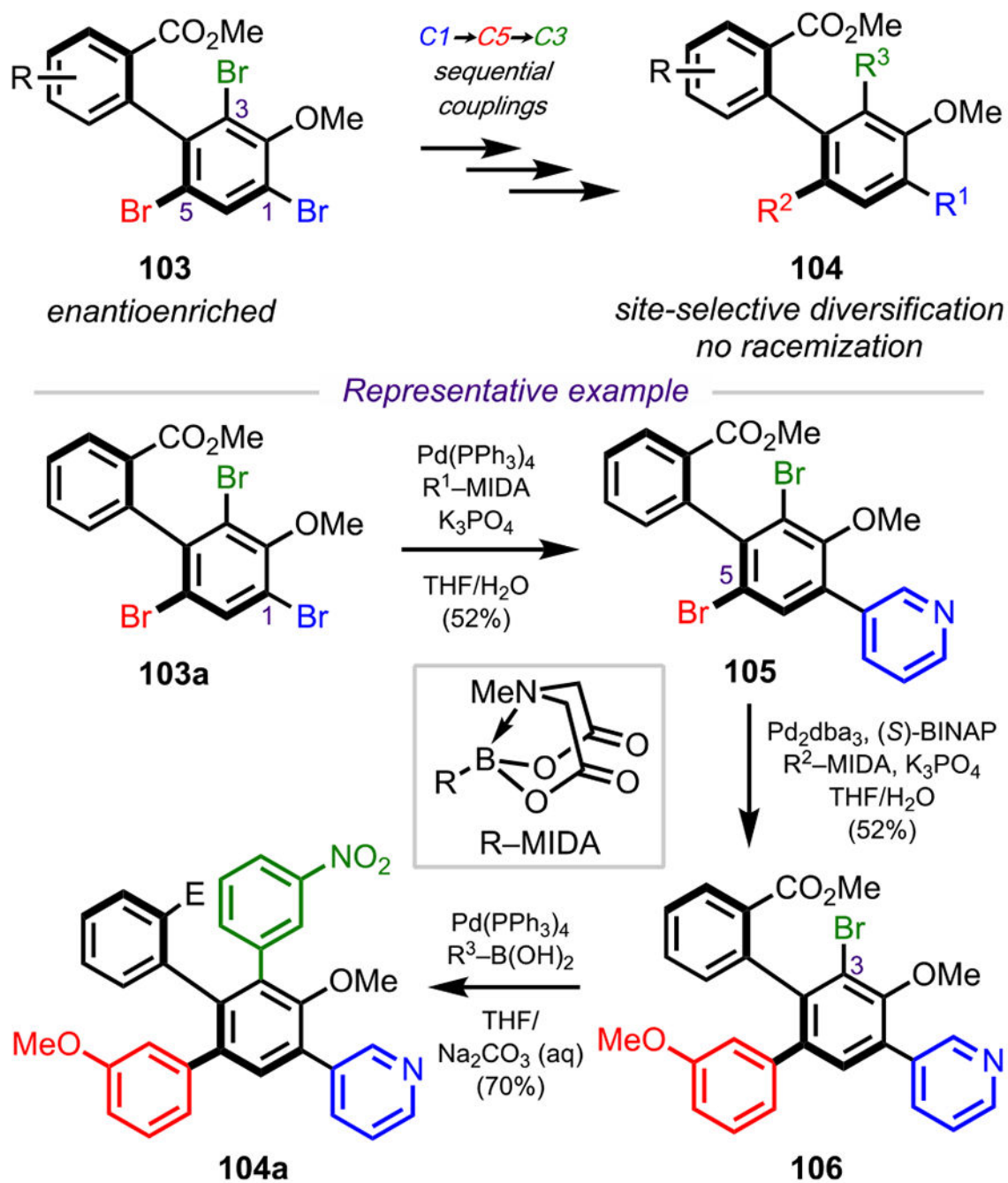
Scheme 25.
 Steric Effects Guiding Cross-Coupling Selectivity

**Scheme 26.**

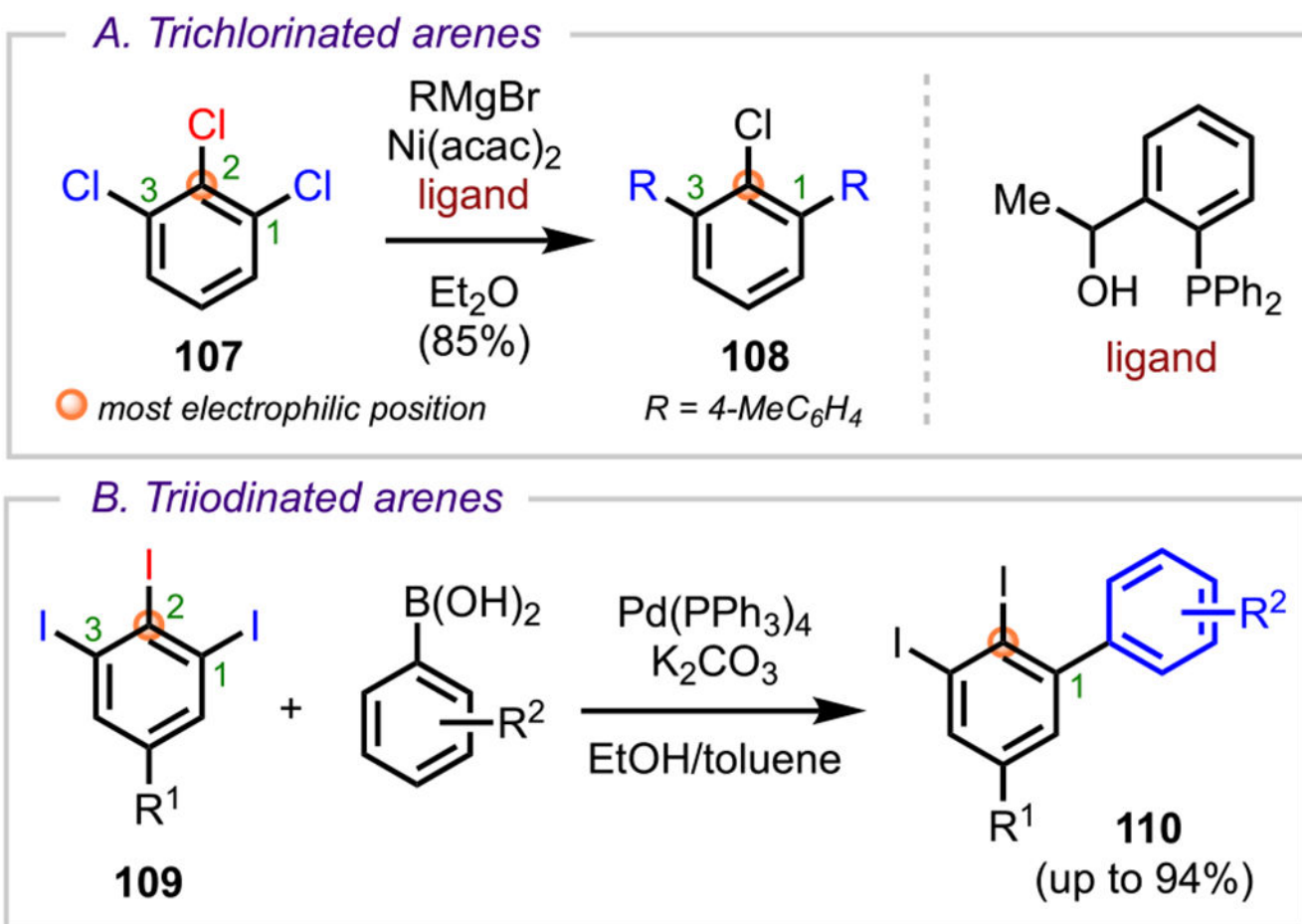
Representative Examples of Steric Effects: (A) Overriding Electronic Effects, (B) Differentiating between Electronically Similar Positions, and (C) Reinforcing Electronic Effects



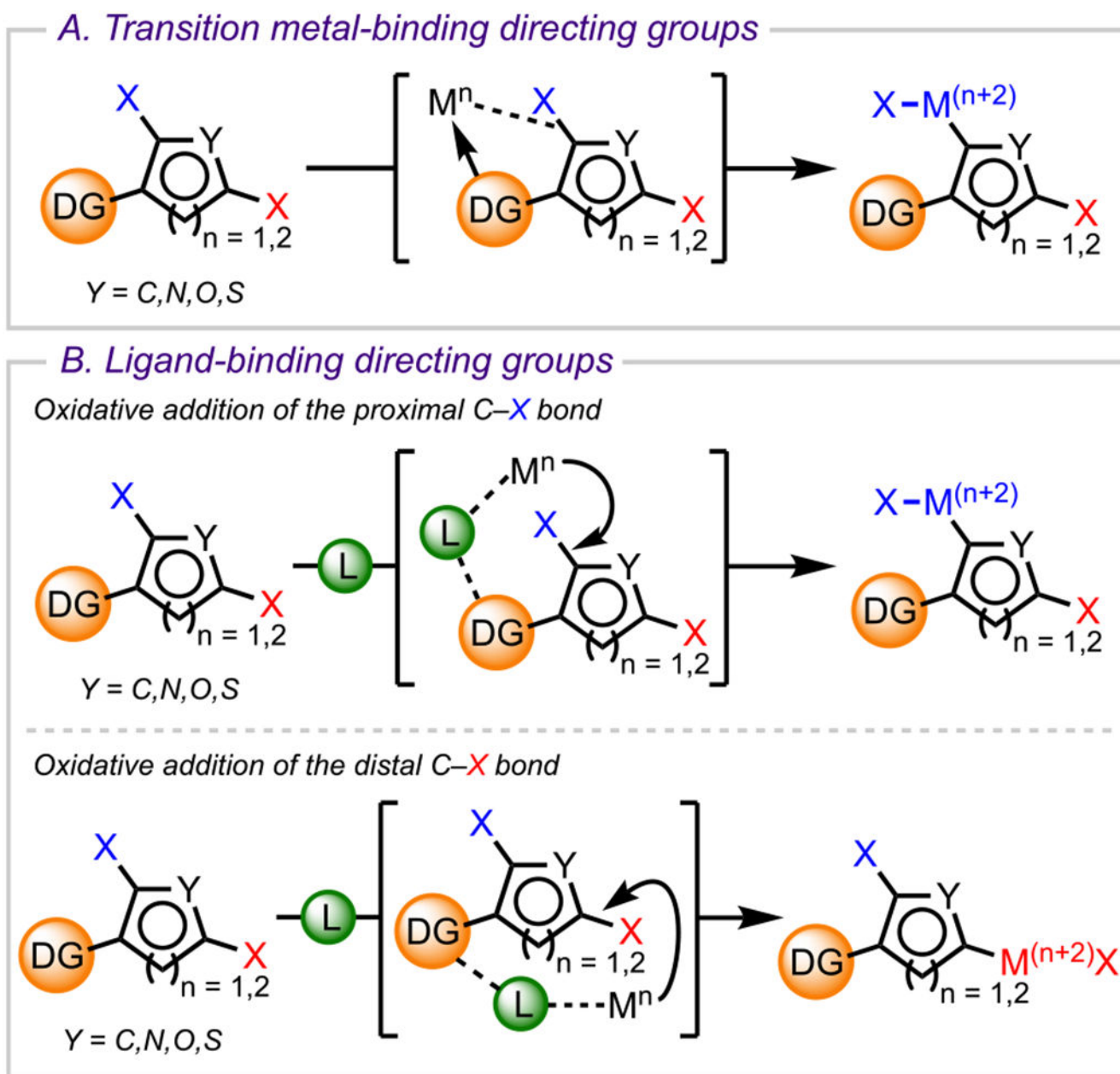
Scheme 27.
Sterically Controlled Coupling in the Total Synthesis of GE2270 A



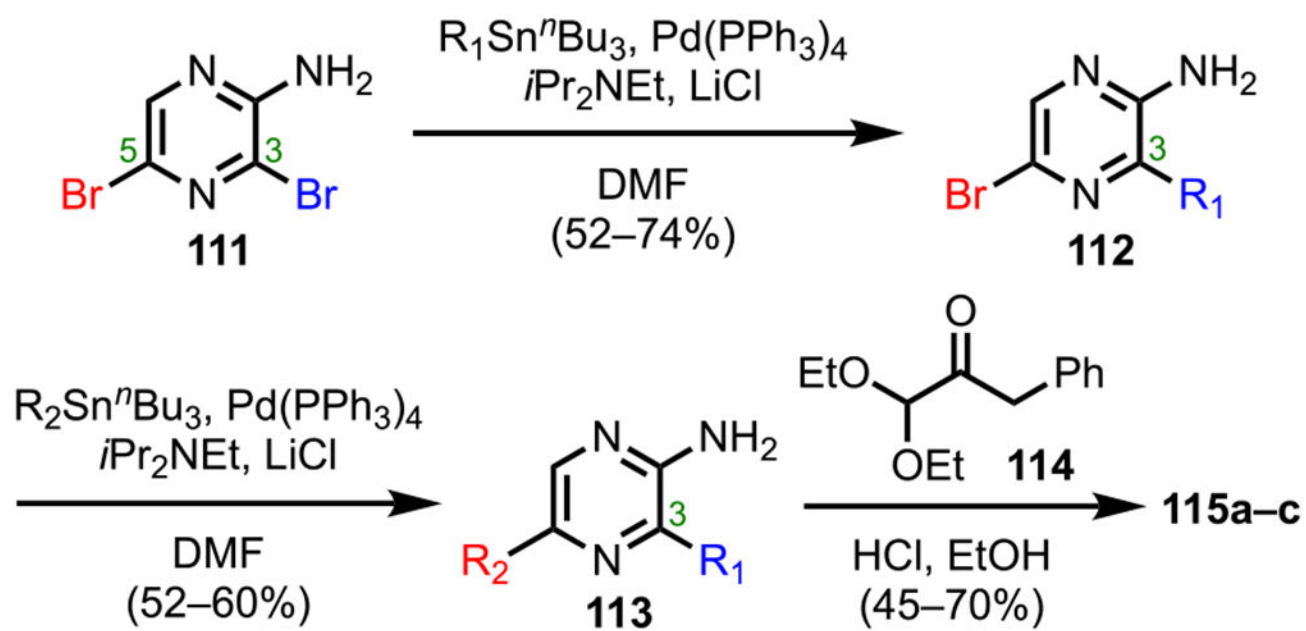
Scheme 28.
Synthesis of Highly Substituted, Enantioenriched Biaryls through Sequential Site-Selective Cross-Couplings



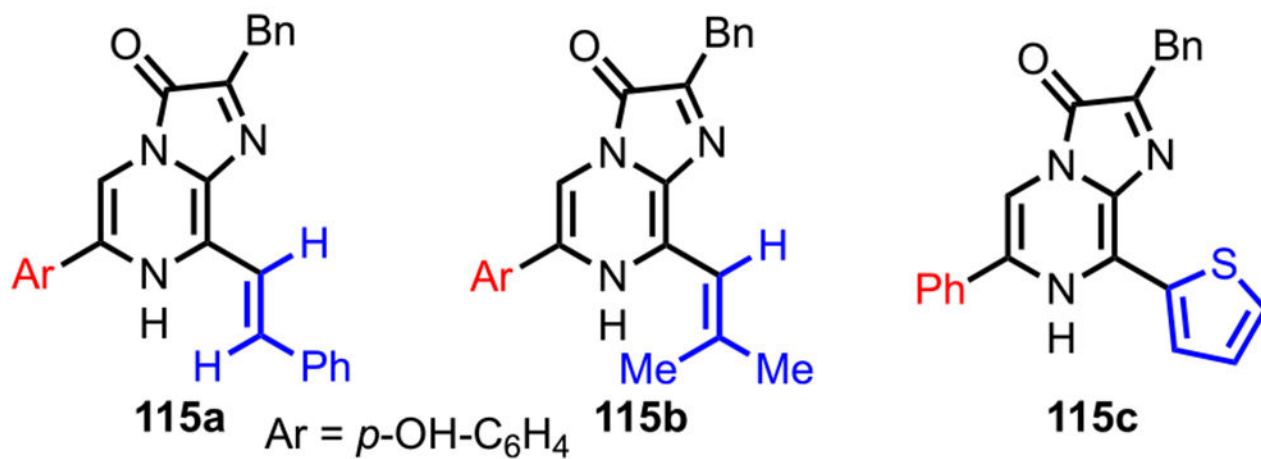
Scheme 29.
 Sterically Controlled Cross-Coupling of (A) 1,2,3-Trichlorinated Benzene and (B) 1,2,3-Triiodinated Benzene

**Scheme 30.**

General Strategy of Achieving Selective Coupling by Using Directing Groups That Either (A) Bind Directly to a Metal Center (Metal-Binding Directing Groups) or (B) Bind to a Ligand (Ligand-Binding Directing Groups)

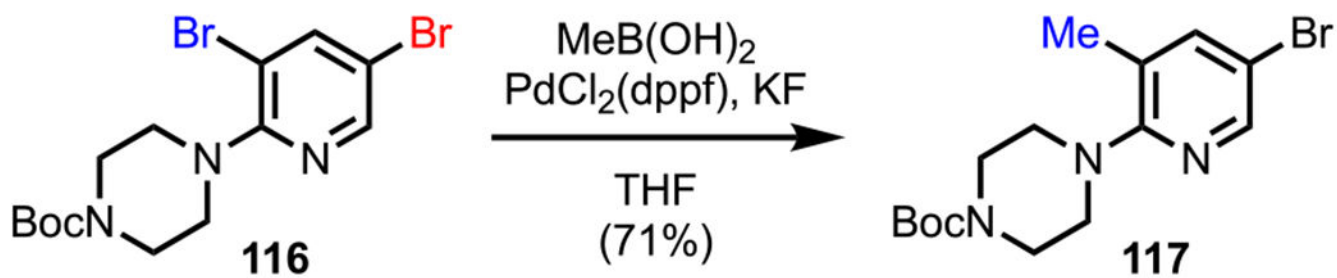


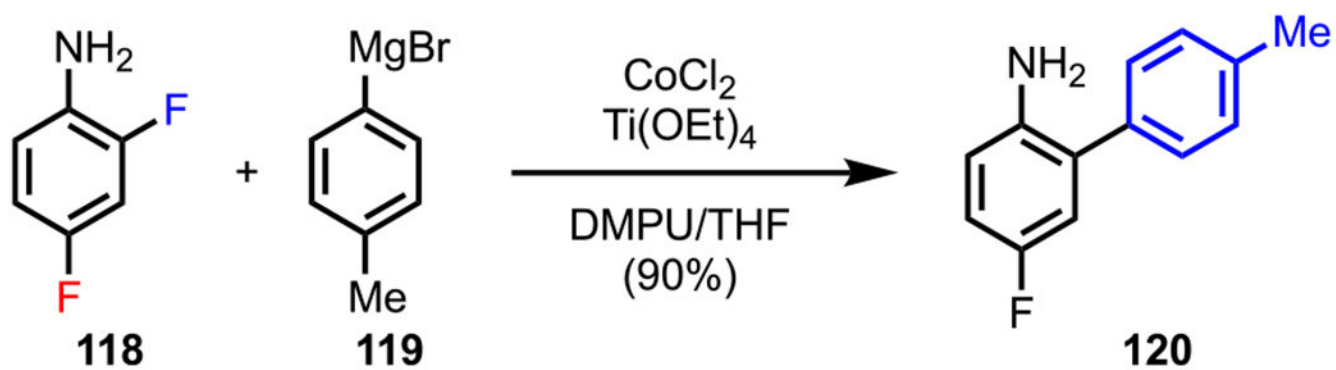
Selected coelenterazine analogues



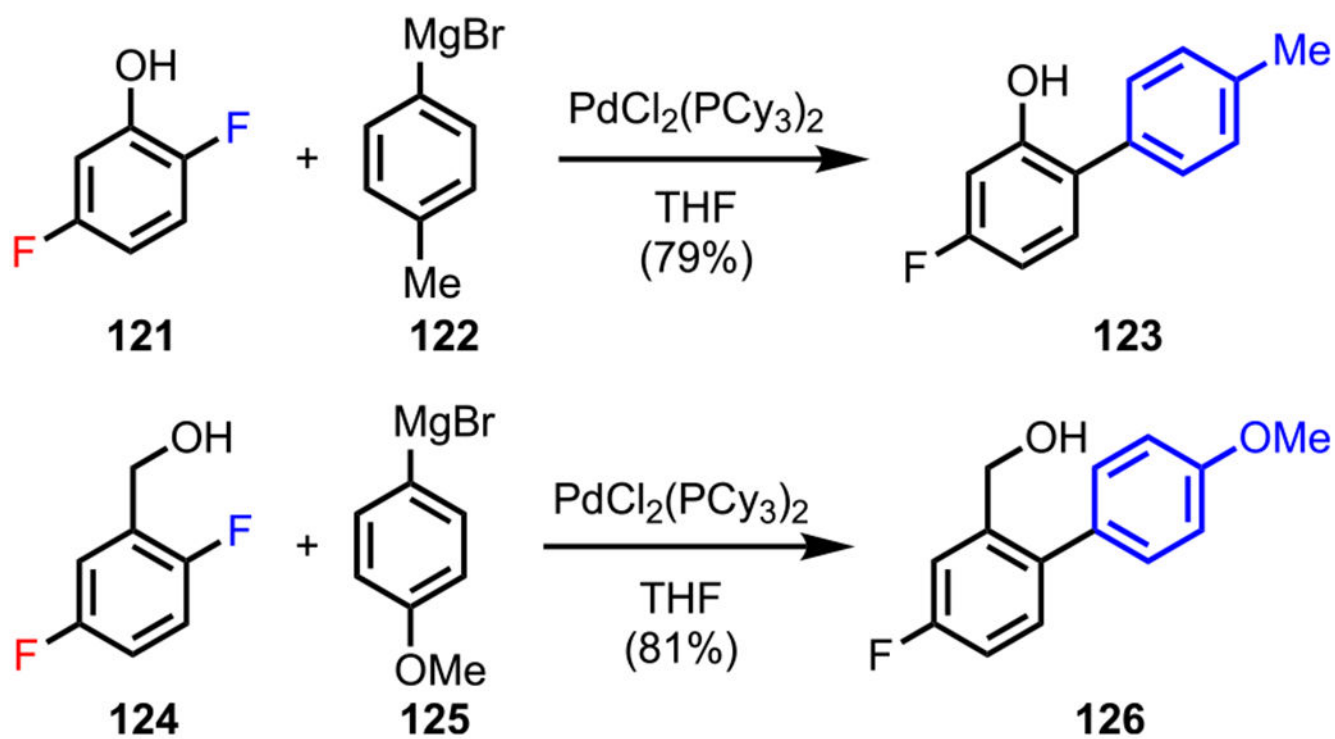
Scheme 31.

Synthesis of Coelenterazine Analogues Starting from 2-Amino-3,5-dibromo Pyrazine (111)

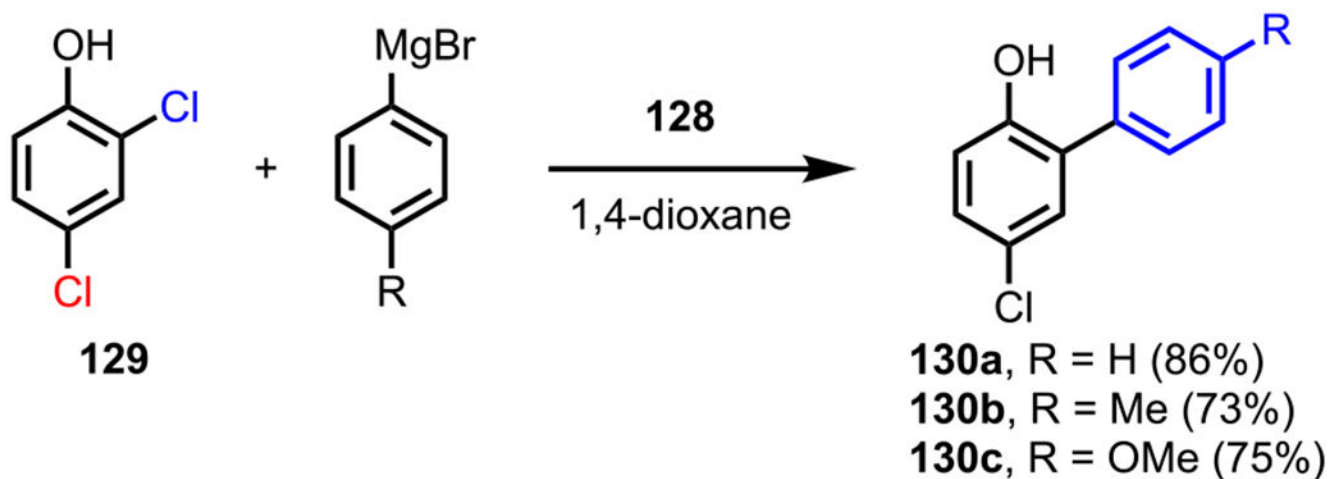
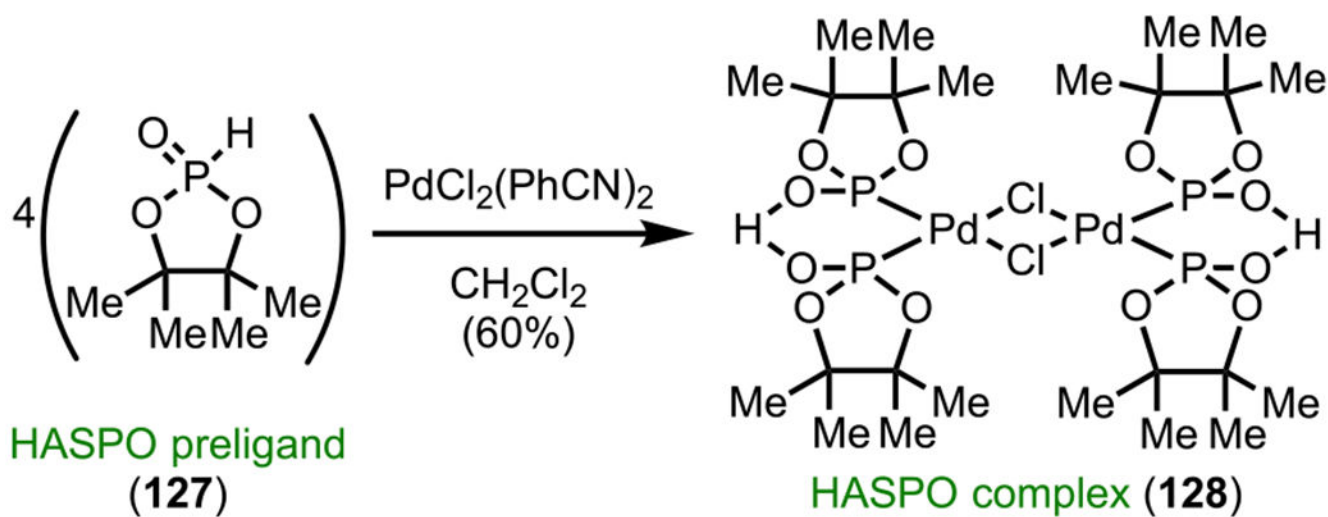
**Scheme 32.**Site-Selective Suzuki–Miyaura Coupling of *N*-(3,5-Dibromo-2-pyridyl)piperazine 116



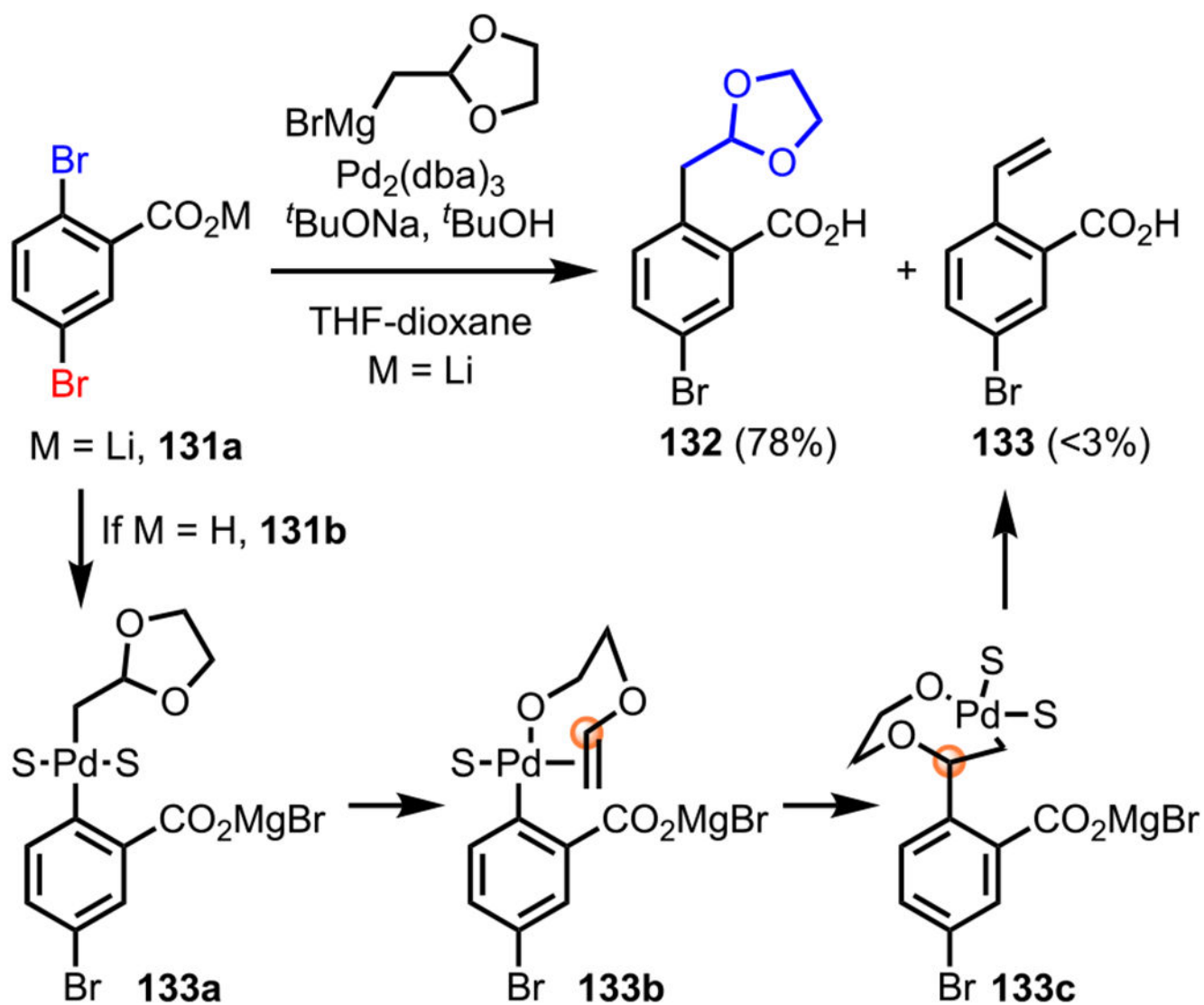
Scheme 33.
Amine-Directed C–F Bond Activation under Cobalt-Catalyzed Conditions



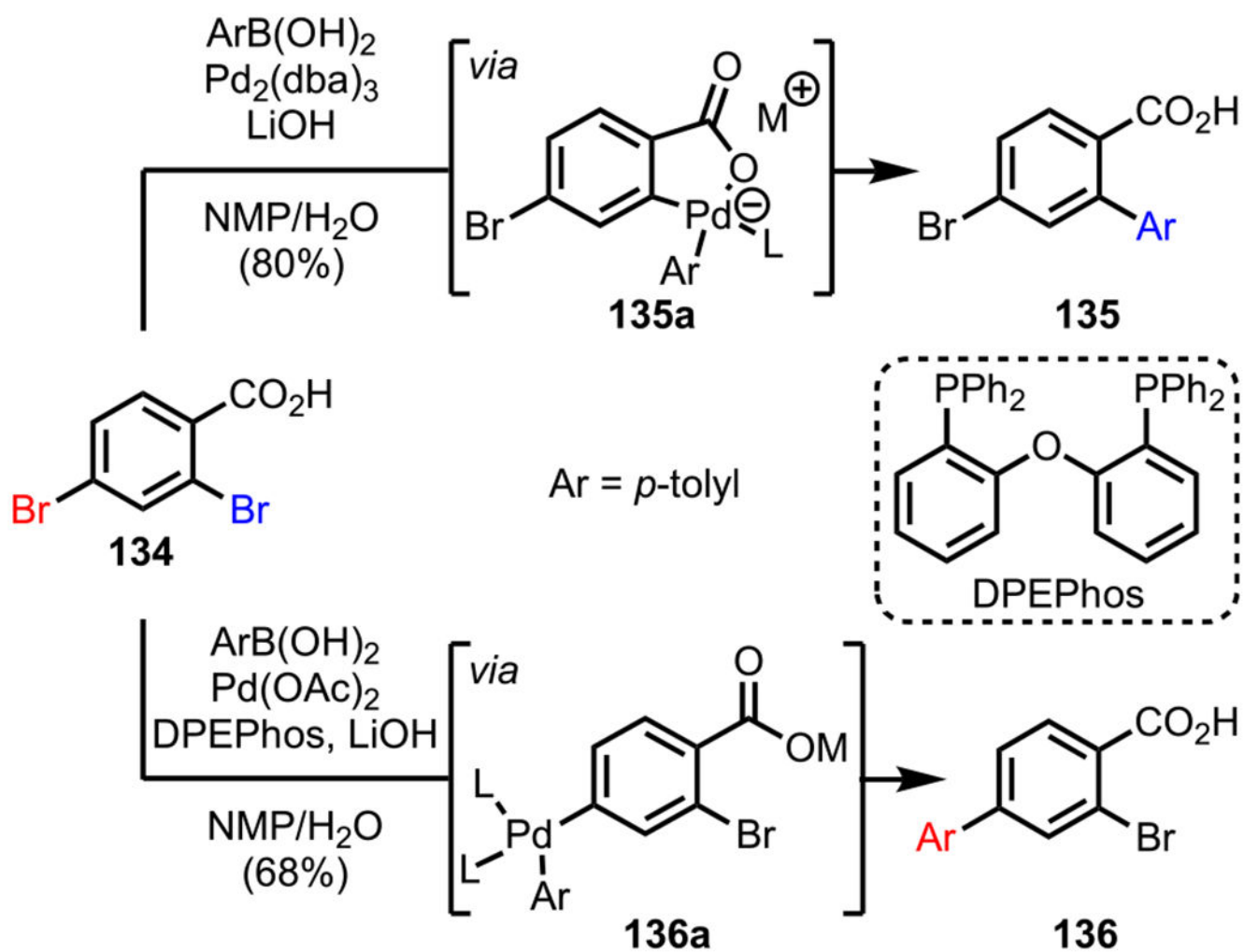
Scheme 34.
ortho-Selective Kumada Coupling of Difluorinated Phenol and Benzylic Alcohol Derivatives



Scheme 35.
 Site-Selective Kumada Coupling of 2,4-Dichlorophenol with the HASPO Complex

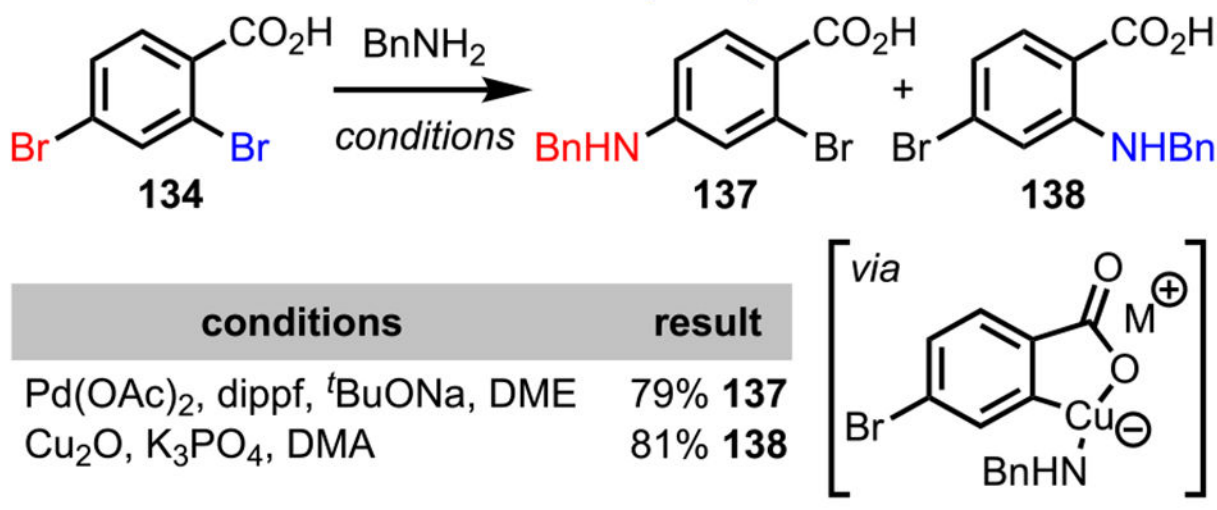


Scheme 36.
ortho-Selective Kumada Coupling with the Lithium Salt of 2,5-Dibromobenzoic Acid

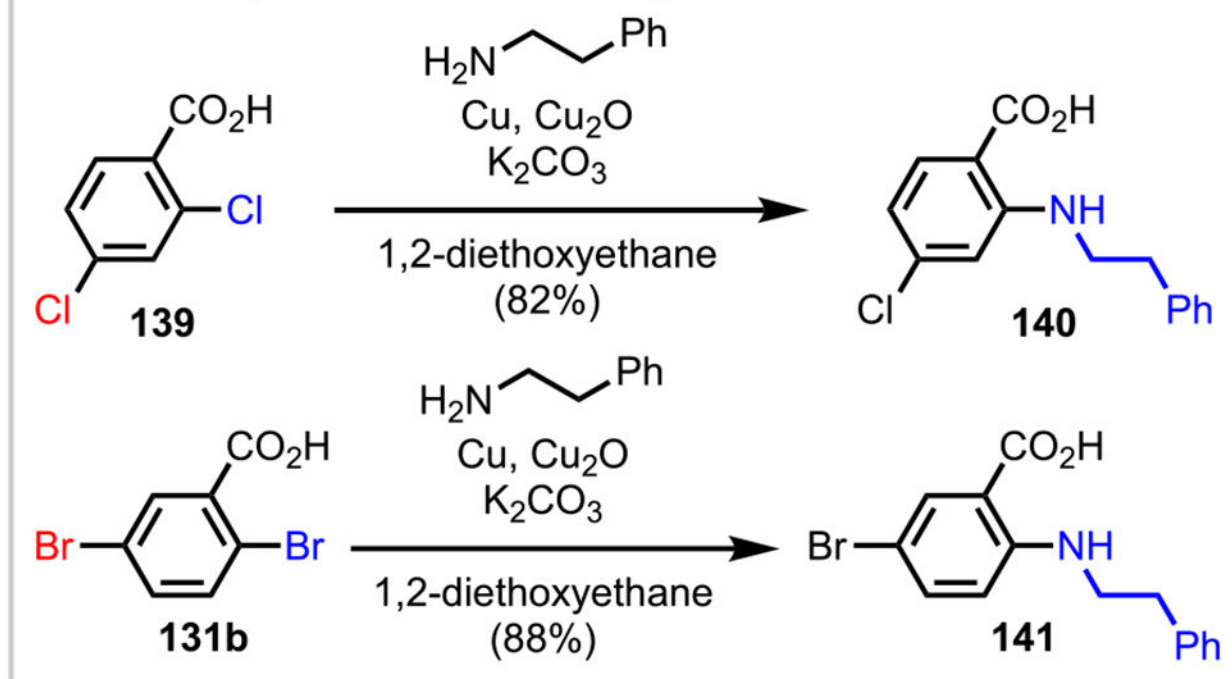


Scheme 37.
Carboxylate-Directed Site-Selective Suzuki–Miyaura Coupling of 2,4-Dibromobenzoic Acid

A. Site-selective monoamination by Houpis and co-workers

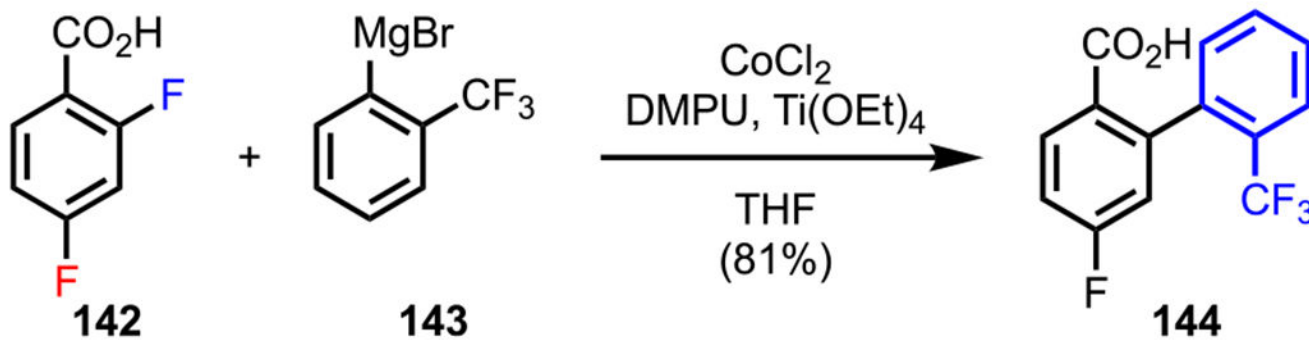


B. Cu-catalyzed monoamination by Wolf and co-workers

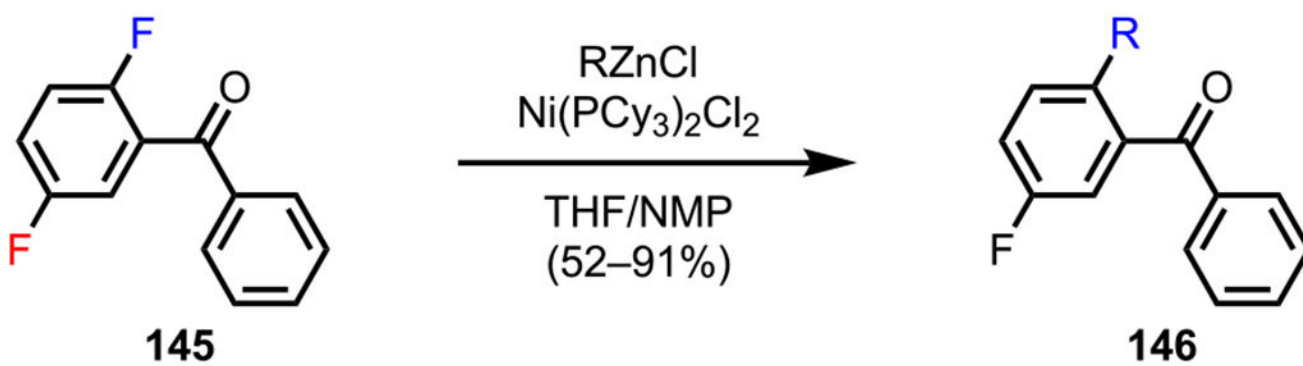


Scheme 38.

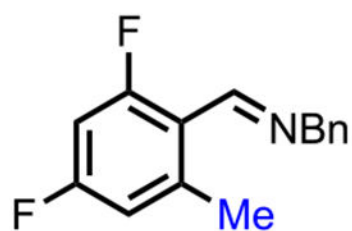
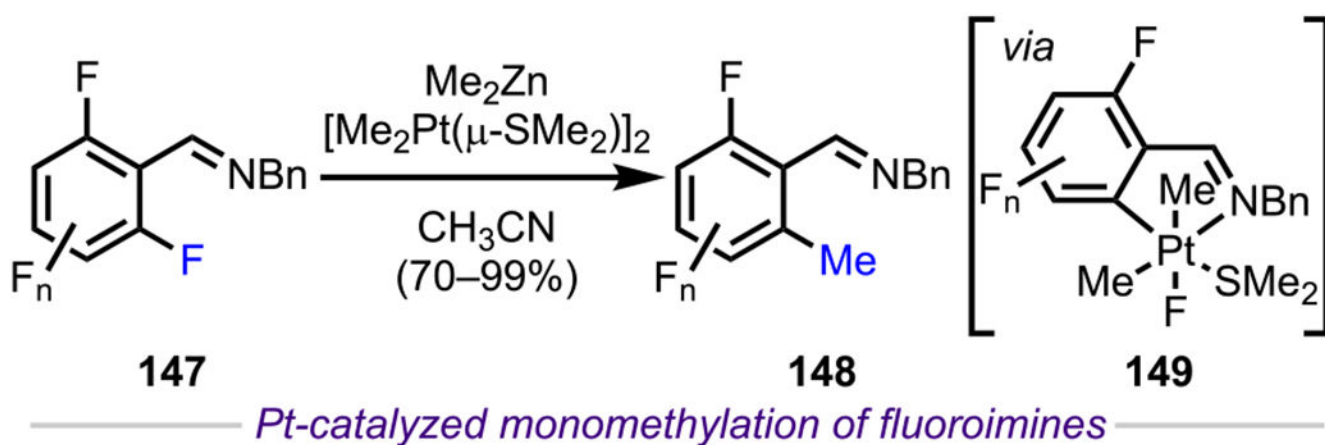
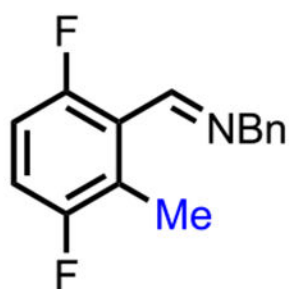
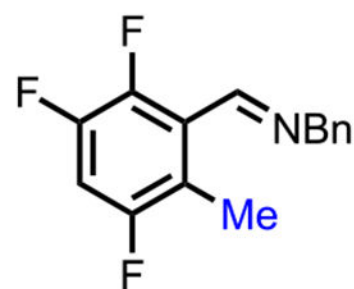
(A) Complementary Selectivity Observed under Pd- and Cu-Catalyzed Conditions and (B) Site-Selective Monoamination under Cu-Catalyzed Conditions



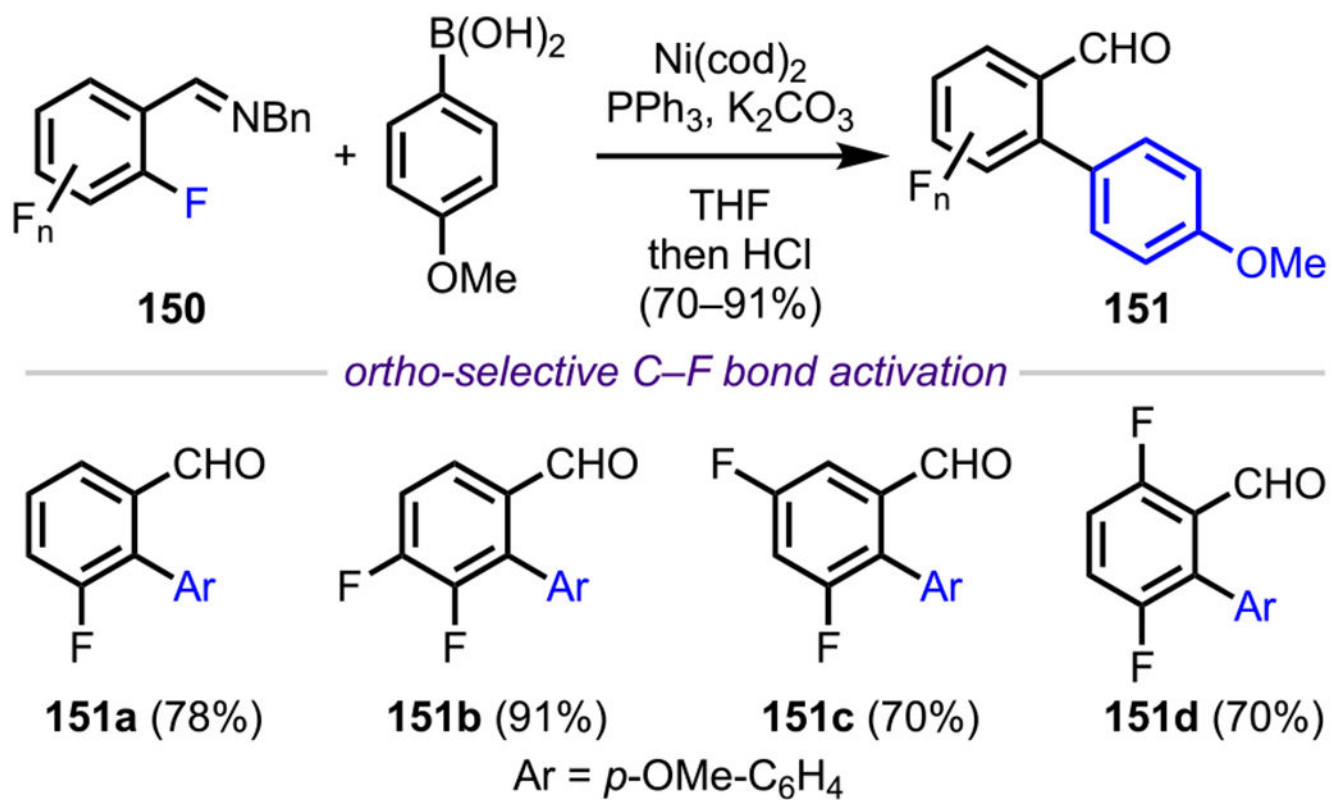
Scheme 39.
ortho-Selective Kumada Coupling of Difluorobenzoic Acid



Scheme 40.
ortho-Selective Functionalization of Difluoroarene 145

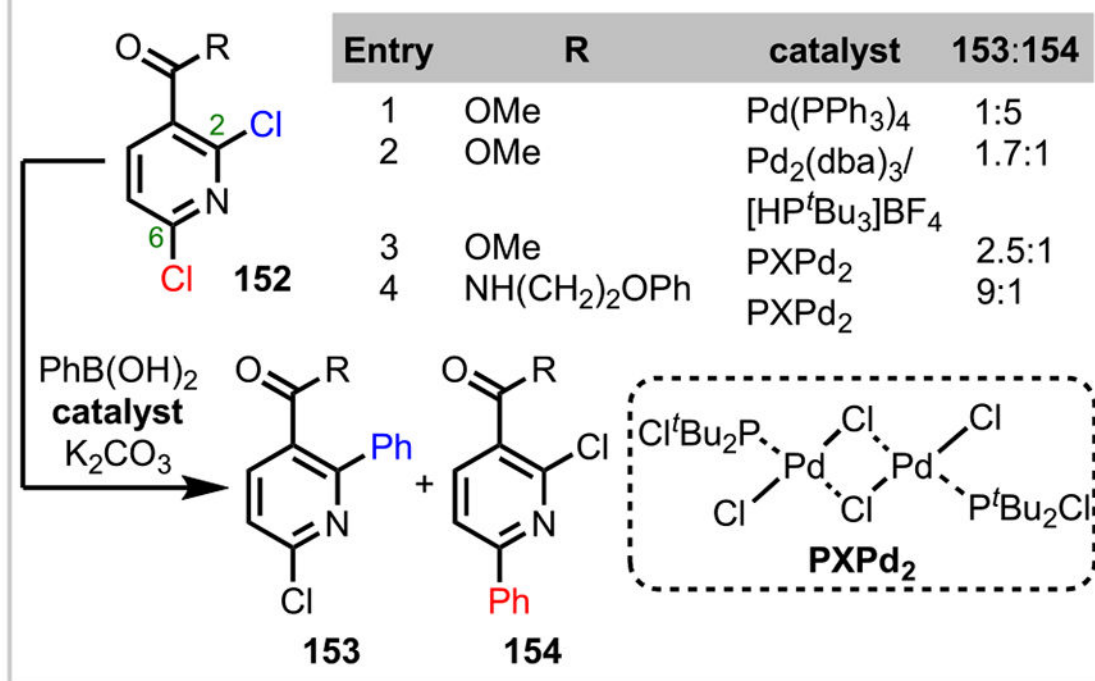
**148a** (95%)**148b** (92%)**148c** (70%)**Scheme 41.**

Platinum(II)-Catalyzed ortho-Methylation of Polyfluoroaryl Imines

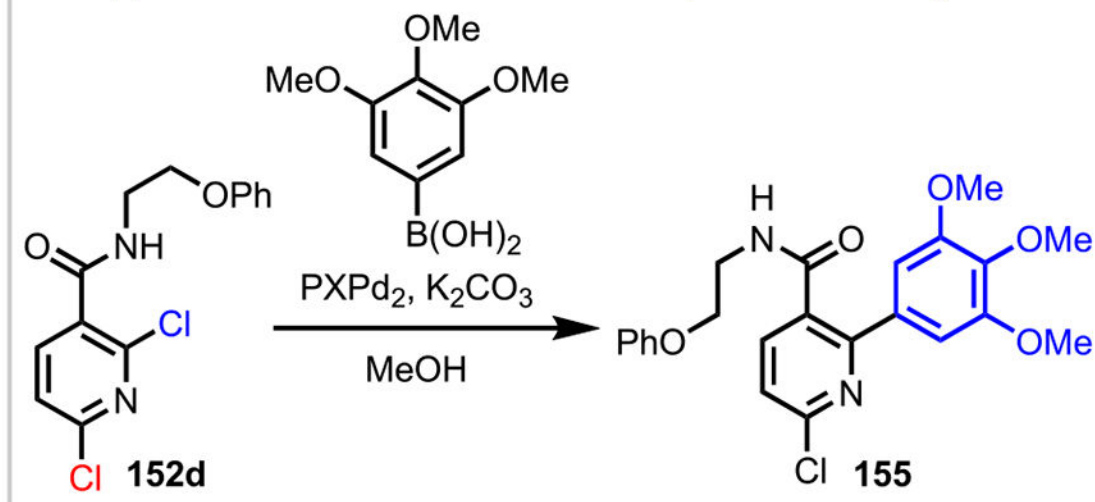


Scheme 42.
Nickel-Catalyzed ortho-Arylation of Polyfluoroaryl Imines

A. Ester/Amide-assisted site-selective monoarylation

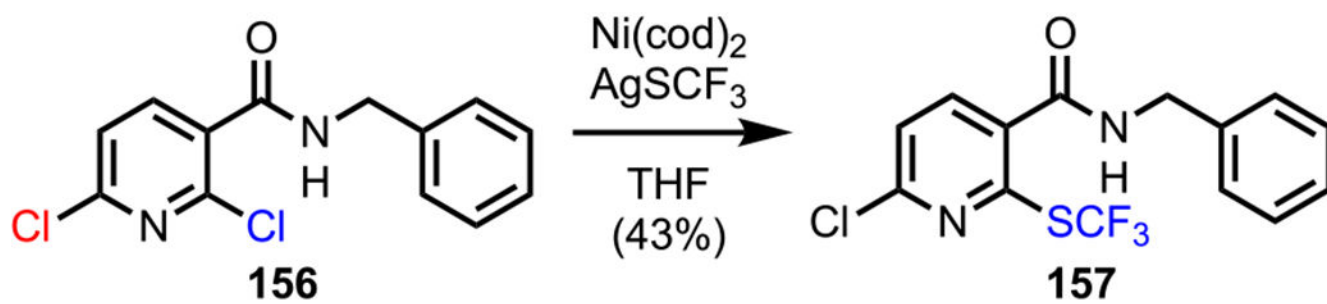


B. Application of amide-assisted monoarylation chemistry

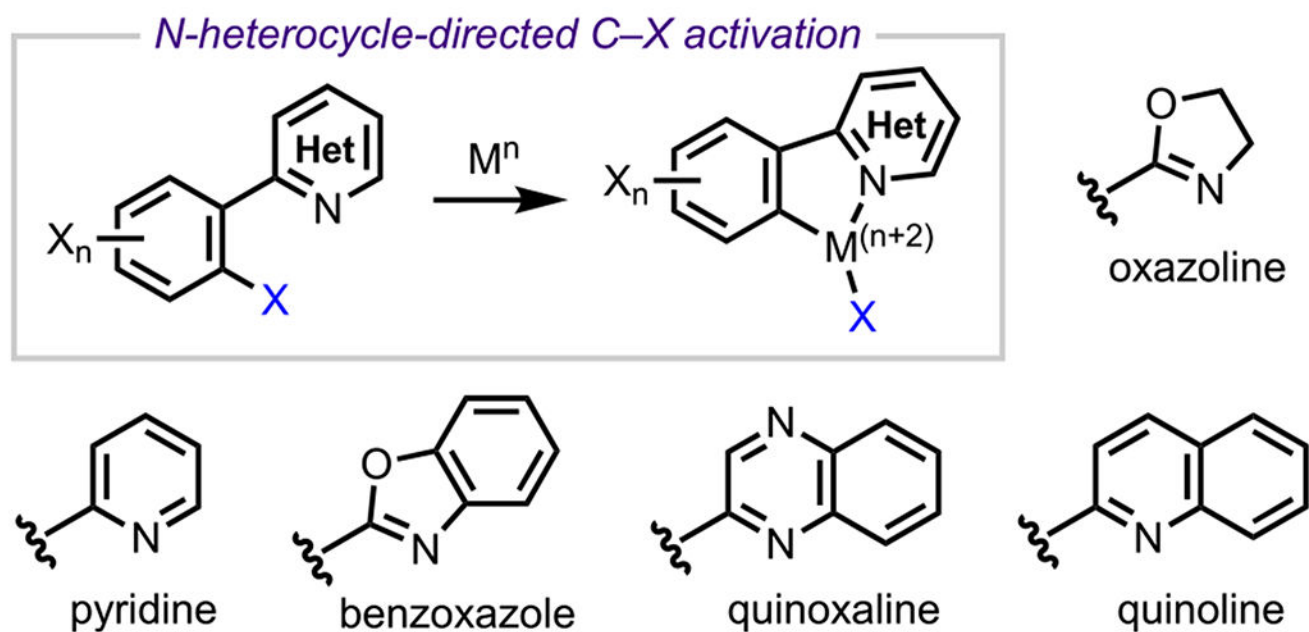


Scheme 43.

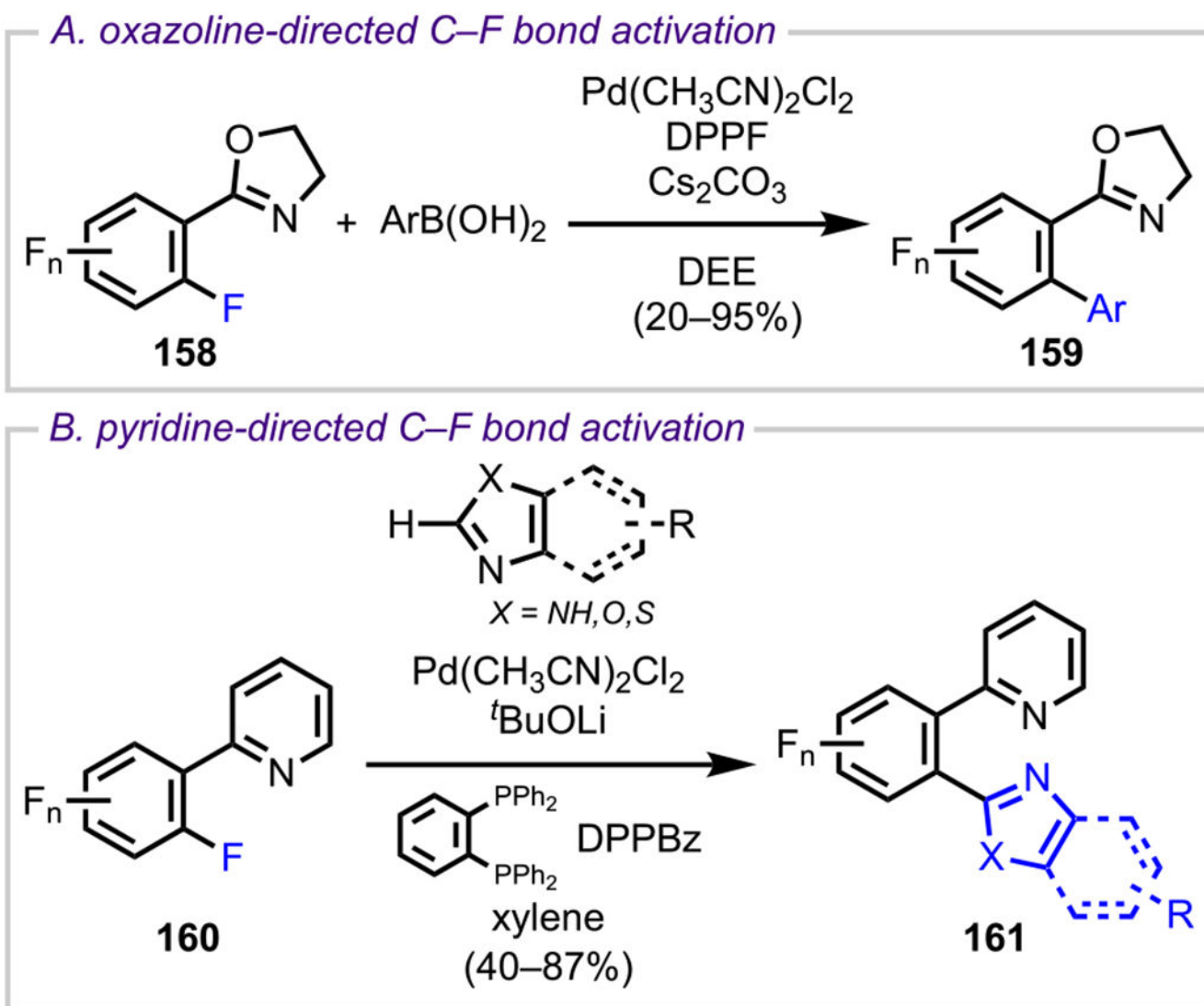
(A) Ester- and Amide-Directed Suzuki–Miyaura Coupling in the Presence of PXPd₂ and (B) Application toward the Syntheses of Negative Allosteric Modulator Analogues



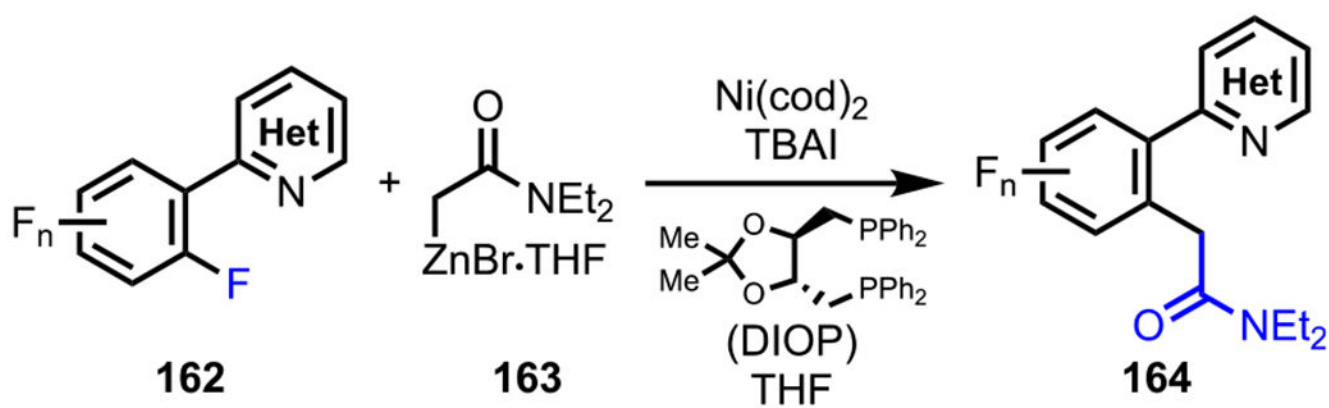
Scheme 44.
Amide-Directed Mono-Trifluoromethylthiolation of Dichloronicotinamide 156

**Scheme 45.**

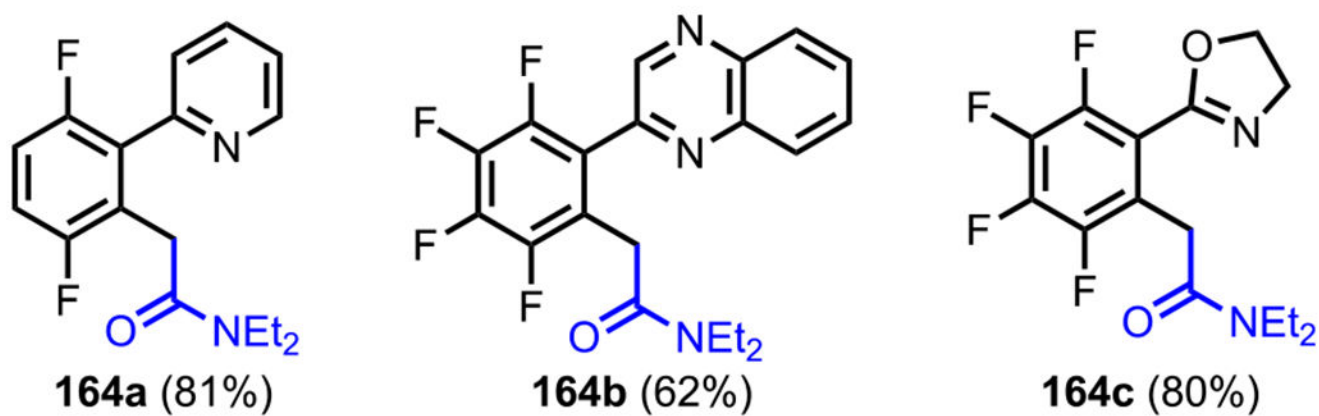
Selected Examples of *N*-Heterocycles Employed for the Selective Functionalization of Polyhaloarenes

**Scheme 46.**

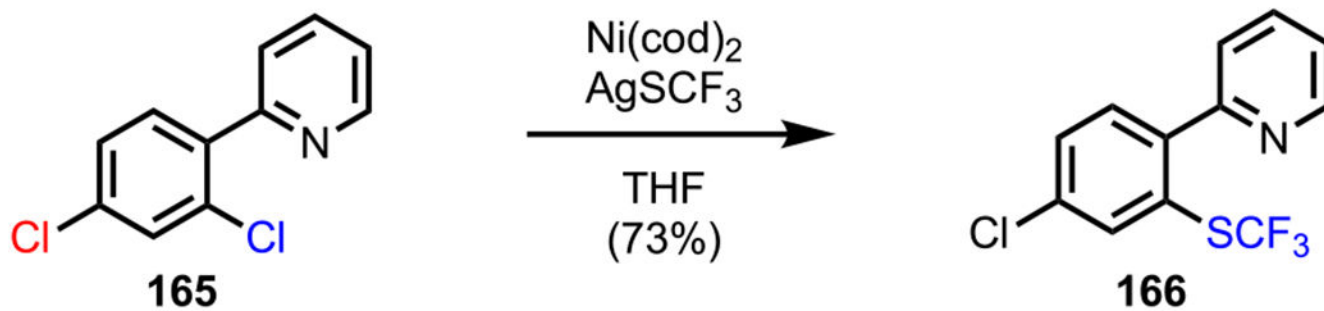
(A) Oxazoline-Directed ortho-Arylation and (B) Pyridine-Directed Concurrent C–F/C–H Bond Activation



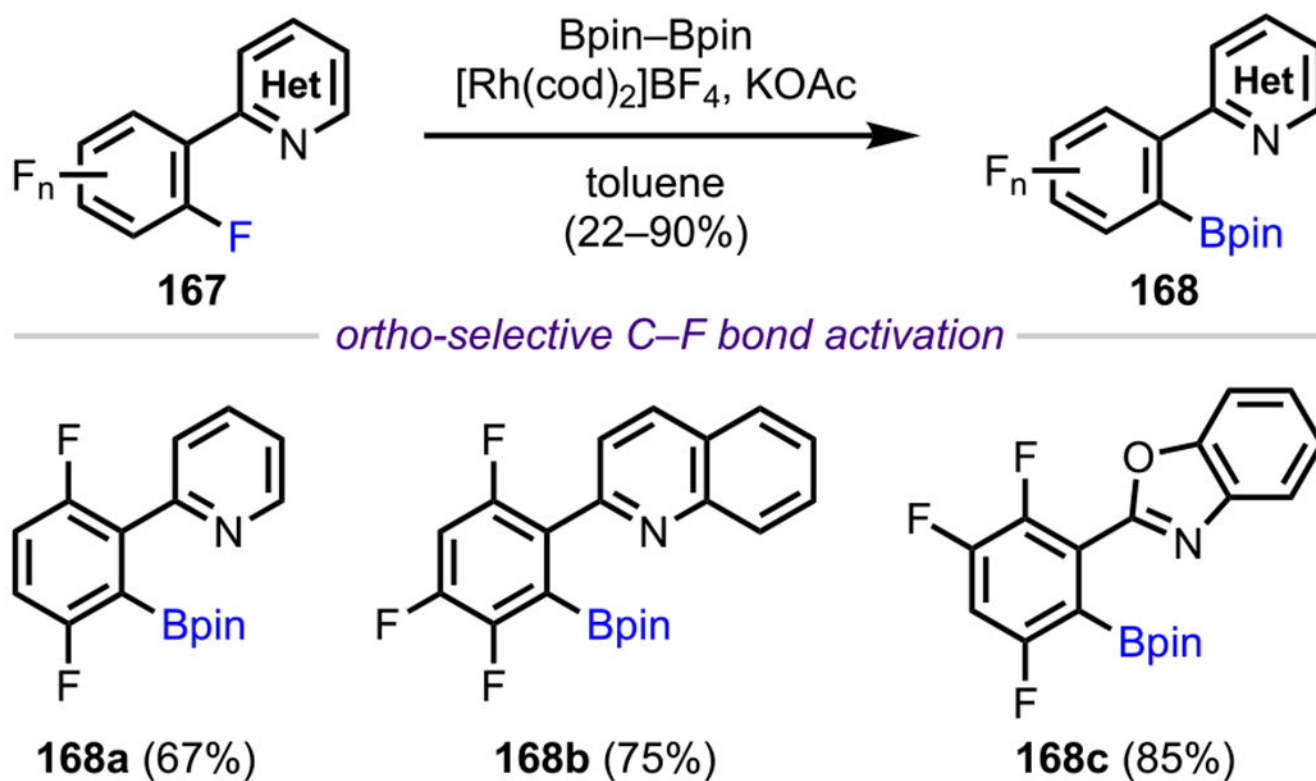
ortho-selective C–F bond activation

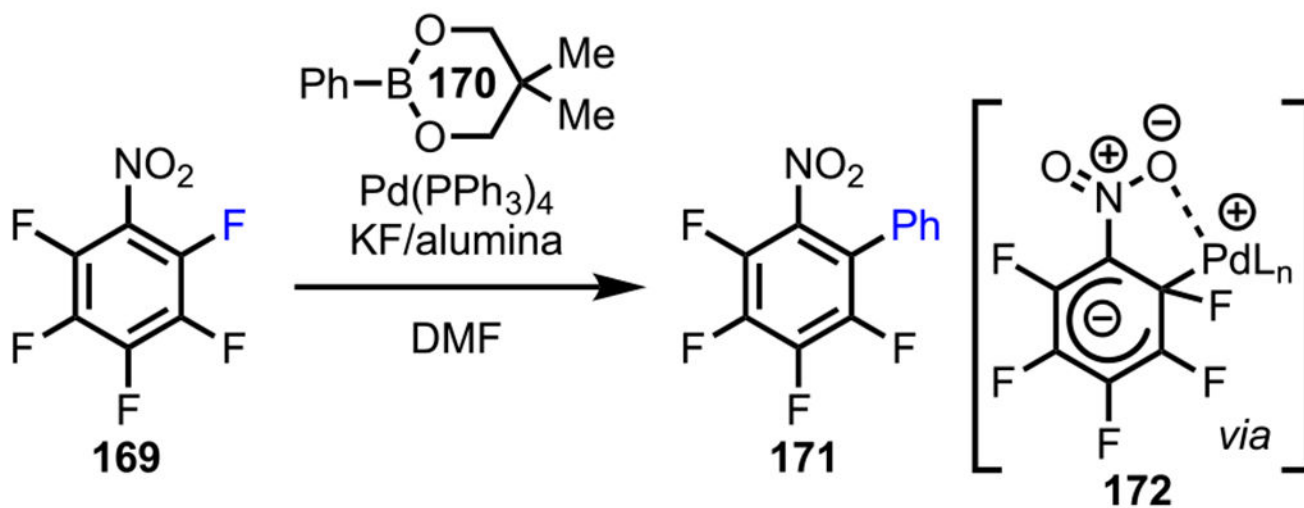


Scheme 47.
ortho-Selective α -Arylation of Polyfluoroarenes with Reformatsky Reagents

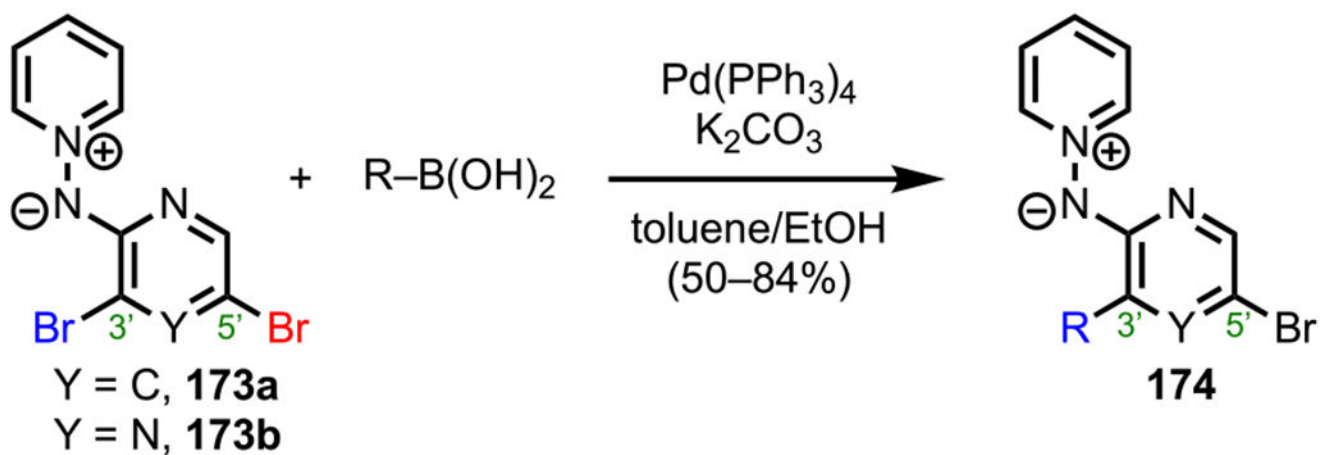
**Scheme 48.**

Pyridine-Directed Mono-Trifluoromethylthiolation of Dichloroarene 165

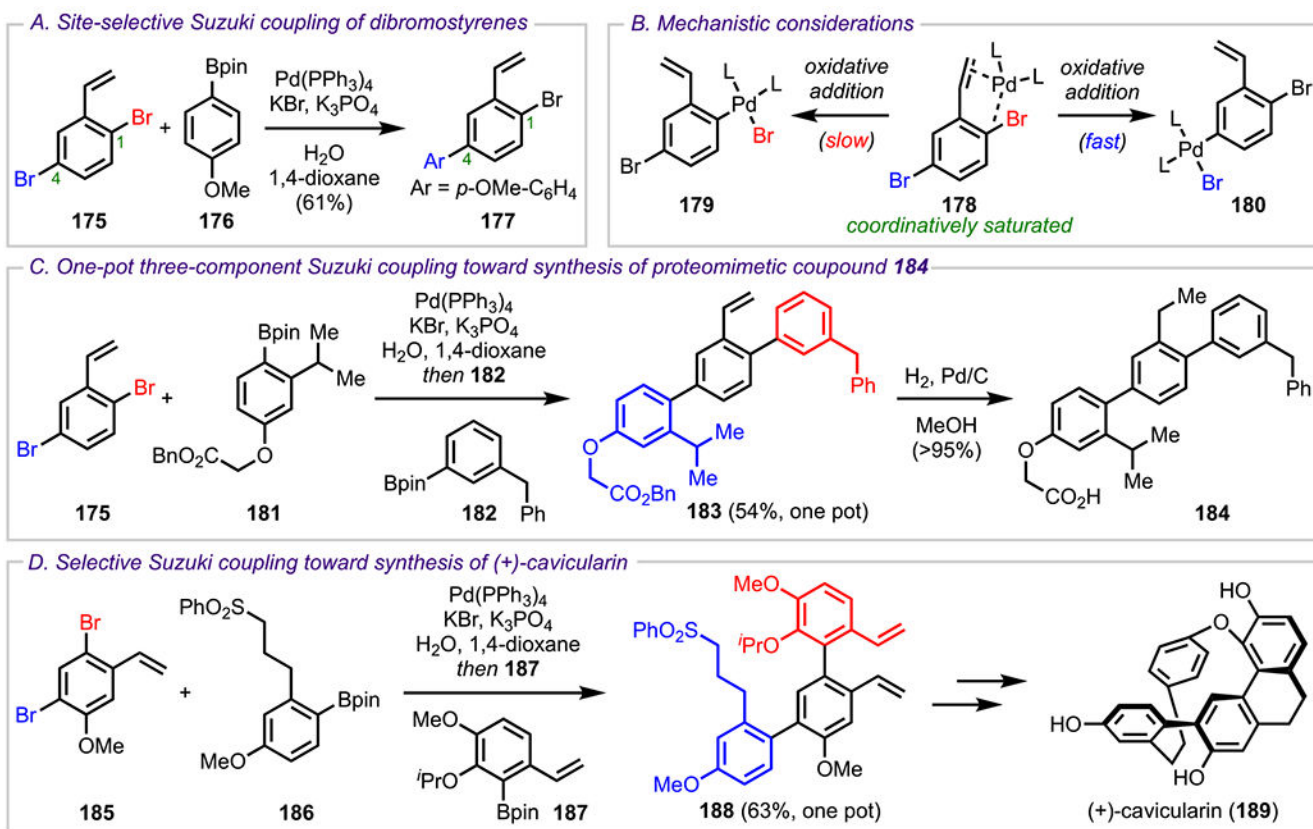
**Scheme 49.***N*-Heterocycle-Directed ortho-Borylation of Polyfluoroarenes



Scheme 50.
ortho-Selective C–F Bond Activation in Perfluorinated Nitroarene 169

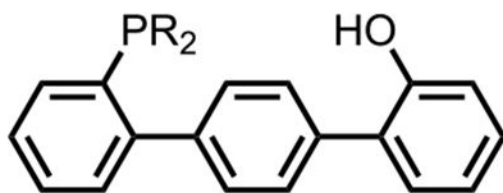


Scheme 51.
Aminide-Directed Selective Suzuki–Miyaura Coupling

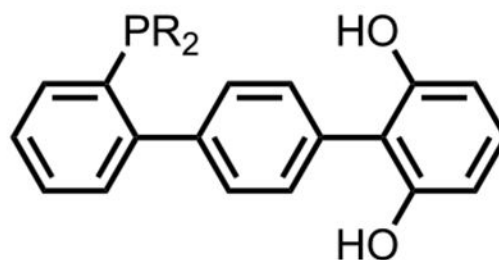
**Scheme 52.**

(A) Olefin-Mediated Site-Selective Suzuki–Miyaura Coupling of Dibromostyrene 175; (B) Mechanistic Considerations for the Observed Selectivity; (C) One-Pot Three-Component Suzuki–Miyaura Reaction for the Synthesis of Terphenyl 184; and (D) One-Pot, Three-Component Suzuki–Miyaura Reaction for the Synthesis of (+)-Cavicularin (189)

A. Synthesized HOPs

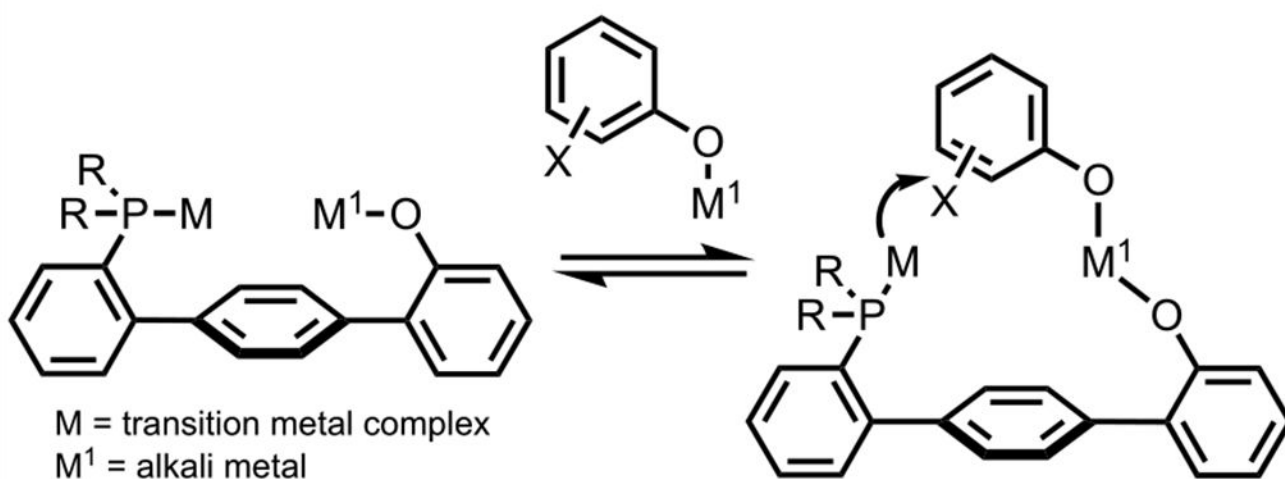


Ph-HTP (R = Ph) **190a**
 Cy-HTP (R = Cy) **190b**



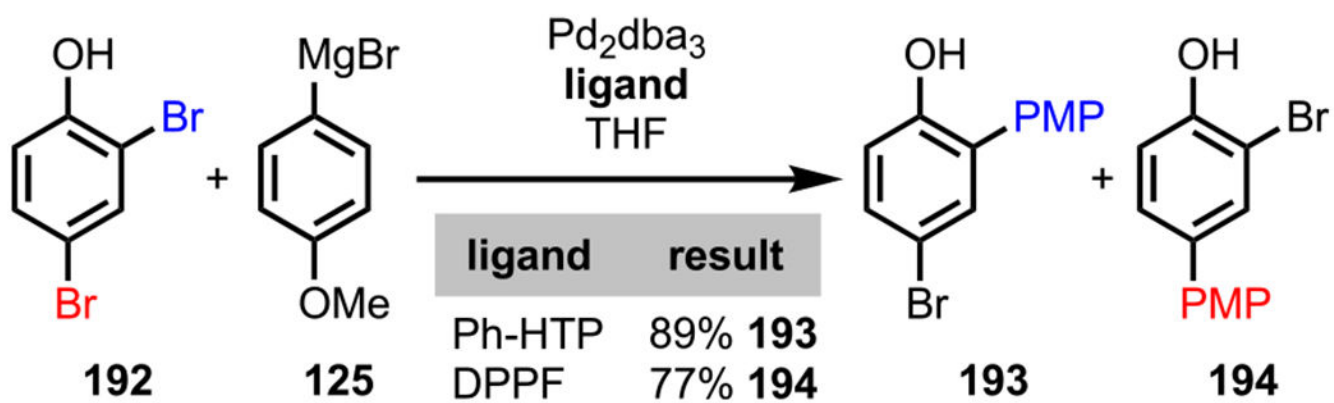
Ph-DHTP (R = Ph) **191a**
 Cy-DHTP (R = Cy) **191b**

B. Mechanistic considerations

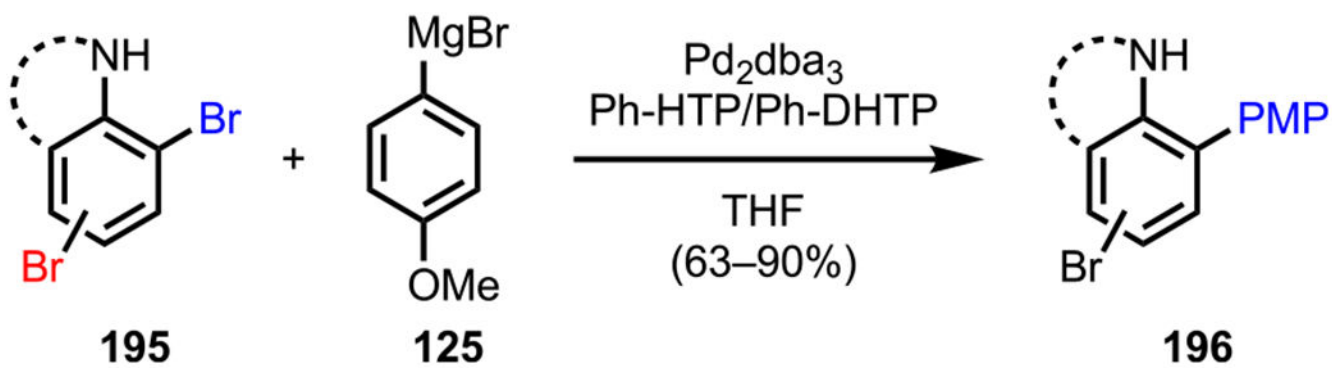


Scheme 53.

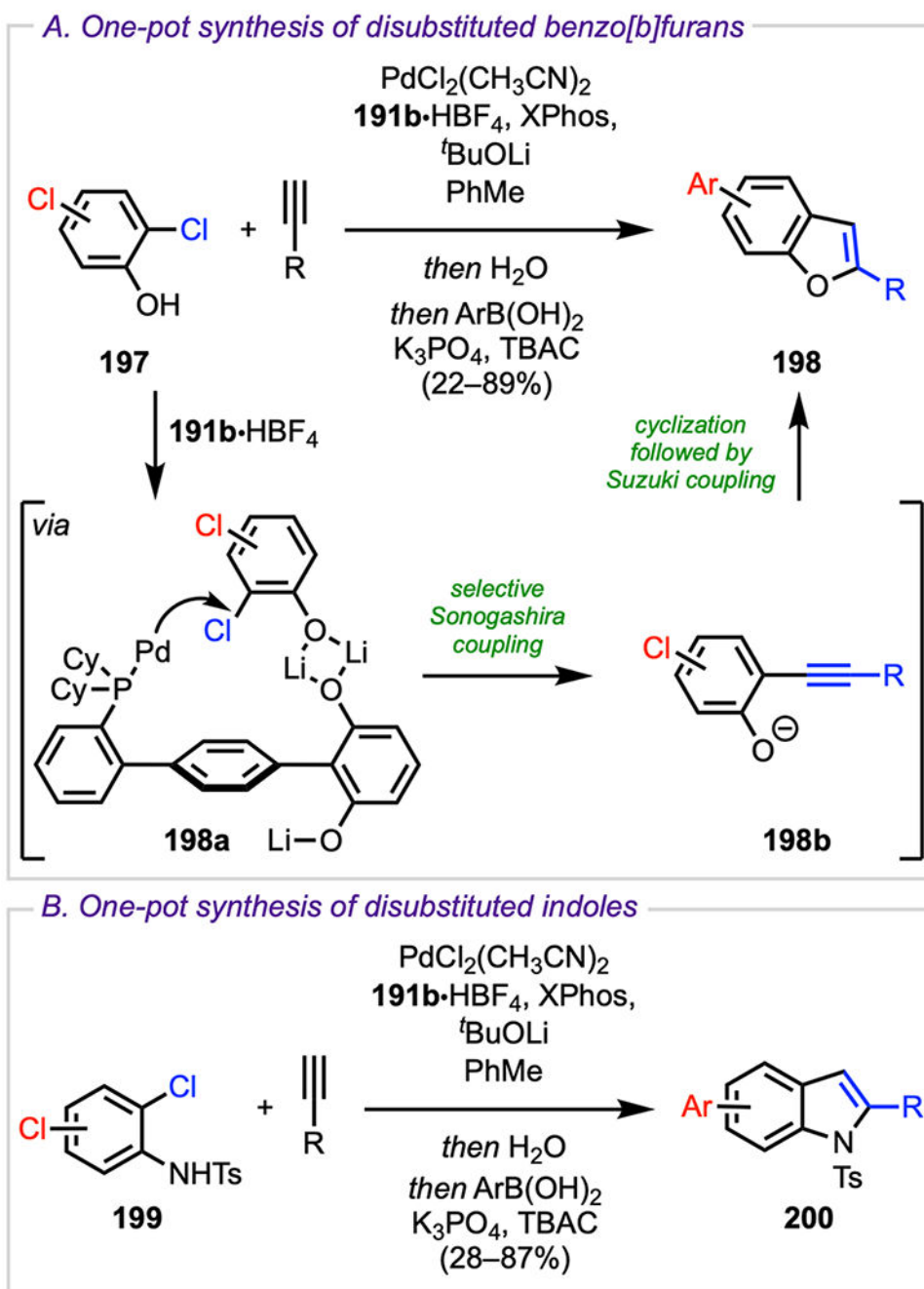
(A) Different HTP and DHTP Ligands and (B) Anticipated Heteroaggregate Formation



Scheme 54.
Site-Selective Kumada Coupling with 2,4-Dibromophenol **192**

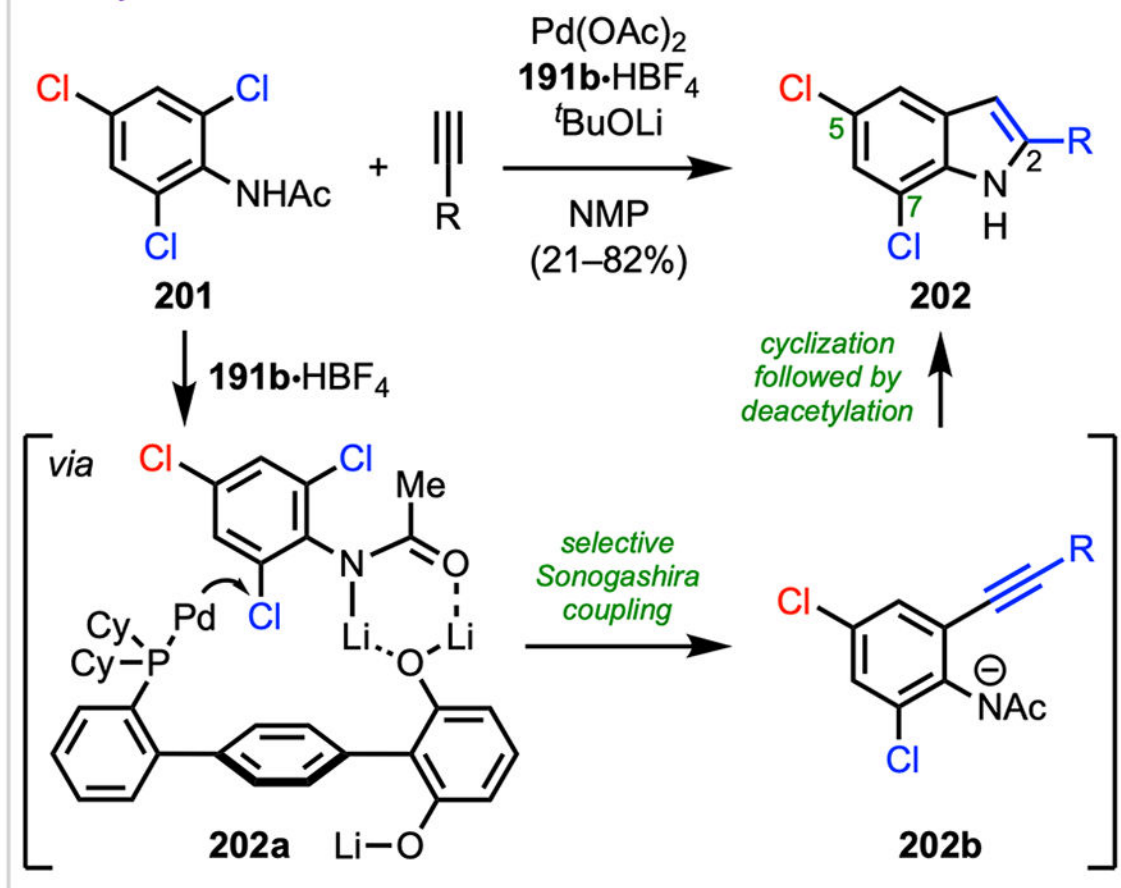


Scheme 55.
ortho-Selective Kumada Coupling with Dibromoaniline Derivatives

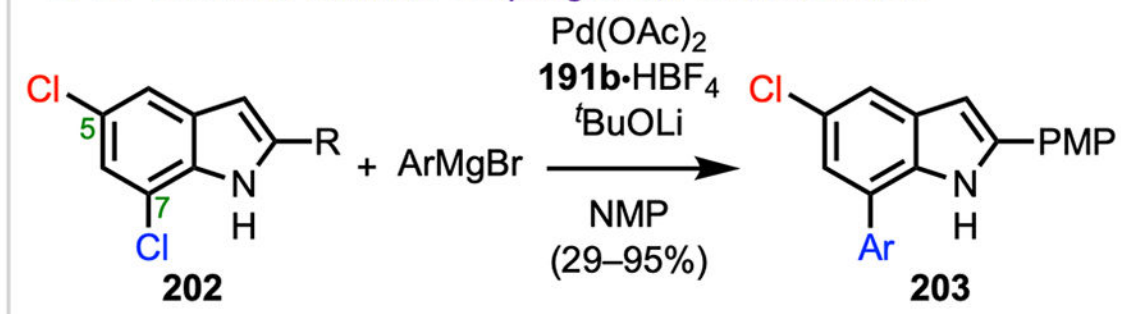
**Scheme 56.**

(A) Reaction Pathway to Access Disubstituted Benzo[*b*]furans and (B) Synthesis of Disubstituted Indoles from *N*-Tosyldichloroaniline Derivatives

A. Synthesis of 2-substituted 5,7-dichloroindole

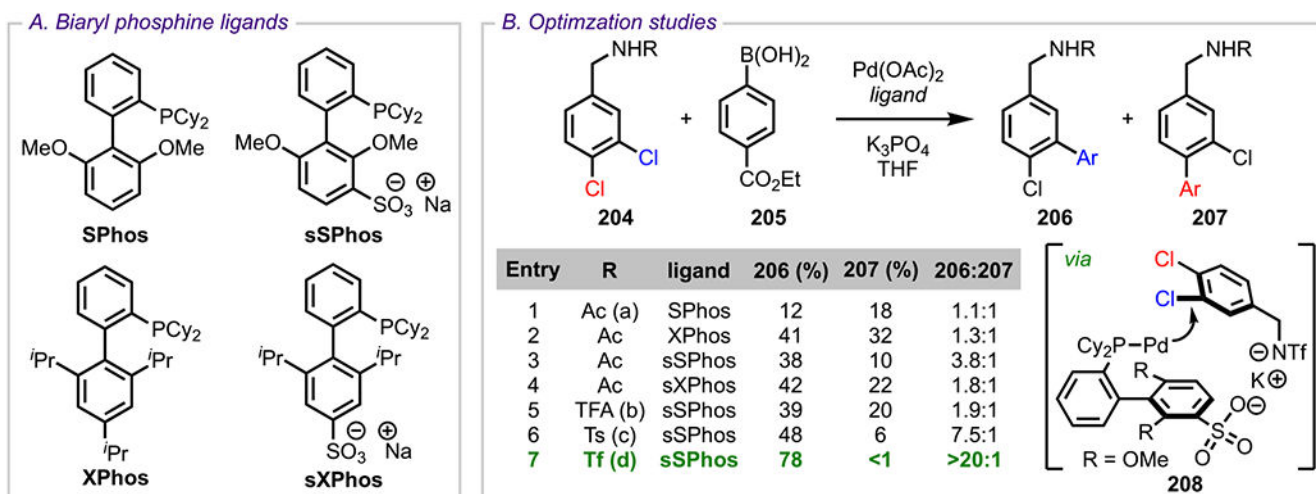


B. C7-selective Kumada coupling of 5,7-dichloroindole

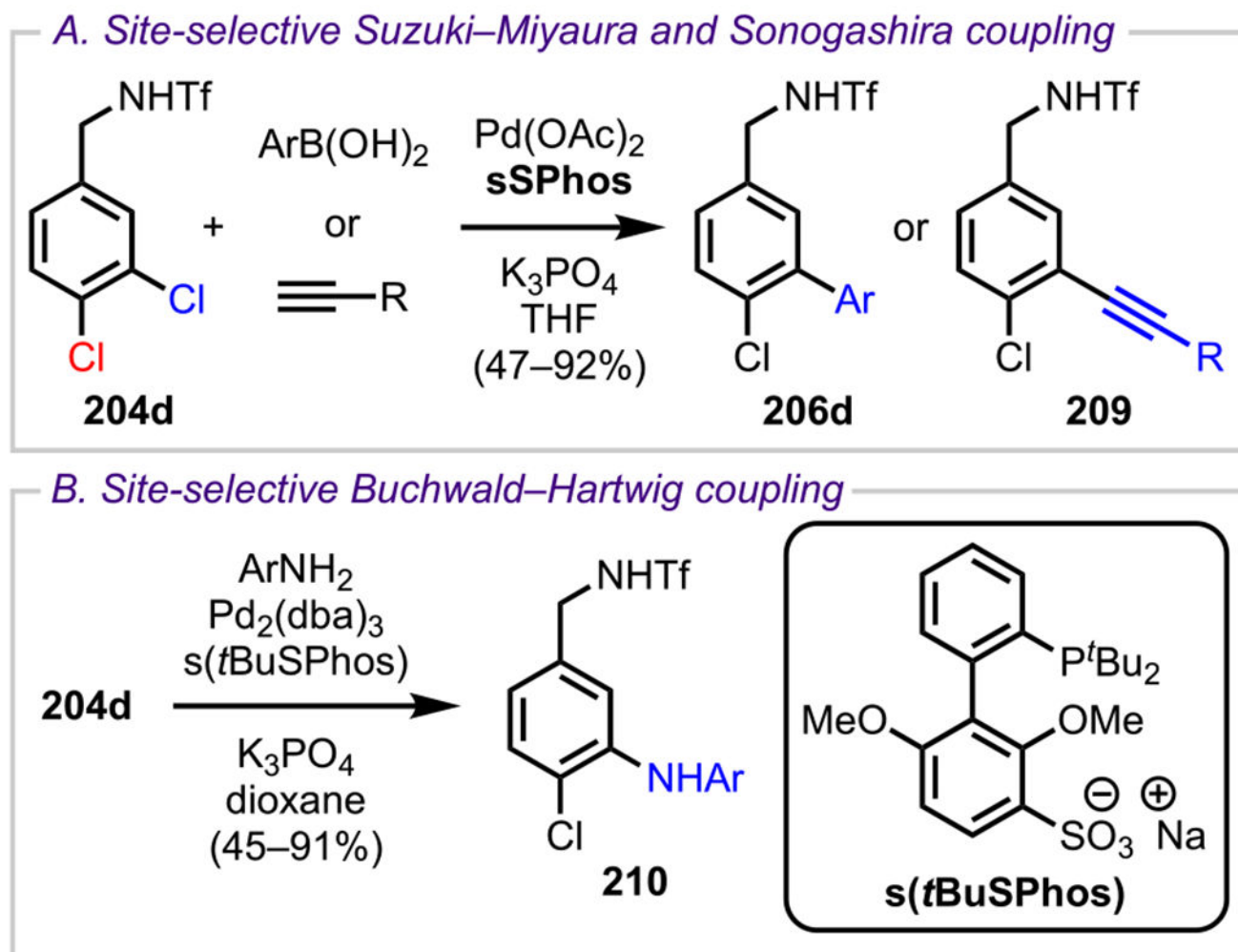


Scheme 57.

(A) Reaction Pathway to Access Two-Substituted 5,7-Dichloroindoles and (B) Site-Selective Kumada Coupling of 5,7-Dichloroindole

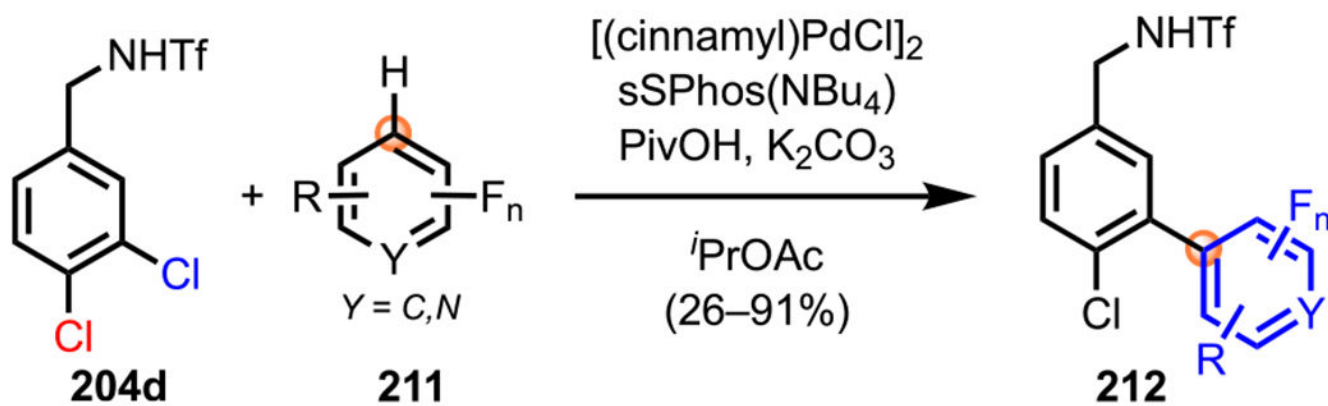
**Scheme 58.**

(A) Selection of Investigated Biarylphosphine Ligands and (B) Optimization Studies to Achieve meta-Selective Coupling

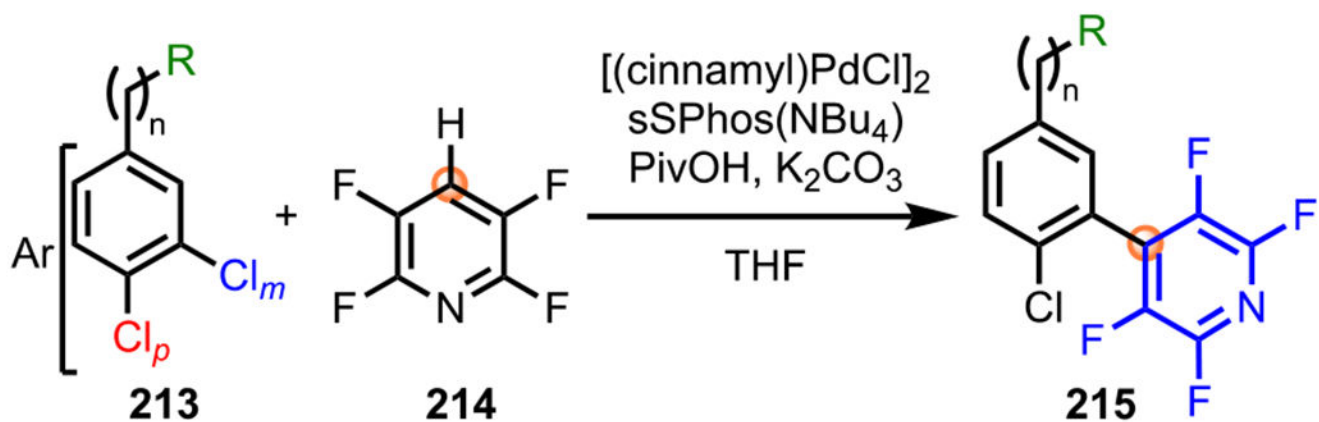


Scheme 59.

(A) Site-Selective Suzuki–Miyaura and Sonogashira Couplings with 204d and (B) Site-Selective Buchwald–Hartwig Amination with 204d

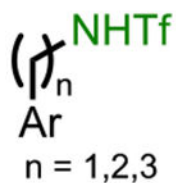


Scheme 60.
meta-Selective C–H Activation/C–C Bond Formation with Fluoroarenes and Fluoroheteroarenes



suitable Brønsted acidic groups

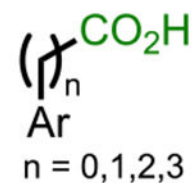
amine triflate



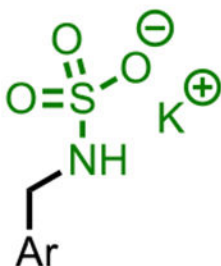
α -branched amine triflate



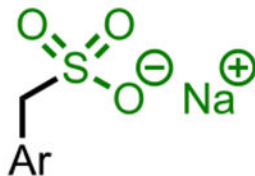
carboxylic acid



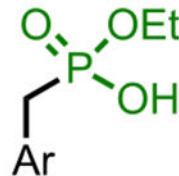
sulfamate



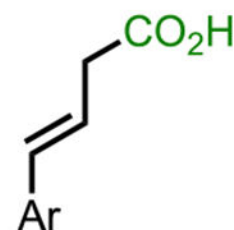
sulfonate



phosphonate

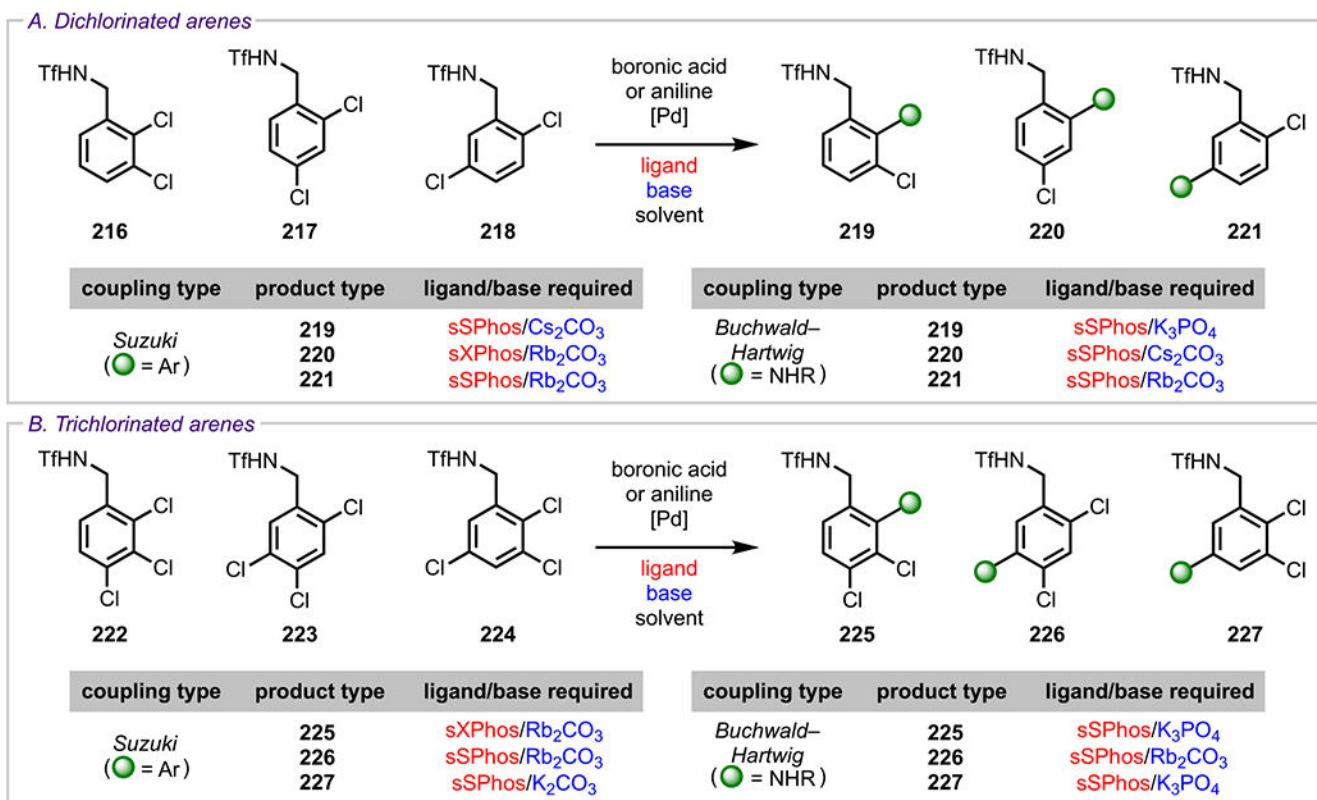


trans-styrylacetic acid

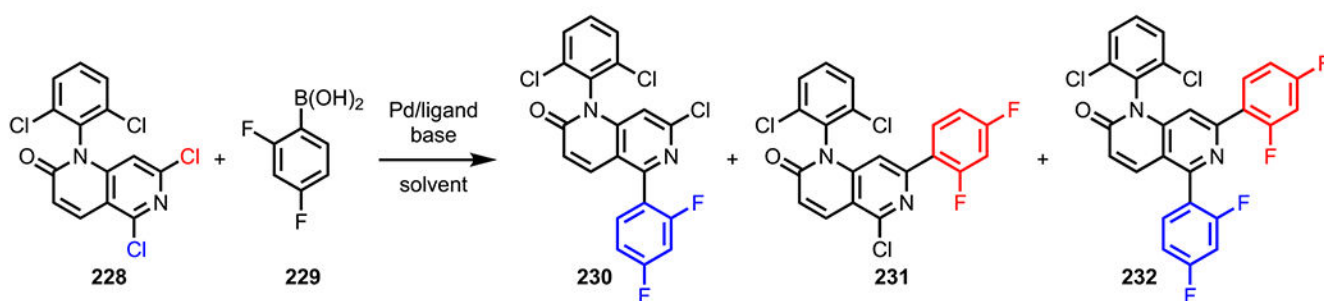


Scheme 61.

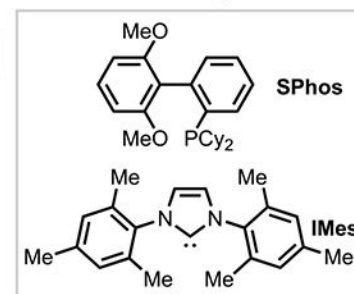
Evaluation of Various Brønsted Acidic Functional Groups

**Scheme 62.**

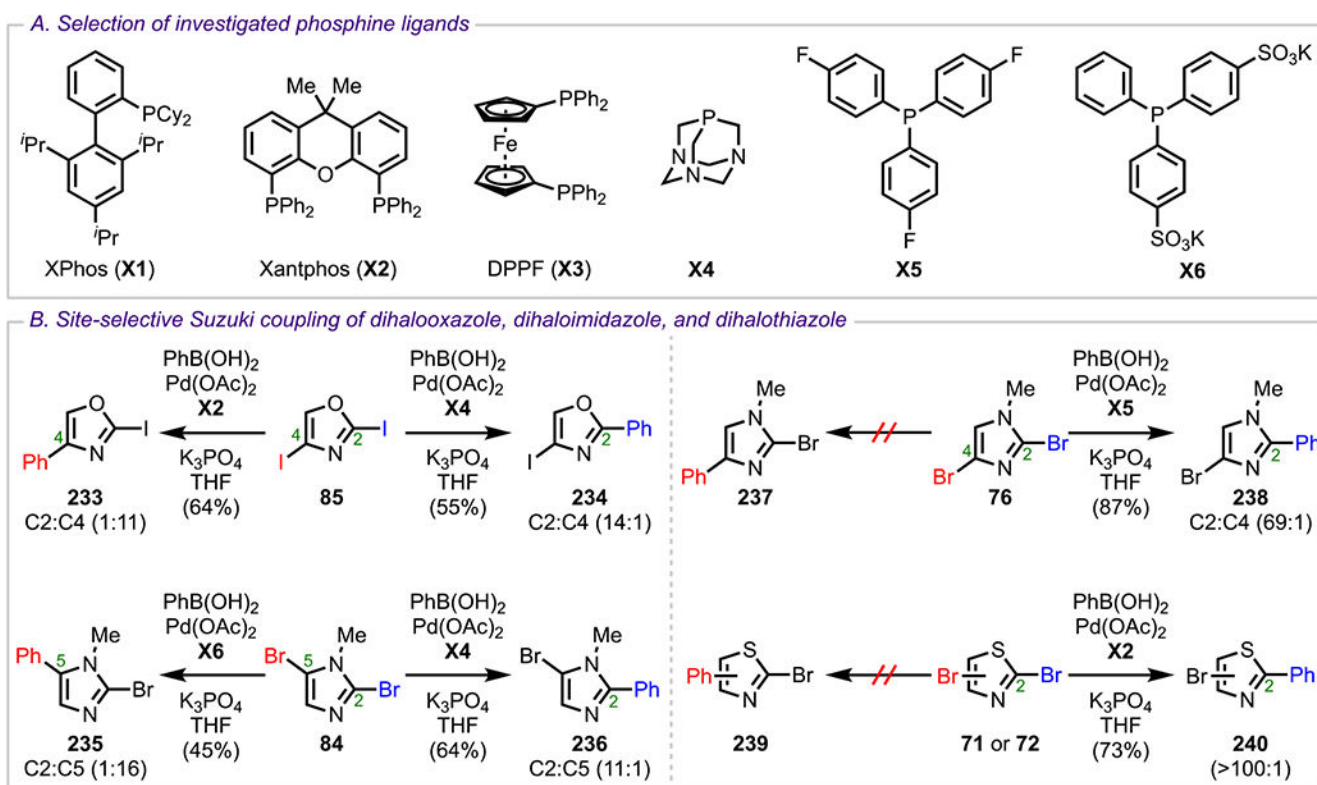
Site-Selective Suzuki–Miyaura and Buchwald–Hartwig Couplings of (A) Dichlorinated and (B) Trichlorinated Arenes



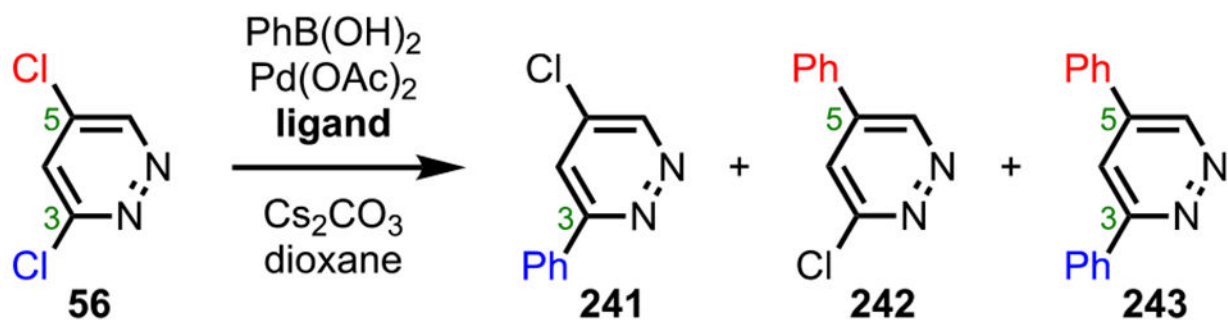
| Entry | Ligand | Pd catalyst | Base | Solvent | T (°C) | 230:231:232 (%) |
|-------|--|---|---------------------------------|---------|--------|-----------------|
| 1 | dppf | PdCl ₂ (dppf) | Cs ₂ CO ₃ | PhMe | 110 | 48:5:47 |
| 2 | dppf | PdCl ₂ (dppf) | Cs ₂ CO ₃ | PhMe | 85 | 79:0:21 |
| 3 | PPh ₃ | Pd(OAc) ₂ | K ₃ PO ₄ | IPA | 100 | 63:6:31 |
| 4 | SPhos | Pd(OAc) ₂ | K ₃ PO ₄ | PhMe | 35 | 82:6:12 |
| 5 | IMes·HCl | Pd(OAc) ₂ | K ₃ PO ₄ | DMF | 50 | 96:2:2 |
| 6 | IMes·HCl | Pd ₂ (dba) ₃ ·CHCl ₃ | K ₃ PO ₄ | DMF | 75 | 97:0:3 |
| 7 | (2-MeOC ₆ H ₄) ₃ P | Pd ₂ (dba) ₃ ·CHCl ₃ | K ₃ PO ₄ | DMF | 40 | 92:3:5 |



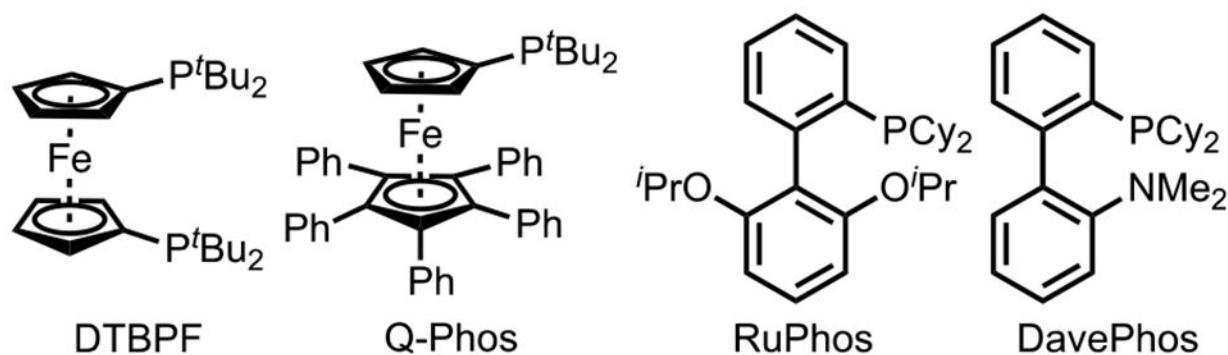
Scheme 63.
Site-Selective Suzuki–Miyaura Coupling of 228

**Scheme 64.**

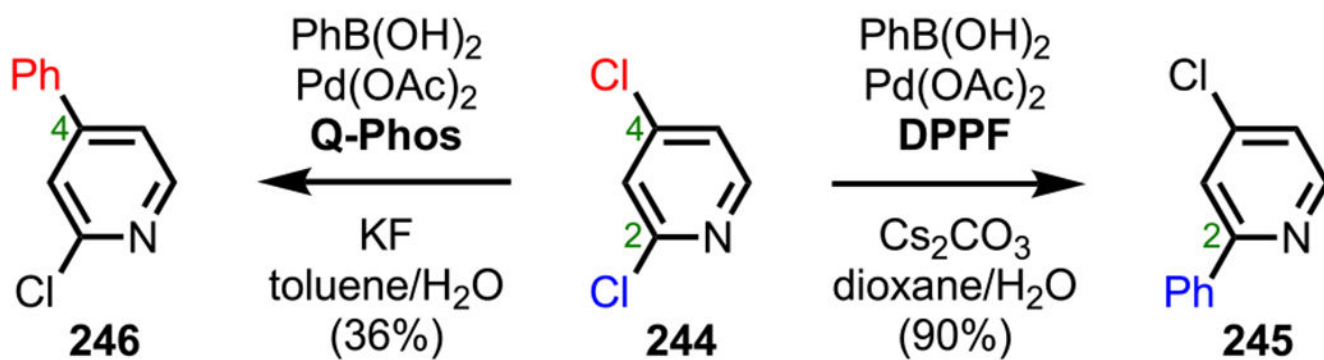
(A) Investigated Ligands and (B) Ligand-Controlled Site-Selective Suzuki–Miyaura Couplings of Various Dihaloazoles



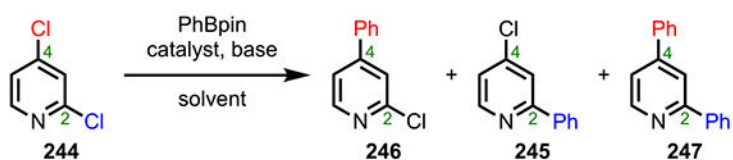
| C-Cl BDEs (kcal/mol) ^a | Entry | ligand | 241 | 242 | 243 |
|--------------------------------------|----------|-------------------------|-------------|-----------|-----------|
| | | 1 | DPPF | 82 | 0 |
| | 2 | Xantphos | 69 | 12 | 19 |
| | 3 | PPh_3 | 76 | 0 | 24 |
| | 4 | DTBPF | 16 | 54 | 30 |
| | 5 | P^tBu_3 | 8 | 71 | 21 |
| | 6 | P(o-tol)_3 | 28 | 60 | 12 |
| | 7 | Q-Phos | 4 | 80 | 16 |
| | 8 | RuPhos | 17 | 4 | 79 |
| | 9 | DavePhos | 14 | 16 | 70 |
| | 10 | XPhos | 10 | 15 | 75 |



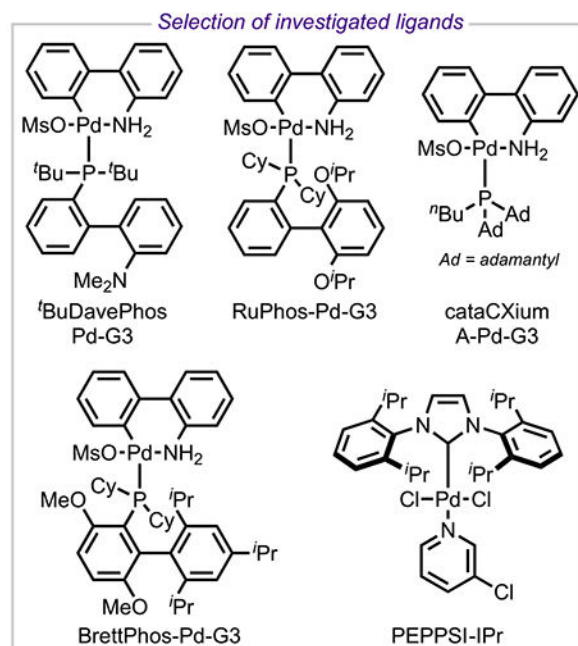
Scheme 65.
C3 versus C5 Complementary Selectivity Observed in 3,5-Dichloropyridazine (**56**)



Scheme 66.
Complementary Selectivity Observed in 2,4-Dichloropyridine (244)

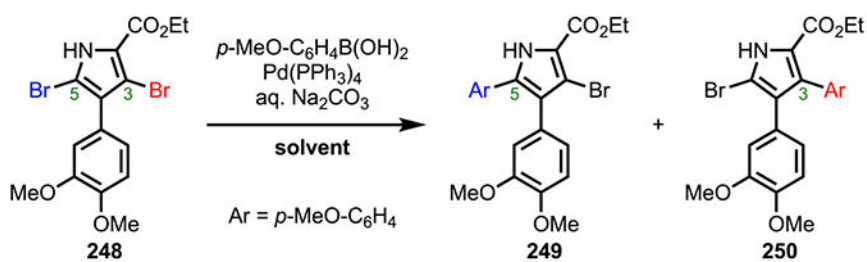


| Entry | Catalyst | Base | Solvent | 246:245:247 (yield of 246) |
|-------|--|---|-------------------------------|-------------------------------|
| 1 | Pd(PPh₃)₄ | Na₂CO₃ | dioxane/H₂O | 2:80:18 |
| 2 | ^t BuDavePhos-Pd-G3 | Na ₂ CO ₃ | dioxane/H ₂ O | 34:52:14 |
| 3 | RuPhos-Pd-G3 | Na ₂ CO ₃ | dioxane/H ₂ O | 15:37:48 |
| 4 | Pd(P ^t Bu ₃) ₂ | Na ₂ CO ₃ | dioxane/H ₂ O | 56:36:8 |
| 5 | cataCXium A-Pd-G3 | Na ₂ CO ₃ | dioxane/H ₂ O | 49:24:27 |
| 6 | BrettPhos-Pd-G3 | Na ₂ CO ₃ | dioxane/H ₂ O | 57:24:19 |
| 7 | PEPPSI-IPr | Na ₂ CO ₃ | dioxane/H ₂ O | 37:8:55 |
| 8 | PEPPSI-IPr | Na ₂ CO ₃ | toluene/H ₂ O | 61:24:15 |
| 9 | PEPPSI-IPr | Na ₂ CO ₃ | PEG400/H ₂ O | 60:14:26 (45%) |
| 10 | PEPPSI-IPr | Na ₂ CO ₃ | PEG400 | 69:16:15 (50%) |
| 11 | PEPPSI-IPr | NaOAc | PEG400 | 83:8:9 (33%) |
| 12 | PEPPSI-IPr | Na₂CO₃ + NaOAc | PEG400 | 99:1:0 (76%) |



Scheme 67.

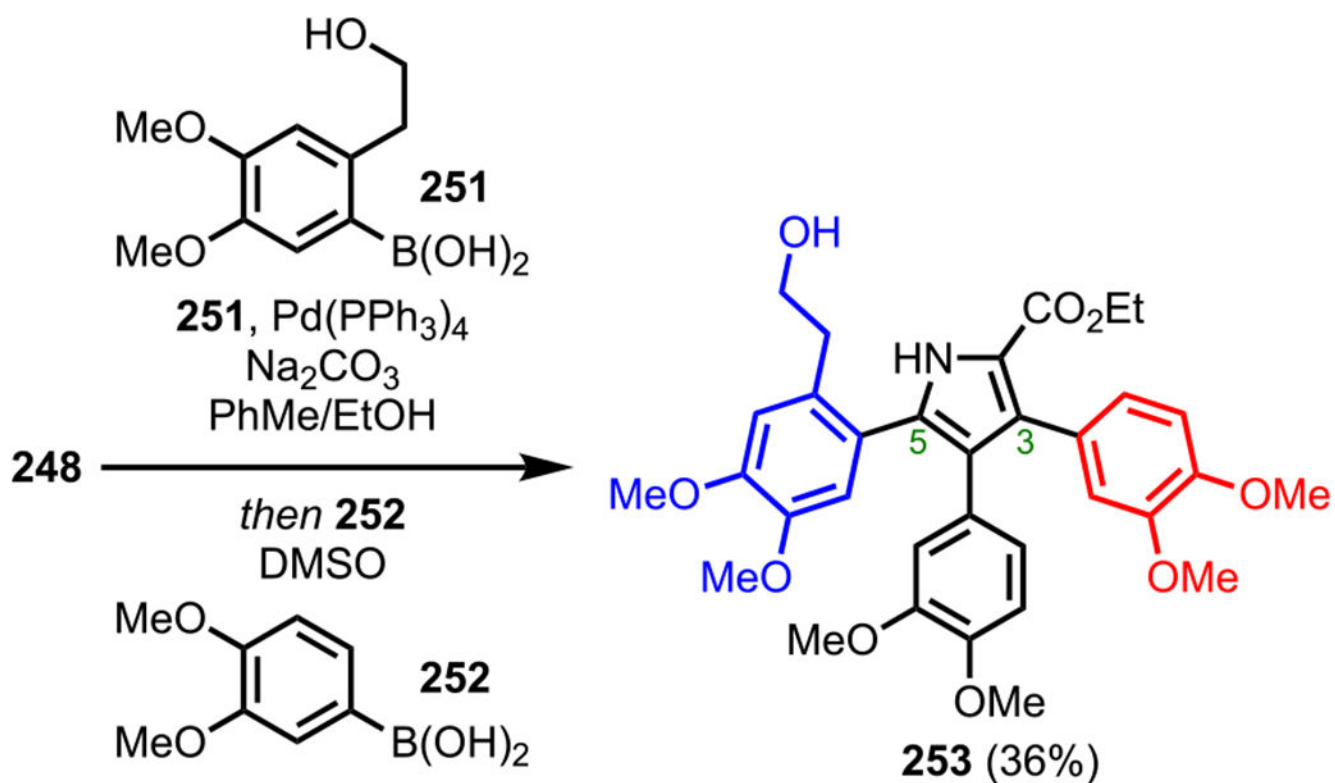
Optimization for the Site-Selective Suzuki–Miyaura Coupling of 2,4-Dichloropyridine (244)



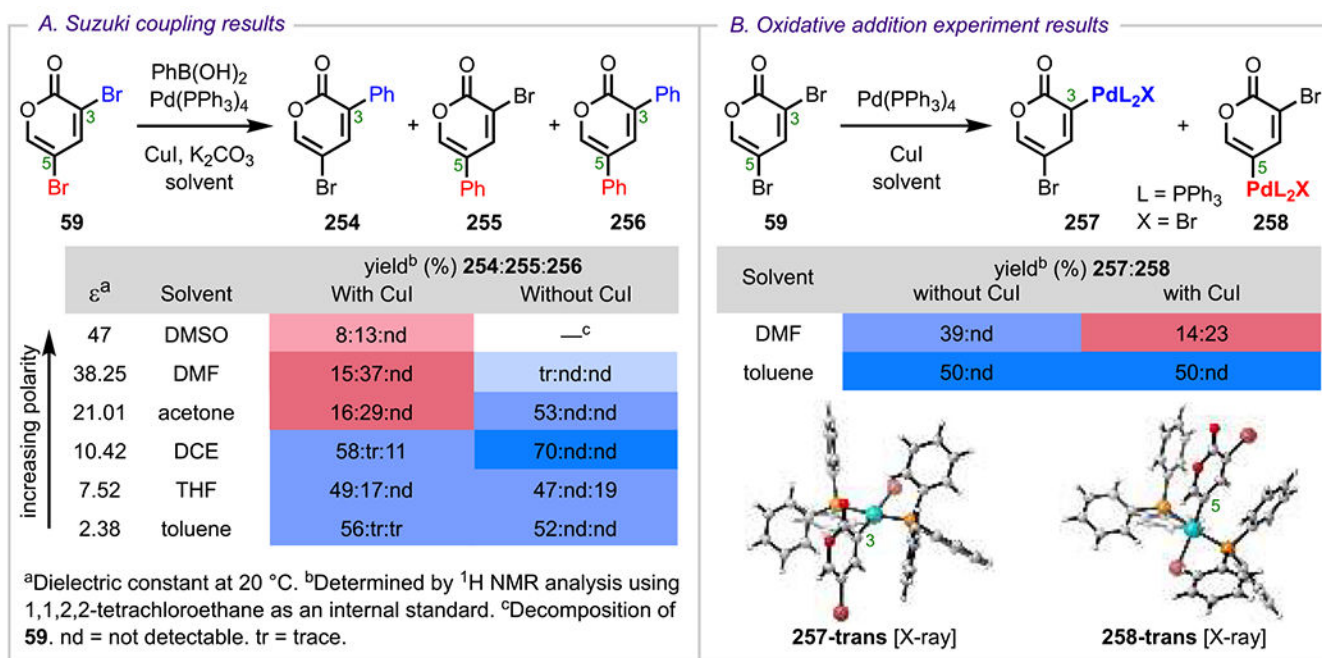
| Entry | Solvent | Conv. (%) | 249:250 (%major) |
|-------|--------------|-----------|------------------|
| 1 | toluene/EtOH | 71 | 22:1 (70%) |
| 2 | acetonitrile | 70 | 1:2 |
| 3 | dioxane | 40 | 2:3 |
| 4 | DMF | >99 | 1:3 (53%) |
| 5 | DMSO | 63 | 1:4 |
| 6 | nitromethane | no rxn | NA |
| 7 | toluene | no rxn | NA |

Scheme 68.

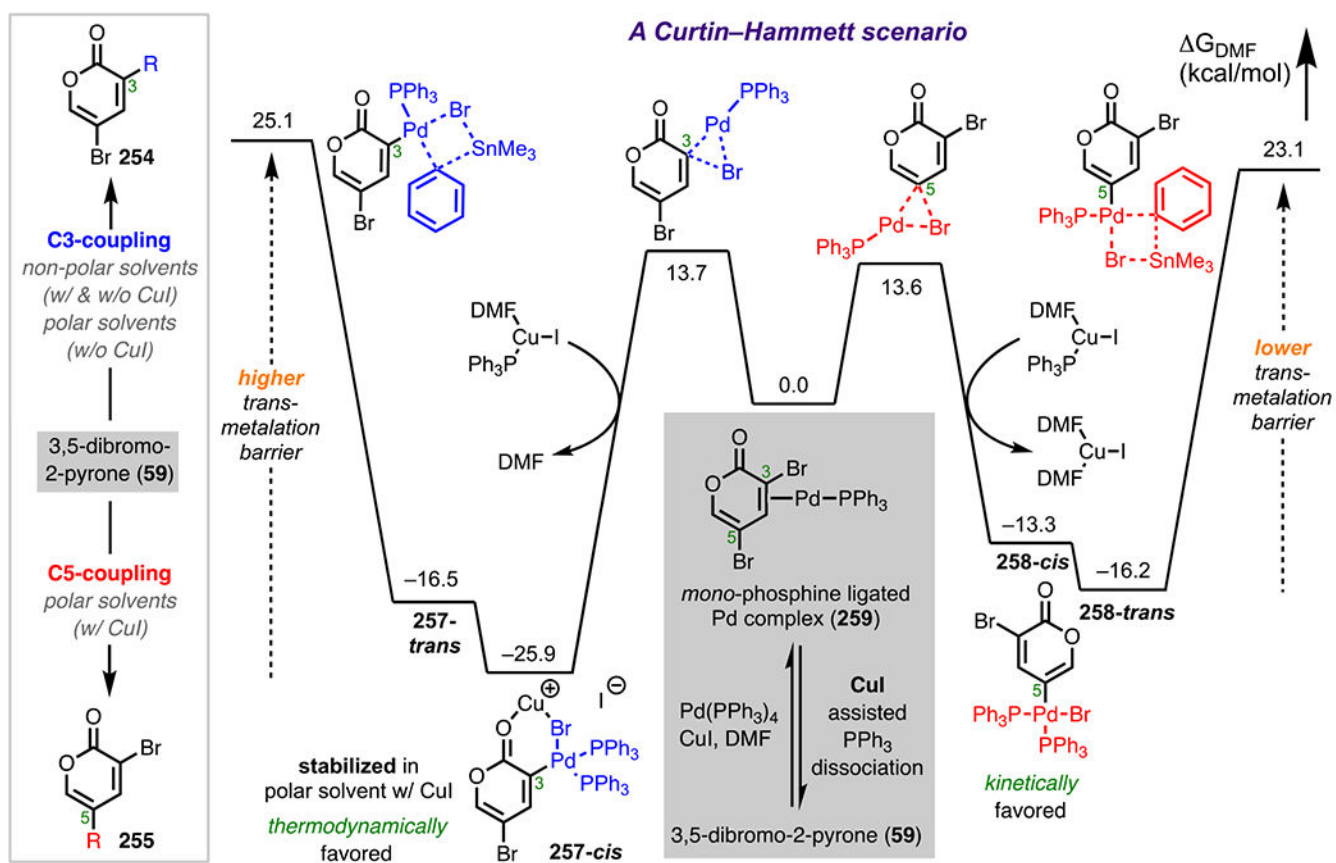
Reversal of Selectivity in 248 upon Changing Reaction Solvent

**Scheme 69.**

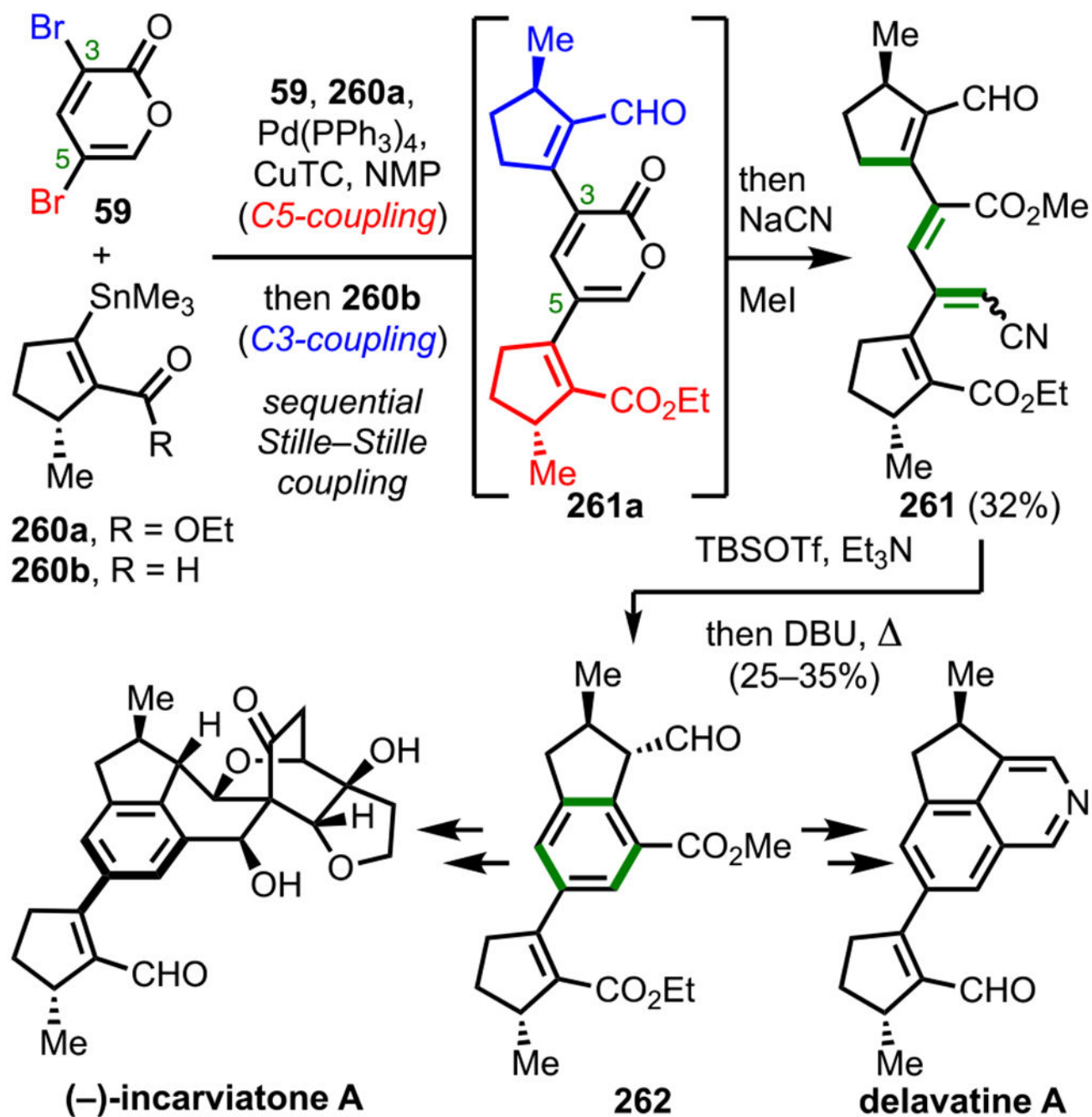
One-Pot Sequential Suzuki-Miyaura Coupling of 248

**Scheme 70.**

(A) Suzuki–Miyaura Coupling with 3,5-Dibromo-2-pyrone (59) and (B) Oxidation Addition Experiments with 3,5-Dibromo-2-pyrone (59) (Adapted from ref 43. Copyright 2019 American Chemical Society)

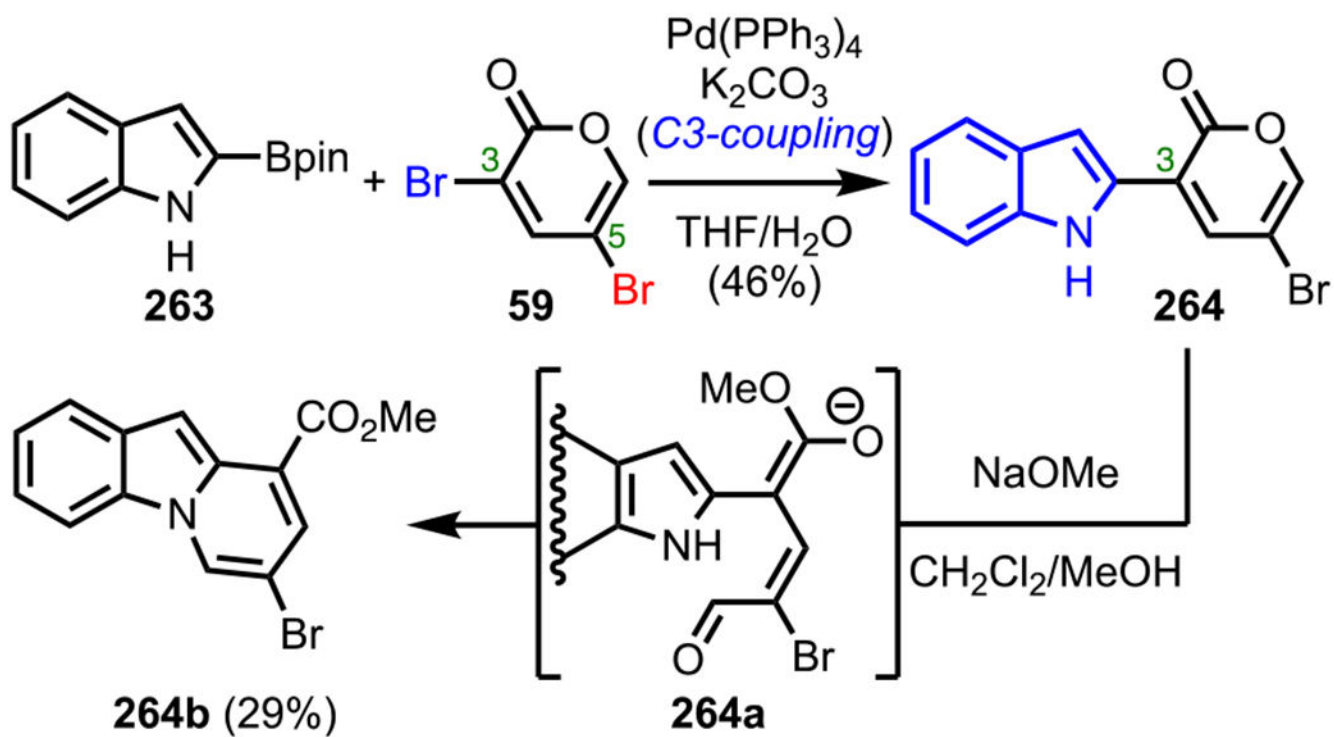


Scheme 71.
Curtin–Hammett Scenario to Favor C5 Coupling over C3 Coupling

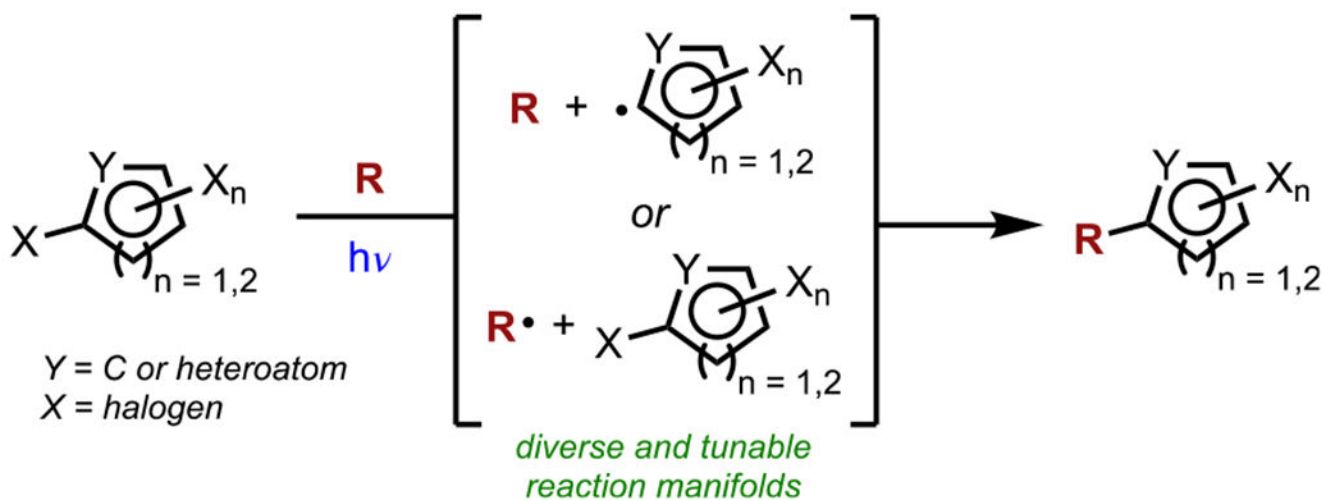


Scheme 72.

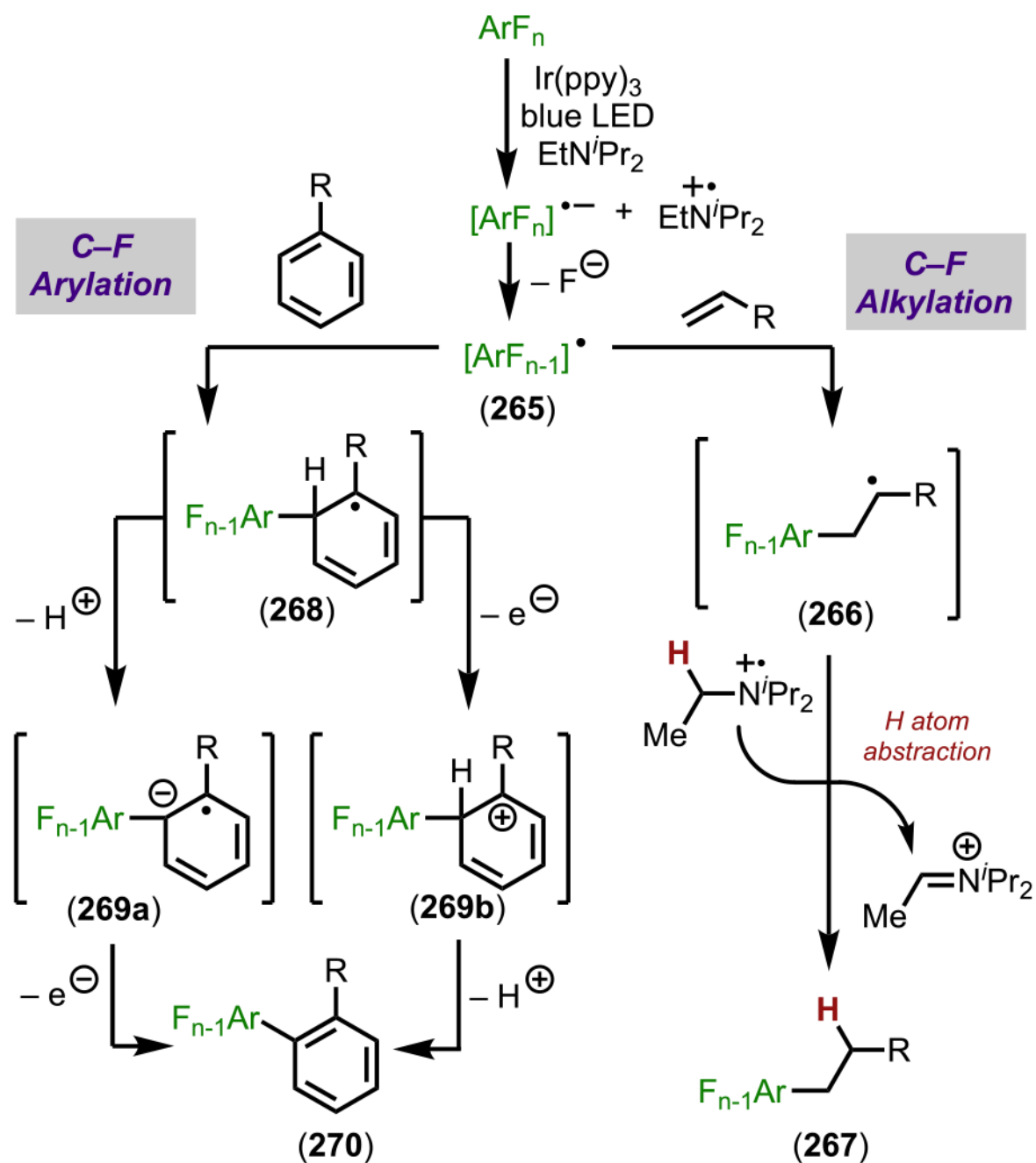
Application of 3,5-Dibromo-2-pyrone (59) Site-Selective Cross-Coupling to the Synthesis of Delavatine A and (–)-Incarviatone A

**Scheme 73.**

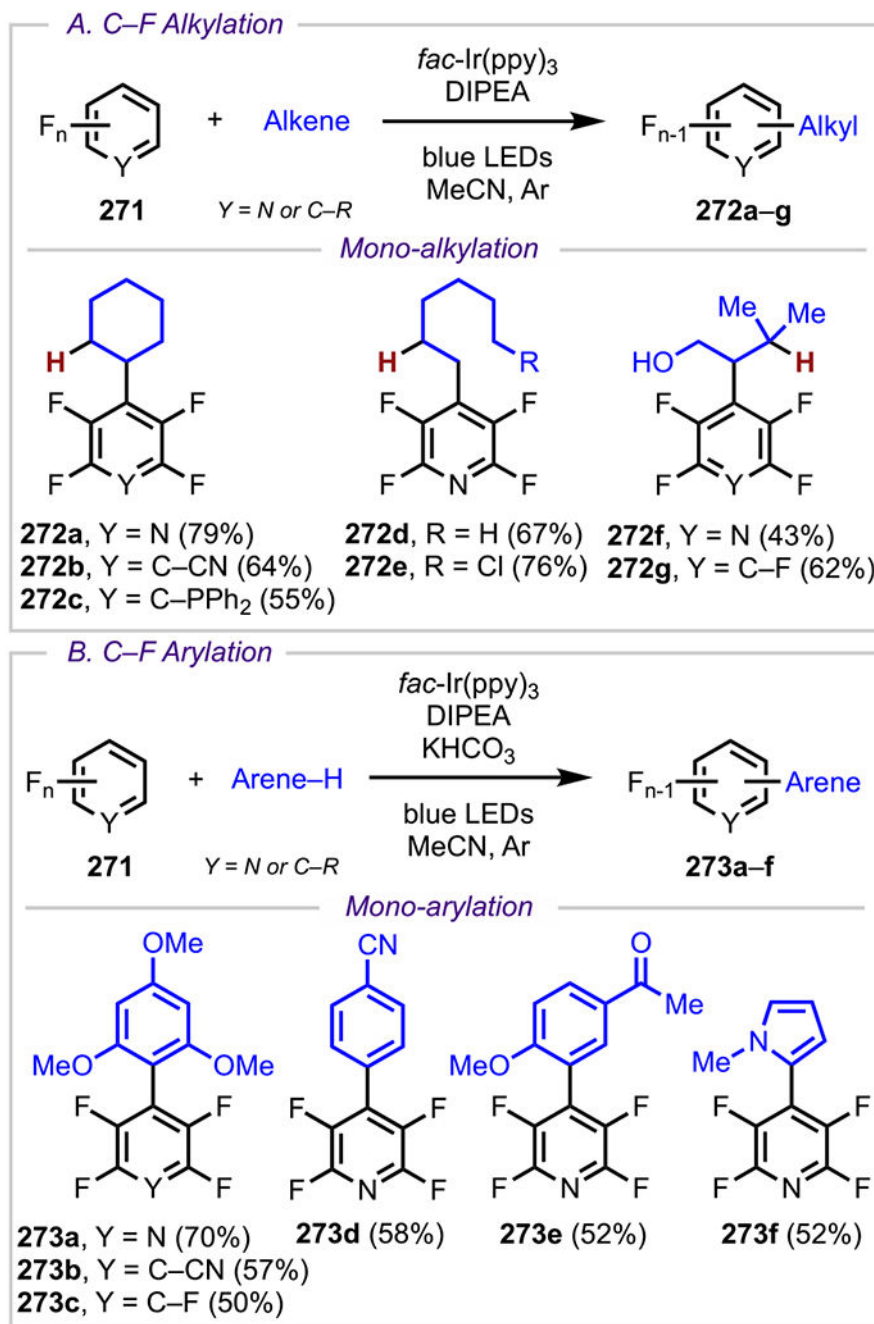
Application of 3,5-Dibromo-2-pyrone (59) Site-Selective Cross-Coupling to the Synthesis of Pyrido[1,2-*a*]indole 264b



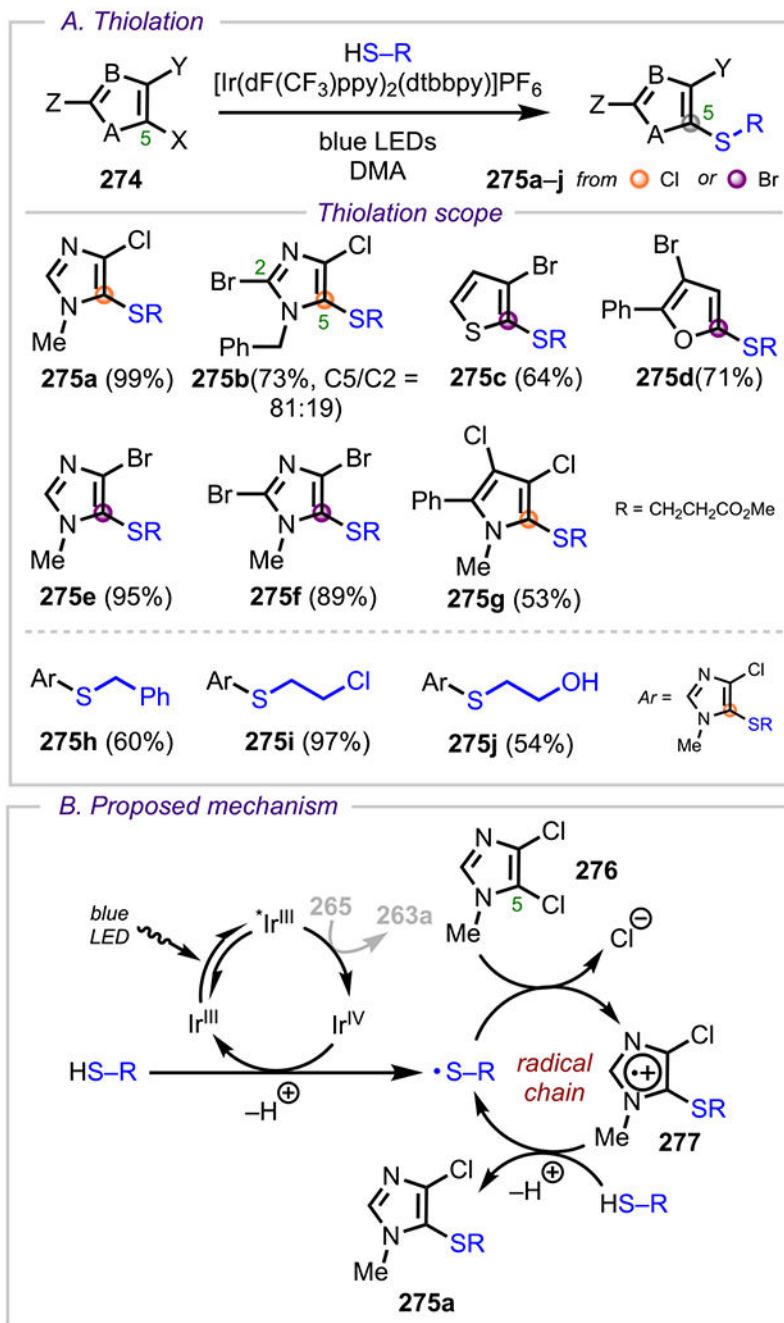
Scheme 74.
 Photochemically Initiated Site-Selective Cross-Coupling



Scheme 75.
Mechanism of Photocatalytic C-F Alkylation and Arylation



Scheme 76.
 Photocatalyzed (A) C–F Alkylation and (B) C–F Arylation

**Scheme 77.**

(A) Photocatalytic Thiolation and (B) Proposed Mechanism